

Washington University in St. Louis
Washington University Open Scholarship

Arts & Sciences Electronic Theses and Dissertations

Arts & Sciences

Spring 5-15-2015

Synthesis, Structure, Spectroscopy, and Reactivity of Azapentadienyl-Ruthenium-Phosphine Complexes

Meghan Leigh Stouffer
Washington University in St. Louis

Follow this and additional works at: https://openscholarship.wustl.edu/art_sci_etds



Part of the [Chemistry Commons](#)

Recommended Citation

Stouffer, Meghan Leigh, "Synthesis, Structure, Spectroscopy, and Reactivity of Azapentadienyl-Ruthenium-Phosphine Complexes" (2015). *Arts & Sciences Electronic Theses and Dissertations*. 469.
https://openscholarship.wustl.edu/art_sci_etds/469

This Dissertation is brought to you for free and open access by the Arts & Sciences at Washington University Open Scholarship. It has been accepted for inclusion in Arts & Sciences Electronic Theses and Dissertations by an authorized administrator of Washington University Open Scholarship. For more information, please contact digital@wumail.wustl.edu.

WASHINGTON UNIVERSITY IN ST. LOUIS

Department of Chemistry

Dissertation Examination Committee:

John R. Bleeke, Chair
Willaim E. Buhro
Sophia Hayes
Liviu M. Mirica
Nigam Rath

Synthesis, Structure, Spectroscopy, and Reactivity of Azapentadienyl-Ruthenium-Phosphine
Complexes

by

Meghan Stouffer

A dissertation presented to the
Graduate School of Arts and Sciences
of Washington University in
partial fulfillment of the
requirements for the degree
of Doctor of Philosophy

May 2015

St. Louis, Missouri

Table of Contents

List of Figures.....	vii
List of Schemes.....	viii
List of Tables.....	xi
List of Compounds.....	xii
Acknowledgements.....	xx
Abstract.....	xxi
Chapter 1: Introduction.....	1
1.1 Allyl-, Cyclopentadienyl-, and Pentadienyl-Transition Metal Complexes.....	2
1.2 Pentadienyl Complexes of Cobalt.....	5
1.3 Pentadienyl Complexes of Ruthenium.....	7
1.4 Heteropentadienyl-Transition Metal Complexes.....	8
1.5 Azapentadienyl-Transition Metal Complexes.....	10
1.5.1 Azapentadienyl-Metal Complex from Oxapentadienyl-Metal Precursors.....	10
1.5.2 Azapentadienyl-Metal Complexes from Anionic Azapentadienide Reagents and Metal Halides.....	11
1.5.3 Half-Open Azapentadienyl-Ruthenium Complexes from Anionic Azapentadienide or Group 14 Enimine.....	14
1.5.4 Additional Work.....	16
1.6 Outline of Dissertation.....	16
1.7 References.....	16

Chapter 2: Neutral <i>bis</i>-Azapentadienyl-Ruthenium-Phosphine Chemistry.....	19
2.1 Introduction.....	20
2.1.1 Azapentadienyl-Metal-Phosphine Complexes (M = Co, Ir, Rh).....	20
2.1.2 Azapentadienyl-Ruthenium-Phosphine Complexes.....	22
2.1.2.1 Comparison to the Analogous Pentadienyl Ruthenium System... <td>24</td>	24
2.2 Results and Discussion.....	25
2.2.1 Synthesis and Characterization of [(1,2,3- η^3)-(5- <i>tert</i> -butylazapentadienyl)] ₂ Ru(PPh ₃) ₂ (1).....	25
2.2.2 Possible Structural Variants for [(1,2,3- η^3)-(5- <i>tert</i> -butylazapentadienyl)] ₂ RuLL' Complexes.....	28
2.2.3 Treatment of Compound 1 with Neutral, 2e ⁻¹ Donor Ligands at Room Temperature.....	30
2.2.3.1 Synthesis and Characterization of [(1,2,3- η^3)-(5- <i>tert</i> -butylazapentadienyl)] ₂ Ru(PPh ₃)(PMe ₃) (2).....	31
2.2.3.2 Synthesis and Characterization of [(1,2,3- η^3)-(5- <i>tert</i> -butylazapentadienyl)] ₂ Ru(PPh ₃)(dmpe) (3).....	34
2.2.3.3 Synthesis and Characterization of [(1,2,3- η^3)-(5- <i>tert</i> -butylazapentadienyl)] ₂ Ru(PPh ₃)[P(OMe) ₃] (4).....	34
2.2.3.4 Synthesis and Characterization of [(1,2,3- η^3)-(5- <i>tert</i> -butylazapentadienyl)] ₂ Ru(PPh ₃)(CNCMe ₃) (5).....	38
2.2.3.5 Synthesis and Characterization of [(1,2,3- η^3)-(5- <i>tert</i> -butylazapentadienyl)] ₂ Ru(PPh ₃)(CO) (6).....	42

2.2.4 Synthesis and Characterization of [(1,2,3- η^3)-(5- <i>tert</i> -butylazapentadienyl)] ₂ Ru(PPh ₃)(PEt ₃) (7) [(1,2,3- η^3)-(5- <i>tert</i> -butylazapentadienyl)] ₂ Ru(PEt ₃) ₂ (8).....	43
2.2.5 Treatment of Compound 1 with Neutral, 2 e ⁻¹ Donor Ligands at Elevated Temperatures.....	48
2.2.5.1 Synthesis and Characterization of [(1,2,3- η^3)-(5- <i>tert</i> -butylazapentadienyl)] ₂ Ru(PMe ₃) ₂ (9).....	48
2.2.5.2 Synthesis and Characterization of [(1,2,3- η^3)-(5- <i>tert</i> -butylazapentadienyl)] ₂ Ru[P(OMe) ₃] ₂ (10).....	52
2.2.5.3 Synthesis and Characterization of [(1,2,3- η^3)-(5- <i>tert</i> -butylazapentadienyl)] ₂ Ru(dmpe) (11).....	53
2.3 Summary and Comparisons.....	53
2.3.1 Comparisons with <i>Mono</i> -Azapentadienyl-Ruthenium-Phosphine Complexes.....	54
2.4 Experimental.....	55
2.5 References.....	65

Chapter 3: Protonation of Neutral *bis*-Azapentadienyl-Ruthenium-Phosphine

Complexes.....	67
3.1 Introduction.....	68
3.1.1 Protonation of Azapentadienyl-Cobalt-Phosphine Complexes.....	69
3.1.2 Protonation of Azapentadienyl-Iridium-Phosphine Complexes.....	71
3.1.3 Protonation of Azapentadienyl-Rhodium-Phosphine Complexes.....	72

3.2 Results and Discussion.....	74
3.2.1 Protonation of [(1,2,3- η^3)-(5- <i>tert</i> -butylazapentadienyl)] ₂ RuL ₂ Complexes.....	74
3.2.1.1 Synthesis and Characterization of {[[(1,2,3- η^3)-(CH ₂ CHCHCH=NCH)(CMe ₃)] ₂ Ru(PEt ₃) ₂ } ²⁺ (O ₃ SCF ₃) ₂ (12).....	75
3.2.1.2 Synthesis and Characterization of {[[(1,2,3- η^3)-(CH ₂ CHCHCH=NCH)(CMe ₃)] ₂ Ru(PMe ₃) ₂ } ²⁺ (O ₃ SCF ₃) ₂ (13)...81	
3.2.1.3 Synthesis and Characterization of {[[(1,2,3- η^3)-(CH ₂ CHCHCH=NCH)(CMe ₃)] ₂ Ru[P(OMe) ₃] ₂ } ²⁺ (O ₃ SCF ₃) ₂ (14).....	82
3.2.2 Protonation of [(1,2,3- η^3)-(5- <i>tert</i> -butylazapentadienyl)] ₂ RuLL'	
Complexes.....	84
3.2.2.1 Synthesis and Characterization of {[[(1,2,3- η^3)-(CH ₂ CHCHCH=NCH)(CMe ₃)] ₂ Ru(PPh ₃)(PMe ₃)} ²⁺ (O ₃ SCF ₃) ₂ (15).....	84
3.2.2.2 Synthesis and Characterization of {[[(1,2,3- η^3)-(CH ₂ CHCHCH=NCH)(CMe ₃)] ₂ Ru(PPh ₃)(L)} ²⁺ (O ₃ SCF ₃) ₂ , where L = P(OMe) ₃ (16) and CNCMe ₃ (17).....	86
3.3 Summary and Comparisons.....	87
3.3.1 Comparison with Azapentadienyl-Cobalt and Azapentadienyl-Rhodium System.....	87
3.4 Experimental.....	88
3.5 References.....	94

Chapter 4: Summary and Future Work.....	95
4.1 Summary of Research.....	96
4.2 Future Work.....	100
4.2.1 Background of <i>bis</i> -Pentadienyl-Iron-Phosphine Complexes.....	100
4.3 Future Direction.....	103
4.4 References.....	106
Appendices.....	108
Appendix A: NMR Spectra of Neutral <i>bis</i> -Azapentadienyl-Ruthenium-Phosphine Complexes.....	108
Appendix B: NMR Spectra of Protonated <i>bis</i> -Azapentadienyl-Ruthenium-Phosphine Complexes.....	146
Appendix C: Selected IR/MS Spectra of <i>bis</i> -Azapentadienyl-Ruthenium-Phosphine Complexes.....	159
Appendix D: X-Ray Crystallographic Data for <i>bis</i> -Azapentadienyl-Ruthenium-Phosphine Complexes.....	166

List of Figures

Figure 1.1	Allyl Ligand.....	3
Figure 1.2	Potential allyl-metal boning modes.....	3
Figure 1.3	Potential bonding modes for cyclopentadienyl and pentadienyl ligands.....	4
Figure 1.4	Drawing of (η^5 -2,4-dimethylpentadienyl)Co(PEt ₃) ₂ (c).....	5
Figure 1.5	Initial 17 e ⁻ monomeric product of reaction of CoCl ₂ with 2 equivalents of 2,4-dimethylpentadienide.....	6
Figure 1.6	Drawing of the cobalt dimer synthesized from the reaction of CoCl ₂ with 2 equivalents of 2,4-dimethylpentadienide.....	6
Figure 2.1	(a) High resolution ESI mass spectrum of 1 ; (b) Experimental isotopic envelope for [M+H] ⁺ ; (c) Predicted isotopic envelope for [M+H] ⁺	27
Figure 2.2	Possible Structural Variants of [(1,2,3- η^3)-(5- <i>tert</i> -butylazapentadienyl)] ₂ RuLL' Complexes.....	29
Figure 2.3	Molecular structure of 2	33
Figure 2.4	Molecular structure of 4	37
Figure 2.5	Molecular structure of 5	40
Figure 2.6	Molecular structure of 7	45
Figure 2.7	Molecular structure of 8	47
Figure 3.1	Molecular structure of 12	79
Figure 3.2	Two possible resonance structures of 12	80
Figure 3.3	(a) $^{31}\text{P}\{\text{H}\}$ NMR of 15 at t = 0 h; (b) $^{31}\text{P}\{\text{H}\}$ NMR of 15 at t = 48 h.....	85

List of Schemes

Scheme 1.1	Synthesis of Ferrocene.....	2
Scheme 1.2	Synthesis of (<i>anti</i> - η^3 -2,4-dimethylpentadienyl)Co(PMe ₃) ₃ (a) and (<i>syn</i> - η^3 -2,4-dimethylpentadienyl)Co(PMe ₃) ₃ (b).....	5
Scheme 1.3	Reactions of (η^5 -pentadienyl)Ru(PPh ₃) ₂ Cl (d) with various phosphine ligands....	7
Scheme 1.4	Potential use of an (η^5 -heteropentadienyl)ML _n in a catalytic cycle.....	9
Scheme 1.5	Synthesis of the first azapentadienyl-metal complexes (η^5 -4-methyl-5-R-5-azapentadienyl)Mn(CO) ₃ (h) (R = i-Pr or t-Bu).....	10
Scheme 1.6	Synthesis of ((1,2,3- η^3)-4-methyl-5-isopropyl-5-azapentadienyl)Mo(Cp)(CO) ₂ (i) and its reaction with HBF ₄ ·OEt ₂	11
Scheme 1.7	Synthesis of potassium <i>tert</i> -butylazapentadienide.....	12
Scheme 1.8	Synthesis of <i>syn</i> - (l) and <i>anti</i> - (m) isomers of ((1,2,3- η^3)-5- <i>tert</i> -butyl-5-azapentadienyl)Ir(PMe ₃) ₃ and their reactions with triflic acid.....	13
Scheme 1.9	Synthesis of (η^5 -azapentadienyl)RuCp* complexes.....	14
Scheme 1.10	Summary of products from the reaction of $\frac{1}{4}$ (Cp*RuCl) ₄ with Me ₃ MCH(R1)C(R2)=C(R3)CH=NCMe ₃	15
Scheme 2.1	Synthesis of ((1,2,3- η^3)-5- <i>tert</i> -butylazapentadienyl)Co(PMe ₃) ₃ (c).....	20
Scheme 2.2	Synthesis of ((1,2,3- η^3)-5- <i>tert</i> -butylazapentadienyl)Rh(PMe ₃) ₂ and ((1,2,3- η^3)-5- <i>tert</i> -butylazapentadienyl)Rh(PMe ₃) ₃	21
Scheme 2.3	Synthesis of ((1,2,3- η^3)-5- <i>tert</i> -butylazapentadienyl)Ir(PEt ₃) ₂ and ((1,2,3- η^3)-5- <i>tert</i> -butylazapentadienyl)Ir(PEt ₃) ₃	22
Scheme 2.4	Synthesis of ((1,2,3- η^3 , 5- η^1)-5- <i>tert</i> -butylazapentadienyl)RuCl(PPh ₃) ₂ (l).....	23
Scheme 2.5	Synthesis of [1-3- η^3 , 5- η^1 -CH ₂ CHCHCHN(t-Bu)]RuCl(PPh ₃)(PPhH ₂).....	24
Scheme 2.6	Synthesis of [(1,2,3- η^3)-(5- <i>tert</i> -butylazapentadienyl)] ₂ Ru(PPh ₃) ₂ (1).....	26
Scheme 2.7	Proposed dissociative mechanism for synthesis of [(1,2,3- η^3)-(5- <i>tert</i> -butylazapentadienyl)] ₂ Ru(PPh ₃)(L).....	30

Scheme 2.8	Proposed associative mechanism for triphenylphosphine substitution.....	31
Scheme 2.9	Synthesis of [(1,2,3- η^3)-(5- <i>tert</i> -butylazapentadienyl)] ₂ Ru(PPh ₃)(PMe ₃) (2).....	32
Scheme 2.10	Proposed mechanism for the synthesis of [(1,2,3- η^3)-(5- <i>tert</i> -butylazapentadienyl)] ₂ Ru(dmpe).....	34
Scheme 2.11	Synthesis of [(1,2,3- η^3)-(5- <i>tert</i> -butylazapentadienyl)] ₂ Ru(PPh ₃)[P(OMe) ₃] (4).....	35
Scheme 2.12	Synthesis of [(1,2,3- η^3)-(5- <i>tert</i> -butylazapentadienyl)] ₂ Ru(PPh ₃)(CNCMe ₃) (5).....	38
Scheme 2.13	Mechanism for conversion of structure A to structure E	41
Scheme 2.14	Proposed mechanism for rearrangement of an azapentadienyl ligand on 5 from “mC3” to “bC3”.....	42
Scheme 2.15	Synthesis of [(1,2,3- η^3)-(5- <i>tert</i> -butylazapentadienyl)] ₂ Ru(PEt ₃) ₂ (8).....	43
Scheme 2.16	Synthesis of [(1,2,3- η^3)-(5- <i>tert</i> -butylazapentadienyl)] ₂ Ru(PMe ₃) ₂ (9).....	48
Scheme 2.17	Synthesis of 9 from Cl ₂ Ru(PMe ₃) ₄	49
Scheme 2.18	Proposed mechanism for conversion of structure A to structure E and structure D	51
Scheme 3.1	Potential protonation sites of azapentadienyl-ruthenium complexes.....	69
Scheme 3.2	Protonation of [(1,2,3- η^3)-5- <i>tert</i> -butylazapentadienyl]Co(PMe ₃) ₃	70
Scheme 3.3	Synthesis of (η^4 -(<i>tert</i> -butylammonium)butadiene)Co(PMe ₃) ₂ [P(OMe) ₃] ²⁺ (O ₃ SCF ₃ ⁻) ₂	70
Scheme 3.4	Protonation of ((1,2,3- η^3)-5- <i>tert</i> -butylazapentadienyl)Ir(PEt ₃) ₃	71
Scheme 3.5	Protonation of ((1,2,3- η^3)-5- <i>tert</i> -butylazapentadienyl)Ir(PEt ₃) ₂	72
Scheme 3.6	Protonation of ((1,2,3- η^3)-5- <i>tert</i> -butylazapentadienyl)Rh(PMe ₃) ₃	73
Scheme 3.7	Protonation of ((1,2,3- η^3)-5- <i>tert</i> -butylazapentadienyl)Rh(PMe ₃) ₂	74
Scheme 3.8	Synthesis of {[[(1,2,3- η^3)-(CH ₂ CHCHCH=NCH)(CMe ₃)] ₂ Ru(PEt ₃) ₂ } ²⁺ (O ₃ SCF ₃) ₂ (12).....	75

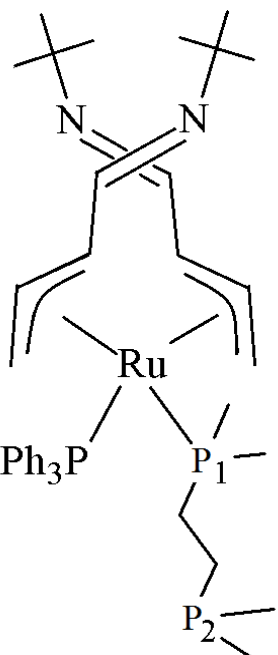
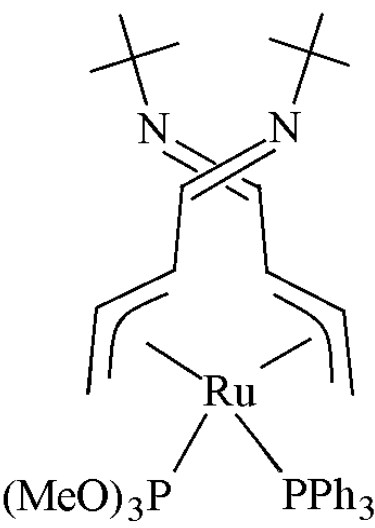
Scheme 3.9	Equilibrium of $[(1,2,3-\eta^3)-(5\text{-}tert\text{-}butylazapentadienyl})_2\text{Ru}(\text{PEt}_3)_2$ (8) and its mono- and di- protonated analogues.....	76
Scheme 3.10	Possible mechanism for conversion of 8 to 12	78
Scheme 3.11	Synthesis of $\{[(1,2,3-\eta^3)\text{-(CH}_2\text{CHCHCH=NC)}(\text{CMe}_3)]_2\text{Ru}(\text{PMe}_3)_2\}^{2+}$ $(\text{O}_3\text{SCF}_3)_2$ (13).....	81
Scheme 3.12	Synthesis of $\{[(1,2,3-\eta^3)\text{-(CH}_2\text{CHCHCH=NC)}(\text{CMe}_3)]_2\text{Ru}[\text{P}(\text{OMe})_3]_2\}^{2+}$ $(\text{O}_3\text{SCF}_3)_2$ (14).....	83
Scheme 4.1	Summary of the synthesis of 2 – 8	97
Scheme 4.2	Summary of the synthesis of 9 – 11	98
Scheme 4.3	Summary of protonation reactions of 8 – 10	100
Scheme 4.4	Synthesis of $(\eta^5\text{-pentadienyl})(\eta^3\text{-pentadienyl})\text{Fe}(\text{PR}_3)$ Complexes.....	101
Scheme 4.5	Protonation reactions of $(\eta^5\text{-pentadienyl})(\eta^3\text{-pentadienyl})\text{Fe}(\text{PEt}_3)$	102
Scheme 4.6	Proposed synthetic route of $(\eta^5\text{-}tert\text{-butylazapentadienyl})(\eta^3\text{-}tert\text{-butylazapentadienyl})\text{Fe}(\text{PEt}_3)$ (e).....	104
Scheme 4.7	Proposed synthetic route of $[(1,2,3-\eta^3, 5\text{-}\eta^1)\text{-}5\text{-}tert\text{-butylazapentadienyl}]\text{Fe}(\text{PMe}_3)_3]^+(\text{OTf})$ (f).....	105

List of Tables

Table 2.1	Cone angles of selected phosphine ligands.....	44
------------------	--	----

List of Compounds

Number	Compound Name	Structure	Page
1	[(1,2,3- η^3)-(5- <i>tert</i> -butylazapentadienyl)] ₂ Ru(PPh ₃) ₂		25
2	[(1,2,3- η^3)-(5- <i>tert</i> -butylazapentadienyl)] ₂ Ru(PPh ₃)(PMe ₃)		31

3	<p>$[(1,2,3-\eta^3)-(5\text{-}tert\text{-}butylazapentadienyl)]_2\text{Ru}$</p> <p>$(\text{PPh}_3)(\text{dmpe})$</p>		34
4	<p>$[(1,2,3-\eta^3)-(5\text{-}tert\text{-}butylazapentadienyl)]_2\text{Ru}$</p> <p>$(\text{PPh}_3)[\text{P}(\text{OMe})_3]$</p>		35

5	<p>$[(1,2,3\text{-}\eta^3)\text{-}(5\text{-}tert\text{-}butylazapentadienyl)}]_2\text{Ru}$</p> <p>$(\text{PPh}_3)(\text{CNCMe}_3)$</p>		38
6	<p>$[(1,2,3\text{-}\eta^3)\text{-}(5\text{-}tert\text{-}butylazapentadienyl)}]_2\text{Ru}$</p> <p>$(\text{PPh}_3)(\text{CO})$</p>		42

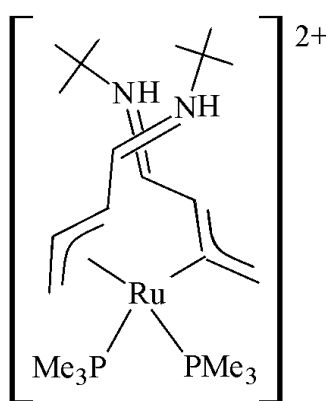
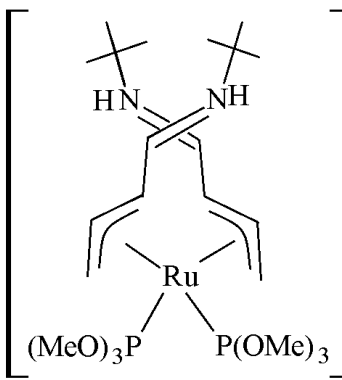
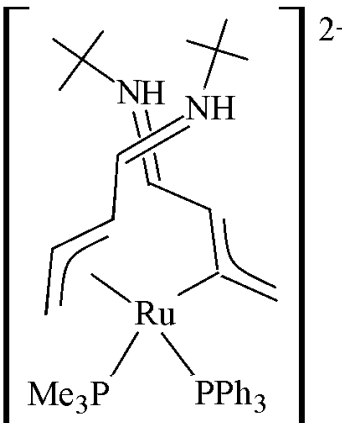
*Proposed structure

7	<p>$[(1,2,3-\eta^3)-(5\text{-}tert\text{-}butylazapentadienyl)]_2\text{Ru}$</p> <p>$(\text{PPh}_3)(\text{PEt}_3)$</p>		43
8	<p>$[(1,2,3-\eta^3)-(5\text{-}tert\text{-}butylazapentadienyl)]_2\text{Ru}(\text{PEt}_3)_2$</p>		43

<p>9a</p> <p>$[(1,2,3\text{-}\eta^3)\text{-}(5\text{-}tert\text{-}butylazapentadienyl})_2\text{Ru}(\text{PMe}_3)_2]$</p>		<p>48</p>
<p>9b</p> <p>$[(1,2,3\text{-}\eta^3)\text{-}(5\text{-}tert\text{-}butylazapentadienyl})_2\text{Ru}(\text{PMe}_3)_2]$</p>		<p>48</p>

10a	<p>$[(1,2,3-\eta^3)-(5\text{-}tert\text{-}butylazapentadienyl)]_2\text{Ru}$</p> <p>$[\text{P}(\text{OMe})_3]_2$</p>		52
10b	<p>$[(1,2,3-\eta^3)-(5\text{-}tert\text{-}butylazapentadienyl)]_2\text{Ru}$</p> <p>$[\text{P}(\text{OMe})_3]_2$</p>		52

11a	$[(1,2,3-\eta^3)-(5\text{-}tert\text{-}butylazapentadienyl)]_2\text{Ru}(\text{dmpe})$	 <small>*Proposed structure</small>	53
12	$\{[(1,2,3-\eta^3)-$ $(\text{CH}_2\text{CHCHCH}=\text{NH(CMe}_3)]_2\text{Ru}$ $(\text{PEt}_3)_2\}^{2+}(\text{O}_3\text{SCF}_3)_2$		75

13	$\{[(1,2,3-\eta^3)-$ $(\text{CH}_2\text{CHCHCH}=\text{NH}(\text{CMe}_3)]_2\text{Ru}$ $(\text{PMe}_3)_2\}^{2+}(\text{O}_3\text{SCF}_3)_2$		81
14	$\{[(1,2,3-\eta^3)-$ $(\text{CH}_2\text{CHCHCH}=\text{NH}(\text{CMe}_3)]_2\text{Ru}$ $[\text{P}(\text{OMe})_3]_2\}^{2+}(\text{O}_3\text{SCF}_3)_2$		82
15	$\{[(1,2,3-\eta^3)-$ $(\text{CH}_2\text{CHCHCH}=\text{NH}(\text{CMe}_3)]_2\text{Ru}$ $(\text{PPh}_3)(\text{PMe}_3)\}^{2+}(\text{O}_3\text{SCF}_3)_2$		84

*proposed structure

ACKNOWLEDGMENTS

There are many people I would like to thank for helping me complete my doctorate. Without you, this could not have been possible. I would like to thank my advisor, Dr. John R. Bleeke, for his guidance and mentoring during my graduate school career. The feedback and advice given during our weekly meetings was invaluable and kept me motivated throughout the past six years. I would also like to thank my graduate committee, Dr. Bill Burho and Dr. Liviu Mirica, for their guidance.

I appreciate the financial support provided by the Chemistry Department, as well as the Graduate School of Arts and Sciences for awarding me the Dean's Dissertation Fellowship. I would also like to thank Dr. Steve Kinsley for always taking me on as a TA and providing me with valuable chemistry and life lessons.

I would like to thank my fellow lab mates, Dr. Bryn Lutes and Dr. Wipark Anutrasakda for their contributions and advice during the research process. Finally I would like to thank my family and friends, in particular my parents, Michael and Lauren Stouffer, and my fiancé, Dr. Josh Lasinski, for their love and support.

Meghan Leigh Stouffer

*Washington University in St. Louis
March 2015*

ABSTRACT OF DISSERTATION

Synthesis, Structure, Spectroscopy, and Reactivity of Azapentadienyl-Ruthenium-Phosphine
Complexes

by

Meghan Stouffer

Doctor of Philosophy in Chemistry

Washington University in St. Louis, 2015

Professor John R. Bleeke, Chair

This dissertation focuses on the systematic synthesis of *bis*-azapentadienyl-ruthenium-phosphine complexes. The synthetic approach involves the treatment of $\text{Cl}_2\text{Ru}(\text{PPh}_3)_3$ with potassium *tert*-butylazapentadienide reagent. The reactivity of this parent compound with other $2e^-$ donor ligands is investigated. These resultant complexes' reactivity with triflic acid is also studied.

Treatment of $\text{Cl}_2\text{Ru}(\text{PPh}_3)_3$ with potassium *tert*-butylazapentadienide produces $[(1,2,3-\eta^3)-5\text{-}tert\text{-butylazapentadienyl}]_2\text{Ru}(\text{PPh}_3)_2$ (**1**). Compound **1** undergoes single substitution of one of the triphenylphosphines when treated with PMe_3 , dmpe, $\text{P}(\text{OMe})_3$, CNCMe_3 , CO, and PEt_3 at room temperature, resulting in $[(1,2,3-\eta^3)-5\text{-}tert\text{-butylazapentadienyl}]_2\text{Ru}(\text{PPh}_3)(\text{L})$ (**2**, $\text{L} = \text{PMe}_3$; **3**, $\text{L} = \text{dmpe}$; **4**, $\text{L} = \text{P}(\text{OMe})_3$; **5**, $\text{L} = \text{CNCMe}_3$; **6**, $\text{L} = \text{CO}$; **7**, $\text{L} = \text{PEt}_3$). By increasing the reaction time of **1** with PEt_3 , double substitution of both triphenylphosphines occurs, resulting in $[(1,2,3-\eta^3)-5\text{-}tert\text{-butylazapentadienyl}]_2\text{Ru}(\text{PEt}_3)_2$ (**8**). Compounds **1 – 8** possess a pseudo-octahedral geometry where both ancillary ligands sit *trans* to the C3's of the azapentadienyl ligands. Compounds **1 – 4**, **7** and **8** exhibit a ligand orientation in which both ancillary ligands

sit in the mouth of each azapentadienyl ligand, denoted as mC3/mC3. In contrast, **5** exhibits a ligand arrangement where the PPh₃ sits in the mouth of one azapentadienyl ligand while CNCMe₃ sits on the backbone of the other azapentadienyl ligand.

Other double substitution reactions occur when **1** is treated with PMe₃, P(OMe)₃, and dmpe in THF *at reflux*, resulting in [(1,2,3- η^3)-5-*tert*-butylazapentadienyl]₂Ru(L)_x (**9**, L = PMe₃, x = 2; **10**, L = P(OMe)₃, x = 2; **11**, L = dmpe, x = 1). Compounds **9** and **10** exist in solution as an equilibrium mixture of two structural isomers. The two isomers in solution have either a mC3/mC3 or mC3/bC1 ligand orientation.

Treatment of **8**, **9** and **10** with triflic acid results in dicationic products, {[(1,2,3- η^3)-(CH₂CHCHCH=N(H)(CMe₃)]₂Ru(L)₂}²⁺(O₃SCF₃)₂ (**12**, L = PEt₃; **13**, L = PMe₃; **14**, L = P(OMe)₃), in which *both* azapentadienyl nitrogen atoms have been protonated. The protonated product, **12**, shows a ligand conversion from mC3/mC3 (seen in **8**) to mC3/bC3. Upon protonation, **9** and **10** each convert to a single isomer, **12** and **13**, respectively. Like **12**, compound **13** possesses a mC3/bC3 orientation while **14** has a ligand orientation in which the azapentadienyl ligands appear to be mC3/mC3. Treatment of **2**, **4** and **5** with triflic acid results in multiple isomers of the diprotonated {[(1,2,3- η^3)-CH₂CHCHCH=N(H)(CMe₃)]₂Ru(PPh₃)(L)}²⁺(O₃SCF₃)₂ (**15**, L = PMe₃; **16**, L = P(OMe)₃; **17**, L = CNCMe₃). All of the compounds have been characterized, in part, by NMR spectroscopy, and the structures of **2**, **4**, **5**, **7**, **8**, and **12** have been confirmed by single-crystal X-ray diffraction.

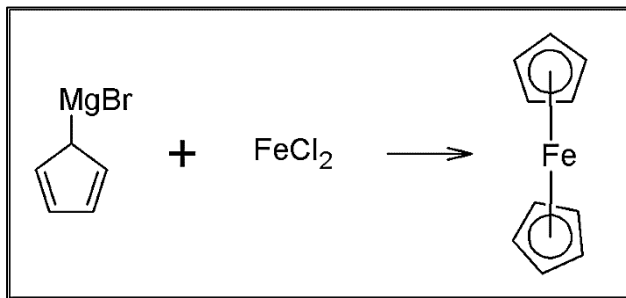
Chapter 1

Introduction

Introduction

1.1 Allyl-, Cyclopentadienyl-, and Pentadienyl-Transition Metal Complexes

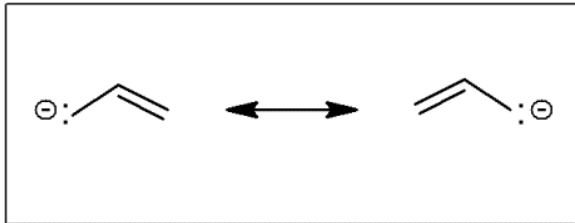
Metal complexes containing the open pentadienyl ligand were first synthesized in the 1980's.¹ Two closely related compound classes, which preceded open pentadienyl-metal complexes, are closed pentadienyl-metal complexes and allyl-metal complexes. The closed pentadienyl (cyclopentadienyl) or “Cp” ligand is a stabilizing ligand most commonly found in “sandwich” complexes such as ferrocene. Ferrocene is a stable metal complex, first synthesized from the Grignard reagent cyclopentadienyl magnesium bromide and iron(II) chloride in 1951 by Pauson and Kealy², as shown in Scheme 1.1. Because of the stability of the cyclopentadienyl ligand³,



Scheme 1.1: Synthesis of Ferrocene

even at elevated temperatures, this “sandwich” metal complex has limited catalytic ability. Other stable Cp-metal complexes such as zirconocene dichloride show more catalytic ability than ferrocene⁴, but typically require the addition of activating agents.

The allyl ligand has formula $\text{H}_2\text{CCHCH}_2^-$. There are two equivalent resonance structures



Figures 1.1: Allyl Ligand.

where the negative charge can reside on either terminal carbon, as shown in Figure 1.1. Allyl-transition metal complexes have been greatly explored, but are generally not as stable as their Cp analogs. When reacted with a metal center, the allyl ligand usually coordinates through all three carbons, producing an η^3 bonding mode. But because the allyl ligand has the ability to shift between bonding modes, allyl-metal complexes exhibit enhanced reactivity, both stoichiometric and catalytic. As shown in Figure 1.2, the allyl ligand can shift between an η^3 bonding mode and an η^1 bonding mode, opening up a coordination site in the process.

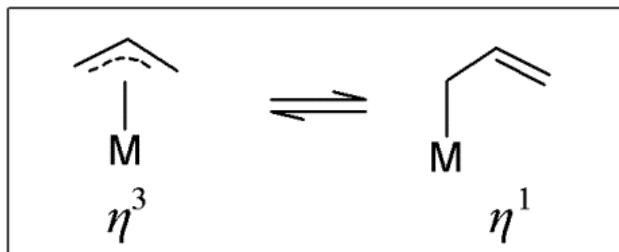


Figure 1.2: Potential allyl-metal bonding modes.

Growing out of cyclopentadienyl- and allyl- transition metal chemistry is open pentadienyl-metal chemistry. These complexes have gained attention because of their potential use as catalysts. The open pentadienyl ligand can form stable bonds to the metal center, like Cp, while maintaining the ability to shift bonding modes, like an allyl ligand. In addition, pentadienyl ligands possess more bonding modes than the three carbon allyl. Figure 1.3 shows the comparison of cyclopentadienyl and pentadienyl ligand bonding modes.

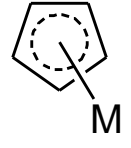
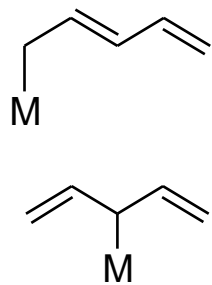
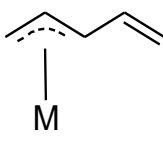
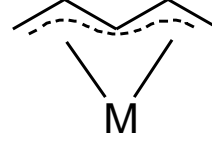
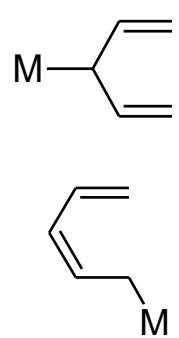
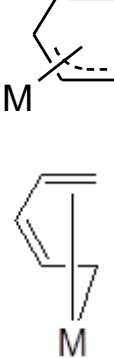
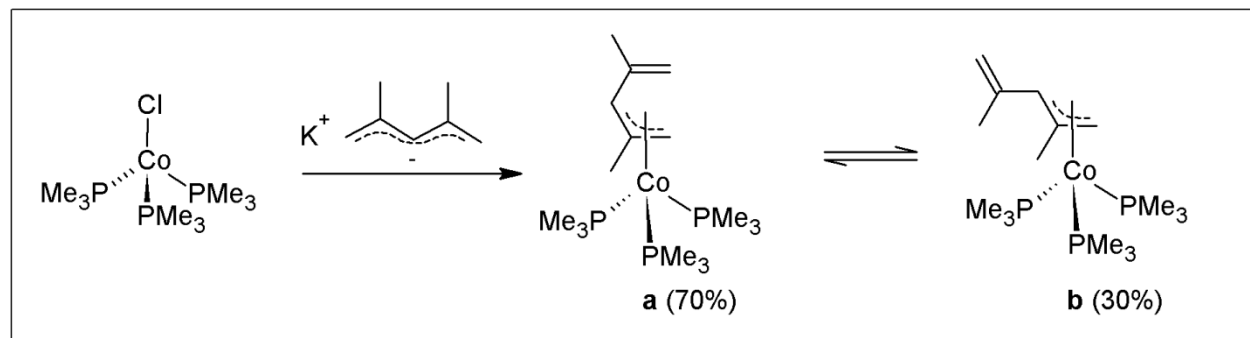
Ligand	η^1	η^3	η^5
Cyclopentadienyl			
Pentadienyl (W-Shaped)			
Pentadienyl (U-Shaped)			

Figure 1.3: Potential bonding modes for cyclopentadienyl and pentadienyl ligands.

Because of the thermal stability and the ability of the pentadienyl ligand to shift between η^5 , η^3 , and η^1 bonding modes, our research group has been interested in studying the synthesis and reactivity of electron-rich pentadienyl-metal complexes.

1.2 Pentadienyl Complexes of Cobalt

Pentadienyl-cobalt complexes were first explored in the Bleeeke group in 1984.⁵ These complexes were synthesized from the reaction of $(Cl)Co(PMe_3)_3$ with potassium 2,4-dimethylpentadienide which resulted in an 18 e^- complex, $(anti\text{-}\eta^3\text{-}2,4\text{-dimethylpentadienyl})Co(PMe_3)_3$, **a**. In solution, the *anti*- isomer, **a**, was in equilibrium with the *syn*- isomer, **b**, in a 70:30 ratio (shown in Scheme 1.2).



Scheme 1.2: Synthesis of $(anti\text{-}\eta^3\text{-}2,4\text{-dimethylpentadienyl})Co(PMe_3)_3$ (**a**) and $(syn\text{-}\eta^3\text{-}2,4\text{-dimethylpentadienyl})Co(PMe_3)_3$ (**b**).

Further reactions involving larger phosphine ligands were carried out. For example, treatment of $CoCl_2$ with 2 equivalents of PEt_3 , followed by potassium 2,4-dimethylpentadienide in the presence of a reducing agent led to $(\eta^5\text{-}2,4\text{-dimethylpentadienyl})Co(PEt_3)_2$ (**c**).⁵

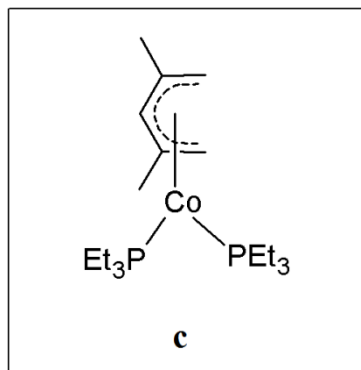


Figure 1.4: Drawing of $(\eta^5\text{-}2,4\text{-dimethylpentadienyl})Co(PEt_3)_2$ (**c**).

When Ernst et. al⁶ treated CoCl_2 with two equivalents of potassium 2,4-dimethylpentadienide without the addition of an ancillary ligand, a dimeric product, $[\text{Co}(\text{C}_7\text{H}_{11})_2]_2$, was obtained (Figure 1.6). The initial monomeric product was a $17e^-$ complex containing two pentadienyl ligands in the η^3 - and η^5 - orientations (see Figure 1.5). Because the monomeric product was

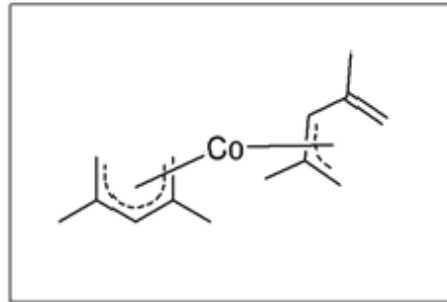


Figure 1.5: Initial $17 e^-$ monomeric product of reaction of CoCl_2 with 2 equivalents of 2,4-dimethylpentadienide.

unstable, it dimerized, resulting in each Co being bonded to an η^5 -2,4-dimethylpentadienyl ligand and to an η^4 -butadiene moiety of half of the dimerized ligand. This allowed for each cobalt metal center to attain an $18e^-$ configuration.

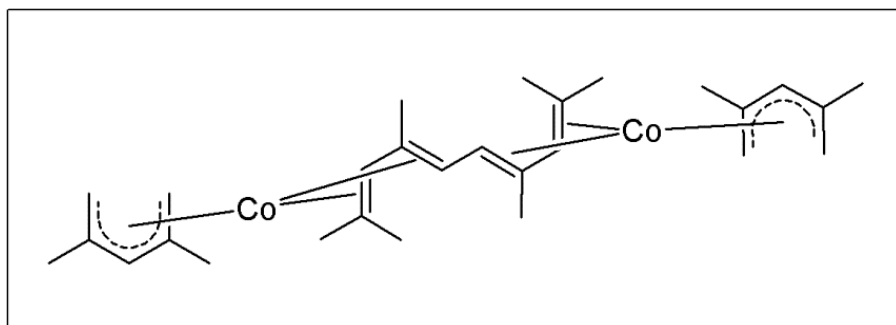
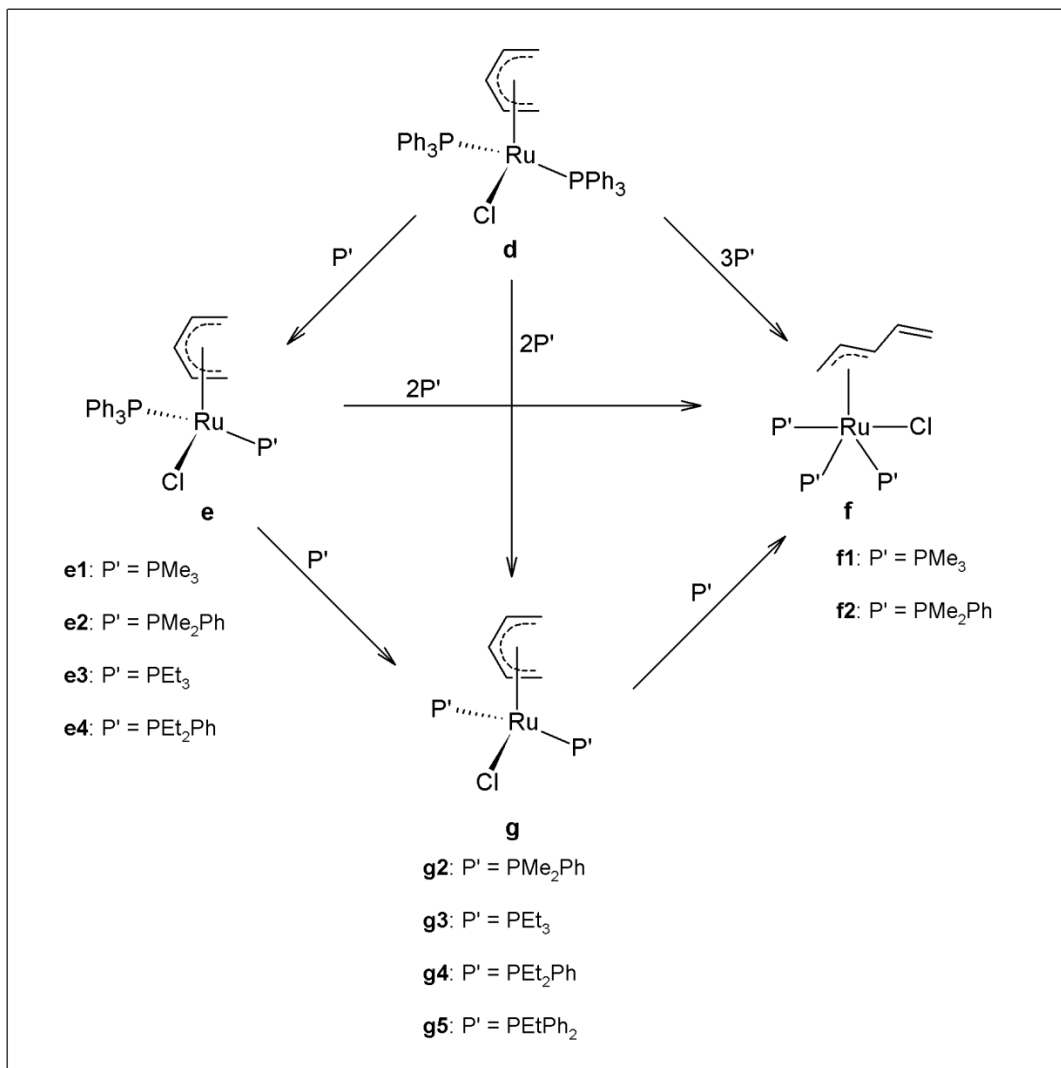


Figure 1.6: Drawing of the cobalt dimer synthesized from the reaction of CoCl_2 with 2 equivalents of 2,4-dimethylpentadienide.

1.3 Pentadienyl Complexes of Ruthenium

Because of the success of the previously synthesized precursor, (η^5 -cyclopentadienyl)RuCl(PPh_3)₂, in forming a large family of cyclopentadienyl-ruthenium-phosphine complexes⁷, the Bleke lab became interested in the open pentadienyl analogue. Treatment of RuCl₂(PPh_3)₃ with pentadienyltributyltin produced the desired (η^5 -pentadienyl)RuCl(PPh_3)₂.⁸ This η^5 product served as a starting material to explore further reactivity with phosphines as shown in Scheme 1.3.



Scheme 1.3: Reactions of (η^5 -pentadienyl)Ru(PPh_3)₂Cl (**d**) with various phosphine ligands.

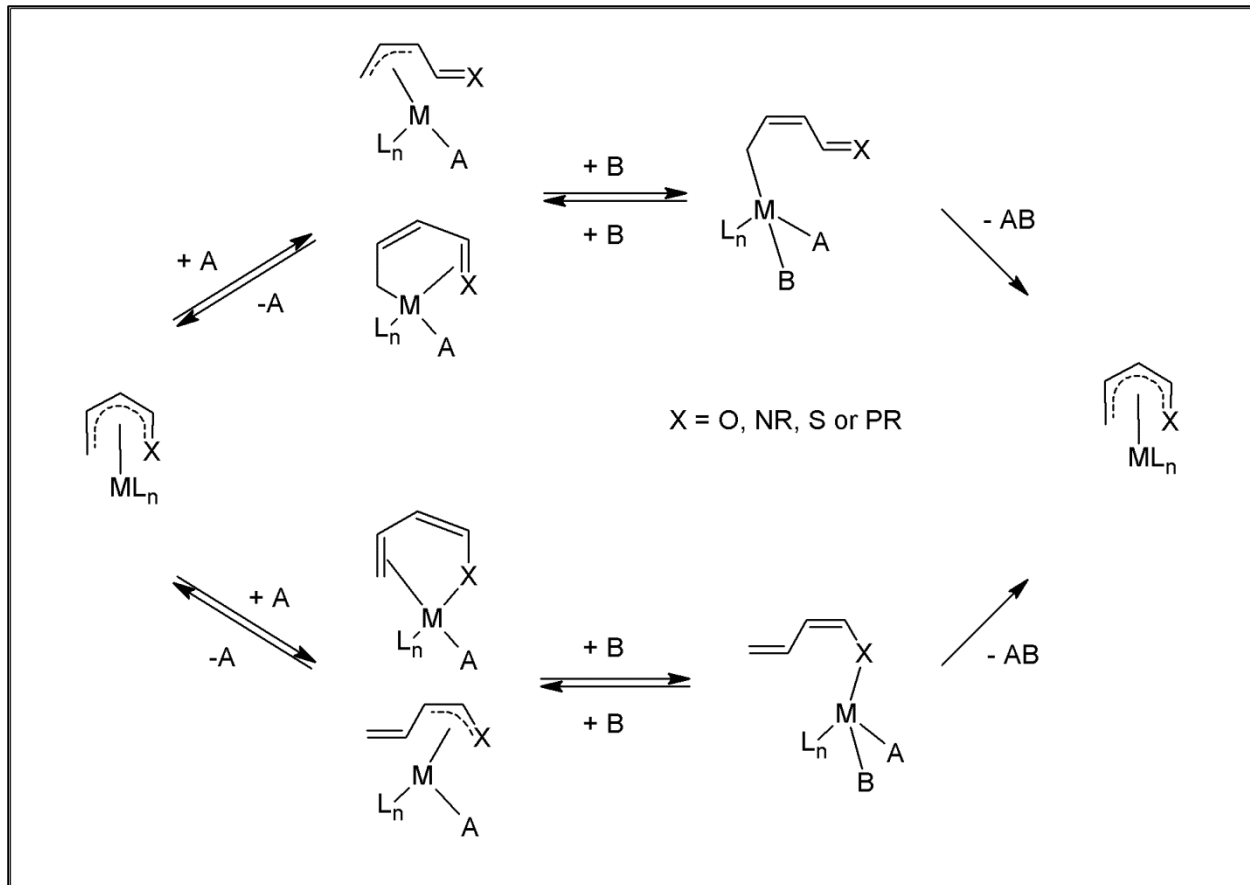
In order to promote bonding mode shifts in the pentadienyl-ruthenium system, compound **d** was reacted with phosphine ligands of various sizes. The addition of one equivalent of PMe_3 led to **e**, where a substitution of one of the PPh_3 was seen. This was most likely accomplished via an associative mechanism. The η^5 -pentadienyl ligand slipped to an η^3 bonding mode because of the bulkiness of the PPh_3 ligands. This opened up a coordination site and allowed for the coordination of the smaller PMe_3 . A bonding mode shift back to η^5 allowed for dissociation of the PPh_3 . When multiple equivalents of PMe_3 were added to **d**, a bonding mode shift to η^3 with the coordination of three small PMe_3 's was seen. This reaction probably proceeded by the same associative mechanism described above. Three PMe_3 were able to coordinate because of the ligand's small size. Treatment of **d** with larger phosphines, regardless of equivalents, did not result in a bonding mode shift.

1.4 Heteropentadienyl-Transition Metal Complexes

Growing out of pentadienyl chemistry is heteropentadienyl chemistry. A heteropentadienyl ligand has one carbon of the pentadienyl ligand replaced by a heteroatom such as oxygen, nitrogen, sulfur, or phosphorus in the terminal position. These ligands maintain thermal stability, like their all carbon analogues, while displaying enhanced reactivity. Heteropentadienyl-metal complexes can undergo reactions at the metal center because of the heteropentadienyl ligand's ability to shift between bonding modes, opening and closing coordination sites. In addition to metal center reactions such as ligand addition and oxidative addition, reactions with simple electrophiles can occur directly on the heteropentadienyl ligand, which can lead to a change in the heteropentadienyl ligand's interaction with the metal center.

These heteropentadienyl complexes have the potential to be used in catalytic cycles.⁹ A *mono-* η^5 complex is preferred for reaction with a small two e⁻ donor ligand, A. The addition of

A, (see Scheme 1.4) allows for the heteropentadienyl to shift from an η^5 to an η^3 bonding mode. The coordination of a second small ligand, B, would promote another bonding mode shift to η^1 . Ligands A and B can then reductively eliminate, allowing the heteropentadienyl ligand to shift back to η^5 , restarting the cycle.



Scheme 1.4: Potential use of an (η^5 -heteropentadienyl) ML_n in a catalytic cycle.

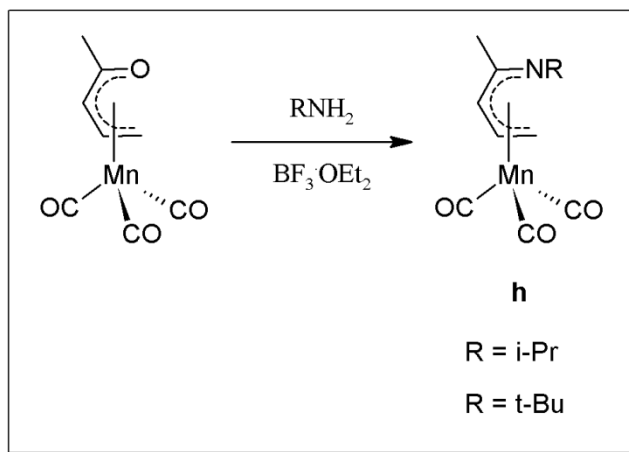
With catalytic cycles like these in mind, the Bleeeke group has methodically explored heteropentadienyl chemistry, including oxapentadienyl¹⁰⁻¹², thiapentadienyl¹³⁻¹⁷, azapentadienyl¹⁸⁻²⁰, phosphapentadienyl²¹⁻²² and silapentadienyl²³⁻²⁴ metal complexes, with late transitions metals, such as Co, Rh, Ir, Fe, and Ru. The Bleeeke group⁹ as well as the Paz-

Sandoval group²⁵ have reported heteropentadienyl-transition metal complexes made from a tin derivative as well as from anionic metal salt derivatives.

1.5 Azapentadienyl-Transition Metal Complexes

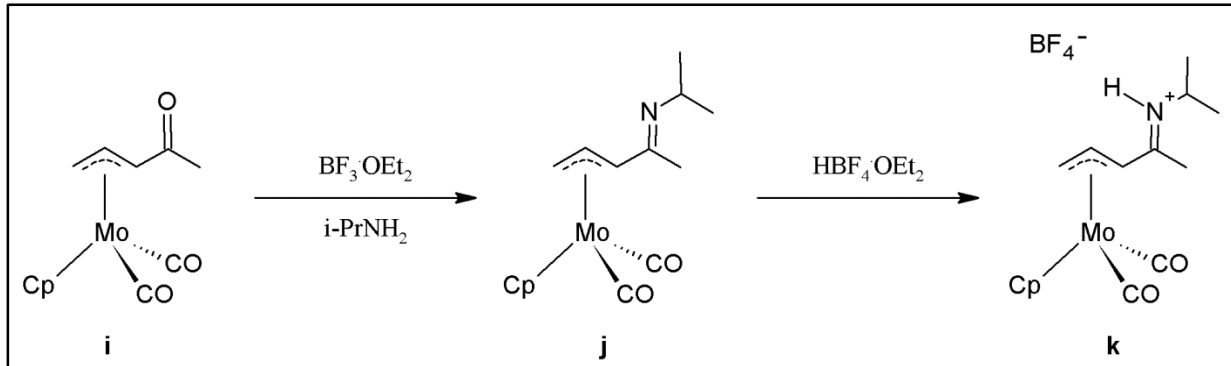
1.5.1 Azapentadienyl-Metal Complexes from Oxpentadienyl-Metal Precursors

The first azapentadienyl-metal complex was prepared from oxpentadienyl-metal precursors by Liu in 1990.²⁶ Treatment of $(\eta^5\text{-4-methyl-5-oxapentadienyl})\text{Mn}(\text{CO})_3$ with $\text{BF}_3\cdot\text{OEt}_2$, followed by addition of RNH_2 ($\text{R} = \text{i-Pr, t-Bu}$) generated $(\eta^5\text{-4-methyl-5-R-5-azapentadienyl})\text{Mn}(\text{CO})_3$, **h**, as seen in Scheme 1.5. The mechanism for this conversion is unknown but probably involved a nucleophilic attack of the amine directly on C4 in either the η^5 or η^3 bonding mode. Liu found that $(\eta^5\text{-4-methyl-5-oxapentadienyl})\text{Mn}(\text{CO})_3$ was reactive towards phosphine at the manganese metal center while $(\eta^5\text{-4-methyl-5-R-5-azapentadienyl})\text{Mn}(\text{CO})_3$ was not. This lack of reactivity suggested stronger bonding of the C=NR moiety to the metal center as compared to the C=O in the starting material. This increased bond strength made an η^5 to η^3 shift less likely.



Scheme 1.5: Synthesis of the first azapentadienyl-metal complexes $(\eta^5\text{-4-methyl-5-R-5-azapentadienyl})\text{Mn}(\text{CO})_3$ (**h**) ($\text{R} = \text{i-Pr}$ or t-Bu).

Similarly, Liu showed that treatment of ((1,2,3- η^3)-4-methyl-5-oxapentadienyl)Mo(Cp)(CO)₂ with BF₃·OEt₂ and i-PrNH₂ resulted in the production of ((1,2,3- η^3)-4-methyl-5-i-Pr-5-azapentadienyl)Mo(Cp)(CO)₂²⁷, (**j**). The *syn* configuration of oxapentadienyl starting material, **i**, was retained in the azapentadienyl product (see Scheme 1.6).

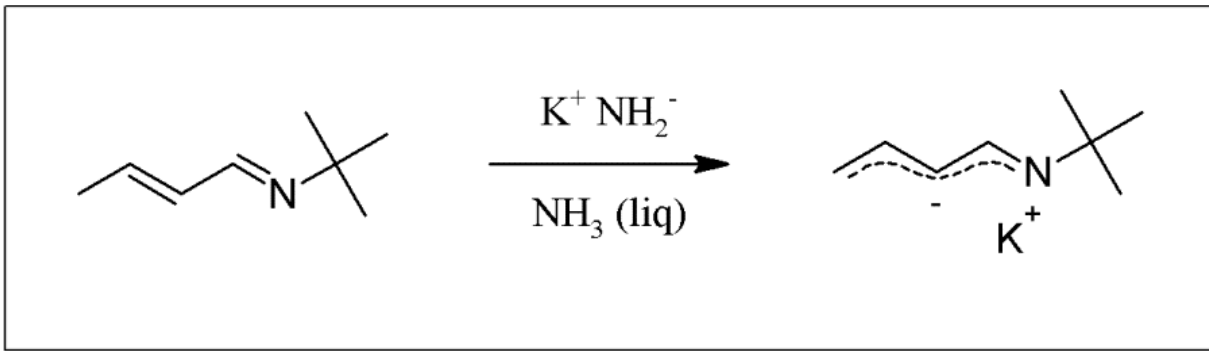


Scheme 1.6: Synthesis of ((1,2,3- η^3)-4-methyl-5-isopropyl-5-azapentadienyl)Mo(Cp)(CO)₂ (**i**) and its reaction with HBF₄·OEt₂.

Upon treatment of **j** with H⁺ from HBF₄·OEt₂, protonation at the nitrogen center was seen and the *syn*- η^3 orientation was maintained.

1.5.2 Azapentadienyl-Metal Complexes from Potassium Azapentadienide Reagents and Metal Halides

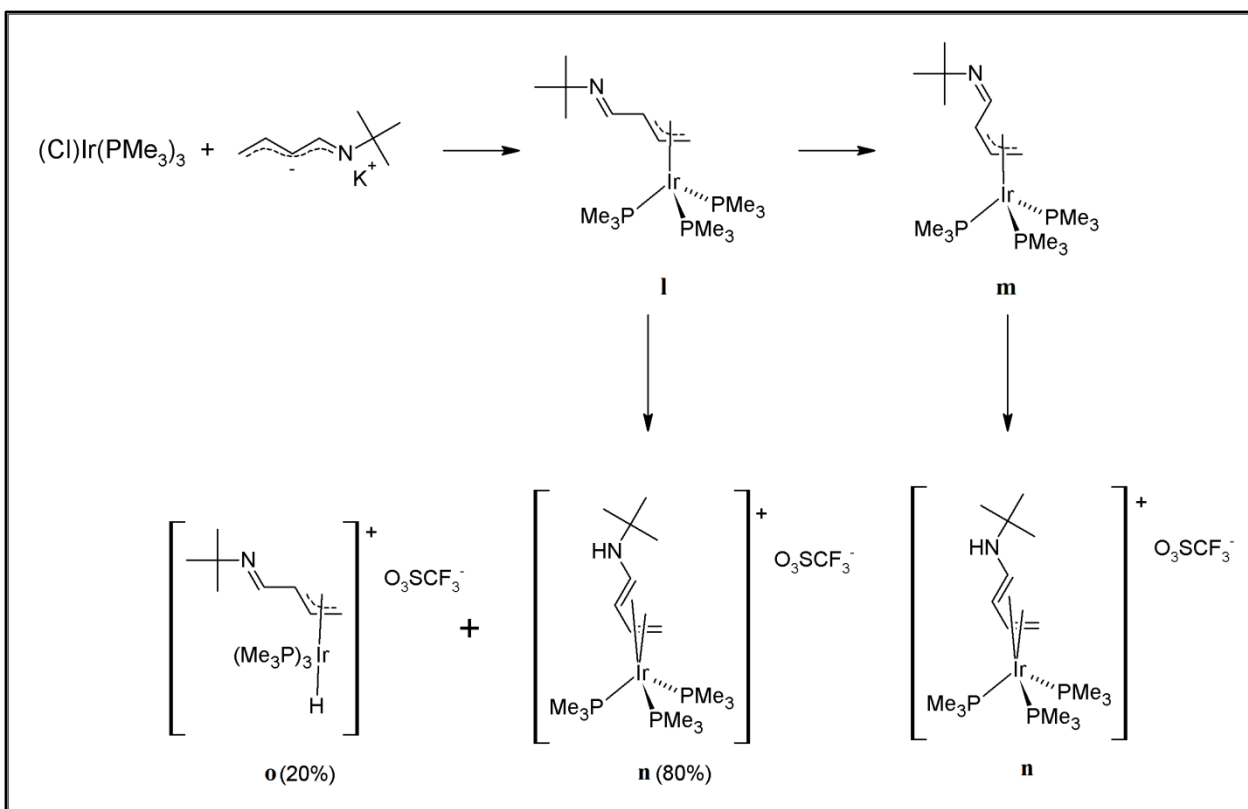
In 1993, the Bleke group started to study azapentadienyl-metal chemistry. By reacting *tert*-butyl azapentadiene with potassium amide in liquid ammonia, potassium *tert*-butylazapentadienide was synthesized and isolated (see Scheme 1.7).²⁰



Scheme 1.7: Synthesis of potassium *tert*-butylazapentadienide.

The NMR spectrum of this salt was identical to the lithium analogue reported by Würthwein,²⁸ and was consistent with a W-shaped, *E-E* isomer.

The reaction of (Cl)Ir(PMe₃)₃ with potassium *tert*-butylazapentadienide resulted in the synthesis of (*syn*-(1,2,3- η)-5-*tert*-butyl-5-azapentadienyl)Ir(PMe₃)₃ (**I**).²⁰ In this reaction, initial nucleophilic attack occurred from the carbon end of the *tert*-butylazapentadienide reagent which differed from the analogous reaction involving oxapentadienide in which the initial attack occurred from the oxygen. This change of reaction site was most likely due to the bulkiness of the t-butyl group on the nitrogen atom, as opposed to a decrease in nucleophilicity of the heteroatom. As seen in Scheme 1.8, there was a slow conversion of (*syn*-(1,2,3- η^3)-5-*tert*-butyl-5-azapentadienyl)Ir(PMe₃)₃ (**I**) to the *anti*- conformer (**m**). This was likely due to resonance stabilization provided by the η^4 -*s-cis* butadiene resonance structure, in which the formal negative charge resided on the most electronegative atom, N, while the formal positive charge was on the iridium metal center and could be neutralized by the PMe₃ ligands.

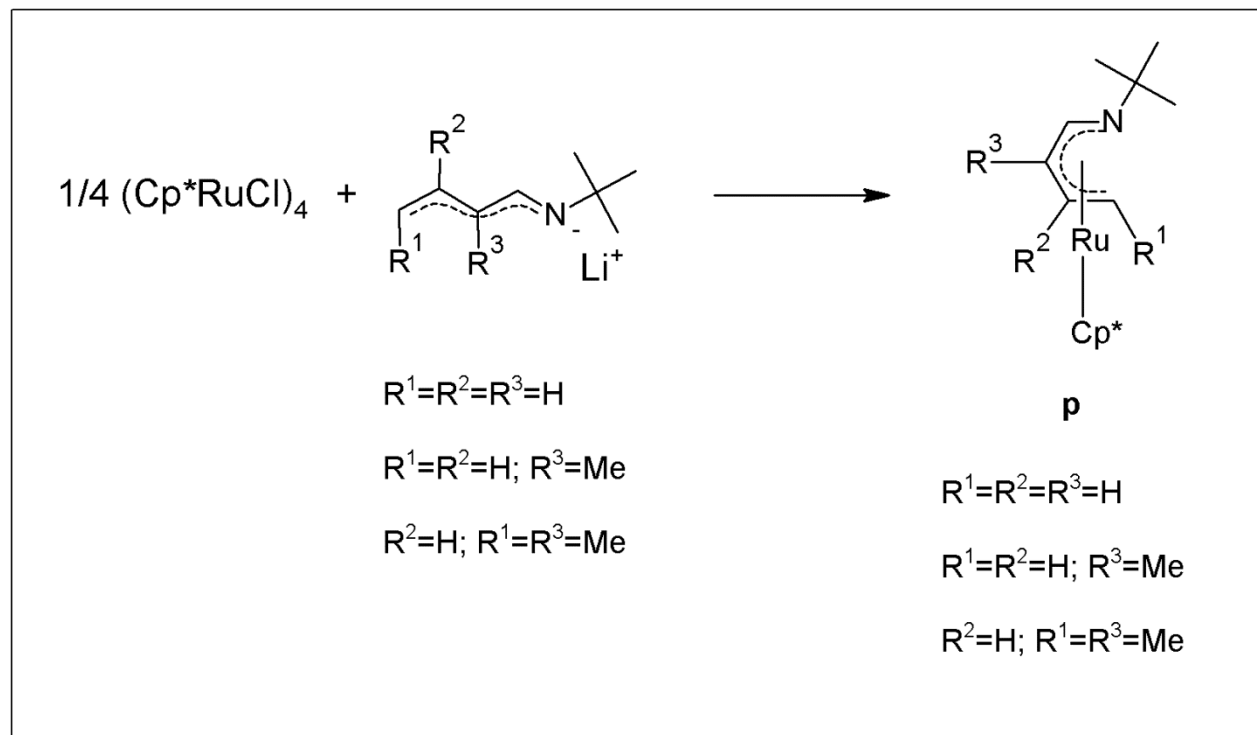


Scheme 1.8: Synthesis of *syn*- (**I**) and *anti*- (**m**) isomers of $((1,2,3-\eta^3)-5\text{-}tert\text{-}butyl\text{-}5\text{-}azapentadienyl)Ir(PMe_3)_3$ and their reactions with triflic acid.

Treatment of $(syn\text{-}(1,2,3-\eta^3)\text{-}5\text{-}tert\text{-}butyl\text{-}5\text{-}azapentadienyl)Ir(PMe_3)_3$ (**I**) with one equivalent of triflic acid, resulted in a mixture of products. The major product, $\eta^4\text{-}(tert\text{-}butylamino)butadiene$ complex (**n**), was seen as 80% of the yield while the minor product, the corresponding iridium hydride complex (**o**), was generated in 20% yield. When the *anti*- isomer, **m** was protonated, only one product ($\eta^4\text{-}(tert\text{-}butylamino)butadiene$ complex) was observed. Upon addition of another equivalent of triflic acid, a second protonation occurred at the nitrogen center, regardless of the η^4 or η^3 -hydride bonding mode.

1.5.3 Half-Open Azapentadienyl-Ruthenium Complexes from Anionic Azapentadienide or Group 14 Enimine

In 1999, Paz-Sandoval and Ernst reported a series of “half open ruthenocenes” containing *tert*-butylazapentadienyl and pentamethylcyclopentadienyl ligands.²⁹ This series of complexes was synthesized by reacting $(Cp^*RuCl)_4$ with lithium *t*-butylazapentadienide reagents, as shown in Scheme 1.9. Compound **p** produced the first x-ray structure

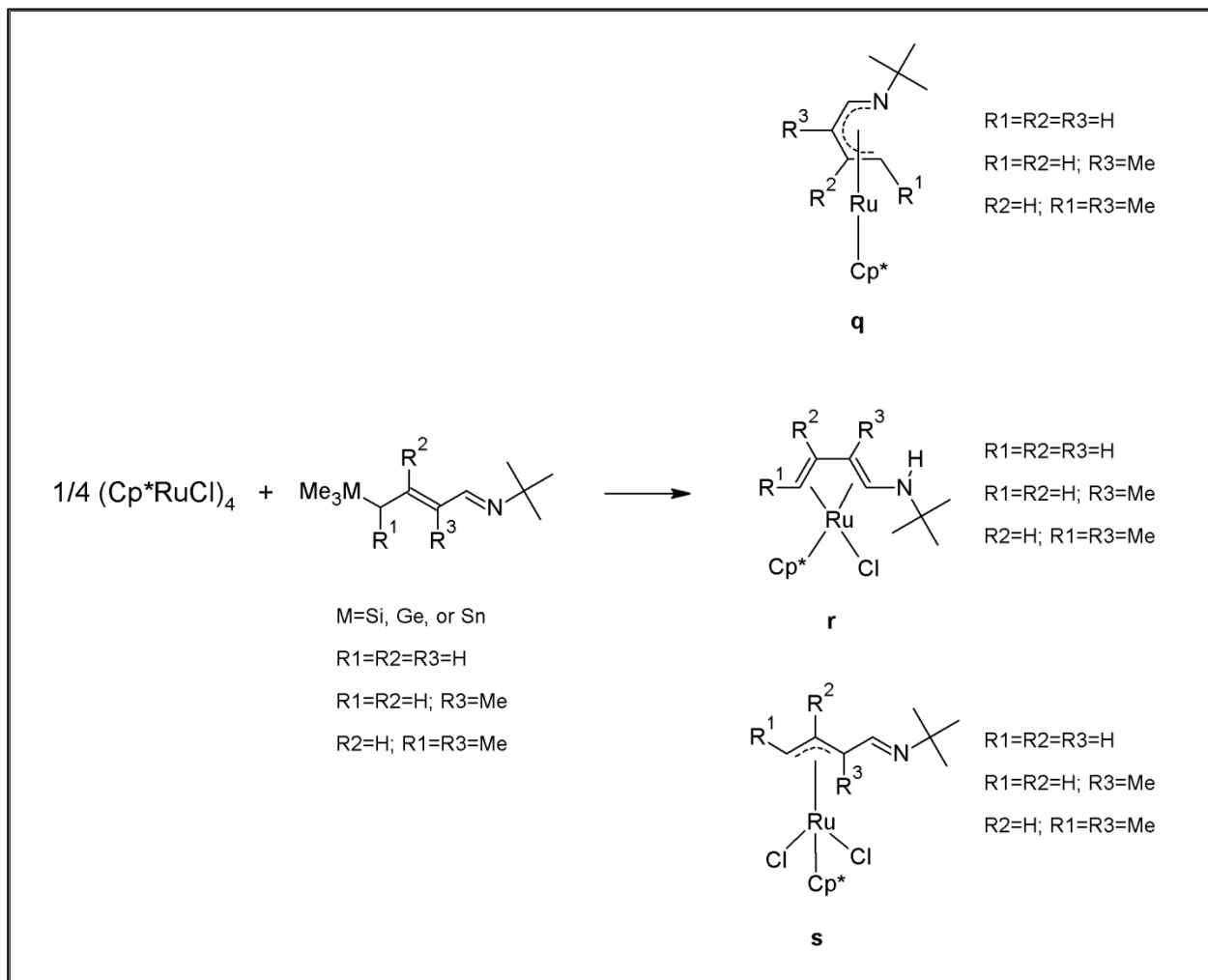


Scheme 1.9: Synthesis of $(\eta^5\text{-azapentadienyl})RuCp^*$ complexes.

of an η^5 azapentadienyl-metal complex. The short bond lengths between the atoms of the azapentadienyl ligand and the ruthenium metal center proved that the ligand was strongly coordinated to the metal center. In addition, the ligand was essentially planar.

In addition to the lithium salt starting material, group 14 enimine derivatives $Me_3MCH(R1)C(R2)=C(R3)CH=NCMe_3$ ($M = Si, Ge, Sn$) were also studied as reagents to coordinate the azapentadienyl ligand to the ruthenium metal center.²⁹ Unlike the lithium starting

materials, these reagents resulted in a mixture of products as shown in Scheme 1.10.



Scheme 1.10: Summary of products from the reaction of $\frac{1}{4}(\text{Cp}^*\text{RuCl})_4$ with $\text{Me}_3\text{MCH}(\text{R}1)\text{C}(\text{R}2)=\text{C}(\text{R}3)\text{CH}=\text{NCMe}_3$.

The yield of each product in the mixture depended on which group 14 metal was used, the methylation pattern of the azapentadienyl, and the reaction solvent. Compound **q**, containing the η^5 azapentadienyl ligand, was favored by the tin enimine reagents while compound **s**, containing the η^3 ligand, was favored by the silicon enimine reagents.

1.5.4 Additional Work

Since 1999, additional azapentadienyl-metal complexes have been synthesized by the Bleeke^{18, 19} and Paz-Sandoval groups³⁰. These will be described in the chapters that follow.

1.6 Outline of Dissertation

This dissertation focuses on the synthesis, characterization, and reactivity of a new family of *bis*-azapentadienyl-ruthenium complexes. Our ultimate goal was to produce new catalysts that could open and close coordination sites through azapentadienyl bonding mode shifts. While that goal was not accomplished, we have discovered new compounds with interesting structures and reactivity. In addition, this work has shown a possible way forward to achieve our goal in the future.

In Chapter 2, the synthesis and characterization of neutral *bis*-azapentadienyl-ruthenium-phosphine complexes are discussed. The multiple possible orientations of the azapentadienyl ligands add another element of interest to these compounds. Chapter 3 describes the reactivity of these neutral compounds towards triflic acid. These reactions allow us to determine the preferred reaction site: the metal center or N atom(s) of the heteropentadienyl ligand(s). Comparisons to related compounds, conclusions, and future work are presented in Chapter 4.

1.7 References

- (1) (a) Wilson, D.R.; DiLullo, A.A.; Ernst, R.D. *J. Am. Chem. Soc.* **1980**, *102*, 5928-5930.
(b) Liu, J. -Z., Ernst, R.D. *J. Am. Chem. Soc.* **1982**, *104*, 3737-3739.
(c) Ernst, R.D.; Cymbaluk, T.H. *Organometallics* **1982**, *1*, 708-713.
- (2) Kealy T.J.; Pauson P.L. *Nature* **1951**, *168*, 1039-1040.
- (3) Wilkinson, G. *Journal of Organometallic Chemistry* **1975**, *100*, 273.

- (4) Kim, S.H.; Ahn, D.; Kang, Y.Y.; Kim, M.; Lee, K.; Lee, J.; Park, M.H.; Kim, Y. *Eur. J. Inorg. Chem.* **2014**, 2014, 5107-5112.
- (5) Bleeke, J.R.; Peng, W.-J. *Organometallics* **1984**, 3, 1422-1426.
- (6) Wilson, D.R.; Ernst, R.D.; Kralik, M.S. *Organometallics* **1984**, 3, 1442-1444.
- (7) (a) Blackmore, T.; Bruce, M.L.; Stone, F.G. *A J. Chem. Soc. A*. **1971**, 2376.
(b) Ashby, G.S.; Bruce, M.L.; Tomkins, I.B.; Wallis, R.C. *Aust. J. Chem.* **1979**, 32, 1003.
(c) Bruce, M.; Wong, F.S.; Skelton, B.W.; White, A.H. *J. Chem. Soc., Dalton Trans.*, **1981**, 1398.
(d) Trechel, P.M.; Komar, D.A. *Synth. React. Inorg. Met.-Org. Chem.* **1980**, 10, 205.
- (8) Bleeke, J.R.; Rauscher, D.J. *Organometallics*, **1988**, 7, 2328 – 2339.
- (9) Bleeke, J.R. *Organometallics*, **2005**, 24, 5190-5207.
- (10) Bleeke, J.R.; Haile, T; New, P.R.; Chiang, M.Y. *Organometallics* **1993**, 12, 517-528.
- (11) Bleeke, J.R.; Donnay, E.; Rath, N.P. *Organometallics*, **2002**, 21, 4099-4112.
- (12) Bleeke, J.R.; Lutes, B.L.; Lipschutz, M.; Sakellariou-Thompson, D.; Lee, J.S.; Rath, N.P *Organometallics*, **2010**, 29, 5057-5067.
- (13) Bleeke, J.R.; Ortwerth, M.F.; Chiang, M.Y. *Organometallics*, **1992**, 11, 2740-2743.
- (14) Bleeke, J.R.; Ortwerth,, M.F.; Rohde, A.M. *Organometallics*, **1995**, 14, 2813-2826.
- (15) Bleeke, J.R.; Wise, E.S.; Shokeen, M.; Rath, N.P. *Organometallics*, **2005**, 24, 805-808.
- (16) Bleeke, J.R.; Shokeen, M.; Wise, E.S.; Rath, N.P. *Organometallics*, **2006**, 25, 2486-2500.
- (17) Bleeke, J.R.; Lutes, B.; Rath, N.P. *Organometallics*, **2009**, 28, 4577-4583.
- (18) Bleeke, J.R.; Anutrasakda, W.; Rath, N.P. *Organometallics*, **2012**, 31, 2219-2230.
- (19) Bleeke, J.R.; Anutrasakda, W.; Rath, N.P. *Organometallics*, **2013**, 32, 6410-6426.

- (20) Bleeke, J.R.; Luaders, S.T.; Robinson, K. D. *Organometallics*, **1994**, *13*, 1592-1600.
- (21) Bleeke, J.R.; Rohde, A.M.; Robinson, K.D. *Organometallics*, **1994**, *13*, 401-403.
- (22) Bleeke, J.R.; Rohde, A.M.; Robinson, K.D. *Organometallics*, **1995**, *14*, 1674-1680.
- (23) Bleeke, J.R.; Thananatthanachon, T.; Rath, N.P. *Organometallics*, **2007**, *26*, 3904-3907.
- (24) Bleeke, J.R.; Thananatthanachon, T.; Rath, N.P. *Organometallics*, **2008**, *27*, 2436-2446.
- (25) Paz-Sandoval, M.A.; Rangel-Salas, I.I. *Coord. Chem. Rev.*, **2006**, *250*, 1071-1106.
- (26) Cheng, M.-H.; Cheng, C.-Y.; Wang, S.-L.; Peng, S. -M.; Liu, R.-S. *Organometallics*, **1990**, *9*, 1853-1861.
- (27) Vong, W.-J.; Peng, S.-M.; Lin, S.-H.; Lin, W.-J.; Liu, R.-S. *J. Am. Chem. Soc.* **1991**, *113*, 573-582.
- (28) Wolf, G.; Würthwein, E.-U. *Chem. Ber.* **1991**, *124*, 889-896.
- (29) Gutierrez, J.A.; Clemente, M.E.N.; Paz-Sandoval, M.A.; Arif, A.M.; Ernst, R.D. *Organometallics*, **1999**, *18*, 1068-1079.
- (30) Reyna-Madrigal, A.; Moreno-Gurrola, A.; Perez-Camacho, O.; Navarro-Clemente, M.E.; Juarez-Saavedra, P.; Leyva-Ramirez, M.A.; Arif, A.M.; Ernst, R.D.; Paz-Sandoval, M.A. *Organometallics* **2012**, *31*, 7125-7145.

Chapter 2

Neutral *bis*-Azapentadienyl-Ruthenium-Phosphine
Chemistry

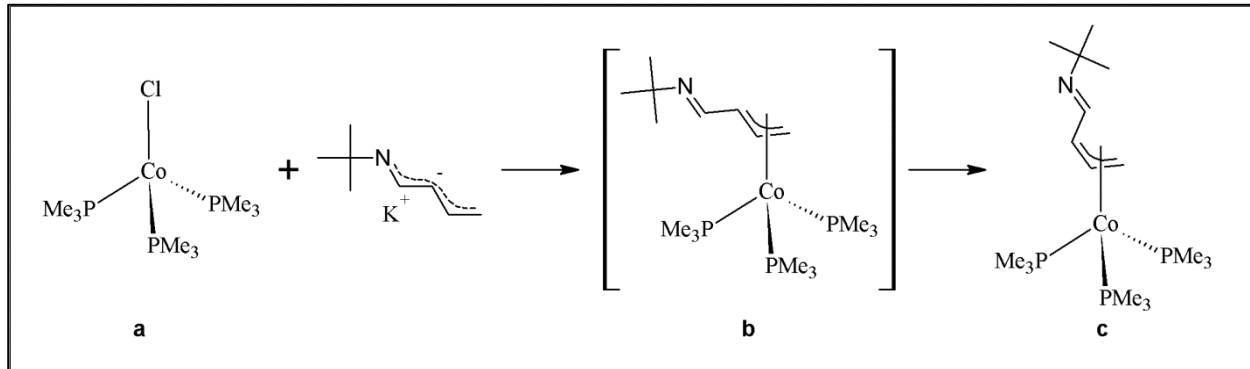
Neutral *bis*-Azapentadienyl-Ruthenium-Phosphine Chemistry

2.1 Introduction

After an initial foray into azapentadienyl-iridium chemistry in the mid-1990's (see Chapter 1), the Bleeke group has recently returned to this topic. Work by Wipark Anutrasakda in our group has focused on the azapentadienyl complexes of Co¹, Rh², and Ir² and the reactions of these species with simple electrophiles. In the sections that follow, that work will be briefly summarized. In addition, the Paz-Sandoval group in Mexico has been actively engaged in azapentadienyl-metal chemistry and recent work from that lab will also be described. With that prior research as a backdrop, I will then discuss my work³, which has recently been published, in synthesizing and characterizing a new family of neutral *bis*-azapentadienyl-RuL₂ complexes.

2.1.1 Azapentadienyl-Metal-Phosphine Complexes (M=Co, Ir, Rh)

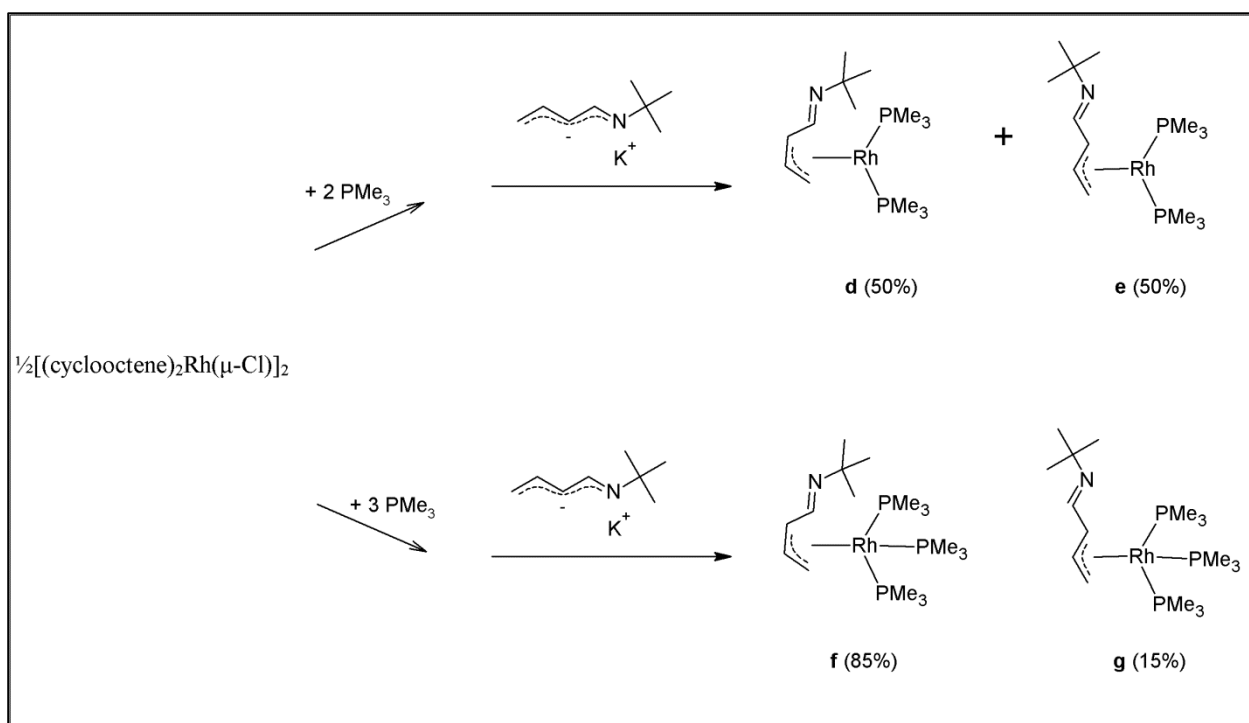
In 2012, the Bleeke group reported that treatment of ClCo(PMe₃)₃ with potassium *tert*-butylazapentadienide resulted in an *anti*- η^3 product that most likely went through the unobserved *syn* intermediate (**b**), as seen in Scheme 2.1.¹ Conversion to the *anti*-product (**c**)



Scheme 2.1: Synthesis of ((1,2,3- η^3)-5-*tert*-butylazapentadienyl)Co(PMe₃)₃ (**c**).

most likely happened because of the additional η^4 resonance structure. Addition of a different ligand, such as $\text{P}(\text{OMe})_3$, showed replacement of one of the PMe_3 while retaining the *anti*- η^3 orientation.

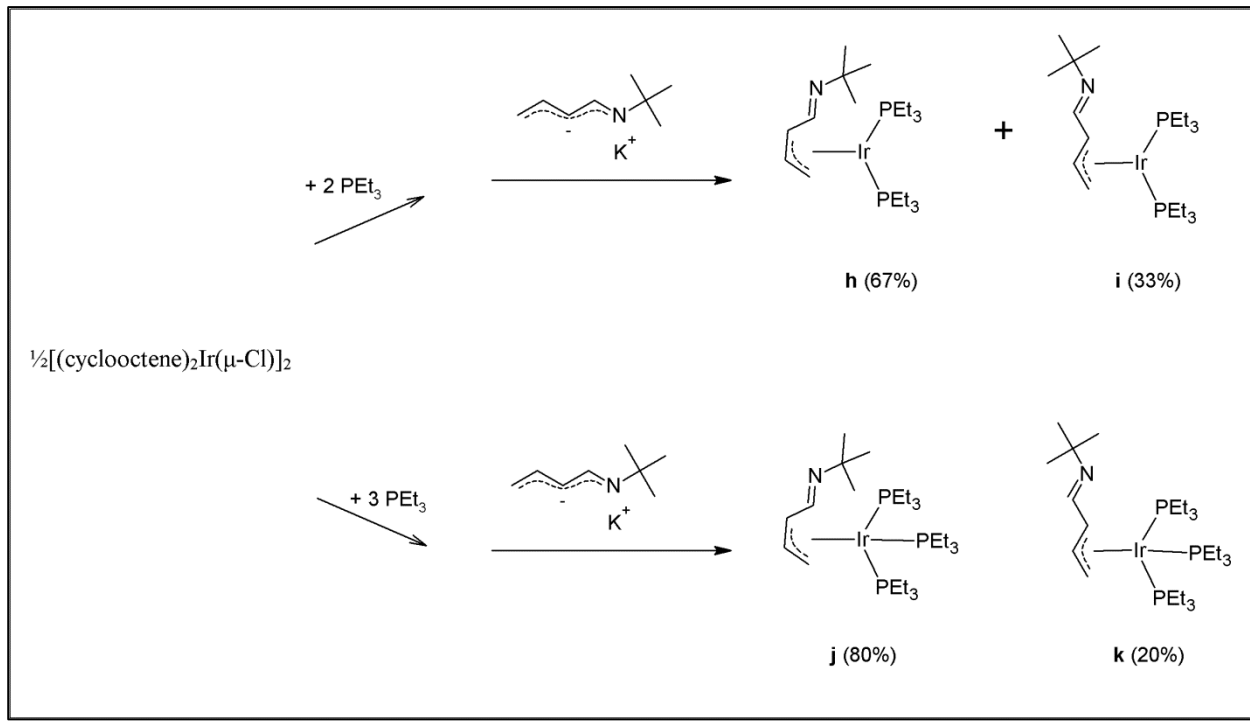
Treatment of $\frac{1}{2}[(\text{cyclooctene})_2\text{Rh}(\mu\text{-Cl})]_2$ with 2 equivalents of PMe_3 , followed by at least one equivalents of potassium azapentadienide resulted in a 50:50 mixture of the *anti*- and *syn*- isomers of $((1,2,3\text{-}\eta^3)\text{-}5\text{-}tert\text{-butylazapentadienyl})\text{Rh}(\text{PMe}_3)_2$, as seen in Scheme 2.2.² The addition of 3 equivalents of PMe_3 to $\frac{1}{2}[(\text{cyclooctene})_2\text{Rh}(\mu\text{-Cl})]_2$, followed by one equivalents of potassium azapentadienide resulted in an 85:15 mixture of the *anti*- (**f**) and *syn*- (**g**) isomers (see Scheme 2.2).²



Scheme 2.2: Synthesis of $((1,2,3\text{-}\eta^3)\text{-}5\text{-}tert\text{-butylazapentadienyl})\text{Rh}(\text{PMe}_3)_2$ and $((1,2,3\text{-}\eta^3)\text{-}5\text{-}tert\text{-butylazapentadienyl})\text{Rh}(\text{PMe}_3)_3$.

The same reactivity was seen with treatment of $\frac{1}{2}[(\text{cyclooctene})_2\text{Ir}(\mu\text{-Cl})]_2$ with 2 or 3 equivalents of PMe_3 , followed by at least one equivalent of potassium azapentadienide² (see

Scheme 2.3). Both *anti*- and *syn*- isomers were seen in the 16e⁻ (**h** and **i**) and 18e⁻ (**j** and **k**) iridium complexes in a 67:33 and 80:20 mixture, respectively.

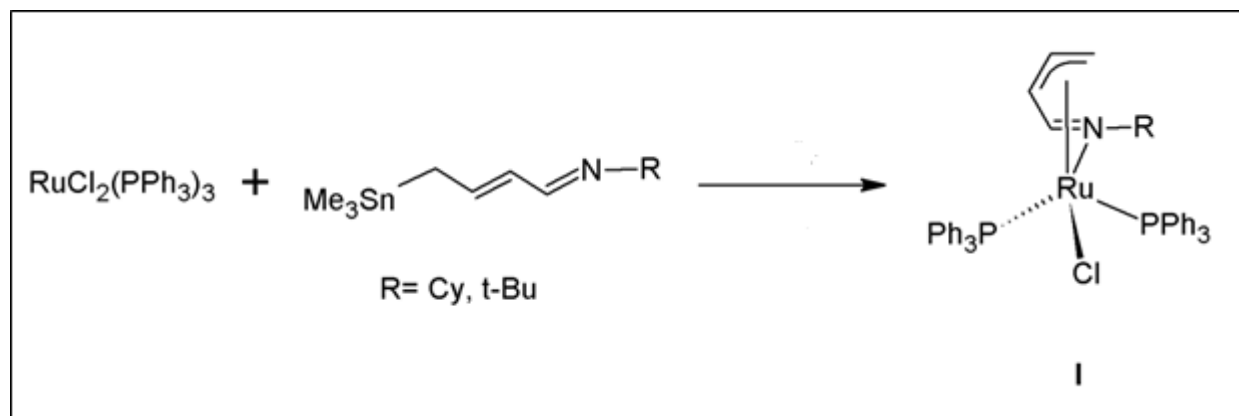


Scheme 2.3: Synthesis of ((1,2,3- η^3)-5-*tert*-butylazapentadienyl)Ir(PEt₃)₂ and ((1,2,3- η^3)-5-*tert*-butylazapentadienyl)Ir(PEt₃)₃.

2.1.2 Azapentadienyl-Ruthenium-Phosphine Complexes

The Paz-Sandoval group was able to synthesize ((1,2,3- η^3 , 5- η^1)-5-*tert*-butylazapentadienyl)RuCl(PPh₃)₂ (**I**) as seen in Scheme 2.4.⁴ Unlike the azapentadienyl-M-phosphine complexes^{1,2} reported in the Bleeke group, a tin enimine reagent⁵ was used in the

synthesis of **I**. Because this compound was a covalent reagent, it was less reactive

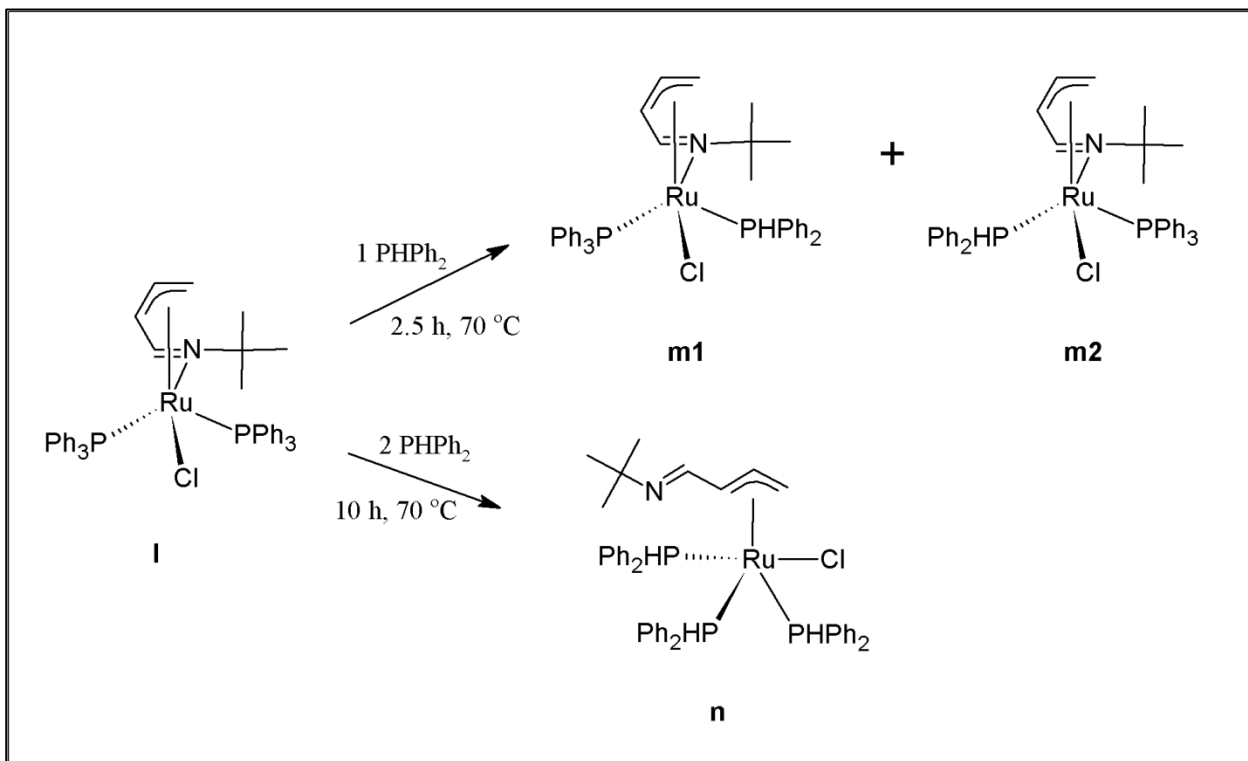


Scheme 2.4: Synthesis of ((1,2,3- η^3 , 5- η^1)-5-*tert*-butylazapentadienyl)RuCl(PPh₃)₂ (**I**).

than the ionic reagent, potassium azapentadienide⁶, used in the Bleeker group. In order to achieve an 18e⁻ complex in the Paz-Sandoval system, bonding involved the nitrogen lone pair as well as the allyl moiety of **I** (Scheme 2.4). This additional nitrogen bonding required that the ligand take on a U-shaped, *anti*- conformation.

Paz-Sandoval studied the reactivity of the *mono*-azapentadienyl complex with various equivalents of PHPh₂ as seen in Scheme 2.5.⁴ Addition of one equivalent of PHPh₂ to **I** at elevated temperatures led to the substitution of one of the triphenylphosphines, resulting in **m1/m2**. The addition of two equivalents of PHPh₂ to **I** at elevated temperatures resulted in the

displacement of both PPh_3 with the coordination of an additional PHPh_2 ligand (**n**).



Scheme 2.5: Synthesis of $[1\text{-}3\text{-}\eta^3,5\text{-}\eta^1\text{-CH}_2\text{CHCHCHN(t-Bu)}]\text{RuCl}(\text{PPh}_3)(\text{PHPh}_2)$.

During the reaction, the azapentadienyl ligand underwent a bonding mode shift from η^3 , η^1 with bonding through the allyl and the nitrogen lone pair to a W-shaped *syn*- η^3 bonding mode. The additionally coordinated PHPh_2 was a result of the compound scavenging a smaller PHPh_2 ligand (in comparison to PPh_3) to complete the $18e^-$ complex.

2.1.2.1 Comparison to the Analogous Pentadienyl Ruthenium System

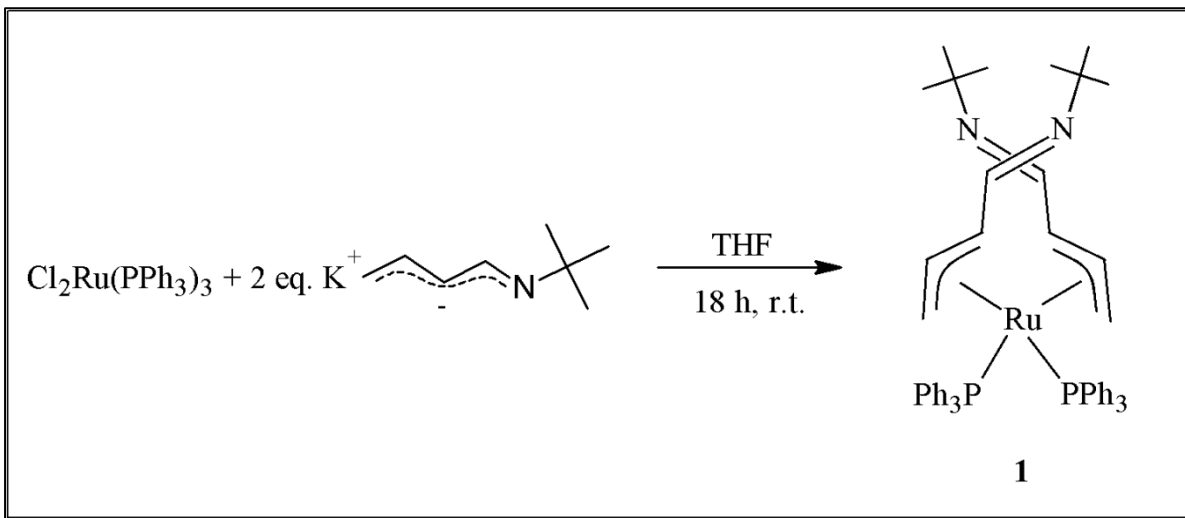
Paz-Sandoval's *mono*-azapentadienyl-ruthenium system was very similar to the all carbon system previously reported by the Bleeeke group⁷ (see Section 1.3). Both compounds result from the addition of a tin reagent with $\text{Cl}_2\text{Ru}(\text{PPh}_3)_3$. In both systems, the addition of one equivalent of a smaller phosphine showed replacement of one triphenylphosphine while retaining the bonding modes of the parent compounds. The difference in reactivity was seen after the

addition of two equivalents of a smaller phosphine. The pentadienyl-ruthenium compound showed replacement of both PPh_3 's with retention of the η^5 bonding mode while the azapentadienyl-ruthenium compounds showed the substitution of both PPh_3 's and the addition of an extra PPh_2 with a bonding mode shift. The η^3, η^1 bonding mode, with bonding through the allyl portion of the ligand and the nitrogen lone pair, shifted to a *syn*- η^3 bonding mode. This shift confirmed the enhanced reactivity of the azapentadienyl as compared to the pentadienyl ligand.

2.2 Results and Discussion

2.2.1 Synthesis and Characterization of $[(1,2,3\text{-}\eta^3)\text{-}(5\text{-}tert\text{-}butylazapentadienyl})]_2\text{Ru}(\text{PPh}_3)_2$ (1)

Treatment of $\text{Cl}_2\text{Ru}(\text{PPh}_3)_3$ ⁸ with two equivalents of potassium *tert*-butylazapentadienide⁶ in tetrahydrofuran resulted in the production of a yellow brown solid $[(1,2,3\text{-}\eta^3)\text{-}(5\text{-}tert\text{-}butylazapentadienyl})]_2\text{Ru}(\text{PPh}_3)_2$ (**1**) in 48% yield as shown in Scheme 2.6. Addition of less than two equivalents of potassium *tert*-butylazapentadienide resulted in the same product in reduced yield. As previously discussed, a *mono*-azapentadienyl-ruthenium complex was synthesized by Paz-Sandoval.^{4,8} However, Compound **1** was the first *bis*-azapentadienyl-ruthenium-phosphine complex to be synthesized. The *bis*-azapentadienyl product is formed even though the same $\text{Cl}_2\text{Ru}(\text{PPh}_3)_3$ starting material was used in both the *mono*- and *bis*- syntheses. This indicates the greater nucleophilicity of potassium azapentadienide versus the tin enimine reagent used by Paz-Sandoval.



Scheme 2.6: Synthesis of $[(1,2,3-\eta^3)-(5\text{-}tert\text{-}butylazapentadienyl})]_2\text{Ru}(\text{PPh}_3)_2$ (**1**)

Compound **1** had two-fold symmetry resulting in the two azapentadienyl ligands being equivalent by NMR. In the ^1H NMR, **1** exhibited a downfield doublet at δ 7.86 corresponding to the uncoordinated H4. The doublet resulted from coupling to the adjacent H3's ($J_{\text{H}4\text{-H}3} = 7.8$ Hz). The coordinated allyl portion of the two symmetrical ligands appeared at δ 4.53 (H2's), 3.30 (H1's), 1.80 (H3's), and 1.15 (H1's). The $^{13}\text{C}\{^1\text{H}\}$ NMR spectrum of **1** showed a downfield singlet at δ 164.7 representing the uncoordinated C4 carbons. The remaining carbon signals appeared further upfield δ 86.2 (C2's), 55.6 (C3's), and 47.2 (C1's). The equivalent C3's showed a coupling to the phosphorus resulting in a doublet from the C3-P *trans* orientation ($J_{\text{C}3\text{-P}} = 18.3$ Hz) in the pseudo-octahedral coordination environment of **1**. Because of the two-fold rotational symmetry axis in **1**, the $^{31}\text{P}\{^1\text{H}\}$ NMR spectrum showed a singlet at δ 57.6. In the infrared spectrum of **1**, the C=N stretch appeared at 1615.8 cm^{-1} . Crystallization attempts were

unsuccessful; however, the high resolution ESI mass spectrum (see Figure 2.1)

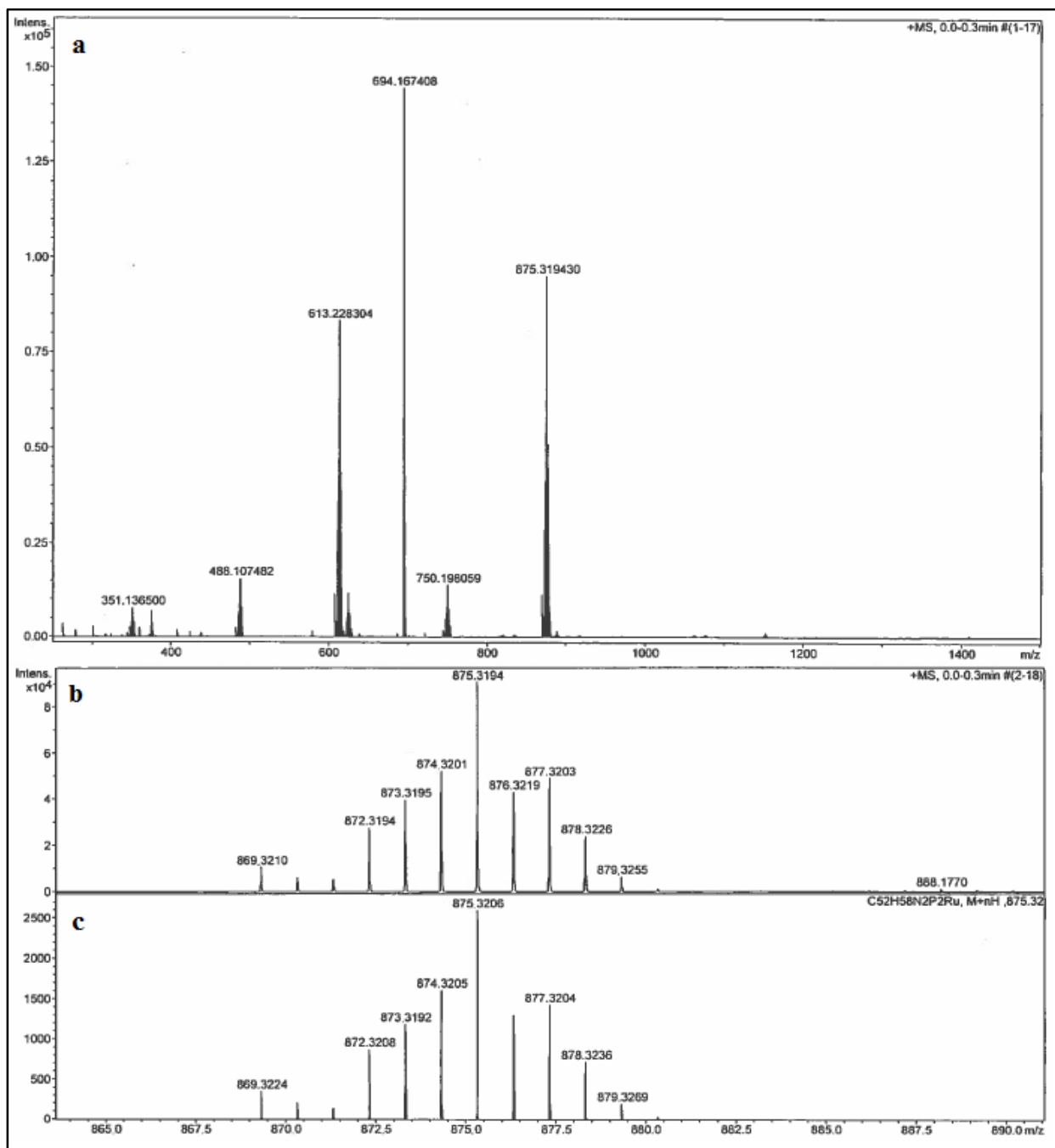


Figure 2.1: (a) High resolution ESI mass spectrum of **1**. Selected ion fragments: 750.1981 (loss of *tert*-butylazapentadiene), 613.2283 (loss of triphenylphosphine) 488.1075 (loss of *tert*-butylazapentadiene and triphenylphosphine). (b) Experimental isotopic envelope for $[M+H]^+$; found, 875.3194. (c) Predicted isotopic envelope for $[M+H]^+$; calc'd, 875.3206.

showed the predicted isotopic pattern for $[M + H]^+$ and for the fragment ions resulting from loss of *tert*-butylazapentadiene, loss of triphenylphosphine, and loss of both *tert*-butylazapentadiene and triphenylphosphine from $[M + H]^+$.

2.2.2 Possible Structural Variants for $[(1,2,3-\eta^3)-(5\text{-}tert\text{-}butylazapentadienyl})_2\text{RuLL}']$ Complexes

There are ten possible structural variations for compounds of the type $[(1,2,3-\eta^3)-(5\text{-}tert\text{-}butylazapentadienyl})_2\text{RuLL}']$ as shown in Figure 2.2. One of the possible structures, structure **A**, shows the L and L' ligands sitting in the mouths of the η^3 -allyl portions of the azapentadienyl ligands. This structure is referred to as a “mouth/mouth” orientation. Structure **A** also shows the C3's of the two azapentadienyl ligands oriented *trans* to the L and L'. When these two features are seen, the complex is denoted as a “mC3/mC3” structure. Structure **B** differs from structure **A** because L is sitting on the “backbone” of the allyl portion of the azapentadienyl. The C3s are still *trans* to each of the L and L' ligands. This type of structure is referred to as “mC3/bC3”. Structure **C** (bC3/bC3) shows L/L' sitting on the backbone of both azapentadienyl ligands while the C3s remain *trans* to the ancillary ligands. One interesting feature of these types of compounds is that the azapentadienyl ligand can rearrange, placing a C1 *trans* to an ancillary ligand. For example, structure **D** shows L and L' sitting in the mouth of each azapentadienyl ligand with a C3 *trans* to L' and C1 on the other azapentadienyl *trans* to L. This is denoted as “mC3/mC1”. Assuming L and L' are the same, structures **A**, **C**, **H**, and **J**, would retain the two-fold axis of symmetry, resulting in chemically equivalent azapentadienyl ligands.

The ^1H and $^{13}\text{C}\{^1\text{H}\}$ NMR spectra of these structures should show one set of ligand signals.

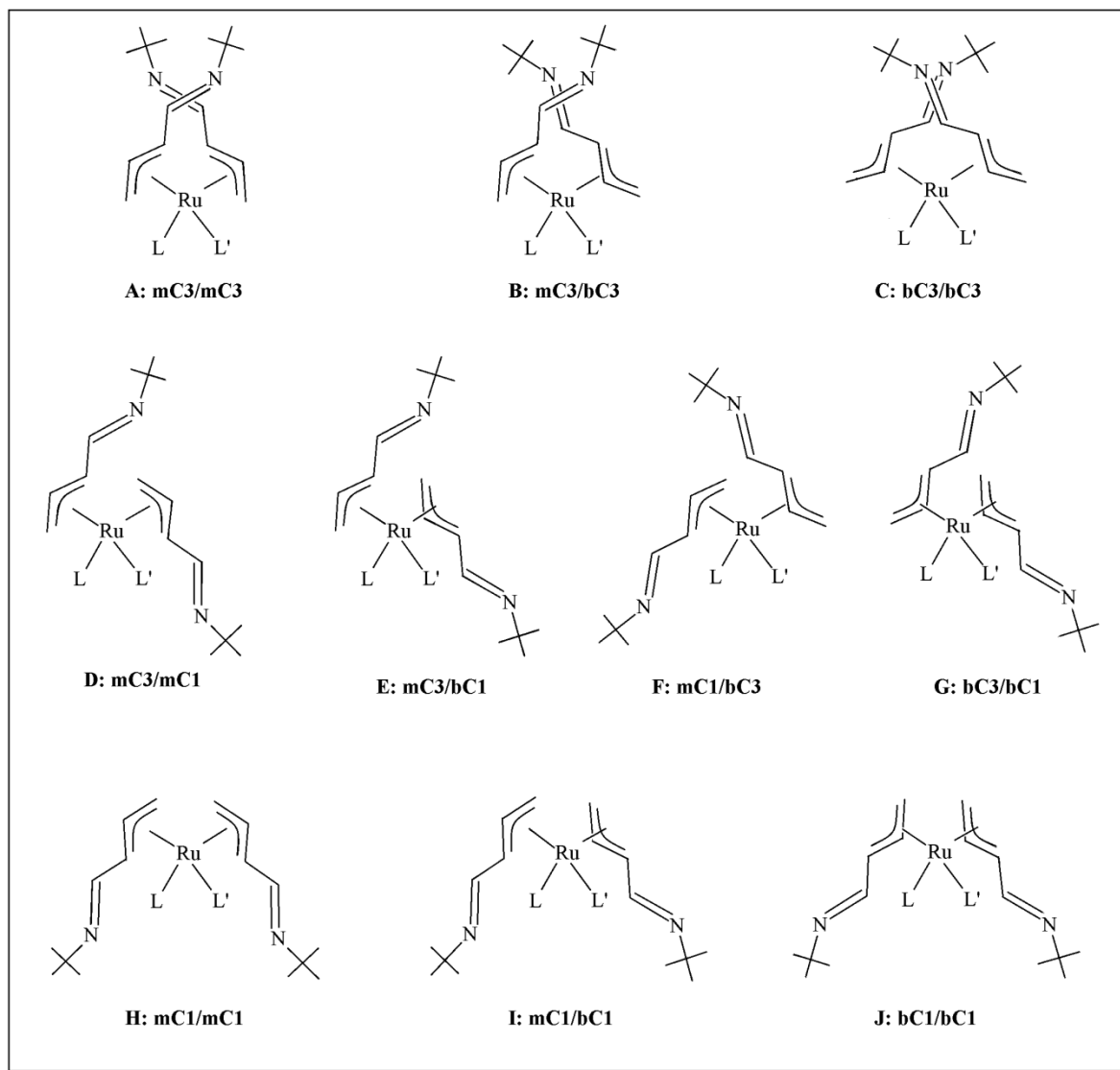


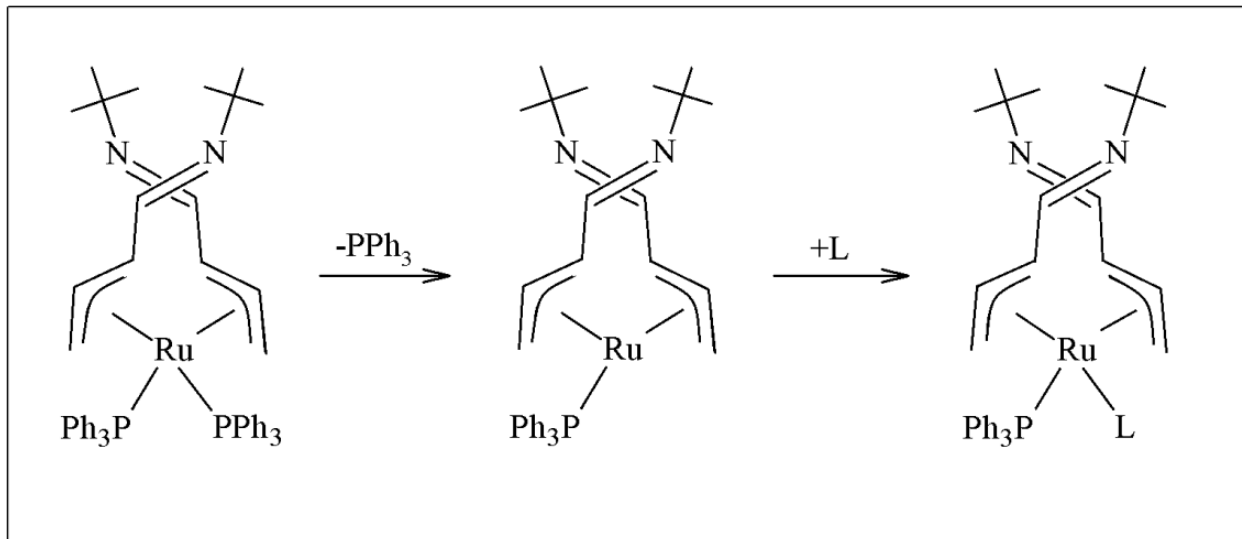
Figure 2.2: Possible Structural Variants of $[(1,2,3-\eta^3)-(5\text{-}tert\text{-}butylazapentadienyl})]_2\text{RuLL}'$ Complexes

The crystal structure of **1** could not be obtained. However, given that the ^1H and $^{13}\text{C}\{^1\text{H}\}$ NMR showed one set of ligand signals, it could be determined that the *tert*-butylazapentadienyl ligands were chemically equivalent. The same could be said about the two triphenylphosphine ligands because of the sharp singlet seen in the $^{31}\text{P}\{^1\text{H}\}$ NMR. From this information,

unsymmetrical structures **B**, **D**, **E**, **F**, **G**, and **I** could be ruled out. Because of the steric bulkiness of the triphenylphosphine (cone angle = 145°)⁹, the phosphine ligand would most likely want to sit in the mouth of the azapentadienyl ligands. This orientation creates the least amount of phosphine/azapentadienyl steric interaction. This assumption allowed structures **C** and **J** to be ruled out. The remaining possible structures include structure **A** and **H**. Because the C3s appeared as doublets in the $^{13}\text{C}\{\text{H}\}$ NMR with $J = 18.3$ Hz, they were most likely *trans* to the PPh₃'s, eliminating structure **H**.

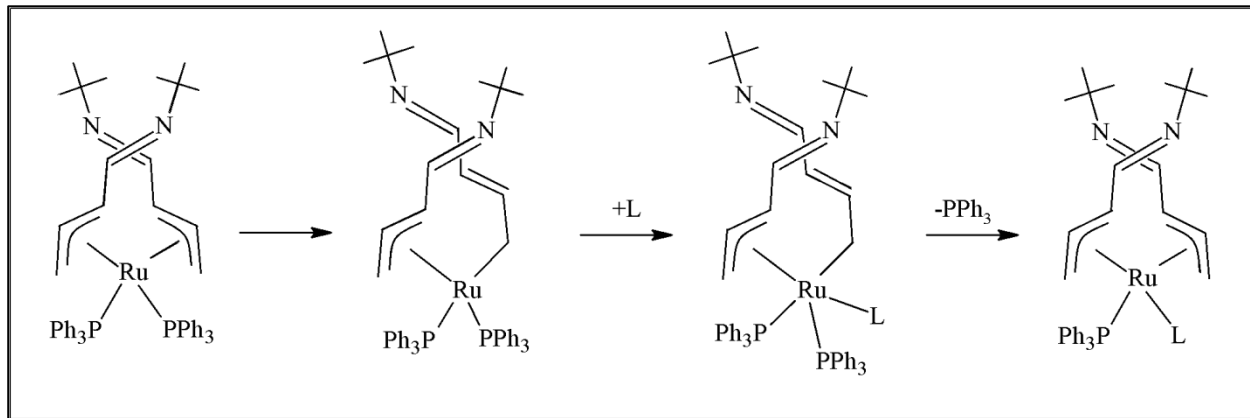
2.2.3 Treatment of Compound 1 with Neutral, 2e⁻ Donor Ligands at Room Temperature

In order to investigate the reactivity of $[(1,2,3-\eta^3)-(5\text{-}tert\text{-}butylazapentadienyl})]_2\text{Ru}(\text{PPh}_3)_2$ (**1**), it was treated with a variety of neutral two electron donor ligands at room temperature. Treatment of **1** with any number of equivalents of L (L = PMe₃, dmpe, P(OMe)₃, CNCMe₃, CO and PEt₃) in THF at room temperature led to displacement of one of the large triphenylphosphine ligands. As seen in Scheme 2.7, this reaction could have



Scheme 2.7: Proposed dissociative mechanism for synthesis of $[(1,2,3-\eta^3)-(5\text{-}tert\text{-}butylazapentadienyl})]_2\text{Ru}(\text{PPh}_3)(\text{L})$.

proceeded via a dissociative mechanism. To relieve steric strain around the metal center, a bulky triphenylphosphine could have dissociated, opening up a coordination site for a smaller L. With the addition of one L, the steric strain was relieved, resulting in a stable 18 e⁻ species. As seen in Scheme 2.8, an associative mechanism was also possible. If a smaller L



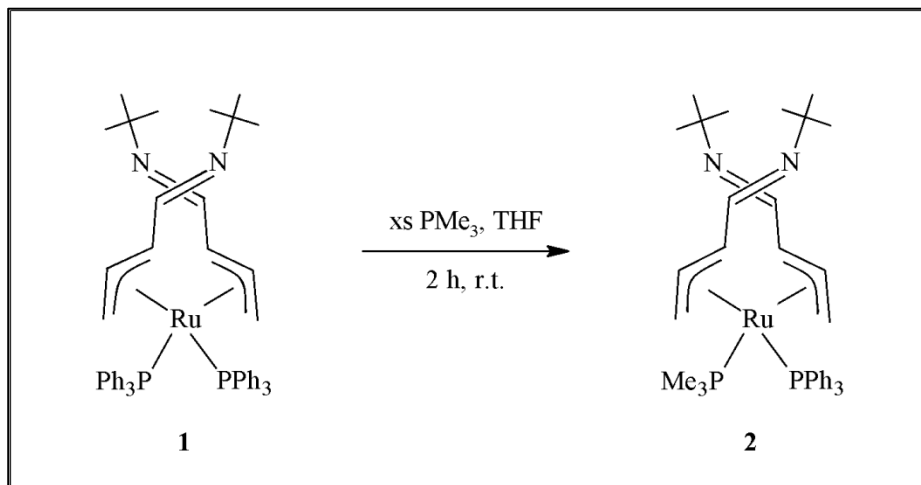
Scheme 2.8: Proposed associative mechanism for triphenylphosphine substitution.

coordinated to the metal center, one of the azapentadienyl ligands would have to shift from η^3 to η^1 in order to open up a coordination site for that new ligand, L. The shift of the azapentadienyl ligand back to an η^3 would result in the dissociation of one of the triphenylphosphine ligands. In order to coordinate a second L, another η^3 to η^1 bonding mode shift must occur to open up a coordination site. However, there was most likely not enough steric bulk remaining around the metal center to promote this shift. Therefore, only a single displacement was seen regardless of the number of equivalents of L added.

2.2.3.1 Synthesis of [(1,2,3- η^3)-(5-*tert*-butylazapentadienyl)]₂Ru(PPh₃)(PMe₃) (**2**)

Treatment of **1** with excess trimethylphosphine in THF at room temperature yielded [(1,2,3- η^3)-(5-*tert*-butylazapentadienyl)]₂Ru(PPh₃)(PMe₃) (**2**) in 56% yield, as seen in Scheme 2.9.

Because two-fold symmetry was broken by the replacement of one of the triphenylphosphines, both sets of ligand signals for the azapentadienyls were observed in the NMR. The $^{13}\text{C}\{\text{H}\}$ NMR showed the C4's downfield at δ 162.1 and 161.6. The coordinated portions of each ligand resonated at δ 84.9/82.3 (C2's), 55.1/52.4 (C3's) and 42.2/40.9 (C1's). The C3 carbons each appeared as a doublet in the $^{13}\text{C}\{\text{H}\}$ spectrum. Because the C3's were oriented *trans* to each of the phosphine ligands, similar to **1**, there was a phosphorus coupling ($J_{\text{C-P}} = 20.6$ Hz and 19.4 Hz). In the $^{31}\text{P}\{\text{H}\}$ NMR spectrum, two doublets were observed at δ 64.1 (PPh_3) and δ 6.6 (PMe_3) with a P-P coupling of 19.8 Hz.



Scheme 2.9: Synthesis of $[(1,2,3\text{-}\eta^3)\text{-}(5\text{-}tert\text{-butylazapentadienyl})]_2\text{Ru}(\text{PPh}_3)(\text{PMe}_3)$ (**2**)

The X-ray crystal structure of **2** is shown in Figure 2.3; selected bond distances are presented in the caption. Both azapentadienyl ligands in **2** were in the *syn, syn* (W) shape, with both phosphorus atoms P1 and P2 sitting in the mouth of the allyl portion of each ligand. The structure of **2** was the **A** structure (see Figure 2.2) where both C3's are *trans* to the PPh₃ and the PMe₃ ligands. We refer to structure **A** as mC3/mC3 because the ancillary ligands sit in the mouth (**m**) of the allyl portion of each azapentadienyl while the **C3** of each azapentadienyl are *trans* to the ancillary ligands.

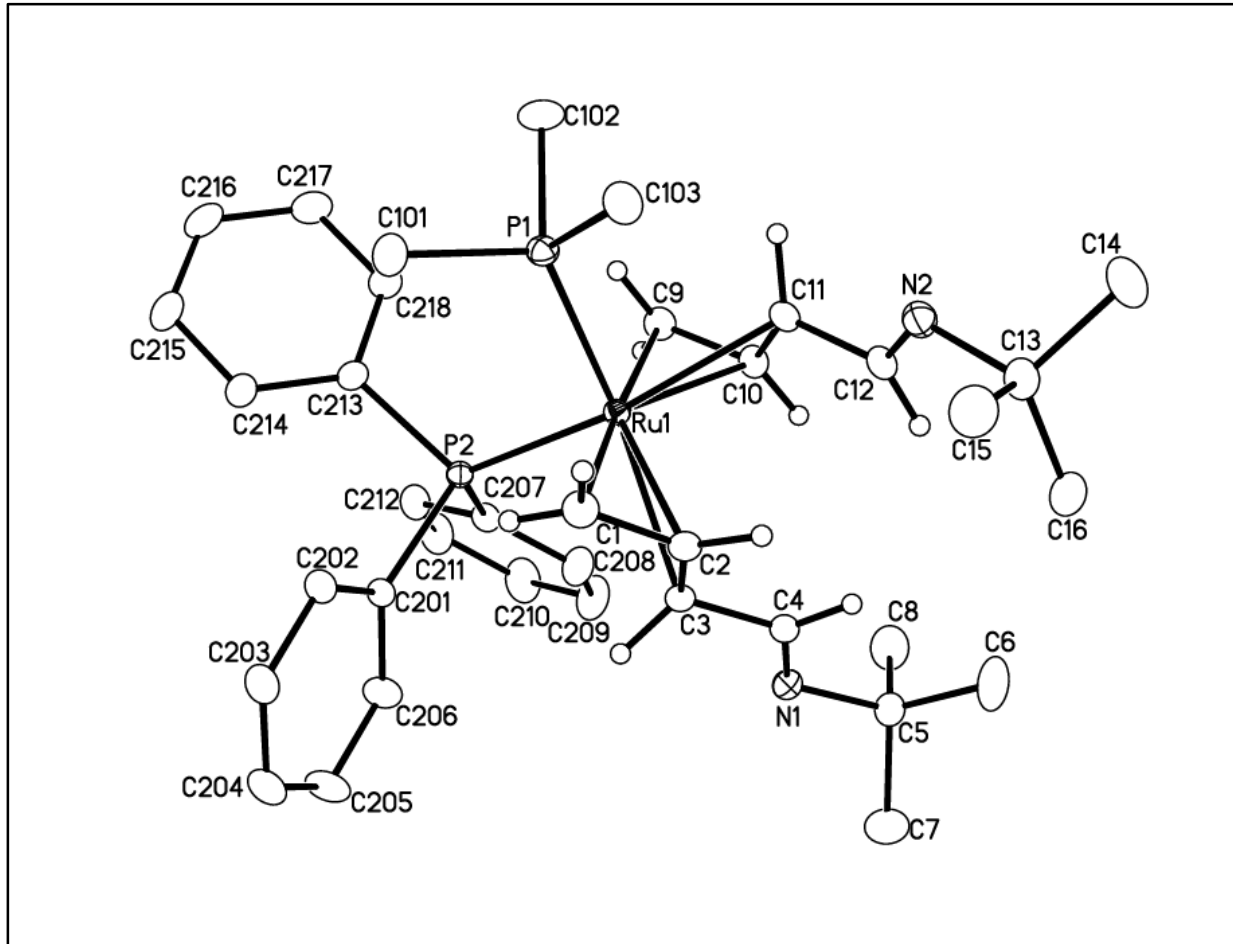
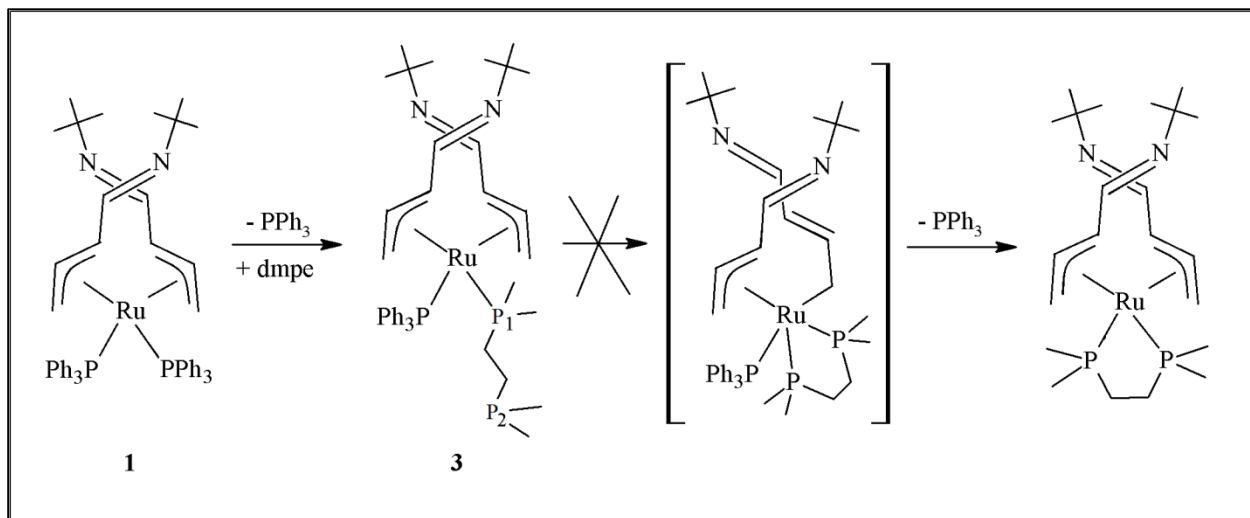


Figure 2.3: Molecular structure of **2**, using thermal ellipsoids at the 50% probability level. The methyl H's on the PMe₃ and PPh₃ ligands and on the *tert*-butyl group are not shown. Selected bond distances (Å): Ru1-P1, 2.3042(4); Ru1-P2, 2.3274(4); Ru1-C1, 2.2178(13); Ru1-C2, 2.1469(13); Ru1-C3, 2.3387(13); C1-C2, 1.4054(19); C2-C3, 1.420(2); C3-C4, 1.4635(19); C4-N1, 1.2711(19); N1-C5, 1.4783(18); Ru1-C9, 2.2187(13); Ru1-C10, 2.1461(13); Ru1-C11, 2.2924(13); C9-C10, 1.4105(19); C10-C11, 1.420(2); C11-C12, 1.4602(19); C12-N2, 1.2733(19); N2-C13, 1.4754(19). Selected bond angles (°): P1-Ru1-C3, 151.12(4); P2-Ru1-C11, 154.56(4); C1-Ru1-C9, 176.40(5); P1-Ru1-P2; 99.617(13).

2.2.3.2 Synthesis and Characterization of [(1,2,3- η^3)-(5-*tert*-butylazapentadienyl)]₂Ru(PPh₃)(dmpe) (3)

As shown in Scheme 2.10, treatment of **1** with a bidentate ligand, 1,2-*bis*(dimethylphosphino)ethane, at room temperature led to [(1,2,3- η^3)-(5-*tert*-butylazapentadienyl)]₂Ru(PPh₃)(dmpe) (**3**) in 88% yield. The ¹H NMR showed two sets of ligand signals while the ³¹P{¹H} NMR showed three phosphorus signals. These signals appeared at δ63.8 (PPh₃), 14.2 (P1) and -47.2 (P2), representing three unique phosphorus atoms. Only one of the phosphorus atoms of dmpe was coordinated to the metal center.

With a cone angle of 108°,⁹ trimethylphosphine was not bulky enough to promote the dissociation of the second triphenylphosphine. A bidentate ligand was chosen in an attempt to encourage the displacement of the second triphenylphosphine. As seen in Scheme 2.10,



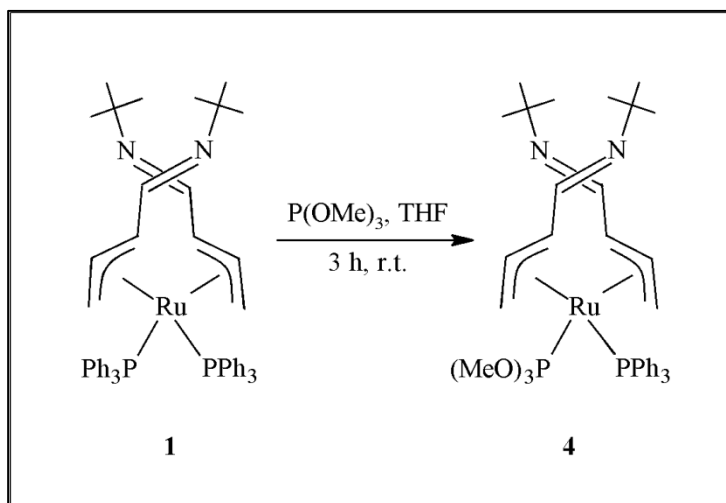
Scheme 2.10: Proposed mechanism for the synthesis of [(1,2,3- η^3)-(5-*tert*-butylazapentadienyl)]₂Ru(dmpe).

after the coordination of the first phosphorus atom, P1, the “tail” of the dmpe ligand is held close to the metal center. Because of the close proximity of the second phosphorus atom, P2, to the

metal center, we thought it would be possible for P2 to coordinate to the ruthenium and promote an azapentadienyl ligand shift from η^3 to η^1 . The displacement of the second triphenylphosphine ligand, followed by a shift back to η^3 , would then result in a neutral 18e⁻ species. However, chelation of the P2 atom did not occur. There was apparently not enough steric bulk around the metal center, so the reaction stopped with a single triphenylphosphine displacement, resulting in **3**.

2.2.3.3 Synthesis and Characterization of [(1,2,3- η^3)-(5-*tert*-butylazapentadienyl)]₂Ru(PPh₃)₂[P(OMe)₃] (**4**)

Compound **1** was reacted with a small, weakly-donating ligand, trimethyl phosphite. Upon addition of at least one equivalent of P(OMe)₃ (**4**), a yellow crystalline solid, [(1,2,3- η^3)-(5-*tert*-butylazapentadienyl)]₂Ru(PPh₃)₂[P(OMe)₃], was observed in a 83% yield (see Scheme 2.11).



Scheme 2.11: Synthesis of [(1,2,3- η^3)-(5-*tert*-butylazapentadienyl)]₂Ru(PPh₃)₂[P(OMe)₃] (**4**).

The ^1H and $^{13}\text{C}\{^1\text{H}\}$ NMR showed two sets of ligand signals for the inequivalent azapentadienyl ligands. Because the two ancillary ligands were inequivalent, the two doublets at δ 156.8 ($J_{\text{P-P}} = 41.1$ Hz, $\text{P}(\text{OMe})_3$) and δ 62.2 ($J_{\text{P-P}} = 41.1$ Hz, PPh_3) seen in the $^{31}\text{P}\{^1\text{H}\}$ NMR gave little insight into the orientation of the two azapentadienyl ligands. In the $^{13}\text{C}\{^1\text{H}\}$ NMR, the C3 signals each appeared as doublets, as the C3's sit *trans* to the ^{31}P nuclei. The coupling between the C3 and the $\text{P}(\text{OMe})_3$ was much larger ($J_{\text{C-P}} = 32.1$ Hz) than the coupling between the other C3 and the *trans* PPh_3 ($J_{\text{C-P}} = 20.6$ Hz).

The X-ray structure of **4** is seen in Figure 2.4; selected bond distances are summarized in the caption. The structure showed that both the PPh_3 and the $\text{P}(\text{OMe})_3$ sit in the mouths of each azapentadienyl ligand. Also, as predicted by the $^{13}\text{C}\{^1\text{H}\}$ NMR, the C3's are oriented *trans* to the ^{31}P nuclei. The structure of **4**, like that of **2**, was the **A** (mC3/mC3) structure where both C3's were *trans* to the PPh_3 and the $\text{P}(\text{OMe})_3$ ligands. As seen in previous structures, the azapentadienyl ligands were W-shaped with the expected delocalization within the allyl moieties.

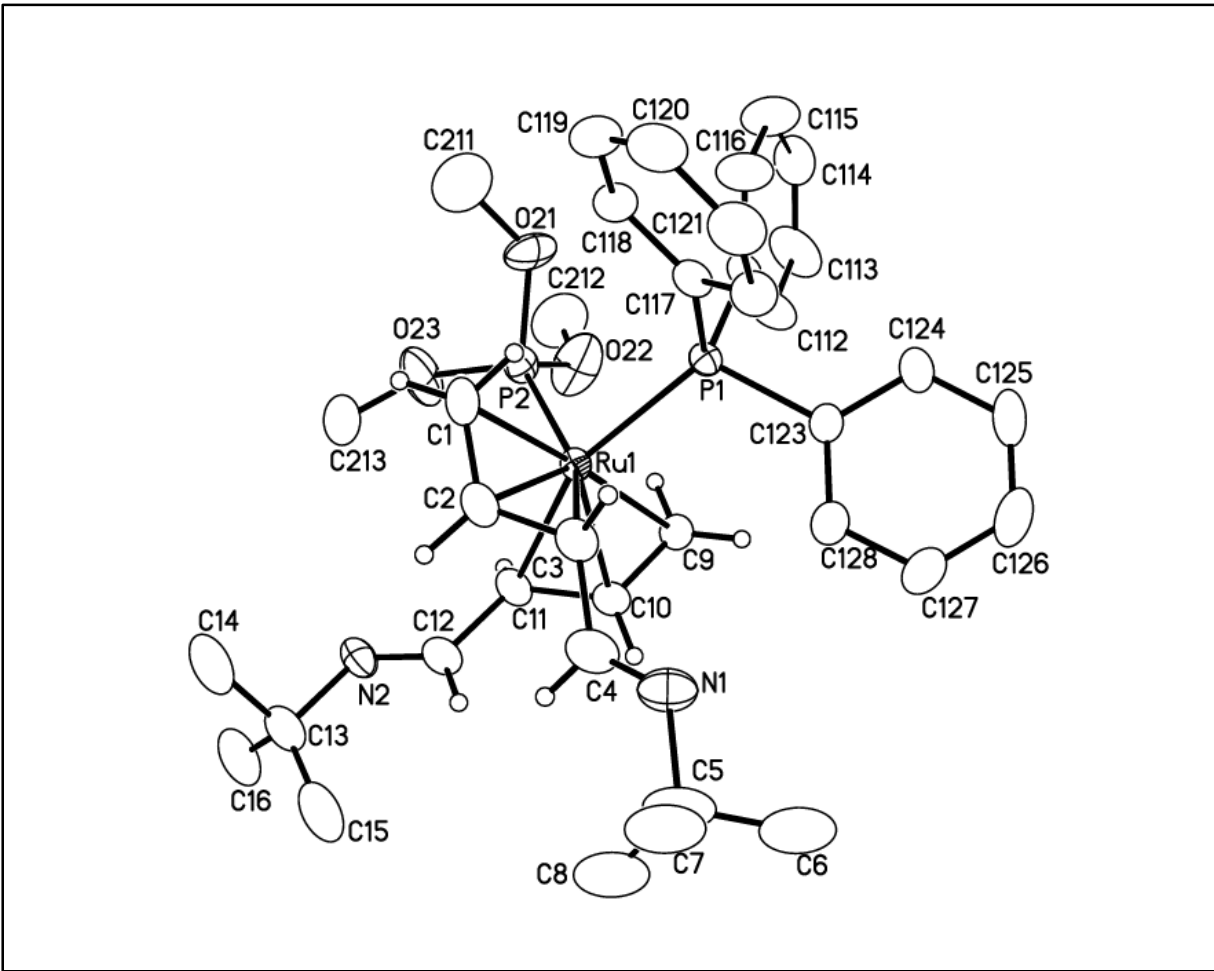
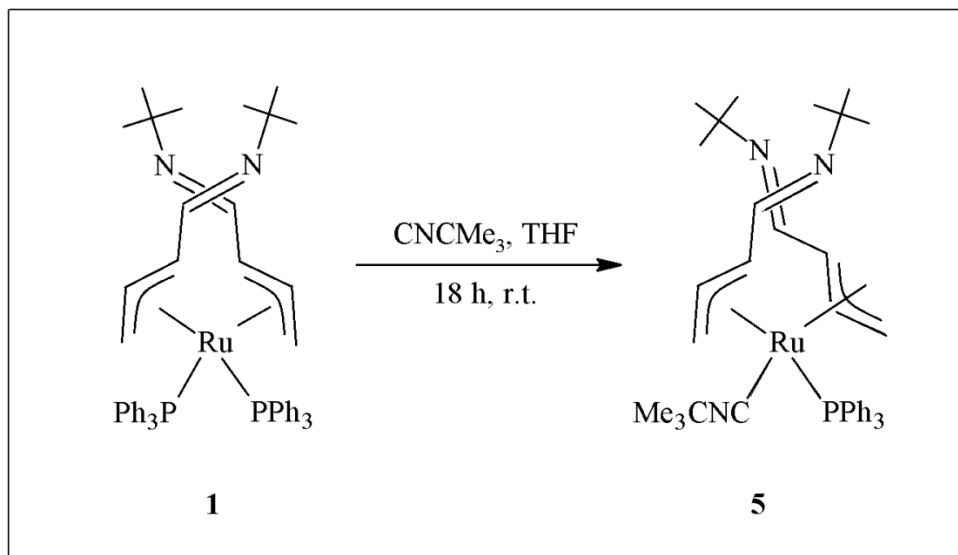


Figure 2.4: Molecular structure of **4**, using thermal ellipsoids at the 50% probability level. The methyl H's on the $\text{P}(\text{OMe})_3$ and PPh_3 ligands and on the *tert*-butyl group are not shown. Selected bond distances (\AA): Ru1-P1, 2.353(11); Ru1-P2, 2.2312(13); Ru1-C1, 2.226(5); Ru1-C2, 2.155(5); Ru1-C3, 2.352(5); C1-C2, 1.391(8); C2-C3, 1.415(7); C3-C4, 1.450(7); C4-N1, 1.246(7); N1-C5, 1.479(8); Ru1-C9, 2.242(4); Ru1-C10, 2.154(4); Ru1-C11, 2.302(4); C9-C10, 1.400(6); C10-C11, 1.410(6); C11-C12, 1.456(7); C12-N2, 1.262(6); N2-C13, 1.484(7). Selected bond angles ($^\circ$): P1-Ru1-C11, 152.89(13); P2-Ru1-C3, 153.10(13); C1-Ru1-C9, 176.28(19); P1-Ru1-P2, 94.26(5).

2.2.3.4 Synthesis and Characterization of [(1,2,3- η^3)-(5-*tert*-butylazapentadienyl)]₂Ru(PPh₃)(CNCMe₃) (**5**)

As shown in Scheme 2.12, treatment of **1** with excess *tert*-butylisocyanide, a small, electron-withdrawing ligand, produced [(1,2,3- η^3)-(5-*tert*-butylazapentadienyl)]₂Ru(PPh₃)(CNCMe₃) (**5**) as a yellow crystalline solid in 89% yield. As in previous single substitution products, two sets of signals for the inequivalent azapentadienyl ligands were observed. In the ¹³C{¹H} NMR spectrum, the C4's appeared downfield at δ 160.8 and 160.4, while the coordinated allyl portion of the ligands appeared at δ 99.5/88.3 (C2's), 62.4/62.3 (C3's), and 46.3/40.5 (C1's). The C3 that was *trans* to the triphenylphosphine ligand appeared as a doublet because of the phosphorus coupling (J_{C-P} = 20.6 Hz) while the other C3, sitting *trans* to the isocyanide ligand, appeared as a singlet. The C1 carbons that were positioned *trans* to each other and appeared as singlets. In the ³¹P{¹H} NMR spectrum, the PPh₃ ligand signal appeared at δ 53.7.



Scheme 2.12: Synthesis of [(1,2,3- η^3)-(5-*tert*-butylazapentadienyl)]₂Ru(PPh₃)(CNCMe₃) (**5**).

The X-ray crystal structure of **5** was obtained and is presented in Figure 2.5. It was similar to the X-ray crystal structures of **2** and **4** in the fact that the ligands were oriented in the *syn, syn* (W) position and the C1's, C3's, triphenylphosphine, and isocyanide ligand occupied octahedral coordination sites. However, the structure of **5** differed from that of **2** and **4** because of the orientation of one of the azapentadienyl ligands with respect to CNCMe₃ ligand. The structure for **5** was the “mC3/bC3” type. The triphenylphospine ligand sat in the mouth of one of the azapentadienyl ligand while the CNCMe₃ sat on the backbone of the other azapentadienyl ligand. The PPh₃ appeared in the mouth of the azapentadienyl ligand because of its greater steric interaction with the ligand.

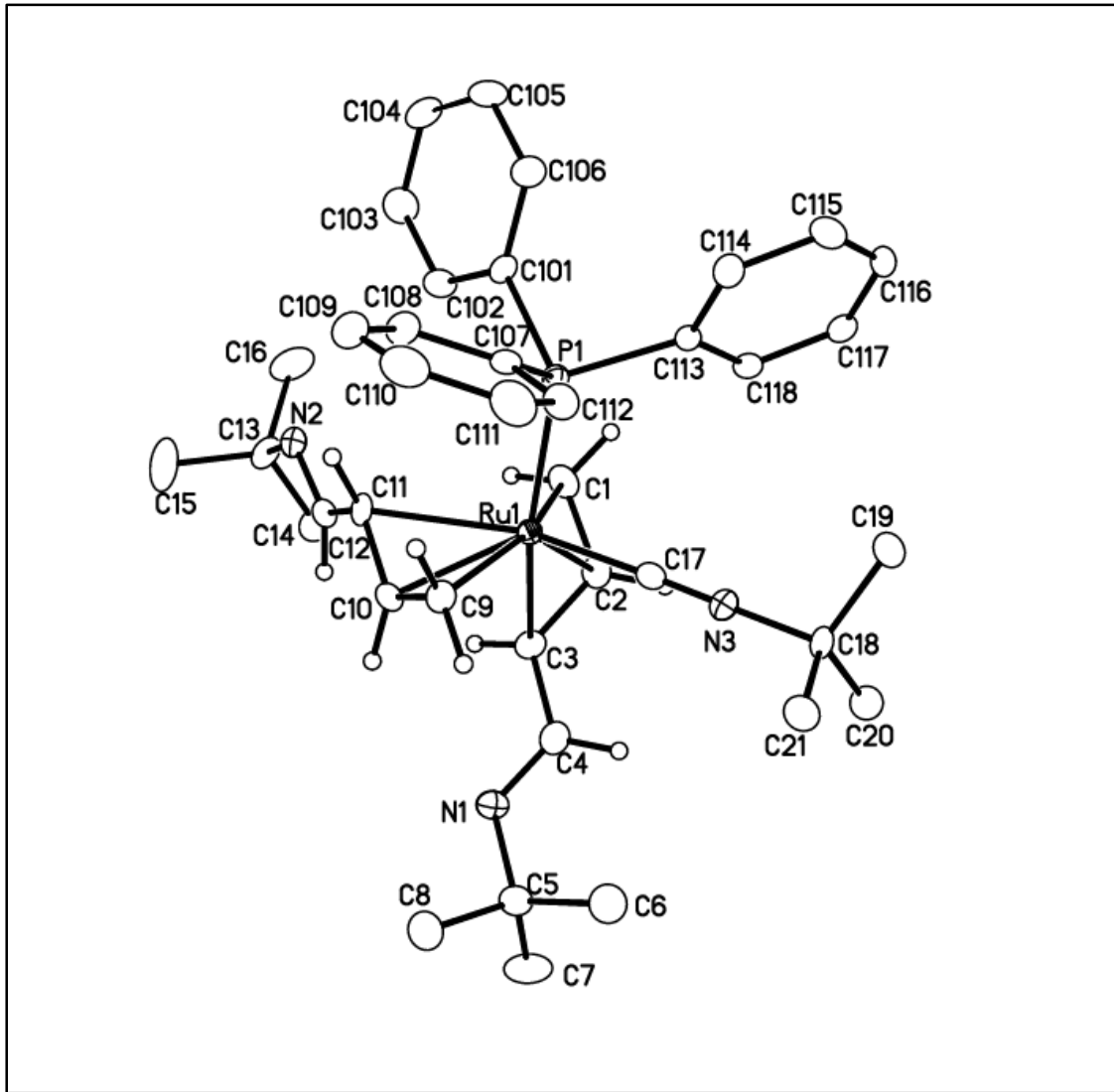
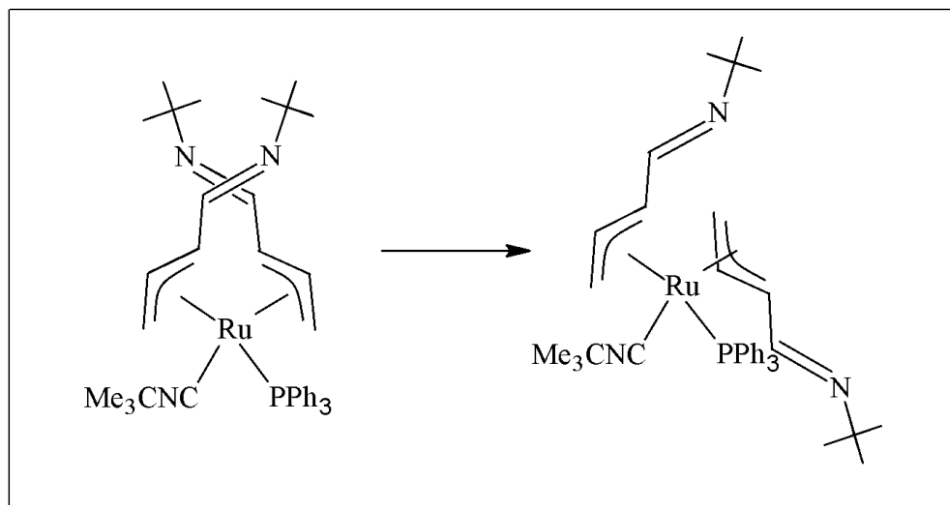


Figure 2.5: Molecular structure of **5**, using thermal ellipsoids at the 50% probability level. The methyl H's on the CNCMe_3 and PPh_3 ligands and on the *tert*-butyl group are not shown. Selected bond distances (\AA): Ru1-P1 , 2.3343(7); Ru1-C17 , 1.927(3); Ru1-C1 , 2.248(2); Ru1-C2 , 2.156(3); Ru1-C3 , 2.236(3); C1-C2 , 1.399(4); C2-C3 , 1.425(3); C3-C4 , 1.452(3); C4-N1 , 1.279(3); N1-C5 , 1.484(3); Ru1-C9 , 2.233(2); Ru1-C10 , 2.156(2); Ru1-C11 , 2.335(2); C9-C10 , 1.404(4); C10-C11 , 1.416(3); C11-C12 , 1.454(3); C12-N2 , 1.276(3); N2-C13 , 1.484(3). Selected bond angles ($^\circ$): C1-Ru1-C9 , 159.93(9); C3-Ru1-P1 , 160.11(6); C11-Ru1-C17 , 154.71(9).

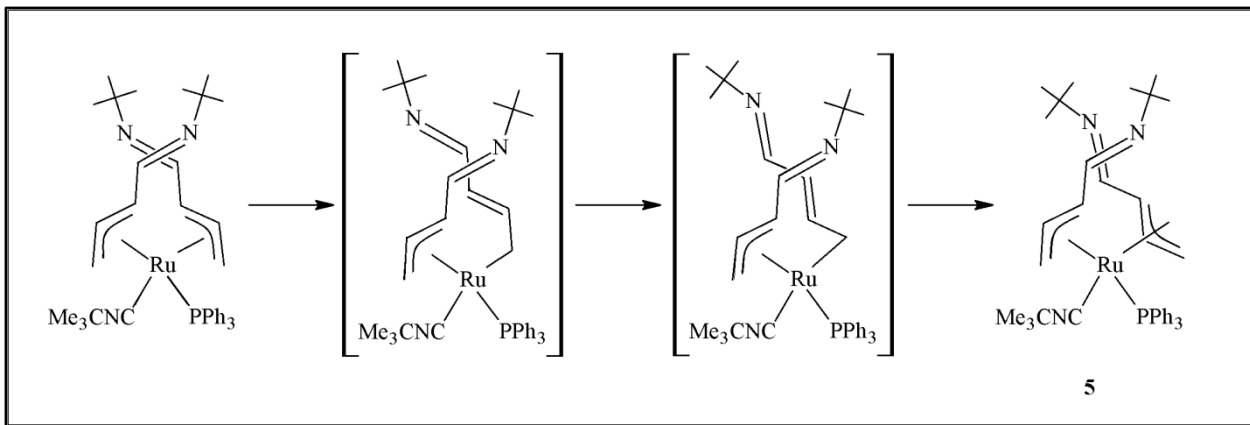
The reason why the CNCMe_3 ligand appeared on the backbone of the azapentadienyl ligand was less clear. Initially, the size of the CNCMe_3 was thought to play a role in ligand orientation; however, other small ligands, PMe_3 (**2**) and $\text{P}(\text{OMe})_3$ (**4**), did not exhibit the “mC3/bC3” structure. CNCMe_3 was the only electron-withdrawing ligand that was used in the reactivity study of **1** that produced an X-ray crystal structure. The crystal structure is needed in order to confirm a “mouth” or “backbone” orientation of each azapentadienyl ligand. For this reason, we could not relate the difference in the structure of **5** to electronics. Although the reason for the structural difference in **5** could not be determined, the mechanism of this transformation can be analyzed. A simple rotation around the Ru-allyl axis would not achieve a “mC3/mC3” to “mC3/bC3” transformation.

As seen in Scheme 2.13,



Scheme 2.13: Mechanism for conversion of structure **A** to structure **E**.

this would put C1 of the rotated azapentadienyl *trans* to the CNCMe_3 , which is not consistent with the crystal structure. In order to achieve the structure seen in **5**, the azapentadienyl must display a ligand shift from η^3 to η^1 , followed by a flip, then reattach to restore the original η^3 bonding mode, as shown in Scheme 2.14.



Scheme 2.14: Proposed mechanism for rearrangement of an azapentadienyl ligand on **5** from “mC3” to “bC3”.

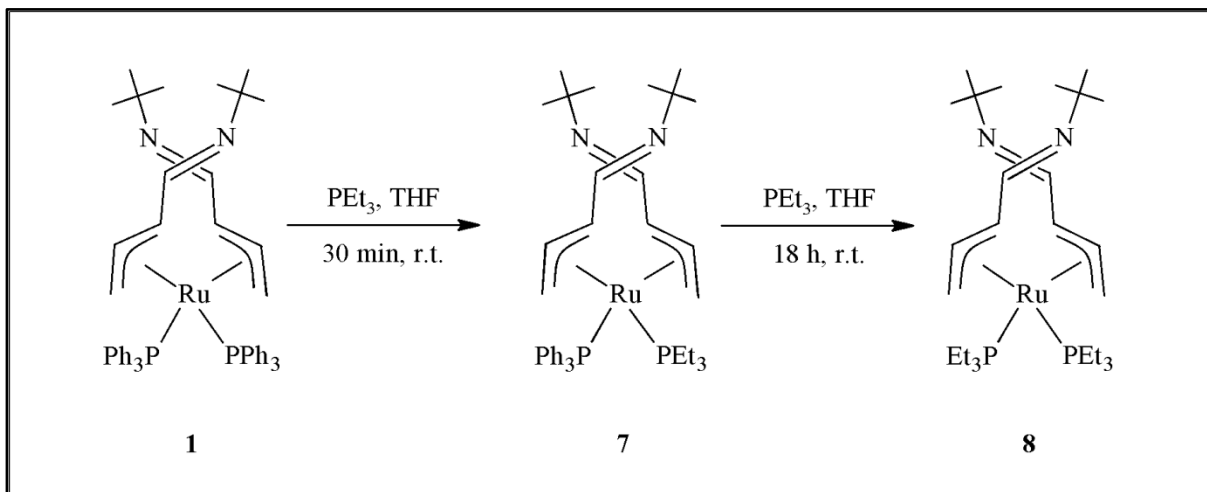
2.2.3.4 Synthesis and Characterization of [(1,2,3- η^3)-(5-*tert*-butylazapentadienyl)]₂Ru(PPh₃)(CO) (**6**)

When carbon monoxide was bubbled through a solution of **1** in THF, a color change from brown-red to orange was seen. ¹H and ³¹P{¹H} NMR analysis showed a mixture of [(1,2,3- η^3)-(5-*tert*-butylazapentadienyl)]₂Ru(PPh₃)(CO) (**6**) and **1**. In the ³¹P{¹H} NMR, one singlet was seen at δ 53.0 representing the single PPh₃ remaining on **6**. As expected, the ¹H NMR showed two sets of ligand signals for the unsymmetrical azapentadienyl ligands. A preliminary inspection of the ¹³C{¹H} NMR showed the C3 signals as a doublet at δ 66.1 (J_{C-P} = 21.6 Hz) and a singlet at δ 65.0, suggesting that one C3 was *trans* to the CO while the other C3 was *trans* to the PPh₃. However, the ¹³C{¹H} NMR did not rule out the possibility of C1 sitting *trans* to the CO ligand. Given this characterization, an assumption could be made that **6** exhibited a structure like **A**, **B**, **C**, **D**, **E**, **F** or **G** (see Figure 2.2), where one C3 lies *trans* to the PPh₃ ligand, and the CO lies *trans* to either the C3 or C1 of the other azapentadienyl. Because the ancillary ligands were not the same, the presence of two azapentadienyl ligand signals in the NMR gave no insight into the ligand orientation around the metal center. CNCMe₃ and CO had the same

characteristics - linear, electron-withdrawing ligand. Knowing the structure of **5** (see above), it seemed likely that **6** was analogous and possessed a “mC₃/bC₃” (**B**) ligand orientation. In order to confirm this, a crystal structure of **6** is needed.

2.2.4 Synthesis and Characterization of [(1,2,3- η^3)-(5-*tert*-butylazapentadienyl)]₂Ru(PPh₃)(PEt₃) (7) and [(1,2,3- η^3)-(5-*tert*-butylazapentadienyl)]₂Ru(PEt₃)₂ (8)

Treatment of **1** with triethylphosphine for short reaction times (e.g., 30 minutes) at room temperature yielded [(1,2,3- η^3)-(5-*tert*-butylazapentadienyl)]₂Ru(PEt₃)₂ (**7**). In solution, compound **7** continued to react with PEt₃, yielding [(1,2,3- η^3)-(5-*tert*-butylazapentadienyl)]₂Ru(PEt₃)₂ (**8**), shown in Scheme 2.15, in 64% yield.



Scheme 2.15: Synthesis of [(1,2,3- η^3)-(5-*tert*-butylazapentadienyl)]₂Ru(PEt₃)₂ (**8**).

Recall that treatment of **1** with smaller neutral ligands (PMe₃, dmpe, P(OMe)₃, CNCMe₃ and CO) yielded single displacement products **2** - **6**, regardless of reaction time. Given the same reaction conditions and similar cone angles, as seen in Table 2.1⁹, a single displacement product was expected when **1** was reacted with triethylphosphine.

Ligand	Cone Angle (°)
P(OMe) ₃	107
dmpe	107
PM ₃	118
PHPH ₂	128
PEt ₃	132
PPh ₃	145

Table 2.1: Cone angles of selected phosphine ligands.

The single displacement product, $\{(1,2,3-\eta^3)-(5\text{-}tert\text{-}butylazapentadienyl)}_2\text{Ru(PEt}_3)(\text{PPh}_3)$ (**7**), could, in fact, be seen via $^{31}\text{P}\{\text{H}\}$ NMR at δ 62.0 (PPh₃) and δ 23.2 (PEt₃) with $J_{\text{P-P}} = 16.2$ Hz after a 30 minute stir time. However, this reaction also yielded **8**. Compound **7** was unable to be isolated, as it did not form as a single product. A poor quality crystal structure was obtained for **7** as seen in Figure 2.6. Compound **7** appeared to be isostructural with **2** and **4**, maintaining the type **A** structure (mC3/mC3).

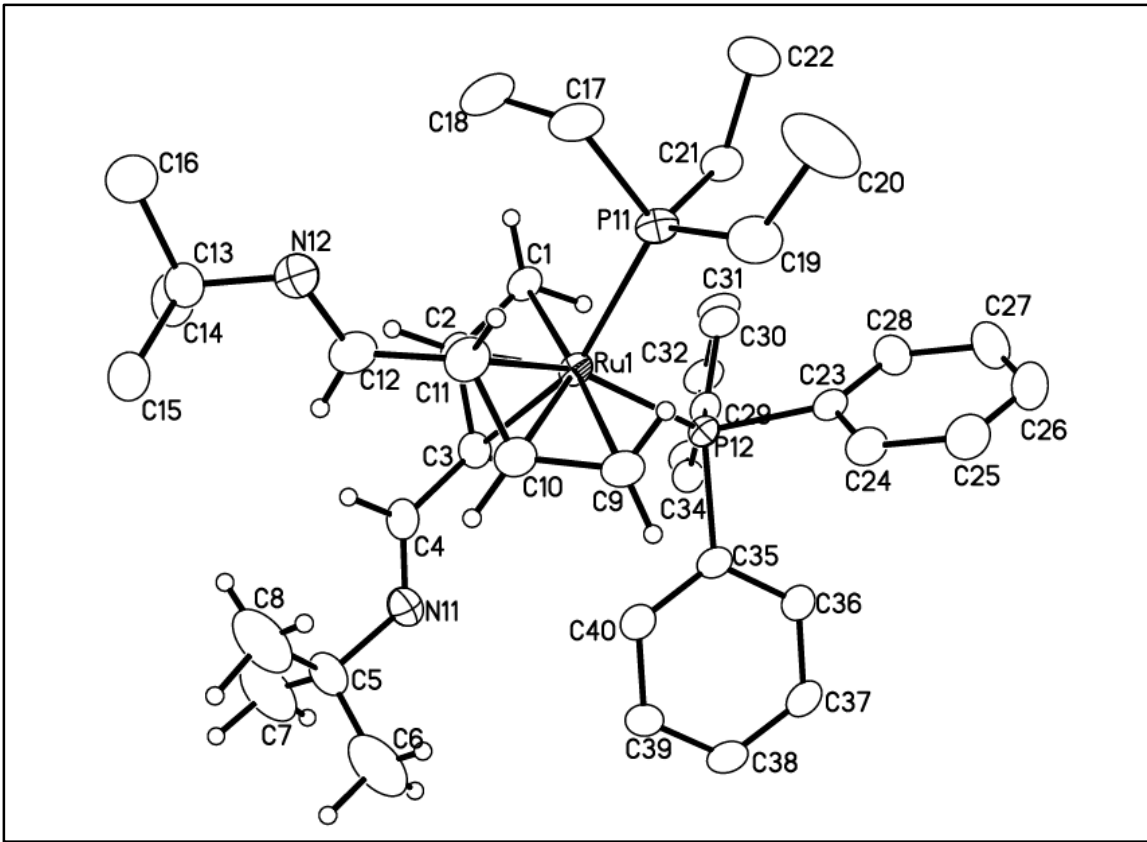


Figure 2.6: Molecular structure of **7**, using thermal ellipsoids at 50% probability level.

The methyl H's on the PEt₃ and PPh₃ ligands and on the *tert*-butyl group are not shown.

Selected bond distances (Å): Ru1-P11, 2.3322(10); Ru1-P12, 2.3162(9); Ru1-C1, 2.237(3); Ru1-C2, 2.167(3); Ru1-C3, 2.352(3); C1-C2, 1.405(5); C2-C3, 1.420(5); C3-C4, 1.453(5); C4-N11, 1.265(5); N11-C5, 1.473(5); Ru1-C9, 2.234(3); Ru1-C10, 2.146(3); Ru1-C11, 2.326(3); C9-C10, 1.400(5); C10-C11, 1.420(5); C11-C12, 1.484(6); C12-N12, 1.259(5); N12-C13, 1.474(5). Selected bond angles (°): P11-Ru1-C3, 153.96(9); P12-Ru1-C11, 153.09(9); C1-Ru1-C9, 176.52(13); P11-Ru1-P12, 97.28(3).

Additional stir time resulted in the single product, **8**. The slight increase in the cone angle of PEt₃, resulting in increased steric bulk around the metal center, promoted the displacement of the second triphenylphosphine ligand. The sum of the cone angles of PPh₃ and

PEt₃ in **7** is 277°. The second substitution seen in **8**, produced a cone angle of 264° which is approximately the same as the sum of the cone angles seen in **2**.⁹

The ¹H NMR spectrum of **8** showed one set of chemically equivalent ligand signals. The chemical shifts of the ligand signals were very similar to those seen in **1** with a downfield signal representing the uncoordinated H4's (δ 7.77) and signals for the H3's (δ 1.80), H2's (δ 4.31), and H1's (δ 2.70/1.39) consistent with *syn-syn* arrangement of the two azapentadienyl ligands. The ³¹P{¹H} NMR showed a singlet at δ 28.4 representing two chemically equivalent triethylphosphines. The ¹³C{¹H} NMR spectrum of **8** showed a downfield singlet at δ 161.8 representing the uncoordinated C4 carbons. The remaining carbon signals appeared further upfield δ 81.6 (C2's), 52.2 (C3's), and 32.4 (C1's). The equivalent C3's had a coupling to the two chemically equivalent, but magnetically inequivalent ³¹P's, resulting in a virtual triplet¹⁰ (J_{C3-P} = 16.5 Hz) in the pseudo-octahedral coordination environment of **8**. This virtual triplet was due to strong coupling of the two phosphorus atoms in the AA'X spin system. In this spin system A and A' represented the ³¹P nuclei while X is the C3. The J-value was the separation in Hz between the outer lines of the virtual triplet and was equal to the absolute value of ($J_{AX} + J_{A'X}$). The equivalent C1's also appeared as a triplet with a smaller coupling (J_{C1-P} = 4 Hz), proving the C1's were sitting *cis* to the two ³¹P nuclei. The infrared spectrum showed the C=N stretch at 1623.9 cm⁻¹.

The X-ray crystal structure of **8** is presented in Figure 2.7; selected bond distances are presented in the caption. The structure of **8** was the A structure where both C3's were *trans* to the two PEt₃ ligands.

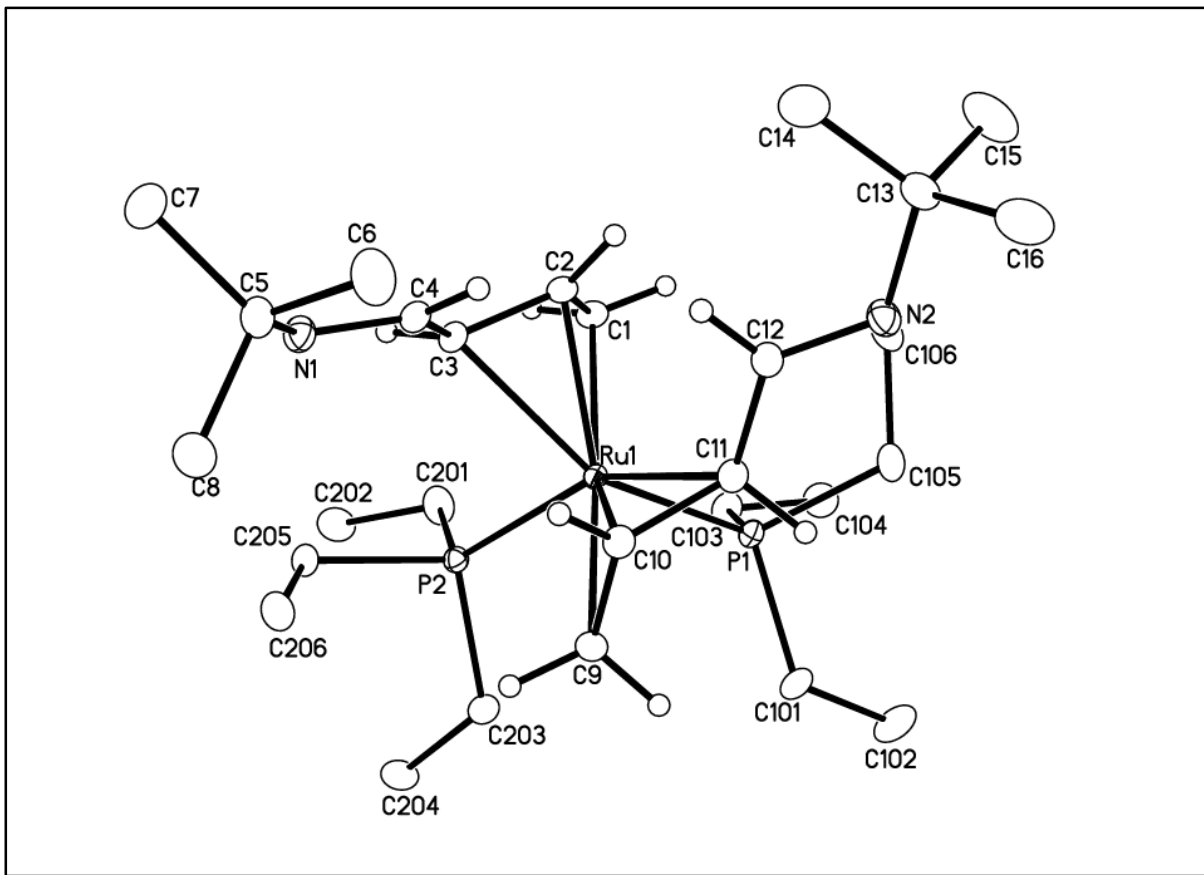


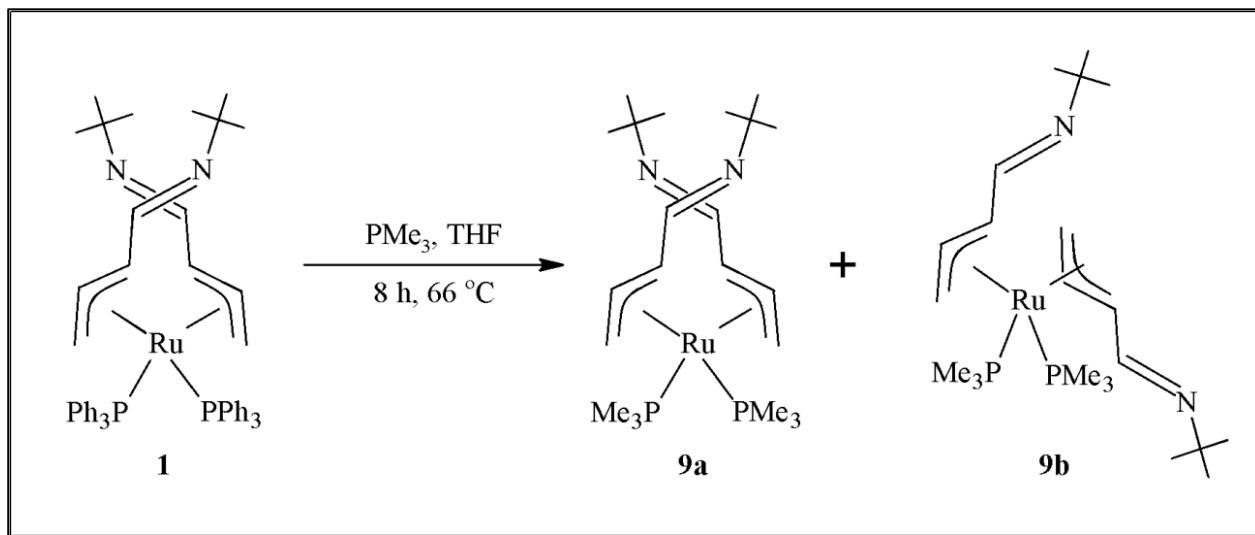
Figure 2.7: Molecular structure of **8**, using thermal ellipsoids at the 50% probability level. The methyl H's on the PEt₃ ligands and on the *tert*-butyl group are not shown. Selected bond distances (Å): Ru1-P1, 2.3274(3); Ru1-P2, 2.3442(2); Ru1-C1, 2.2372(9); Ru1-C2, 2.1507(8); Ru1-C3, 2.3231(8); C1-C2, 1.4140(12); C2-C3, 1.4248(12); C3-C4, 1.4570(12); C4-N1, 1.2783(12); N1-C5, 1.4776(12); Ru1-C9, 2.2437(9); Ru1-C10, 2.1571(8); Ru1-C11, 2.3142(8); C9-C10, 1.4132(12); C10-C11, 1.4246(12); C11-C12, 1.4561(12); C12-N2, 1.2805(11); N2-C13, 1.4750(12). Selected bond angles (°): P1-Ru1-C3, 153.64(2); P2-Ru1-C11, 152.98(2); C1-Ru1-C9, 176.16(3); P1-Ru1-P2; 97.354(9).

2.2.5 Treatment of Compound **1** with Neutral, 2e⁻ Donor Ligands at Elevated Temperatures

Treatment of **1** with a variety of neutral, two electron donor ligands in THF at reflux yielded a mixture of products for each respective ligand. Addition of any number of equivalents of PMe₃, P(OMe)₃, or dmpe resulted in a mixture of two isomers (identified by NMR), both showing double substitution of the two triphenylphosphine ligands.

2.2.5.1 Synthesis of [(1,2,3- η^3)-(5-*tert*-butylazapentadienyl)]₂Ru(PMe₃)₂ (**9**)

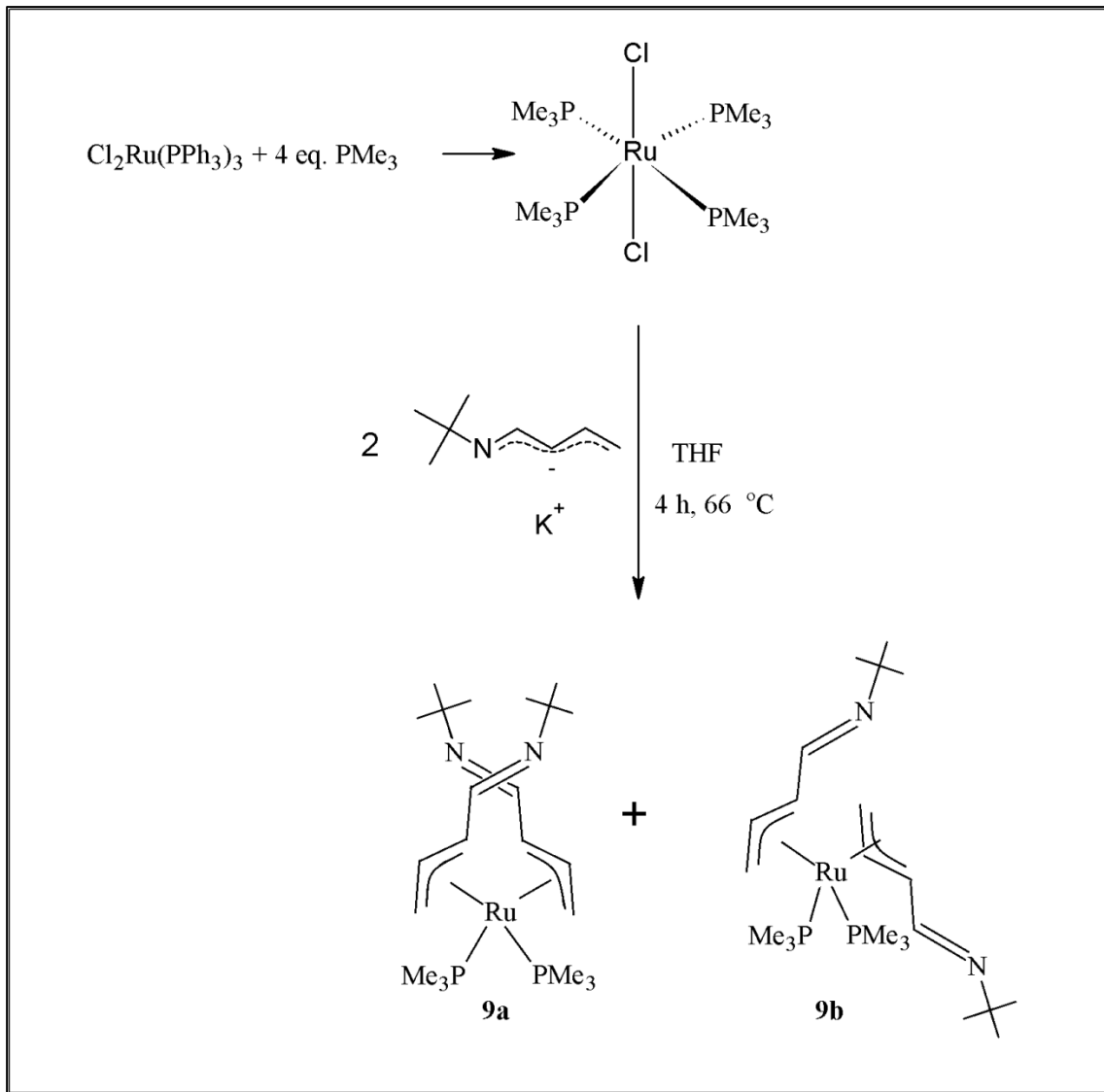
Treatment of **1** with excess PMe₃ in refluxing tetrahydrofuran led to the double substitution of the triphenylphosphine ligands, resulting in [(1,2,3- η^3)-(5-*tert*-butylazapentadienyl)]₂Ru(PMe₃)₂ (**9**) in 87% yield, as seen in Scheme 2.16.



Scheme 2.16: Synthesis of [(1,2,3- η^3)-(5-*tert*-butylazapentadienyl)]₂Ru(PMe₃)₂ (**9**).

A shortened reflux time showed a mixture of compounds **1**, **2**, and **9**, proving formation of **2** before **9**. Compound **9** could also be synthesized from **2** with the addition of an extra equivalent

of PMe_3 , as well as via a $\text{Cl}_2\text{Ru}(\text{PMe}_3)_4$ ¹¹ starting material with the addition of at least two equivalents of potassium *tert*-butylazapentadienide⁶, as seen in Scheme 2.17.



Scheme 2.17: Synthesis of **9** from $\text{Cl}_2\text{Ru}(\text{PMe}_3)_4$.

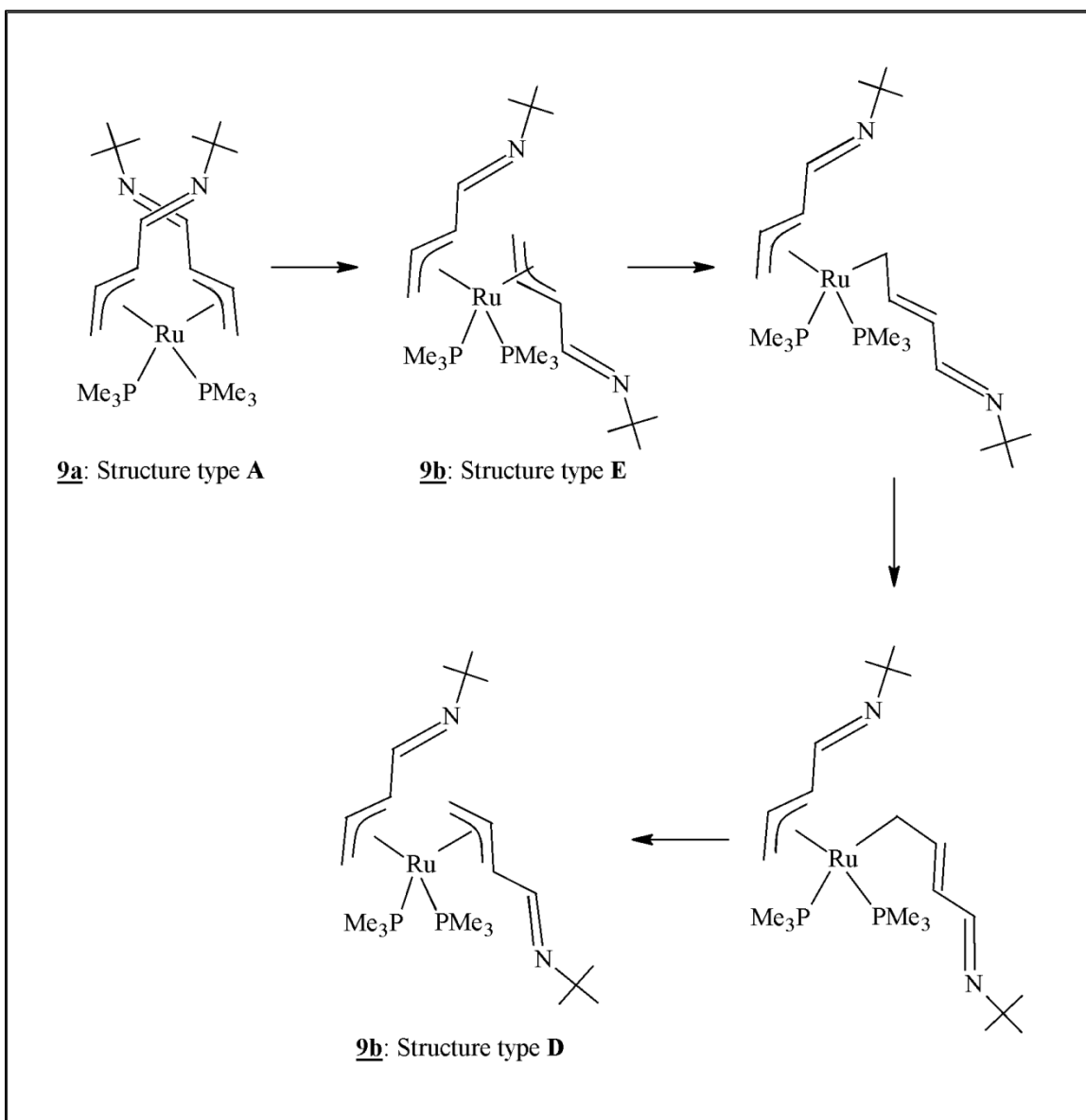
The $^{31}\text{P}\{^1\text{H}\}$ NMR spectrum of **9** showed two isomers in a 55:45 equilibrium mixture. The major isomer **9a** gave rise to a singlet at $\delta 10.5$ while the minor isomer **9b**, is represented by two doublets at $\delta 9.5$ ($J_{\text{P-P}} = 31.6 \text{ Hz}$) and 1.6 ($J_{\text{P-P}} = 31.6 \text{ Hz}$). Based on the $^{31}\text{P}\{^1\text{H}\}$ NMR spectrum, the major isomer, **9a**, had two-fold rotational symmetry, very similar to compound **1**.

The $^{13}\text{C}\{^1\text{H}\}$ NMR spectrum of the major isomer showed typical chemical shifts for C1-C4. The C3 signal at δ 54.7 appeared as a characteristic virtual triplet¹⁰ with $J = 16.0$ Hz. Like compound **8**, the spin system AA'X could be applied where A and A' were representative of the PMe₃'s and X represented C3. The *trans* relationship between C3 and the PMe₃'s was confirmed by the large coupling. The C1 signal at δ 35.4 appeared as a triplet as well. This triplet showed a C-P coupling of only 4.1 Hz. This smaller coupling confirmed a *cis* relationship between the C1 and PMe₃'s. The NMR features of **9a** were consistent with mC3/mC3 (**A**) or bC3/bC3 (**C**). Given the similarities in the NMR spectra to **8**, compound **9a** most likely had a mC3/mC3 orientation.

Based on the pair of doublets, seen in the $^{31}\text{P}\{^1\text{H}\}$ NMR, representing the minor isomer **9b**, the two-fold symmetry was broken. The two azapentadienyl ligands were no longer chemically equivalent due to an apparent ligand rearrangement. The $^{13}\text{C}\{^1\text{H}\}$ NMR gave insight into the new ligand orientations of **9b**. The C3 signals appeared as a triplet at δ 57.0 ($J_{\text{C-P}} = 3.0$ Hz) and a doublet of doublets at δ 53.1 ($J_{\text{C-P}} = 19.4, 3.7$ Hz). These splitting patterns were very telling in determining the orientation of both azapentadienyl ligands.

The C3 signal that appeared as a doublet of doublets is the “expected” multiplicity as it sat *trans* to one ^{31}P nuclei and *cis* to the other. The other C3 signal that showed the weakly coupled triplet ($J_{\text{C-P}} = 3.0$ Hz) indicated that C3 sits *cis* to both PMe₃'s, where the PMe₃'s were coupled as well. Similarly, the C1 region of the $^{13}\text{C}\{^1\text{H}\}$ NMR spectrum showed the same pattern – one C1 resonated as a doublet of doublets ($J_{\text{C-P}} = 22.2$ Hz, 5.5 Hz) while the other C1 showed a triplet ($J_{\text{C-P}} = 3.7$ Hz). Like in the case of the C3's, the C1 that appeared as a doublet of doublets is the usual splitting pattern for the C1 being *trans* to one PMe₃ and *cis* to the other PMe₃. The other C1 that appeared as a weakly coupled triplet was *cis* to both PMe₃. With this information, it was determined that **9b** must have had one of the structures **D**, **E**, **F**, or **G**, shown

schematically in Figure 2.2. The most likely structure of **9b** was **E** (mC3/bC1). A simple 180° rotation around the Ru-allyl axis of one of the azapentadienyl ligands of **9a** would result in a mC3/bC1 (**E**) ligand orientation. The only other possible structure that was likely is **D** (mC3/mC1). To obtain the ligand orientation seen in **D**, a conversion of **9a** to **9b** was possible with a rotation and flip (via an η^1 -intermediate) of one of the azapentadienyl ligands, as seen in Scheme 2.18.



Scheme 2.18: Proposed mechanism for conversion of structure **A** to structure **E** and structure **D**.

2.2.5.2 Synthesis and Characterization of [(1,2,3- η^3)-(5-*tert*-butylazapentadienyl)]₂Ru[P(OMe)₃]₂ (**10**)

Treatment of **1** with excess P(OMe)₃ in refluxing THF resulted in a double substitution of both triphenylphosphine ligands, resulting in [(1,2,3- η^3)-(5-*tert*-butylazapentadienyl)]₂Ru[P(OMe)₃]₂ (**10**) in a 73% yield. Compound **10** could also be formed from **4**, when treated with an additional equivalent of P(OMe)₃ in refluxing THF. Also, **10** could be synthesized like **9**, using a Cl₂Ru[P(OMe)₃]₄ starting material as seen in Scheme 2.17.

The ³¹P{¹H} NMR spectrum showed two isomers, **10a** and **10b**, in a 80:20 equilibrium mixture. The major isomer **10a** appeared as a singlet proving the presence of a two-fold rotational symmetry. In order to confirm the orientation of each azapentadienyl ligand, the C3 and C1 regions of the ¹³C{¹H} NMR were inspected. The C3 signal of **10a** showed a virtual triplet⁹ (J_{C-P} = 27.4 Hz). The large splitting proved that C3 sits *trans* to the P(OMe)₃. The C1 signal also appeared as a triplet with much smaller coupling ($J < 4$ Hz) indicating a weak *cis* coupling to each ³¹P nucleus. With this information, the structure of **10a** could be narrowed down to **A** (mC3/mC3) or **C** (bC3/bC3). Given the similarities in NMR spectra to previous compounds, **10a** most likely had a “mC3/mC3” (**A**) orientation. The ¹H and ¹³C{¹H} NMR were analogous to other symmetrical compounds **1**, **8**, and **9a**.

The minor isomer, **10b**, gave rise to two doublets in the ³¹P{¹H} NMR. The concentration of this isomer was too low to analyze its ¹H and ¹³C{¹H} NMR spectra. Because of the similarities in the sizes of trimethylphosphine and trimethyl phosphite ligands (Table 2.1), as

well as the similarities in reactivities in the monosubstituted compounds **2** and **4**, it is likely that the minor isomer **10b** behaved similarly to **9b** and probably had a mC3/bC1 (**E**) orientation.

2.2.5.3 Synthesis and Characterization of [(1,2,3- η^3)-(5-*tert*-butylazapentadienyl)]₂Ru(dmpe) (**11**)

As previously discussed, the reaction of **1** with 1,2-*bis*(dimethylphosphino)ethane (dmpe) at room temperature resulted in the coordination of one of the phosphorus atoms, but not both. The same reaction done in refluxing THF led to [(1,2,3- η^3)-(5-*tert*-butylazapentadienyl)]₂Ru(dmpe) (**11**). The ³¹P{¹H} NMR showed two singlets as well as a pair of doublets in the appropriate region (40-55 ppm) for coordinated dmpe. The singlets appeared at δ 54.5 and 44.8 and were probably due to two different isomers of **11**, each containing symmetrical azapentadienyl ligands. The doublets appeared at δ 53.6 and 43.9 (J_{P-P} = 21.7 Hz). These doublets most likely corresponded to an isomer of **11** containing two unsymmetrical azapentadienyl ligands. Further inspection of the ¹H NMR and COSY showed the presence of four signals in the 7.0-8.0 ppm region that could correspond to four H4 signals. A speculation could be made that two of the four possible H4 signals corresponded to the complex containing the unsymmetrical azapentadienyl ligands, while the remaining two potential H4 signals corresponded to two different complexes each containing symmetrical azapentadienyl ligands. Without full characterization (more specifically ¹³C{¹H} spectra) and crystallization, the ten possible structures in Figure 2.2 could not be narrowed down.

2.3 Summary and Comparisons

This chapter described the synthesis, structure, and spectroscopy of eleven new *bis*-azapentadienyl-ruthenium-phosphine complexes. The reaction of Cl₂Ru(PPh₃)₃⁸ with potassium *tert*-butylazapentadienide⁶ led to the formation of [(1,2,3- η^3)-(5-*tert*-

$\text{butylazapentadienyl}]_2\text{Ru}(\text{PPh}_3)_2$ (**1**). Compound **1** was treated with various neutral, $2e^-$ donor ligands in order to probe its reactivity. Ligands were chosen with a variety of cone angles as well as differing electronics. When reacted with **1**, ligands with smaller cone angles underwent a monosubstitution of PPh_3 at room temperature, resulting in $[(1,2,3-\eta^3)-(5\text{-}tert\text{-butylazapentadienyl})]_2\text{Ru}(\text{PPh}_3)(\text{L})$ where $\text{L} = \text{PMe}_3$ (**2**), dmpe (**3**), $\text{P}(\text{OMe})_3$ (**4**), CNCMe_3 (**5**), and CO (**6**). A larger ligand, PEt_3 , when reacted with **1** at room temperature, resulted in a *bis*-substitution of the PPh_3 ligands, $[(1,2,3-\eta^3)-(5\text{-}tert\text{-butylazapentadienyl})]_2\text{Ru}(\text{PEt}_3)_2$ (**8**). Treatment of **1** with the smaller phosphines (PMe_3 , $\text{P}(\text{OMe})_3$, and dmpe) at elevated temperatures also resulted in the double displacement of the PPh_3 ligands, forming $[(1,2,3-\eta^3)-(5\text{-}tert\text{-butylazapentadienyl})]_2\text{Ru}(\text{L})_x$ where $\text{L} = \text{PMe}_3$, $x = 2$ (**9**); $\text{L} = \text{P}(\text{OMe})_3$, $x = 2$ (**10**); and $\text{L} = \text{dmpe}$, $x = 1$ (**11**). These reactions gave a mixture of isomers. Compounds **1-11** exhibited different ligand orientations where the ancillary ligands were either *trans* to the C3's or the C1's of the azapentadienyl ligands and either in the mouth or on the backbone of the η^3 -allyl portion of the azapentadienyl ligands.

2.3.1 Comparisons with *Mono-Azapentadienyl-Ruthenium-Phosphine Complexes*

As previously discussed, Paz-Sandoval and Ernst⁴ synthesized a series of *mono*-azapentadienyl-ruthenium-phosphine complexes (see Scheme 2.4) using a covalent tin enimine reagent. It was our desire to uncover a synthetic route that produced the desired compound **1** in higher yield at moderate conditions. A more reactive ionic reagent, potassium *tert*-butylazapentadienide, was chosen to accomplish this goal. Surprisingly, we did not obtain **1**, but were able to synthesize the first series of *bis*-azapentadienyl-ruthenium complexes. It is important to note that these reactions were done in good yield under moderate reaction conditions. The *mono*-azapentadienyl-ruthenium system was reacted with 1 and 2 equivalents of

PPh_2 and showed substitution reactions that were similar to those seen in the *bis*-azapentadienyl-ruthenium system. A key feature of the Paz-Sandoval work was the U-shaped, *anti*- conformation seen in **I**. The additional bonding through the N lone pair filled a coordination site and reduced the need for a second azapentadienyl ligand (as seen in our system). Our desire to achieve a *mono*-azapentadienyl-ruthenium complex led us to protonation reactions, described in Chapter 3.

2.4 Experimental

2.4.1 General Comments on Experimental Techniques

All manipulations were carried out under a nitrogen atmosphere, using either glovebox or double-manifold Schlenk techniques. Solvents were stored under nitrogen after being distilled from the appropriate drying agents. Deuterated NMR solvents were obtained in sealed vials and used as received. $\text{Cl}_2\text{RuPPh}_3^8$ and potassium *tert*-butylazapentadienide⁶ were prepared by literature procedures. $\text{RuCl}_3 \cdot 3\text{H}_2\text{O}$ (Pressure Chemical Co.), triphenylphosphine (Aldrich), *tert*-butyl isocyanide (Aldrich), trimethyl phosphite (Aldrich), trimethyl phosphine (Aldrich), triethylphosphine (VWR), high-purity carbon monoxide gas (Praxair) and trifluoromethanesulfonic acid (VWR and Aldrich) were used as received.

NMR experiments were performed on a Varian Unity Plus-300 spectrometer (^1H , 300 MHz; ^{13}C , 75 MHz; ^{31}P , 121 MHz), a Varian Inova-300 spectrometer (^1H , 300 MHz; ^{13}C , 75 MHz; ^{31}P , 121 MHz), a Varian Unity-500 spectrometer (^1H , 500 MHz; ^{13}C 125 MHz; ^{31}P , 202 MHz), or a Varian Unity-600 spectrometer (^1H , 600 MHz; ^{13}C , 150 MHz; ^{31}P , 242 MHz). ^1H and ^{13}C spectra were referenced to tetramethylsilane, while ^{31}P spectra were referenced to external H_3PO_4 . HMQC (^1H -detected multiple quantum coherence), DEPT (distortion-less enhancement by polarization transfer) and COSY (correlation spectroscopy) experiments aided

in assigning some of the ^1H and ^{13}C peaks. In all of the NMR spectra, carbon atoms and associated hydrogens are numbered by starting at the end of the chain *opposite* nitrogen.

Mass spectra were obtained on a high resolution quadrupole time-of-flight (Q-ToF) mass spectrometer (Maxis 4G) using electrospray ionization (ESI) as source. Infrared spectra were obtained on a Perkin-Elmer Spectrum BX FT-IR spectrometer.

2.4.2 Synthesis of $[(1,2,3\text{-}\eta^3)\text{-}(5\text{-}tert\text{-}butylazapentadienyl})]_2\text{Ru}(\text{PPh}_3)_2$ (**1**)

Potassium *tert*-butylazapentadienide (0.17 g, 1.0 mmol) was added to a stirred solution of $\text{Cl}_2\text{Ru}(\text{PPh}_3)_3$ (0.46 g, 0.48 mmol) in 100 mL of tetrahydrofuran (THF). The resulting red-brown solution was stirred at room temperature overnight. After removal of the solvent under vacuum, the remaining solid was then triturated with pentane. The resulting precipitate was filtered and washed with pentane, giving a yellow-brown microcrystalline powder. Yield: 0.20 g (48 %).

High resolution ESI-MS: calcd for $[\text{M} + \text{H}]^+$ ($\text{C}_{52}\text{H}_{59}\text{N}_2\text{RuP}_2^+$), 875.3206; found, 875.3194.

IR (Nujol mull): $1615.8\text{ cm}^{-1}(\text{C}=\text{N})$.

^1H NMR (THF-d₈, 22 °C): δ 7.86 (d, $J_{\text{H}4\text{-H}3} = 7.8$ Hz, 2, H4's), 7.50-6.60 (m, 30, PPh₃'s), 4.53 (m, 2, H2's), 3.03 (m, 2, H1's), 1.80 (m, 2, H3's), 1.30 (s, 18, *tert*-butyl's), 1.15 (m, 2, H1's).

$^{13}\text{C}\{\text{H}\}$ NMR (THF-d₈, 22 °C): δ 164.7 (s, C4's), 138.2-127.8 (m, PPh₃'s), 86.2 (s, C2's), 58.5 (s, *tert*-butyl C's), 55.6 (filled-in d, $J_{\text{C-P}} = 18.3$ Hz, C3's), 47.2 (s, C1's), 32.1 (s, *tert*-butyl CH₃'s).

$^{31}\text{P}\{\text{H}\}$ NMR (THF-d₈, 22 °C): δ 57.6 (s, 2, PPh₃'s).

2.4.3 Synthesis of $[(1,2,3\text{-}\eta^3)\text{-}(5\text{-}tert\text{-}butylazapentadienyl})]_2\text{Ru}(\text{PPh}_3)(\text{PMe}_3)$ (**2**)

Compound **1** (0.23 g, 0.26 mmol) was dissolved in 45 mL tetrahydrofuran. Trimethylphosphine (0.26 g, 3.42 mmol) was added and the resulting solution was stirred for 2 h at room temperature.

During this time, the solution changed from dark red-brown to yellow-orange. After removal of the solvent under vacuum, the residue was then extracted with pentane and filtered through Celite. Removal of the pentane under vacuum yielded **2** as an orange oil. The residue was dissolved in a small quantity of diethyl ether and cooled to -30 °C. Yellow crystals of **2** formed overnight. Yield: 0.10 g (56 %)

High resolution ESI-MS: calcd for [M + H]⁺ (C₃₇H₅₃N₂RuP₂⁺), 689.2732; found, 689.2742.

IR (Nujol mull): 1621.7 cm⁻¹(C=N).

¹H NMR (acetone-d₆, 22 °C): δ 7.94 (d, J_{H4-H3} = 8.4 Hz, 1, H4), 7.87 (d, J_{H4'-H3'} = 7.2 Hz, 1, H4'), 7.50-6.75 (m, 15, PPh₃), 4.58 (m, 1, H2), 4.49 (m, 1, H2'), 2.72 (m, 1, H1'), 2.49 (m, 1, H1), 1.82 (m, 1, H3), 1.69 (m, 1, H3'), 1.60 (m, 1, H1'), 1.34 (s, 9, *tert*-butyl), 1.21 (s, 9, *tert*-butyl), 1.16 (d, J_{H-P} = 8.1 Hz, 9, PMe₃), 0.92 (m, 1, H1).

¹³C{¹H} NMR (acetone-d₆, 22 °C): δ 162.1 (s, C4'), 161.6 (s, C4), 137.8-127.5 (m, PPh₃), 84.9 (s, C2), 82.3 (s, C2'), 56.5 (s, *tert*-butyl C), 56.4 (s, *tert*-butyl C), 55.1 (d, J_{C-P} = 20.6 Hz, C3), 52.4 (d, J_{C-P} = 19.4 Hz, C3'), 42.2 (s, C1), 40.9 (s, C1'), 30.5 (s, *tert*-butyl CH₃'s), 30.1 (s, *tert*-butyl CH₃'s), 17.6 (d, J_{C-P} = 26.3 Hz, PMe₃).

³¹P{¹H} NMR (acetone-d₆, 22 °C): δ 64.1 (d, J_{P-P} = 19.8 Hz, 1, PPh₃), 6.6 (d, J_{P-P} = 19.8 Hz, 1, PMe₃).

2.4.4 Synthesis of [(1,2,3- η^3)-(5-*tert*-butylazapentadienyl)]₂Ru(PPh₃)(dmpe) (**3**)

Compound **1** (0.26 g, 0.29 mmol) was dissolved in 40 mL tetrahydrofuran. 1,2-*bis*(dimethylphosphine)ethane (dmpe) (0.13 g, 0.85 mmol) was added and the resulting solution was stirred for 2 h at room temperature. During this time, the solution changed from dark red-brown to a lighter orange-red color. After removal of the solvent under vacuum, the residue was

then extracted with pentane and filtered through Celite. Removal of the pentane under vacuum yielded **3** as a light orange oil. Yield: 0.15 g (68 %).

¹H NMR (acetone-d₆, 22 °C): δ 7.91 (d, J_{H4-H3'} = 8.4 Hz, 1, H4), 7.82 (d, J_{H4'-H3'} = 7.5 Hz, 1, H4'), 7.70-6.80 (m, 15, PPh₃), 4.54 (m, 1, H2'), 4.44 (m, 1, H2), 2.68 (m, 1, H1), 2.50 (m, 1, H1'), 1.80 (m, 1, H3), 1.75 (m, 1, H1), 1.60 (m, 1, H3'), 1.31 (s, 9, *tert*-butyl), 1.19 (s, 9, *tert*-butyl), 0.80 (m, 1, H1').

³¹P{¹H} NMR (acetone-d₆, 22 °C): δ 63.8 (d, J_{P-P} = 13.8 Hz, 1, PPh₃), 14.2 (dd, J_{P-P} = 19.7 Hz, 1, dmpe), -47.2 (d, J_{P-P} = 21.3 Hz, 1, dmpe) .

2.4.5 Synthesis of [(1,2,3-*η*³)-(5-*tert*-butylazapentadienyl)]₂Ru(PPh₃)₂[P(OMe)₃] (**4**)

Compound **1** (0.23 g, 0.26 mmol) was dissolved in 45 mL tetrahydrofuran. Trimethyl phosphite (0.15 g, 1.21 mmol) was added and the resulting solution was stirred for 3 h at room temperature. During this time, the solution changed from dark red-brown to yellow-orange. After removal of the solvent under vacuum, the residue was then extracted with pentane and filtered through Celite. Removal of the pentane under vacuum yielded **4** as a yellow-orange oil. The residue was dissolved in a minimal amount of diethyl ether and cooled to -30°C. Orange crystals of **4** formed overnight. Yield: 0.16 g (83 %).

High resolution ESI-MS: calcd for [M + H]⁺ (C₃₇H₅₃O₃N₂RuP₂⁺), 737.2577; found, 737.2580.

IR (Nujol mull): 1622.4 cm⁻¹(C=N).

¹H NMR (acetone-d₆, 22 °C): δ 7.91 (d, J_{H4-H3'} = 8.7 Hz, 1, H4'), 7.86 (d, J_{H8-H7} = 8.1 Hz, 1, H4), 7.70-7.20 (m, 15, PPh₃), 4.52 (m, 2, H2/H2'), 3.42 (d, J_{H-P} = 10.5 Hz, 9, P(OMe)₃), 2.93 (m, 2 H1/H1'), 2.47 (m, 1, H3'), 2.25 (m, 1, H1), 1.76 (m, 1, H3), 1.34 (s, 9, *tert*-butyl), 1.22 (s, 9, *tert*-butyl), 0.70 (m, 1, H1').

$^{13}\text{C}\{\text{H}\}$ NMR (acetone-d₆, 22 °C): δ 161.8 (s, C4'), 161.7 (s, C4), 137.5-126.1 (m, PPh₃), 86.5 (s, C2), 84.7 (s, C2'), 56.5 (s, *tert*-butyl C's), 54.0 (d, $J_{\text{C-P}} = 32.1$ Hz, C3), 52.4 (d, $J_{\text{C-P}} = 20.6$ Hz, C3'), 52.4 (d, $J_{\text{C-P}} = 8.0$ Hz, P(OMe)₃), 42.1 (s, C1), 39.5 (s, C1'), 30.3 (s, *tert*-butyl CH₃'s), 29.9 (s, *tert*-butyl CH₃'s).

$^{31}\text{P}\{\text{H}\}$ NMR (acetone-d₆, 22 °C): δ 156.8 (d, $J_{\text{P-P}} = 41.1$ Hz, 1, P(OMe)₃), 62.2 (d, $J_{\text{P-P}} = 41.1$ Hz, 1, PPh₃).

2.4.6 Synthesis of [(1,2,3- η^3)-(5-*tert*-butylazapentadienyl)]₂Ru(CNCMe₃) (**5**)

Compound **1** (0.39 g, 0.45 mmol) was dissolved in 45 mL tetrahydrofuran. *Tert*-butyl isocyanide (0.10 g, 1.2 mmol) was added and the resulting solution was stirred overnight at room temperature. During this time, the solution changed from dark red-brown to yellow-orange. After removal of the solvent under vacuum, the residue was then extracted with pentane and filtered through Celite. Removal of the pentane under vacuum yielded **5** as a yellow oil. The residue was dissolved in a small quantity of diethyl ether and cooled to -30 °C. Yellow crystals of **5** formed overnight. Yield: 0.28 g (89%)

High resolution ESI-MS: calcd for [M + H]⁺ (C₃₉H₅₃N₃RuP⁺), 696.3026; found, 696.2988.

IR (Nujol mull): 1628 cm⁻¹(C=N).

^1H NMR (dichloromethane-d₂, 22 °C): δ ~7.5 (obscured, 1, H4'), ~7.4 (obscured, 1, H4), 7.66-7.10 (m, 15, PPh₃), 4.89 (m, 1, H2), 4.51 (m, 1, H2'), 3.24 (m, 1, H3), 2.66 (d, $J = 10.5$ Hz, 1, H1'), 2.09 (m, 1, H1'), 1.45 (m, 1, H3'), 1.31 (s, 9, *tert*-butyl), 1.24 (s, 9, *tert*-butyl), 1.23 (s, 9, *tert*-butyl), 0.93 (m, 1, H1), 0.41 (m, 1, H1).

$^{13}\text{C}\{\text{H}\}$ NMR (dichloromethane-d₂, 22 °C): δ 160.8 (s, C4'), 160.4 (s, C4), 137.5-127.8 (m, PPh₃), 99.5 (s, C2), 88.3 (s, C2'), 62.9 (d, $J_{\text{C-P}} = 22.9$ Hz, C7), 62.4 (s, C3), 56.0 (s, *tert*-butyl C),

55.8 (s, *tert*-butyl C), 55.7 (s, *tert*-butyl C), 46.3 (s, C1), 40.5 (s, C1'), 31.0 (s, *tert*-butyl CH₃'s), 30.5 (s, *tert*-butyl CH₃'s), 30.0 (s, *tert*-butyl CH₃'s).

³¹P{¹H} NMR (dichloromethane-d₂, 22 °C): δ 53.7 (s, 1, PPh₃).

2.4.7 Synthesis of [(1,2,3- η^3)-(5-*tert*-butylazapentadienyl)]₂Ru(PPh₃)(CO) (6)

Compound **1** (0.38 g, 0.43 mmol) was dissolved in 45 mL tetrahydrofuran. Carbon monoxide was bubbled through the solution for **7.5** h. During this time, a color change from dark red-brown to orange was seen. After removal of the solvent under vacuum, the residue was then extracted with pentane and filtered through Celite. Removal of the pentane under vacuum yielded **6** as an red-orange oil.

¹H NMR (acetone-d₆, 22 °C): δ 7.45 (obsured, 1, H4), 7.40 (obsured, 1, H4'), 7.60-7.20 (m, 15, PPh₃), 5.09 (m, 1, H2), 4.98 (m, 1, H2'), 3.68 (m, 1, H3), 2.86 (m, 1, H1'), 2.27 (m, 1, H1'), 1.88 (m, 1, H3'), 1.10 (m, 1, H1), 0.75 (m, 1, H1), 1.25 (s, 9, *tert*-butyl), 1.09 (s, 9, *tert*-butyl).

¹³C{¹H} NMR (acetone-d₆, 22 °C): δ 160.3 (s, C4), 159.9 (s, C4'), 137.4-128.3 (m, PPh₃), 101.4 (s, C2), 90.0 (s, C2'), 65.9 (d, JC-P = 21.6 Hz, 1, C3'), 65.0 (s, C3), 56.4 (s, *tert*-butyl C), 55.8 (s, *tert*-butyl C), 49.3 (s, C1), 43.2 (s, C1'), 32.1 (s, *tert*-butyl CH₃'s), 31.3 (s, *tert*-butyl CH₃'s).

³¹P{¹H} NMR (acetone-d₆, 22 °C): δ 53.0 (s, 1, PPh₃).

2.4.8 Synthesis of [(1,2,3- η^3)-(5-*tert*-butylazapentadienyl)]₂Ru(PPh₃)(PEt₃) (7)

Compound **1** (0.29 g, 0.33 mmol) was dissolved in 45 mL tetrahydrofuran. Triethylphosphine (0.025 g, 0.21 mmol) was added and the resulting solution was stirred for 30 min at room temperature. During this time, the solution changed from dark red-brown to lighter red-orange. After removal of the solvent under vacuum, the residue was then extracted with pentane and

filtered through Celite. Removal of the pentane under vacuum yielded an oily mixture of **7** and **8** in an approximate 3:1 ratio. Attempts to separate **7** from **8** were unsuccessful.

$^{31}\text{P}\{\text{H}\}$ NMR (acetone-d₆, 22 °C): δ 62.0 (d, $J_{\text{P-P}} = 16.2$ Hz, 1, PPh₃), 23.2 (d, $J_{\text{P-P}} = 16.1$ Hz, 1, PEt₃).

2.4.9 Synthesis of [(1,2,3- η^3)-(5-*tert*-butylazapentadienyl)]₂Ru(PEt₃)₂ (**8**)

Compound **1** (0.35 g, 0.40 mmol) was dissolved in 45 mL tetrahydrofuran. Triethylphosphine (0.12 g, 1.02 mmol) was added and the resulting solution was stirred overnight at room temperature. During this time, the solution changed from dark red-brown to lighter red-orange. After removal of the solvent under vacuum, the residue was then extracted with pentane and filtered through Celite. Removal of the pentane under vacuum yielded **8** as a red oil. The residue was dissolved in a small quantity of diethyl ether and cooled to -30 °C. Orange crystals of **8** formed overnight. Yield: 0.15 g (64%)

Anal. Calcd for C₂₈H₅₈RuN₂P₂: C, 57.41; H, 9.98. Found: C, 57.83; H, 9.95.

IR (Nujol mull): 1623.9 cm⁻¹(C=N).

^1H NMR (acetone-d₆, 22 °C): δ 7.77 (d, $J_{\text{H4-H3}} = 8.1$ Hz, 2, H4's), 4.31 (m, 2, H2's), 2.70 (m, 2, H1's), ~1.8 (obscured, H3's), 1.88-1.71 (m, 12, PEt₃ CH₂'s), 1.39 (m, 2, H1's), 1.16 (s, 18, *tert*-butyl's), 1.08-0.98 (m, 18, PEt₃ CH₃'s).

$^{13}\text{C}\{\text{H}\}$ NMR (acetone-d₆, 22 °C): δ 161.8 (s, C4's), 81.6 (s, C2's), 56.2 (s, *tert*-butyl C's), 52.2 (virtual t, $J_{\text{C-P}} = 16.5$ Hz, C3's), 32.4 (t, $J_{\text{C-P}} = 4.1$ Hz, C1's), 30.3 (s, *tert*-butyl CH₃'s), 21.1 (filled-in d, $J_{\text{C-P}} = 22.9$ Hz, PEt₃ CH₂'s), 8.9 (s, PEt₃ CH₃'s).

$^{31}\text{P}\{\text{H}\}$ NMR (acetone-d₆, 22 °C): δ 28.4 (s, 2, PEt₃'s).

2.4.10 Synthesis of [(1,2,3- η^3)-(5-*tert*-butylazapentadienyl)]₂Ru(PMe₃)₂ (9**)**

Compound **1** (0.36 g, 0.41 mmol) was dissolved in 100 mL tetrahydrofuran. Trimethylphosphine (0.68 g, 8.9 mmol) was added and the resulting solution was refluxed for 8 h. During this time, the solution changed from dark red-brown to lighter red-orange. After removal of the solvent under vacuum, the residue was then extracted with pentane and filtered through Celite. Removal of the pentane under vacuum yielded **9** as a red oil. Yield: 0.18 g (87%)

2.4.10.1 Synthesis of Cl₂Ru(PMe₃)₄.

Cl₂Ru(PPh₃)₃ (1.73 g, 1.8 mmol) was added to 30 mL tetrahydrofuran. Trimethylphosphine (0.55 g, 7.23 mmol) was added and the resulting solution was stirred for 1 h at room temperature. There was an immediate change from a dark brown-red solution with precipitate to a clear yellow solution. After removal of the solvent under vacuum, the remaining white-yellow solid was triturated with pentane. The pale white-yellow solid was collected on a frit. Yield: 0.66 g (86 %)

2.4.10.1 Alternate Synthesis of [(1,2,3- η^3)-5-*tert*-butylazapentadienyl]₂Ru[P(Me)₃]₂ (9**)**

Cl₂Ru(PMe₃)₄ (0.45 g, 0.94 mmol) was dissolved in 100 mL tetrahydrofuran. Potassium *tert*-butylazapentadienide (0.39 g, 2.4 mmol) was added and the solution was refluxed for 4 h. During this time the solution changed from dark red-brown to lighter orange. The solution was allowed to cool, and the solvent was removed under vacuum. The residue was extracted with pentane and filtered through Celite. Removal of the pentane under vacuum yielded **9** as an orange oil. Yield: 0.43 g (91 %).

High resolution ESI-MS: calcd for [M-H]⁺ ($C_{22}H_{47}N_2RuP_2^+$), 503.2259; found, 503.2253.

IR (Nujol mull): 1622.4 cm⁻¹(C=N)

Isomer A (55%)

¹H NMR (acetone-d₆, 22 °C): δ 7.78 (d, $J_{H4\text{-}H3'} = 8.1$ Hz, 2, H4's), 4.43 (m, 2, H2's), 2.34 (m, 2, H1's), 1.76 (m, 2, H3's), 1.5-1.3 (m, 18, PMe₃'s), 1.48 (partially obscured, 2, H1's), 1.19 (s, 18, *tert*-butyl's).

¹³C{¹H} NMR (acetone-d₆, 22 °C): δ 160.8 (s, C4's), 82.8 (s, C2's), 55.9 (s, *tert*-butyl C's), 54.7 (virtual t, $J_{C\text{-}P} = 16.0$ Hz, C3's), 35.4 (t, $J_{C\text{-}P} = 4.1$ Hz, C1's), 30.2 (s, *tert*-butyl CH₃'s), 19.0 (filled-in d, $J_{C\text{-}P} = 28.6$ Hz, PMe₃'s),

³¹P{¹H} NMR (acetone-d₆, 22 °C): δ 10.5 (s, 2, PMe₃'s).

Isomer B (45%)

¹H NMR (acetone-d₆, 22 °C): δ 7.59 (d, $J_{H4'\text{-}H3'} = 7.5$ Hz, 1, H4'), 7.39 (d, 1, H4), 4.40 (m, 1, H2'), 4.38 (m, 1, H2), 2.72 (m, 1, H3), 2.28 (m, 1, H1'), 2.02 (m, 1, H1), 1.78 (m, 1, H3'), 1.5-1.3 (m, 18, PMe₃'s), 1.40 (s, 9, *tert*-butyl), 1.37 (s, 9, *tert*-butyl), 1.36 (partially obscured, 1, H1'), 0.54 (m, 1, H1),

¹³C{¹H} NMR (acetone-d₆, 22 °C): δ 162.3 (s, C4), 161.7 (s, C4'), 85.8 (s, C2), 80.7 (s, C2'), 57.0 (t, $J_{C\text{-}P} = 3.0$ Hz, C3), 56.1 (s, *tert*-butyl C), 55.6 (s, *tert*-butyl C), 53.1 (dd, $J_{C\text{-}P} = 19.4$ Hz, 3.7 Hz, C3'), 33.8 (dd, $J_{C\text{-}P} = 22.2$ Hz, 5.3 Hz, C1), 33.5 (t, $J_{C\text{-}P} = 3.7$ Hz, C1'), 30.0 (s, *tert*-butyl CH₃'s), 29.0 (s, *tert*-butyl CH₃'s), 19.7 (dd, $J_{C\text{-}P} = 26.3$ Hz, 2.6 Hz, PMe₃), 18.2 (dd, $J_{C\text{-}P} = 24.0$ Hz, 2.2 Hz, PMe₃).

³¹P{¹H} NMR (acetone-d₆, 22 °C): δ 9.5 (d, $J_{P\text{-}P} = 31.6$ Hz, 1, PMe₃), 1.6 (d, $J_{P\text{-}P} = 31.6$ Hz, 1, PMe₃).

2.4.11 Synthesis of [(1,2,3- η^3)-(5-*tert*-butylazapentadienyl)]₂Ru[P(OMe)₃]₂, (10)

Compound **1** (0.32 g, 0.37 mmol) was dissolved in 100 mL tetrahydrofuran. Trimethylphosphite (0.20 g, 1.61 mmol) was added and the resulting solution was refluxed for 6 h. During this time, the solution changed from dark red-brown to lighter red-orange. After removal of the solvent under vacuum, the residue was then extracted with pentane and filtered through Celite. Removal of the pentane under vacuum yielded **10** as a red oil. Yield: 0.16 g (72%)

2.4.11.1 Synthesis of Cl₂Ru[P(OMe)₃]₄.

Cl₂Ru(PPh₃)₃ (1.08 g, 1.12 mmol) was added to 30 mL tetrahydrofuran. Trimethyl phosphite (0.56 g, 4.48 mmol) was added and the resulting solution was stirred for 1 h at room temperature. There was an immediate change from a dark brown-red solution with precipitate to a clear yellow solution. After removal of the solvent under vacuum, the remaining white-yellow solid was triturated with pentane. The pale white-yellow solid was collected on a frit. Yield: 0.62 g (83 %)

2.4.11.2 Alternate synthesis [(1,2,3-*η*³)-(5-*tert*-butylazapentadienyl)]₂Ru[P(OMe)₃]₂, (10**)**

Cl₂Ru[P(OMe)₃]₄ (0.45 g, 0.94 mmol) was dissolved in 100 mL tetrahydrofuran. Potassium *tert*-butylazapentadienide (0.39 g, 2.4 mmol) was added and the solution was refluxed for 4 h. During this time the solution changed from dark red-brown to lighter orange. The solution was allowed to cool, and the solvent was removed under vacuum. The residue was extracted with pentane and filtered through celite. Removal of the pentane under vacuum yielded **9** as an orange oil. Yield: 0.43 g (91 %).

High resolution ESI-MS: calcd for [M-H]⁺ (C₂₂H₄₇N₂O₆RuP₂⁺), 599.1954; found, 599.1952.

IR (Nujol mull): 1626.9 cm⁻¹(C=N).

Isomer A (80%)

¹H NMR (acetone-d₆, 22 °C): δ 7.76 (d, J_{H4-H3} = 8.7 Hz, 2, H4's), 4.38 (m, 2, H2's), 3.55 (m, 18, P(OMe)₃'s), 2.73 (m, 2, H1's), 2.42 (m, 2, H3's), 2.15 (m, 2, H1's), 1.19 (s, 18, *tert*-butyl's).

¹³C{¹H} NMR (acetone-d₆, 22 °C): δ 160.5 (s, C4's), 85.5 (s, C2's), 56.3 (s, *tert*-butyl C's), 53.6 (virtual t, J_{C-P} = 27.4 Hz, C3's), 51.3 (br s, P(OMe)₃'s), 35.4 (br t, C1's), 29.9 (s, *tert*-butyl CH₃'s).

³¹P{¹H} NMR (acetone-d₆, 22 °C): δ 168.6 (s, 2, P(OMe)₃'s).

Isomer B (20%)

³¹P{¹H} NMR (acetone-d₆, 22 °C): δ 166.3 (d, J_{P-P} = 54.7 Hz, 1, P(OMe)₃), 163.6 (d, J_{P-P} = 54.7 Hz, 1, P(OMe)₃).

2.4.12 Synthesis of [(1,2,3-*η*³)-(5-*tert*-butylazapentadienyl)]₂Ru(dmpe), (11)

Compound **1** (0.28 g, 0.32 mmol) was dissolved in 100 mL tetrahydrofuran. 1,2-*bis*(dimethylphosphino)ethane (dmpe) (0.21 g, 1.40 mmol) was added and the solution was refluxed for 1 h. After removal of the solvent under vacuum, the residue was extracted with pentane and filtered through Celite. Removal of the pentane under vacuum yield **11** as an orange oil. Yield: 0.10 g (61 %).

Isomer A

³¹P{¹H} NMR (acetone-d₆, 22 °C): δ 54.5 (s, 2, dmpe).

Isomer B

³¹P{¹H} NMR (acetone-d₆, 22 °C): δ 45.0 (s, 2, dmpe)

Isomer C

³¹P{¹H} NMR (acetone-d₆, 22 °C): δ 53.5 (d, J_{P-P} = 21.3 Hz, 1, dmpe), 44.4 (d, J_{P-P} = 21.8 Hz, 1, dmpe).

2.5 References

- (1) Bleeke, J.R.; Anutrasakda, W.; Rath, N.P, *Organometallics*, **2012**, *31*, 2219-2230.
- (2) Bleeke, J.R.; Anutrasakda, W.; Rath, N.P, *Organometallics*, **2013**, *32*, 6410-6426.
- (3) Bleeke, J.R.; Stouffer, M.; Rath, N.P, *J. of Organometallic Chem.*, **2015**, *781*, 11-21.
- (4) Reyna-Madrigal, A.; Moreno-Gurrola, A.; Perez-Camacho, O.; Navarro-Clemente, M.E.; Juarez-Saavedra, P.; Leyva-Ramirez, M.A.; Arif, A.M.; Ernst, R.D.; Paz-Sandoval, M.A. *Organometallics* **2012**, *31*, 7125-7145.
- (5) Paz-Sandoval, M.A.; Powel, P.J. *Organomet. Chem* **1981**, *219*, 81.
- (6) Bleeke, J.R.; Luaders, S.T.; Robinson, K.D. *Organometallics*, **1994**, *13*, 1592-1600.
- (7) Bleeke, J.R.; Rauscher, D.J. *Organometallics* **1988**, *7*, 2328-2339
- (8) (a) Stephenson, T.A.; Wilkinson, G. *J. Inorg. Nucl. Chem.* **1966**, *28*, 945.
(b) Hallman, P.S.; Stephenson, T.A.; Wilkinson, G. *Inorg. Synth.* **1970**, *12*, 237.
- (9) Tolman, C.A. *Chem. Rev.* **1977**, *77*, 313 – 348.
- (10) (a) Becker, E.D. *High Resolution NMR, Theory and Chemical Applications, Second Edition*; Academic Press, New York, **1980**, 149-171.
(b) Crabtree, R.H. *The Organometallic Chemistry of the Transition Metals, Fourth Edition*; John Wiley and Sons, Inc., Hoboken, NJ **2005**, 276-279.
- (11) Holmes, N.J.; Levason, W.; Webster, M. *J. Chem. Soc., Dalton Trans.* **1997**, 4223-4229.

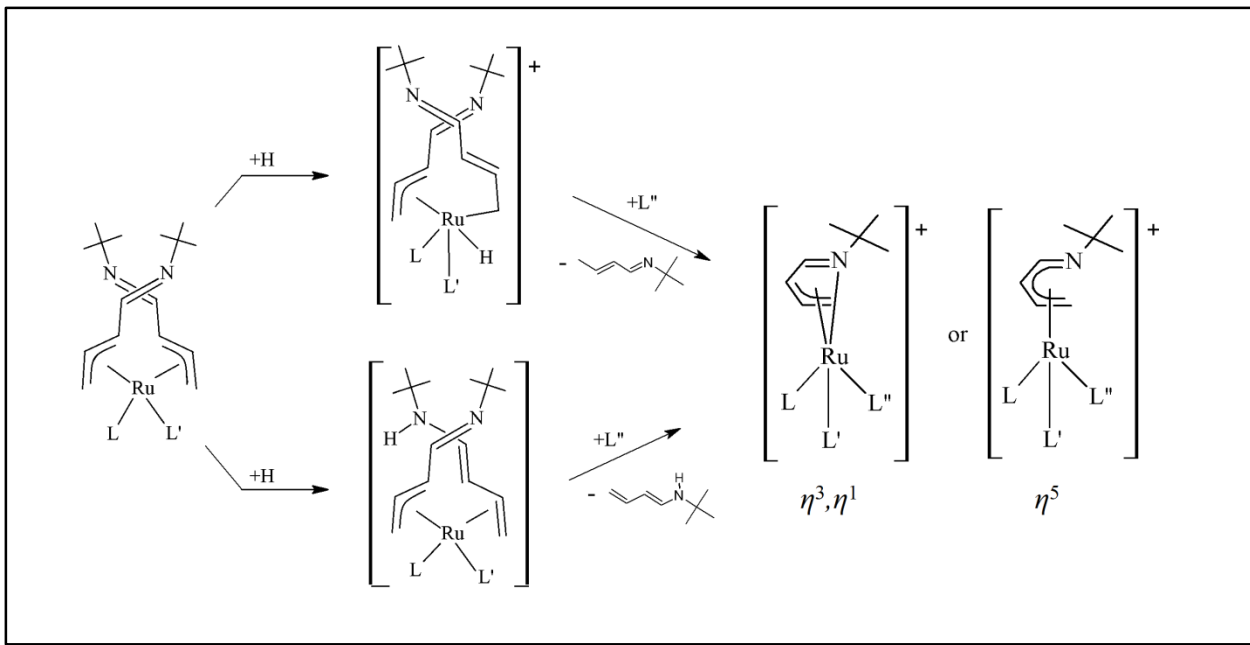
Chapter 3

Protonation of Neutral *bis*-Azapentadienyl-
Ruthenium-Phosphine Complexes

Protonation of Neutral *bis*-Azapentadienyl-Ruthenium-Phosphine Complexes

3.1 Introduction

There are two possible sites of *mono*-protonation on azapentadienyl-ruthenium complexes. When introduced to an acid source, these compounds can either protonate at the metal center or at an N atom. As seen in Scheme 3.1, protonation at the ruthenium metal center (Path 1) could result in an intermediate that could prompt a reductive elimination of a neutral t-butylcrotonaldimine and shift of the remaining η^3 ligand to an η^5 or η^3, η^1 mode with bonding through the nitrogen lone pair. This species could then add a trapping ligand, L" to attain an 18 e⁻ configuration. Similarly, protonation at the nitrogen center (Path 2) could prompt one of the η^3 azapentadienyl ligands to shift to a terminal olefin. Because this ligand is now weakly coordinated to the ruthenium, the presence of an additional ligand, L", could promote the displacement of the neutral t-butylaminobutadiene. This allows the remaining azapentadienyl to shift from η^3 to η^5 or η^3, η^1 with bonding through the allyl moiety and the nitrogen lone pair, filling in the remaining coordination sites around the ruthenium. These potential *mono*-azapentadienyl products are particularly desirable as possible catalysts (see Scheme 1.4).

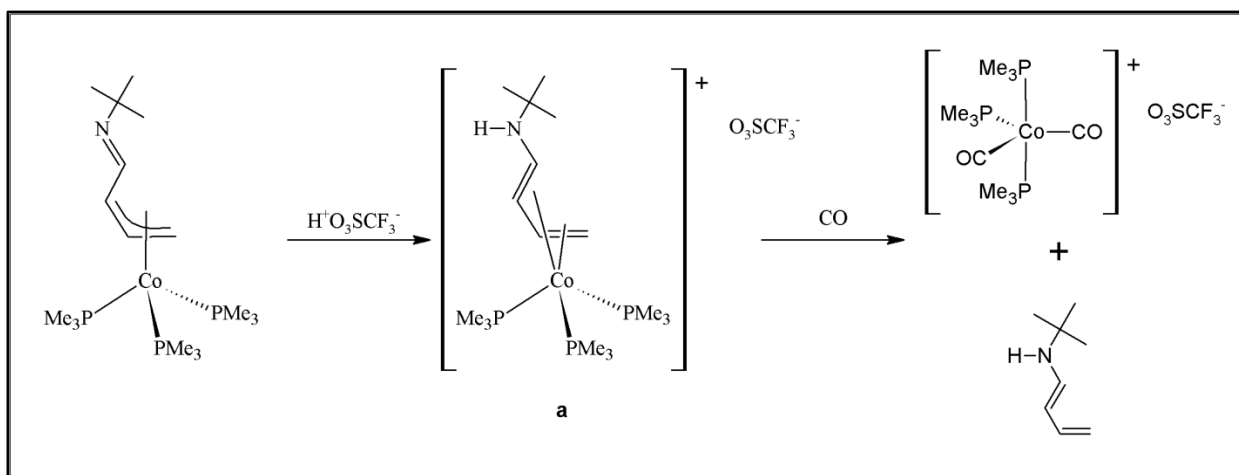


Scheme 3.1: Potential protonation sites of azapentadienyl-ruthenium complexes.

The possibility of double protonation must also be considered, particularly when more than one equivalent of acid is added. One can imagine protonation at M and N, protonation at both N's or even double protonation at a single N. Prior to presenting my results, previous protonation reactions, involving group 9 azapentadienyl complexes are summarized below.

3.1.1 Protonation of Azapentadienyl-Cobalt-Phosphine Complexes

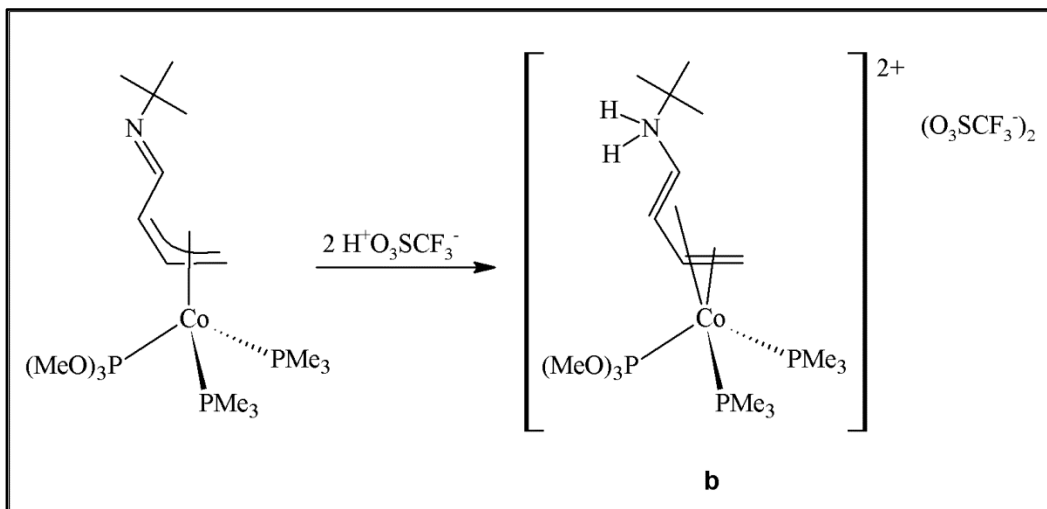
Protonation studies of complexes containing azapentadienyl ligands have been done previously in the Bleeeke group. As seen in Scheme 3.2, ((1,2,3- η^3)-5-*tert*-butylazapentadienyl)Co(PMe₃)₃ was protonated at the nitrogen center, prompting the formation of (η^4 -(*tert*-butylamino)butadiene)Co(PMe₃)₃⁺O₃SCF₃⁻ (**a**).¹



Scheme 3.2: Protonation of $[(1,2,3-\eta^3)-5\text{-}tert\text{-butylazapentadienyl}]Co(PMe_3)_3$.

When the singly protonated cobalt complex (**a**) was reacted with an ancillary ligand, such as CO or P(OMe)₃, displacement of *tert*-butylaminobutadiene and the formation of Co(PMe₃)₃L₂ was seen.

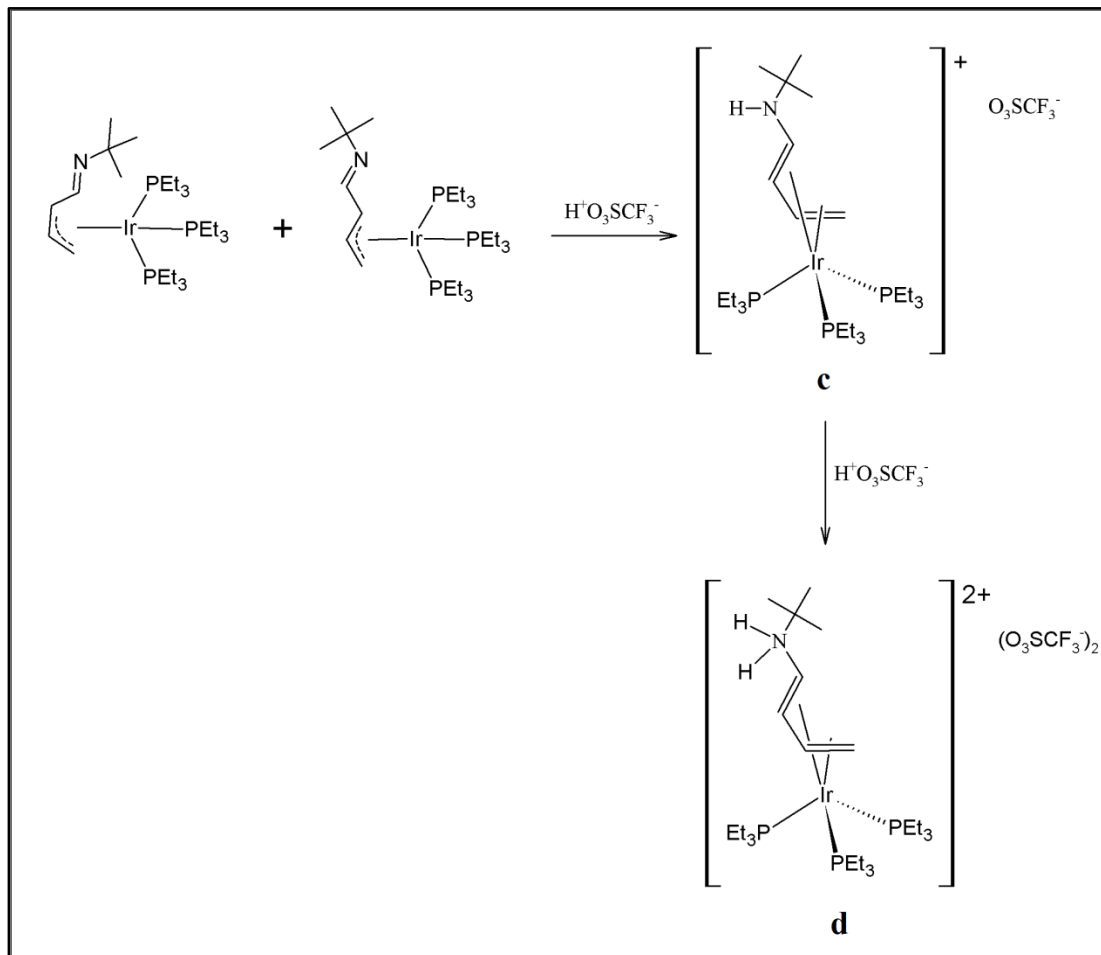
Reaction of the neutral *tert*-butylazapentadienyl-cobalt complexes with two equivalents of triflic acid led to the double protonation at the nitrogen center, while retaining the η^4 -*tert*-butylazapentadiene orientation¹ (see Scheme 3.3).



Scheme 3.3: Synthesis of $(\eta^4\text{-(}tert\text{-butylammonium})\text{butadiene})Co(PMe_3)_2[P(OMe)_3]^{2+}(O_3SCF_3^-)_2$.

3.1.2 Protonation of Azapentadienyl-Iridium-Phosphine Complexes

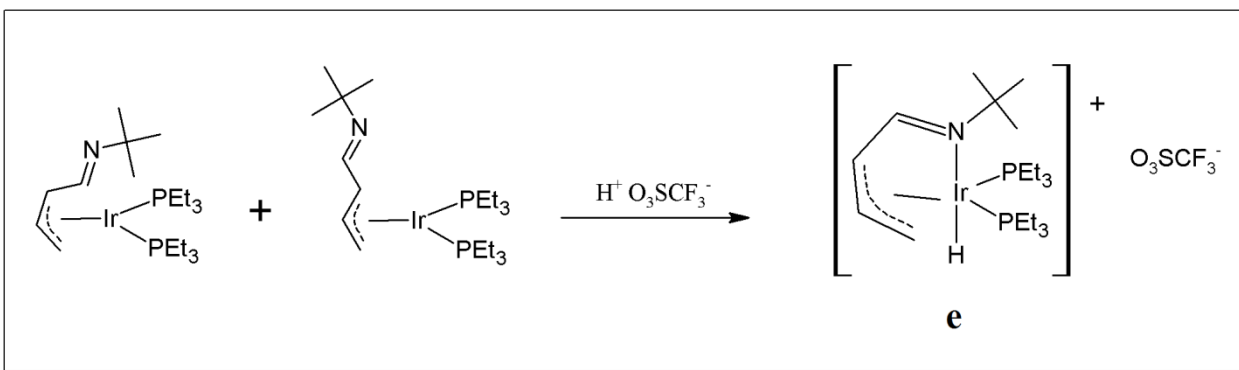
This pattern of protonation at the nitrogen center followed by a ligand rearrangement to an η^4 diene was also seen for $((1,2,3\text{-}\eta^3)\text{-}5\text{-}tert\text{-}butylazapentadienyl})\text{Ir}(\text{PEt}_3)_3$ (see Scheme 3.4).²



Scheme 3.4: Protonation of $((1,2,3\text{-}\eta^3)\text{-}5\text{-}tert\text{-}butylazapentadienyl})\text{Ir}(\text{PEt}_3)_3$.

Addition of a second equivalent of triflic acid led to double protonation at the nitrogen center.

In contrast, the 16e⁻ complex $((1,2,3\text{-}\eta^3)\text{-}5\text{-}tert\text{-}butylazapentadienyl})\text{Ir}(\text{PEt}_3)_2$, when reacted with one equivalent of triflic acid, protonated at the iridium metal center and the η^3 -allyl coordination was retained with additional bonding through the nitrogen lone pair, forming $((1,2,3\text{-}\eta^3, 5\text{-}\eta^1)\text{-}5\text{-}tert\text{-}butylazapentadienyl})\text{Ir}(\text{H})(\text{PEt}_3)_2^+\text{O}_3\text{SCF}_3^-$ (**e**) (see Scheme 3.5).² This

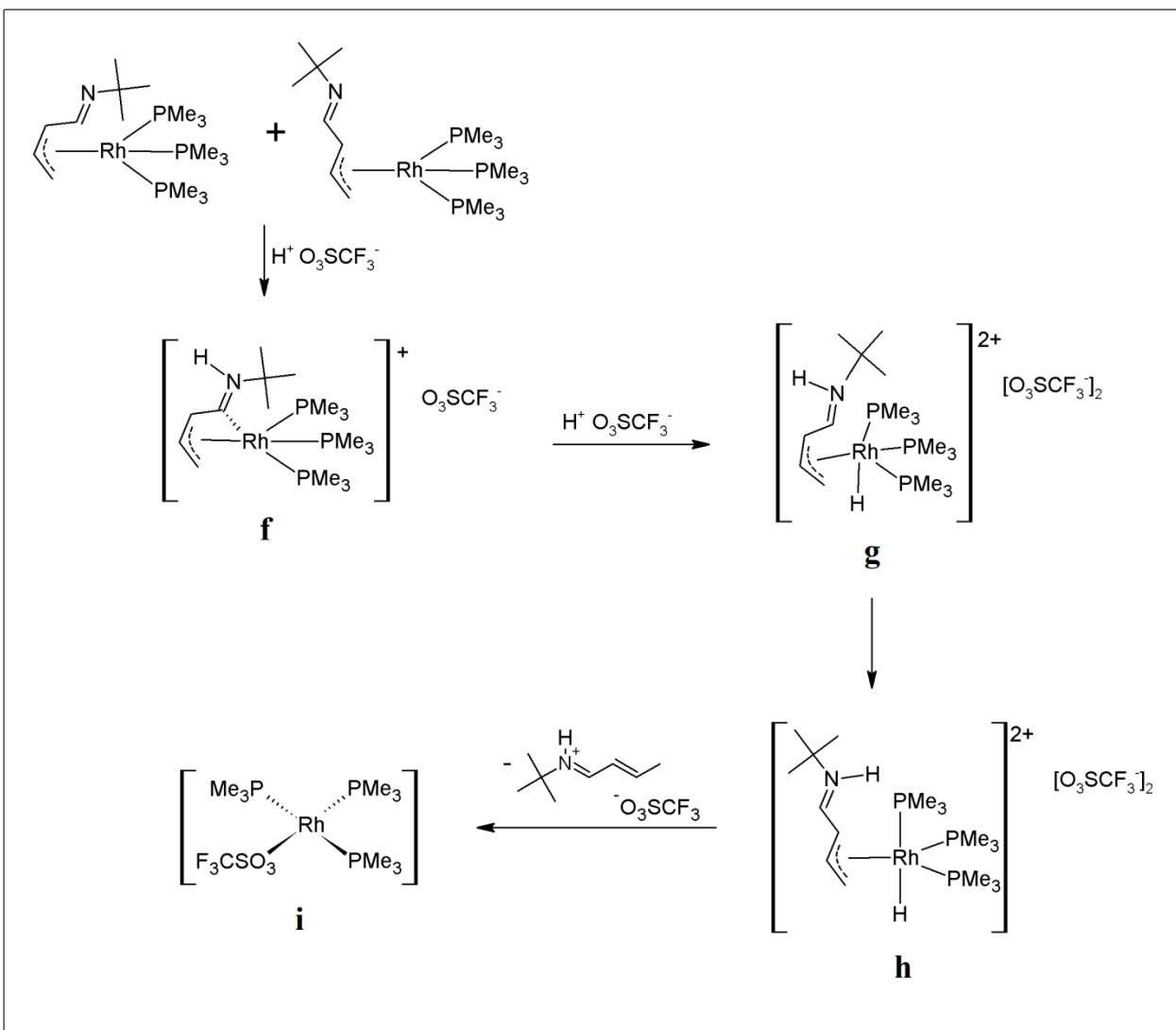


Scheme 3.5: Protonation of $((1,2,3\text{-}\eta^3)\text{-}5\text{-}tert\text{-butylazapentadienyl})\text{Ir}(\text{PEt}_3)_2$.

protonation at the metal center was due to iridium's tendency to assume $18e^-$ octahedral Ir(III) geometries.

3.1.3 Protonation of Azapentadienyl-Rhodium-Phosphine Complexes

Protonation of the *syn*- and *anti*- mixture of neutral $((1,2,3\text{-}\eta^3)\text{-}5\text{-}tert\text{-butylazapentadienyl})\text{Rh}(\text{PMe}_3)_3$ resulted in the monoprotonated product $(\eta^4\text{-}(tert\text{-butylamino})\text{butadiene})\text{Rh}(\text{PMe}_3)_3^+ \text{O}_3\text{SCF}_3^-$ (**f**)², as seen in Scheme 3.6.

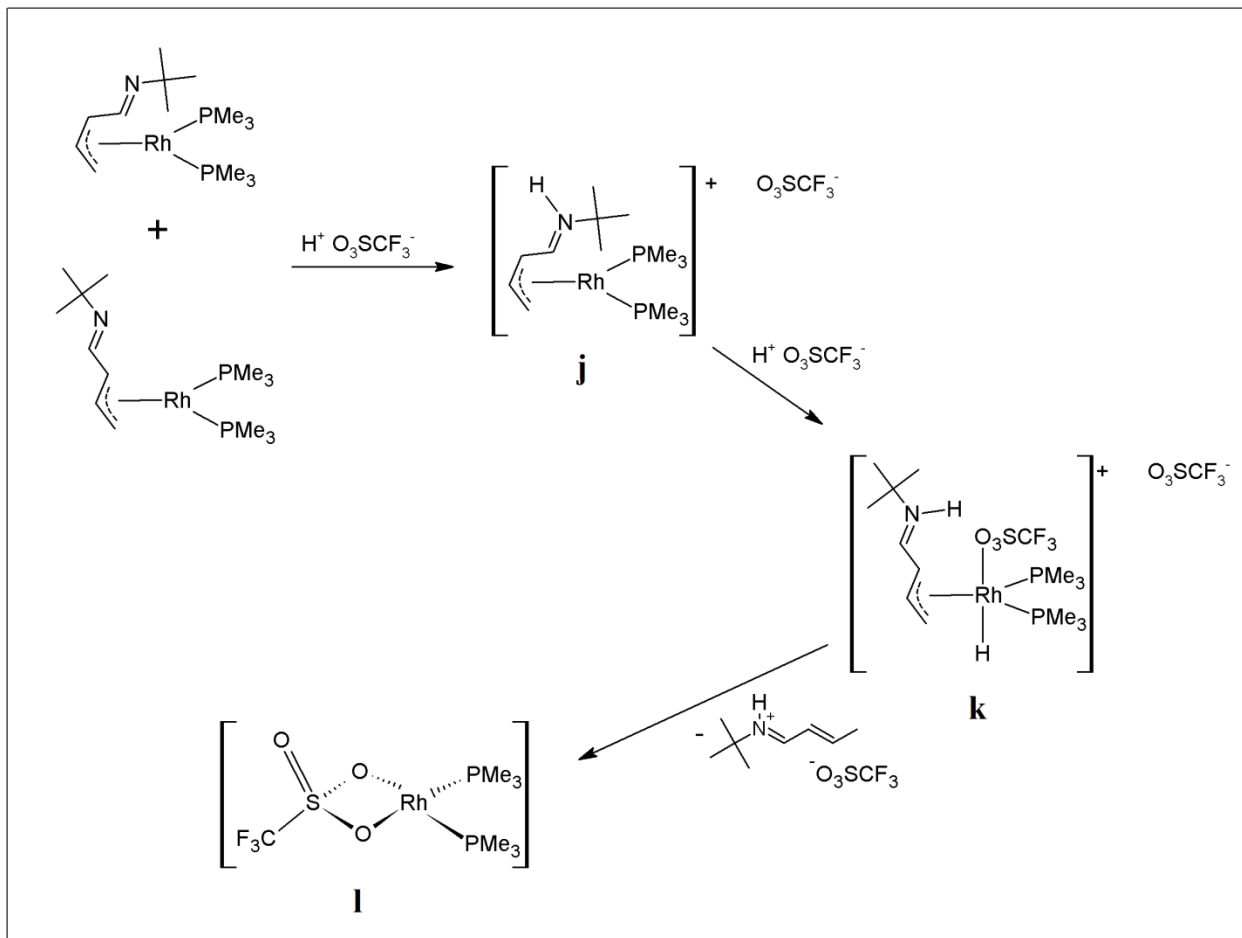


Scheme 3.6: Protonation of $((1,2,3-\eta^3)\text{-}5\text{-}tert\text{-butylazapentadienyl})\text{Rh}(\text{PMe}_3)_3$.

Treatment of **f** with an additional equivalent of triflic acid resulted in protonation at the rhodium center, followed by reductive elimination of the protonated *tert*-butylcrotonaldimine. Before this reductive elimination, the protonated azapentadienyl ligand isomerized from *anti* to *syn* (**h**).

The reaction of $((1,2,3-\eta^3)\text{-}5\text{-}tert\text{-butylazapentadienyl})\text{Rh}(\text{PMe}_3)_2$ with triflic acid resulted in the monoprotonation at the nitrogen center (see Scheme 3.7).² The mixture of *syn*- and *anti*- isomers in the starting material was completely converted to the *anti*- conformation (**j**).

in the monoprotonated product. Similar to the *tris*-PMe₃ system, the introduction of another equivalent of triflic acid resulted in the protonation of the rhodium center (**k**) followed by the reductive elimination of the protonated ligand (**l**).



Scheme 3.7: Protonation of ((1,2,3- η^3)-5-*tert*-butylazapentadienyl)Rh(PMe₃)₂.

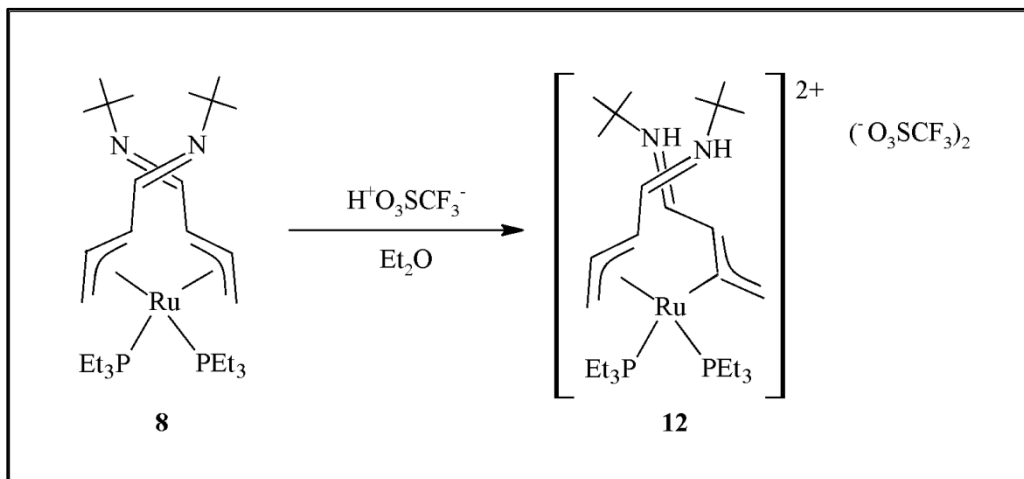
3.2 Results and Discussion

3.2.1 Protonation of [(1,2,3- η^3)-(5-*tert*-butylazapentadienyl)]₂RuL₂ Complexes

In order to investigate the potential protonation sites of the series of *bis-tert*-butylazapentadienyl complexes, [(1,2,3- η^3)-(5-*tert*-butylazapentadienyl)]₂RuL₂, they were reacted with a small electrophile, triflic acid (H⁺). As discussed below, these reactions led to protonation at both nitrogen centers, regardless of how much triflic acid was used.³

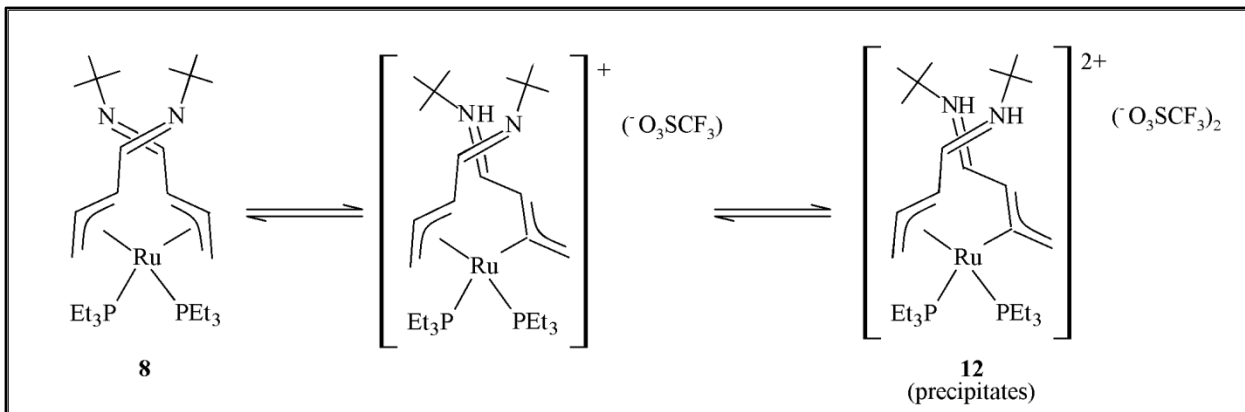
3.2.1.1 Synthesis and Characterization of $\{[(1,2,3-\eta^3)\text{-}(\text{CH}_2\text{CHCHCH=NCH})(\text{CMe}_3)]_2\text{Ru}(\text{PEt}_3)_2\}^{2+}(\text{O}_3\text{SCF}_3)_2$ (**12**)

Treatment of **8** with *one* equivalent of triflic acid in diethyl ether led to the precipitation of a red solid, $\{[(1,2,3-\eta^3)\text{-}(\text{CH}_2\text{CHCHCH=NCH})(\text{CMe}_3)]_2\text{Ru}(\text{PEt}_3)_2\}^{2+}(\text{O}_3\text{SCF}_3)_2$ (**12**), shown in Scheme 3.8. This product showed protonation at both nitrogen centers. This reaction resulted in an 84% yield of **12**, based on the limiting reagent (triflic acid).



Scheme 3.8: Synthesis of $\{[(1,2,3-\eta^3)\text{-}(\text{CH}_2\text{CHCHCH=NCH})(\text{CMe}_3)]_2\text{Ru}(\text{PEt}_3)_2\}^{2+}(\text{O}_3\text{SCF}_3)_2$ (**12**).

After precipitation of **12**, the diethyl ether solution remained an orange-red color. A ¹H and ³¹P{¹H} NMR were taken of the remaining solution and showed the presence of unreacted neutral **8**. The reaction of **8** with *two* equivalents of triflic acid resulted in **12** in a much higher yield (based on starting material **8**). The inability to synthesize the monoprotonated compound would suggest that the monoprotonated compound was more reactive than the neutral starting material. But another possibility is that there was an equilibrium between the neutral, monoprotonated, and diprotonated compounds and that the insolubility of the dicationic salt, **12**, in diethyl ether drove the reaction to the diprotonated product as seen in Scheme 3.9.



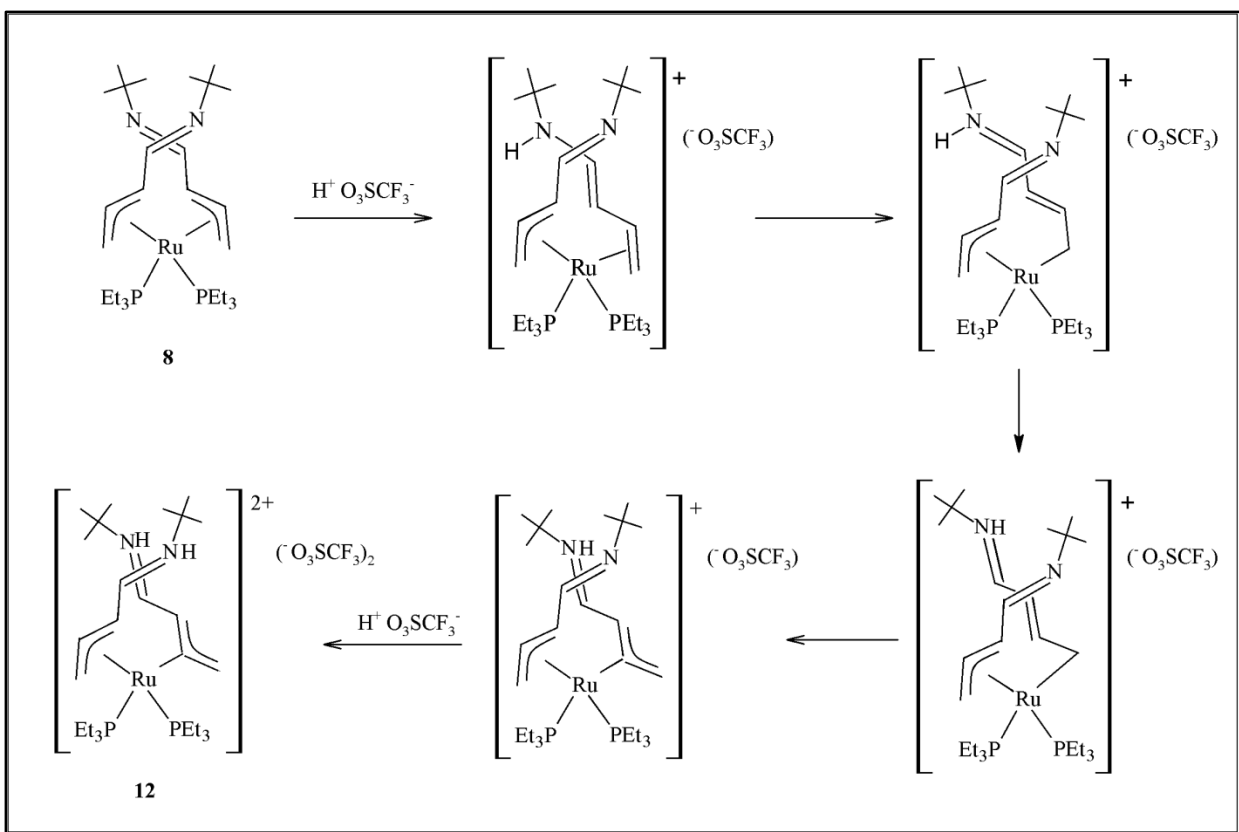
Scheme 3.9: Equilibrium of $[(1,2,3\text{-}\eta^3)\text{-}(5\text{-}tert\text{-}butylazapentadienyl})]_2\text{Ru}(\text{PEt}_3)_2$ (**8**) and its mono- and di- protonated analogues.

The ^1H NMR of **12** showed two sets of ligands signals. Two doublets were seen downfield at δ 10.51 ($J_{\text{NH-H}4} = 15.6$ Hz) and δ 9.76 ($J_{\text{NH-H}4} = 15.3$ Hz) representing the NH protons. The two peaks due to the H4s were each seen as doublet of doublets at δ 8.08 and 7.72 due to splitting by the NH's and H3's. All other ligand signals H3's (δ 3.51/2.92), H2's (δ 5.60/5.43) and H1's (δ 3.49/2.56 and 3.40/2.92) were seen shifted slightly downfield from their positions in the spectrum of neutral **8**. In the ^1H NMR, the location of the H4 signals showed no interaction with the ruthenium metal center, proving retention of the η^3 orientation of both azapentadienyl ligands. In the $^{13}\text{C}\{\text{H}\}$ NMR, two downfield signals at δ 168.3 and 167.1 were seen, representing the two uncoordinated C4s. This data further supported the η^3 arrangement of both azapentadienyl ligands. The C3 signals were both doublets at δ 60.9 ($J_{\text{C-P}} = 12.8$ Hz) and δ 54.0 ($J_{\text{C-P}} = 12.6$ Hz). The doublets arose from the *trans* coupling of the C3's and the PEt₃'s in the pseudo-octahedral coordination geometry of **12**. The C1 signals appeared as weakly coupled doublets ($J_{\text{C-P}} = 3.8$ Hz and 5.3 Hz). These smaller coupling constants confirmed that the C1s lie *cis* to the PEt₃'s. Further supporting the presence of two unsymmetrical ligands was the $^{31}\text{P}\{\text{H}\}$ NMR: a pair of doublets at δ 37.5 ($J_{\text{P-P}} = 31.6$ Hz) and 26.9 ($J_{\text{P-P}} = 31.2$ Hz). With this NMR

evidence, **12** was confirmed to be structure **B** (mC3/bC3) with both C3's *trans* to the PEt₃'s and a mouth/backbone orientation of the azapentadienyl ligands.

The reorientation of one of the azapentadienyl ligands from mouth (in **8**) to backbone (in **12**) most likely proceeded by the same mechanism seen in **5**. In order to achieve the mC3/bC3 structure seen in **12**, an azapentadienyl shift to η^1 , followed by a flip, then reattachment on the opposite face was probable. *When* this rearrangement occurred with respect to the first and second nitrogen protonations was unclear. One possibility was that the first protonation occurred, followed by the azapentadienyl ligand rearrangement to a “backbone” orientation. The second protonation would then “trap” the mC3/bC3 structure.

This rearrangement of one of the azapentadienyl ligands to a backbone orientation may have been due to protonation of one of the nitrogen centers, which could have allowed the affected azapentadienyl ligand to shift to a terminal olefin. The terminal olefin may have been a more direct route to attain the necessary η^1 bonding mode needed to achieve the “backbone” orientation as seen in Scheme 3.10. This is a speculated route of rearrangement, but the order of protonation and ligand conversion from mouth to backbone could not be definitively established.



Scheme 3.10: Possible mechanism for conversion of **8** to **12**.

An X-ray crystal structure of **12** was obtained, confirming the mC3/bC3 (**B**) orientation, shown in Figure 3.1. Based on the crystal structure, P2 sat in the mouth of the allyl portion of the azapentadienyl carbons C9-C11, while P1 sat on the backbone of carbons C1-C3. C3 was approximately *trans* to P2 (C3-Ru1-P2, 152.24(4) $^\circ$) while C11 was *trans* to P1 (C11-Ru1-P1, 151.50(4) $^\circ$). In order to further investigate the structure of **12**, selected bond lengths were compared to the neutral analogue. When **8** was protonated to produce **12**, the C3-C4 bond lengths were shortened (1.4570(12) Å and 1.4567 Å in **8** vs. 1.415(2) Å and 1.401(2) Å in **12**). Also the C4-N bonds lengthened (1.2783(12) Å and 1.2805(11) Å in **8** vs. 1.299(2) Å and 1.306(2) Å in **12**).

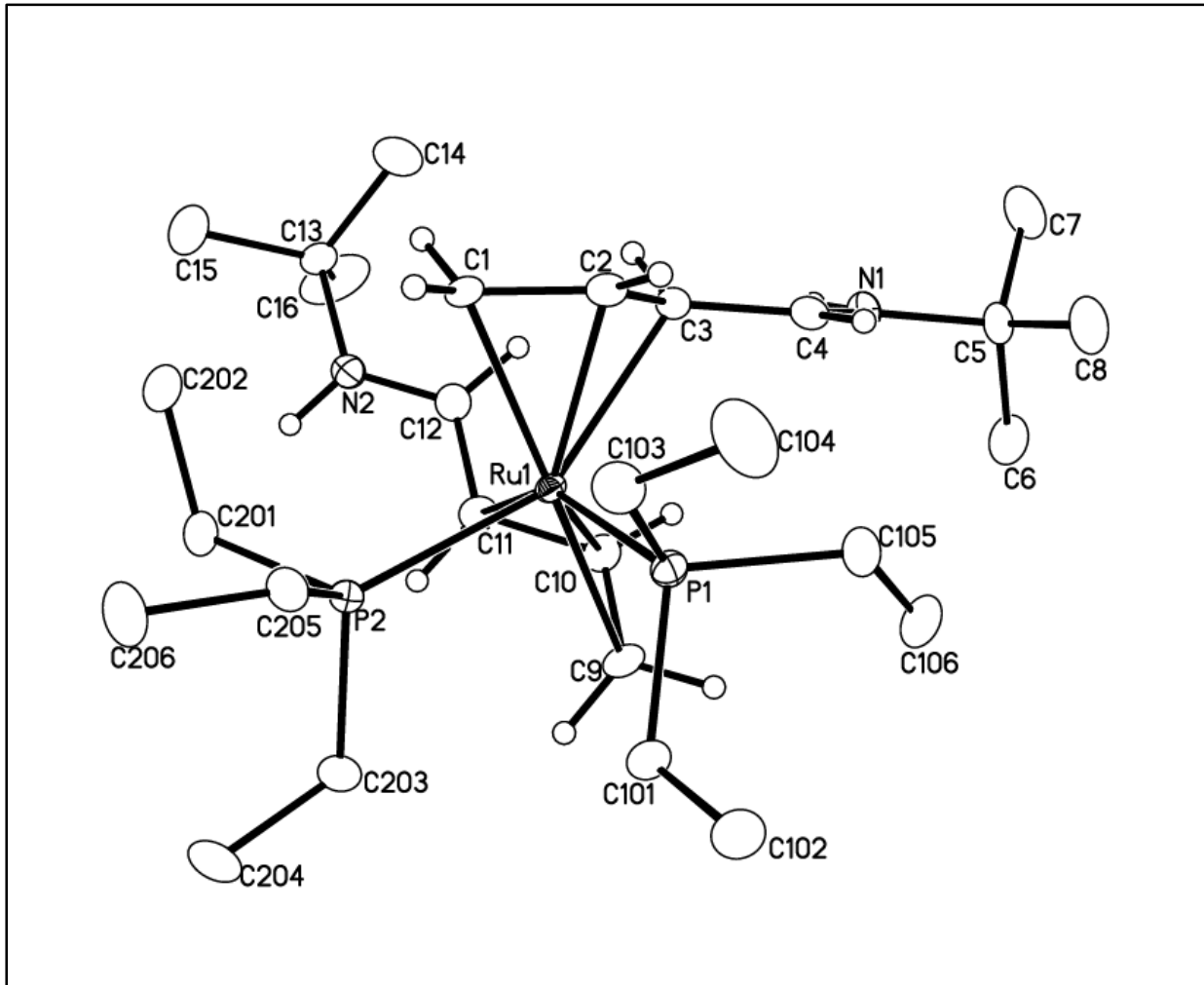


Figure 3.1: Molecular structure of **12**, using thermal ellipsoids at the 50% probability level. The methyl H's on the PEt₃ ligands and on the *tert*-butyl group are not shown. Selected bond distances (Å): Ru1-P1, 2.3209(4); Ru1-P2, 2.3719(4); Ru1-C1, 2.2407(16); Ru1-C2, 2.1683(16); Ru1-C3, 2.3331(15); C1-C2, 1.408(2); C2-C3, 1.425(2); C3-C4, 1.415(2); C4-N1, 1.299(2); N1-C5, 1.489(2); Ru1-C9, 2.2660(16); Ru1-C10, 2.1472(16); Ru1-C11, 2.3781(16); C9-C10, 1.405(2); C10-C11, 1.429(2); C11-C12, 1.401(2); C12-N2, 1.306(2); N2-C13, 1.484(2).

The bond length changes could have possibly been attributed to a small contribution from the η^4 resonance structure in **12** (see Figure 3.2) where the formal positive charge lies on the ruthenium

center. In the infrared spectrum, peaks at 1632 and 1622 cm^{-1} were observed for the C=N stretches.

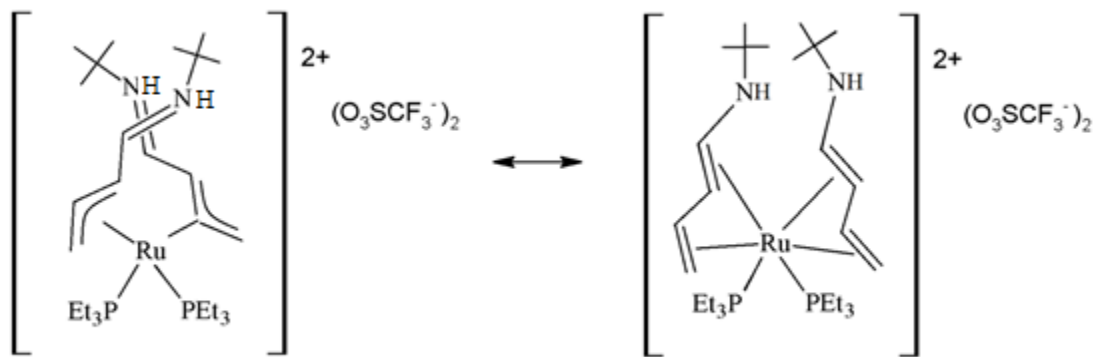


Figure 3.2: Two possible resonance structures of **12**.

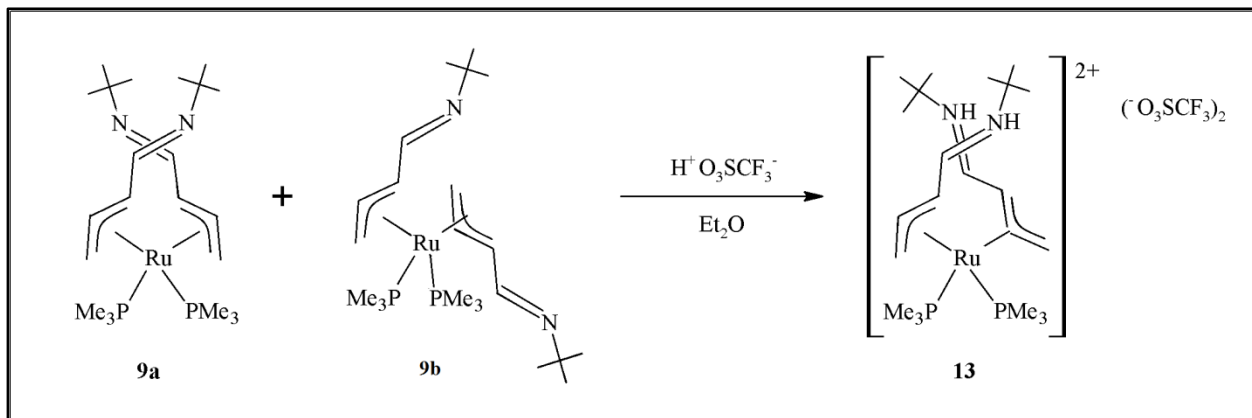
In an attempt to isolate the monoprotonated product, reactions were carried out with **12** and lithium diisopropyl amine (LDA). Compound **12** was dissolved in tetrahydrofuran and a solution of LDA in THF was added. When excess LDA was added, both nitrogen centers were deprotonated as expected, resulting in **8**. When one equivalent of LDA was reacted with **12**, both nitrogen centers were, again, deprotonated. Addition of one equivalent of LDA followed by extraction with pentane, led to an orange solution, **8**, and an insoluble portion. This insoluble portion showed evidence of **12**. The monoprotonated compound was unable to be isolated. As **8** went into the pentane, the equilibrium shifted to make more of it until finally only **8** and **12** remained.

Based on the hypothesis that the addition of a trapping ligand could potentially lead to the displacement of one of the protonated azapentadienyl ligands (Scheme 3.1, Path 2), compound **12** was reacted with PEt₃. These attempts proved unsuccessful as the $^{31}\text{P}\{^1\text{H}\}$ NMR showed

only the presence of $[HPEt_3]^+$ and $O=PEt_3$. Signals for coordinated azapentadienyl as well as free *tert*-butylaminobutadiene were unable to be identified by 1H NMR.

3.2.1.2 Synthesis and characterization of $\{(1,2,3\text{-}\eta^3)\text{-(CH}_2\text{CHCHCH=N(H)(CMe}_3)\text{)}_2\text{Ru(PMe}_3\text{)}_2\}^{2+}(\text{O}_3\text{SCF}_3)_2$ (13)

Treatment of **9** with one equivalent of triflic acid resulted in the precipitation of a dark red solid, the diprotonated product $\{(1,2,3\text{-}\eta^3)\text{-(CH}_2\text{CHCHCH=N(H)(CMe}_3)\text{)}_2\text{Ru(PMe}_3\text{)}_2\}^{2+}$ ($\text{O}_3\text{SCF}_3)_2$ (**13**) in 86% yield (based on the limiting reagent, triflic acid).



Scheme 3.11: Synthesis of $\{(1,2,3\text{-}\eta^3)\text{-(CH}_2\text{CHCHCH=N(H)(CMe}_3)\text{)}_2\text{Ru(PMe}_3\text{)}_2\}^{2+}$ ($\text{O}_3\text{SCF}_3)_2$ (**13**)

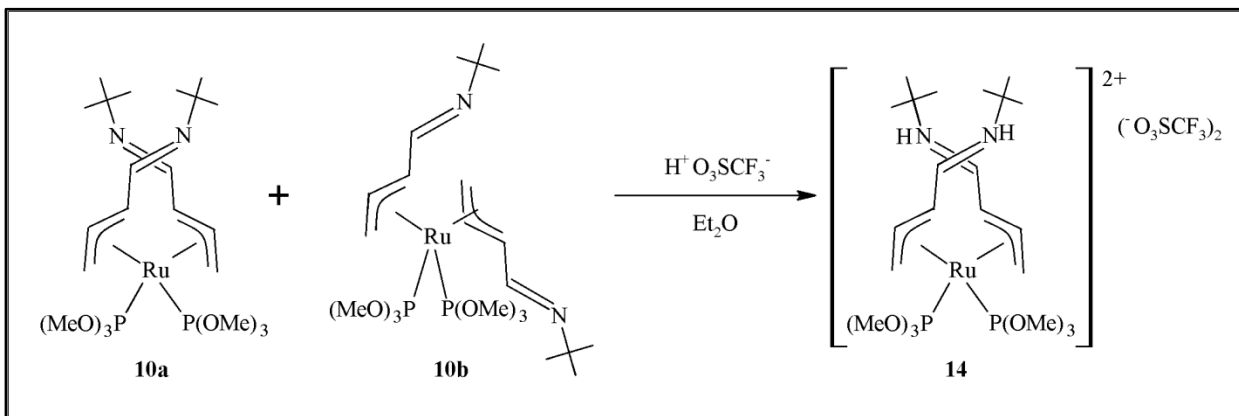
As previously stated, **9** was a mixture of two isomers (**9a** and **9b**). When diprotonated, a single product (**13**) was seen. The $^{31}\text{P}\{^1\text{H}\}$ of **13** showed two doublets at δ 19.1 and δ 12.2 ($J_{\text{P-P}} = 37.6$ Hz). The ^1H and $^{13}\text{C}\{^1\text{H}\}$ NMR also showed two sets of azapentadienyl ligands proving they are unsymmetrical. The ^1H NMR showed two downfield signals at δ 10.15 and δ 9.62, representing the two NH protons. These signals appeared as doublets ($J_{\text{NH-H4}} = 15.3$ Hz) due to the splitting by the adjacent H4. The H4s appeared as doublets of doublets due to the splitting by NH's and H3's. In the $^{13}\text{C}\{^1\text{H}\}$ NMR, the C3's each appeared as doublets at δ 58.8 and 54.9 ($J_{\text{C-P}} = 13.8$

Hz) indicating coupling to a *trans* PMe₃ while the C1's also appeared as doublets with a much smaller coupling constant ($J_{C-P} = 2.9$ Hz) indicating a *cis* position to each PMe₃.

Similar to **12**, compound **13** was reacted with LDA to try to isolate the monoprotonated product. Addition of any number of equivalents of LDA resulted in the neutral compound **9**. After deprotonation, a different ratio of the two isomers (**9a** and **9b**) was seen in the $^{31}\text{P}\{\text{H}\}$ NMR. Compounds **9a** and **9b** were seen in a 1:2 ratio as opposed to the almost 1:1 ratio seen in the initial synthesis of **9**. A $^{31}\text{P}\{\text{H}\}$ NMR was taken of the deprotonated sample 48 h later and the 1:1 ratio of isomers was restored. Assuming the original mC3/mC3 (**9a**) and mC3/bC1 (**9b**) structures of **9** are reformed, the change in ratio of the two isomers could be a clue as to how the conversion of **13** to **9** occurred. Compound **9b** was seen in greater abundance after the deprotonation of **13** which means upon deprotonation, the **B** (mC3/bC3) type structure of **13** was converted to the **E** type structure (mC3/bC1) of **9b**, then converted to the **A** (mC3/mC3) structure of **9a**. In order for this azapentadienyl ligand rearrangement from bC3 to bC1 to occur, a 180° rotation around the Ru-allyl bond must occur, followed by a ligand flip via an η^1 -intermediate. There is another possible explanation of the 1:2 ratio seen in Compound **9** after deprotonation. The monoprotonated form of **9** could have an **E** type structure. After deprotonation of one of the N atoms in **13**, a conversion of one azapentadienyl ligand to a bC1 orientation is possible, followed by the deprotonation of the second N atom, forming **9b**.

3.2.1.3 Synthesis and Characterization of $\{[(1,2,3-\eta^3)\text{-}(\text{CH}_2\text{CHCHCH=NCH})(\text{CMe}_3)]_2\text{Ru}[\text{P}(\text{OMe})_3]_2\}^{2+}(\text{O}_3\text{SCF}_3)_2$ (14)

As shown in Scheme 3.12, treatment of **10** with triflic acid in diethyl ether resulted in a red-brown precipitate, $\{[(1,2,3-\eta^3)\text{-}(\text{CH}_2\text{CHCHCH=NCH})(\text{CMe}_3)]_2\text{Ru}[\text{P}(\text{OMe})_3]_2\}^{2+}(\text{O}_3\text{SCF}_3)_2$ (14).



Scheme 3.12: Synthesis of $\{[(1,2,3-\eta^3)-(\text{CH}_2\text{CHCHCH=NCH})(\text{CMe}_3)]_2\text{Ru}[\text{P}(\text{OMe})_3]_2\}^{2+}\{\text{O}_3\text{SCF}_3\}_2$ (**14**).

Compound **10** showed different ligand connectivity to the metal center than the analogous **9** when introduced to triflic acid. Similar to **9**, compound **10** underwent protonation at both nitrogen centers; however, **14** did not undergo a mouth to backbone rearrangement of one of the azapentadienyl ligands. The $^{31}\text{P}\{\text{H}\}$ NMR showed a singlet at δ 145.6, consistent with the presence of two symmetrical azapentadienyl ligands and two equivalent $\text{P}(\text{OMe})_3$ ligands. In the ^1H NMR, the NH proton resonated at δ 9.69 ($J_{\text{NH-H}4} = 14.1$ Hz). The H4 signal appeared downfield at δ 8.46 as a doublet of doublet due to splitting by NH and H3 protons. The rest of the azapentadienyl ligand signals H3 (δ 2.31), H2 (δ 6.56), and H1 (δ 3.15/1.13) appeared downfield from the signals seen in the neutral **10**. Compound **14** decomposed quickly and made it difficult to obtain a $^{13}\text{C}\{\text{H}\}$ NMR. Based on the acquired data, **14** must have had structure **A**, **C**, **H**, or **J** (Figure 2.2). The mC3/mC3 (**A**) orientation was most probable, given the structure of **10** and the fact that structure **C**, **H**, and **J** have not been seen in this series of *bis*-azapentadienyl-ruthenium complexes thus far. The decomposition of **14** could have been a result of an attempted ligand rearrangement from mC3/mC3 to mC3/bC3, which was the favored orientation

of the other diprotonated compounds **9** and **10**. However, without a $^{13}\text{C}\{\text{H}\}$ NMR and crystal structure, the orientation of the azapentadienyl could not be confirmed.

3.2.2 Protonation of [(1,2,3- η^3)-(5-*tert*-butylazapentadienyl)]₂RuLL' Complexes

Treatment of [(1,2,3- η^3)-(5-*tert*-butylazapentadienyl)]₂RuLL' type complexes, where L and L' are different, with triflic acid resulted in a mixture of products. Unlike the series of complexes containing equivalent ancillary ligands where one isomer was seen, two and three isomers were seen in the monosubstituted complexes.

3.2.2.1 Synthesis and Characterization of {[(1,2,3- η^3)-(CH₂CHCHCH=N(H)(CMe₃))]₂Ru(PPh₃)(PMe₃)²⁺(O₃SCF₃)₂ (**15**)}

Treatment of compound **2** with one or two equivalents of triflic acid in diethyl ether resulted in a brown-red solid {[(1,2,3- η^3)-(CH₂CHCHCH=N(H)(CMe₃))]₂Ru(PPh₃)(PMe₃)²⁺(O₃SCF₃)₂ (**15**)}. The $^{31}\text{P}\{\text{H}\}$ NMR showed three pair of doublets. Each doublet in the PPh₃ region (δ50-60 ppm) had a corresponding doublet in the PMe₃ region (δ7 - 14 ppm) with equivalent coupling constants. These doublets were seen at δ58.2 and 13.6 (J = 26.4 Hz), δ54.4 and 7.9 (J = 26.3 Hz) and δ54.1 and 12.7 (J = 26.3 Hz) and most likely represented three unique isomers. Because **15** had two unique phosphines, none of the structures in Figure 2.2 could be ruled out. The ¹H NMR could not be deciphered because of the large number of ligand signals which was consistent with the presence of six unique azapentadienyl ligands.

Compound **15** was allowed to sit in an NMR tube (in d₆-acetone) for 48 hours at which point a ¹H and $^{31}\text{P}\{\text{H}\}$ NMR were taken. After 48 hrs, the $^{31}\text{P}\{\text{H}\}$ NMR showed one set of

doublets as opposed to the three pairs seen at $t = 0$ h (see Figure 3.3).

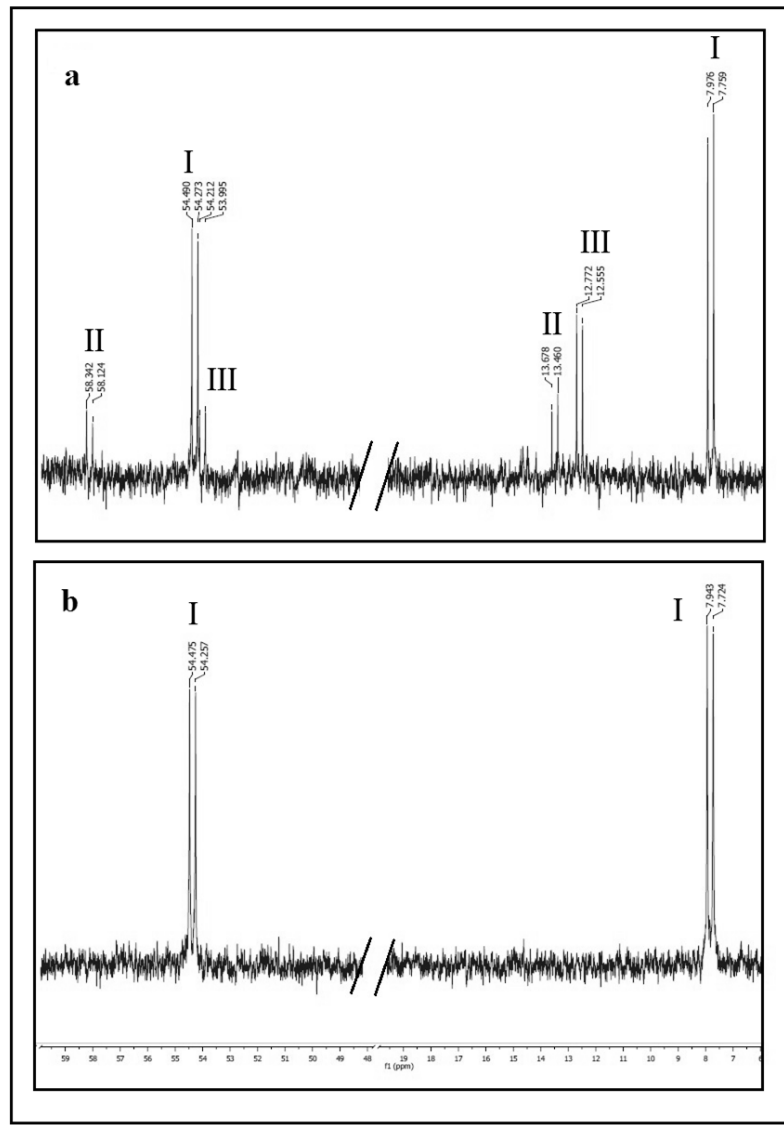


Figure 3.3: (a) $^{31}\text{P}\{\text{H}\}$ NMR of **15** at $t = 0$ h, showing three sets of doublets representing three different isomers. (b) $^{31}\text{P}\{\text{H}\}$ NMR of **15** at $t = 48$ h, showing one set of doublets, representing one isomer.

After 48 hrs, the ^1H NMR showed two sets of azapentadienyl ligand signals. The NH signals appeared downfield at $\delta 10.68/10.27$ ($J_{\text{NH-H}4} = 14.1$ Hz) while the H4s appeared at $\delta 8.13/6.83$ with a doublet of doublet multiplicity from NH and H3 splitting. The H3's ($\delta 3.61/2.99$), H2's

(δ 6.55/4.39), and H1's (δ 3.91/2.88 and δ 3.70/3.03) appeared in the expected regions. These ^1H and $^{31}\text{P}\{^1\text{H}\}$ NMR were consistent with the presence of a single isomer after 48 hrs. Attempts at crystallization proved unsuccessful. Without a crystal structure, the orientation of the azapentadienyl ligands in **15** could not be determined.

3.2.2.2 Synthesis and Characterization of $\{[(1,2,3-\eta^3)-(\text{CH}_2\text{CHCHCH}=\text{NH})(\text{CMe}_3)]_2\text{Ru}(\text{PPh}_3)(\text{L})\}^{2+}(\text{O}_3\text{SCF}_3)_2$, where L = P(OMe)₃ (**16**) and CNCMe₃ (**17**).

Treatment of $[(1,2,3-\eta^3)-(5\text{-}tert\text{-butylazapentadienyl})]_2\text{Ru}(\text{PPh}_3)(\text{L})$ (where L = P(OMe)₃ (**4**) or L = CNCMe₃ (**5**)) with triflic acid in diethyl ether resulted in $\{[(1,2,3-\eta^3)-(\text{CH}_2\text{CHCHCH}=\text{NCH})(\text{CMe}_3)]_2\text{Ru}(\text{PPh}_3)(\text{L})\}^{2+}(\text{O}_3\text{SCF}_3)_2$ (L = P(OMe)₃ (**16**) and L = CNCMe₃ (**17**)). From their NMR spectra, both **16** and **17** appeared to be mixtures of two isomers.

The ^1H NMR of **16** and **17** showed four sets of azapentadienyl ligands, all of which had protonated nitrogens, as evidenced by the four doublets between δ 9.5 and 11.5. The H4 signals appeared at the appropriate shifts and had a doublet of doublet multiplicity from splitting by NH and H3. The H3s, H2s, and H1s signals appeared at similar shifts to those in the spectra of compounds **4** and **5**.

For **16** the $^{31}\text{P}\{^1\text{H}\}$ NMR showed two pairs of doublets. Most likely, the pair of doublets at δ 137.3 (P(OMe)₃) and 53.5 (PPh₃) with $J_{\text{P-P}} = 47.2$ Hz represent one isomer while δ 141.1 (P(OMe)₃) and 50.3 (PPh₃) with $J_{\text{P-P}} = 42.6$ Hz represented the second isomer. Similarly, the $^{31}\text{P}\{^1\text{H}\}$ NMR of **17** showed two singlets at δ 56.3 and 53.6, each corresponding to a PPh₃ on the two isomers.

Without crystal structures of **16** and **17**, the orientations of the azapentadienyl ligands could not be confirmed; none of the ten possible structures in Figure 2.2 could be ruled out.

NMR analysis was done on compounds **16** and **17** at $t = 24$ and 48 h after synthesis. Unlike **15**, these compounds did not convert to one isomer, preventing additional analysis.

3.3 Summary and Comparisons

This chapter reported the synthesis, structure, and spectroscopy of protonated *bis*-azapentadienyl-ruthenium complexes. The compounds described in Chapter 2 were reacted with various equivalents of triflic acid (H^+). Treatment of compounds **2**, **4**, **5**, and **8-10** with triflic acid resulted in the protonation of both nitrogen centers of the azapentadienyl ligands. The $[(1,2,3-\eta^3)-(5\text{-}tert\text{-}butylazapentadienyl})_2RuL_2$ (**8-10**) complexes reacted cleanly with H^+ to give single products (**12-14**). The $[(1,2,3-\eta^3)-(5\text{-}tert\text{-}butylazapentadienyl})_2RuLL'$ (**2**, **4**, and **5**) complexes when reacted with H^+ resulted in a mixture of three isomers (**15**) or two isomers (**16** and **17**), each isomer being diprotonated.

3.3.1 Comparison with Azapentadienyl-Cobalt and Azapentadienyl-Rhodium System

The azapentadienyl-cobalt system¹ showed displacement of the azapentadienyl ligand upon protonation of the nitrogen and the addition of another ligand, such as CO. This system suggested that it was possible to prompt a ligand displacement via the protonation route described in Scheme 3.1. However, protonation of the *bis*-azapentadienyl-ruthenium system did not show ligand rearrangement or displacement. A key feature of the cobalt system was the bonding mode of the protonated azapentadienyl ligand. Scheme 3.1 shows that upon protonation of the nitrogen center, the ligand adopted an η^4 bonding mode to the cobalt metal center. The η^4 azapentadienyl ligand in **a** (Scheme 3.1) was a neutral ligand which was much easier to displace than the ionic η^3 ligand. In the azapentadienyl-ruthenium system, the azapentadienyl ligands never adopted the *anti*- conformation required to achieve the η^4 bonding mode. The *syn*- η^4

conformation was not a major resonance contributor to the protonated product, preventing ligand displacement with the addition of a trapping ligand.

As shown Schemes 3.6 and 3.7, the azapentadienyl-rhodium system² underwent ligand displacement. In order for this ligand displacement to be achieved, a protonation at the nitrogen center, followed by a second protonation at the rhodium metal center was required. A reductive elimination then occurred, displacing the protonated amine. Given the *syn*- η^3 bonding mode of the azapentadienyl ligands in the ruthenium system, an additional protonation at the ruthenium metal center is most likely required.

3.4 Experimental

3.4.1 General Comments on Experimental Techniques

All manipulations were carried out under a nitrogen atmosphere, using either glovebox or double-manifold Schlenk techniques. Solvents were stored under nitrogen after being distilled from the appropriate drying agents. Deuterated NMR solvents were obtained in sealed vials and used as received. Triethylphosphine (VWR), lithium diisopropyl amine (Aldrich) and trifluoromethanesulfonic acid (VWR and Aldrich) were used as received.

NMR experiments were performed on a Varian Unity Plus-300 spectrometer (¹H, 300 MHz; ¹³C, 75 MHz; ³¹P, 121 MHz), a Varian Inova-300 spectrometer (¹H, 300 MHz; ¹³C, 75 MHz; ³¹P, 121 MHz), a Varian Unity-500 spectrometer (¹H, 500 MHz; ¹³C 125 MHz; ³¹P, 202 MHz), or a Varian Unity-600 spectrometer (¹H, 600 MHz; ¹³C, 150 MHz; ³¹P, 242 MHz). ¹H and ¹³C spectra were referenced to tetramethylsilane, while ³¹P spectra were referenced to external H₃PO₄. HMQC (¹H-detected multiple quantum coherence), DEPT (distortion-less enhancement by polarization transfer) and COSY (correlation spectroscopy) experiments aided

in assigning some of the ^1H and ^{13}C peaks. In all of the NMR spectra, carbon atoms and associated hydrogens are numbered by starting at the end of the chain *opposite* nitrogen.

Infrared spectra were obtained on a Perkin-Elmer Spectrum BX FT-IR spectrometer.

Microanalyses were performed by Galbraith Laboratories, Inc., Knoxville, TN.

3.4.2 Synthesis of $\{[(1,2,3-\eta^3)-(\text{CH}_2\text{CHCHCH}=\text{N(H)(CMe}_3)]_2\text{Ru(PEt}_3)_2\}^{2+}(\text{O}_3\text{SCF}_3)_2$, 12.

Compound **8** (0.17 g, 0.29 mmol) was dissolved in 10 mL of diethyl ether. A cold 1.33 M solution of triflic acid in diethyl ether (0.04 g, 0.27 mmol) was then added dropwise, causing a dark red residue to form immediately. The red ether solution was decanted and the residue was washed with diethyl ether and pentane, giving a dark red residue. The residue was dissolved in a small quantity of acetone/diethyl ether and cooled to -30 °C. Red crystals of **12** formed in a few days. Yield: 0.10 g (85%)

Anal. Calcd for $\text{C}_{30}\text{H}_{60}\text{RuN}_2\text{O}_6\text{F}_8\text{P}_2\text{S}_2$: C, 40.68; H, 6.84. Found: C, 40.90; H, 6.41.

IR (Nujol mull): 1632 cm⁻¹ (C=N), 1622 cm⁻¹(C=N).

^1H NMR (acetone-d₆, 22 °C): δ 10.51 (br d, $J_{\text{NH}1-\text{H}4} = 15.6$ Hz, 1, NH1), 9.76 (br d, $J_{\text{NH}2-\text{H}8} = 15.3$ Hz, 1, NH2), 8.08 (dd, $J_{\text{H}4-\text{NH}1} = 15.6$ Hz, $J_{\text{H}4-\text{H}3} = 10.8$ Hz, 1, H4), 7.72 (dd, $J_{\text{H}8-\text{NH}2} = 15.3$ Hz, $J_{\text{H}8-\text{H}7} = 12.0$ Hz, 1, H8), 5.60 (m, 1, H2), 5.43 (m, 1, H6), 3.49 (m, 1, H1), 3.40 (m, 1, H5), 3.15 (m, 1, H7), 2.92 (m, 1, H3), 2.92 (m, 1, H5), 2.56 (m, 1, H1), 2.2-1.8 (m, 12, PEt₃ CH₂'s), 1.44 (s, 9, *tert*-butyl), 1.38 (s, 9 *tert*-butyl), 1.4-1.0 (m, 18 PEt₃ CH₃'s).

$^{13}\text{C}\{\text{H}\}$ NMR (acetone-d₆, 22 °C): δ 168.3 (s, C4), 167.1 (s, C8), 94.8 (s, C2), 93.2 (s, C6), 60.9 (d, $J_{\text{C-P}} = 12.8$ Hz, C7), 58.3 (s, *tert*-butyl C), 57.0 (s, *tert*-butyl C), 54.0 (d, $J_{\text{C-P}} = 12.6$ Hz, C3), 43.8 (d, $J_{\text{C-P}} = 3.8$ Hz, C5), 39.5 (d, $J_{\text{C-P}} = 5.3$ Hz, C1), 29.9 (s, *tert*-butyl CH₃'s), 27.5 (s, *tert*-butyl CH₃'s), 23.2 (d, $J_{\text{C-P}} = 26.3$ Hz, PEt₃ CH₂'s), 20.4 (d, $J_{\text{C-P}} = 26.3$ Hz, PEt₃ CH₂'s), 9.1 (d, $J_{\text{C-P}} = 5.3$ Hz, PEt₃ CH₃'s), 8.7 (d, $J_{\text{C-P}} = 5.3$ Hz, PEt₃ CH₃'s).

$^{31}\text{P}\{\text{H}\}$ NMR (acetone-d₆, 22 °C): δ37.5 (d, $J_{\text{P-P}} = 31.6$ Hz, 1, PEt₃), 26.9 (d, $J_{\text{P-P}} = 30.9$ Hz, 1, PEt₃)

3.4.2.1 Deprotonation of $\{[(1,2,3-\eta^3)\text{-}(\text{CH}_2\text{CHCHCH}=\text{N(H)(CMe}_3)]_2\text{Ru(PEt}_3)_2\}^{2+}$ (O_3SCF_3^-)₂, **12**.

Compound **12** (0.17 g, 0.28 mmol) was dissolved in 5 mL of tetrahydrofuran. A solution of lithium diisopropyl amine (0.07 g, 0.61 mmol) in tetrahydrofuran was made and added to the solution of **12**. The resulting solution was stirred for 30 minutes after which, a color change from dark red to orange was seen. The solvent was removed under vacuum and an orange-red residue remained. The residue was extracted with pentane and decanted. The pentane was removed under vacuum and yielded **8** as an orange oil.

3.4.3 Synthesis of $\{[(1,2,3-\eta^3)\text{-}(\text{CH}_2\text{CHCHCH}=\text{N(H)(CMe}_3)]_2\text{Ru(PMe}_3)_2\}^{2+}$ (O_3SCF_3^-)₂, **13**.

Compound **9** (0.13 g, 0.26 mmol) was dissolved in 10 mL of diethyl ether. A cold 1.33 M solution of triflic acid in diethyl ether (0.04 g, 0.27 mmol) was then added dropwise, causing a dark red residue to form immediately. The red ether solution was decanted and the residue was washed with diethyl ether and pentane, giving a dark red product, **13**. Yield: 0.09 g (84%).

Anal. Calcd for C₂₄H₄₈RuN₂O₆F₈P₂S₂: C, 35.93; H, 6.05. Found: C, 35.95; H, 6.03.

IR (Nujol mull): 1633 cm⁻¹, 1626 cm⁻¹ (C=N).

^1H NMR (acetone-d₆, 22 °C): δ10.15 (d, $J_{\text{NH}_2\text{-H}_8} = 15.3$ Hz, 1, NH₂), 9.62 (d, $J_{\text{NH}_1\text{-H}_4} = 15.3$ Hz, 1, NH₁), 7.92 (m, 1, H₈), 7.71 (m, 1, H₄), 5.63 (m, 1, H₆), 5.03 (m, 1, H₂), 3.24 (m, 1, H₃), 3.21 (m, 1, H₅), 3.17 (m, 1, H₁), 3.03 (m, 1, H₇), 2.89 (m, 1, H₁), 2.64 (m, 1, H₅), 1.67 (d, $J_{\text{P-H}} = 9.9$ Hz, 9, PMe₃ CH₃'s), 1.62 (d, $J_{\text{P-H}} = 9.3$ Hz, 9, PMe₃ CH₃'s), 1.47 (s, 9, *tert*-butyl), 1.42 (s, 9 *tert*-butyl).

$^{13}\text{C}\{\text{H}\}$ NMR (acetone-d₆, 22 °C): δ164.9 (s, C4), 164.9 (s, C8), 95.6 (s, C2), 93.6 (s, C6), 58.8 (m, C3), 57.3 (s, *tert*-butyl C), 56.6 (s, *tert*-butyl C), 54.9 (m, C7), 49.2 (s, C1), 43.1 (s, C5), 28.6 (s, *tert*-butyl CH₃'s), 28.1 (s, *tert*-butyl CH₃'s), 21.2 (d, $J_{\text{C-P}} = 33.2$ Hz, PMe₃ CH₃'s), 17.4 (d, $J_{\text{C-P}} = 32.8$ Hz, PMe₃ CH₃'s).

$^{31}\text{P}\{\text{H}\}$ NMR (acetone-d₆, 22 °C): δ19.1 (d, $J_{\text{P-P}} = 37.6$ Hz, PMe₃), 12.2 (d, $J_{\text{P-P}} = 37.6$ Hz, PMe₃).

3.4.3.1 Deprotonation of $\{[(1,2,3\text{-}\eta^3)\text{-}(\text{CH}_2\text{CHCHCH=NH})(\text{CMe}_3)]_2\text{Ru}(\text{PMe}_3)_2\}^{2+}$ (O_3SCF_3^-)₂, **13**.

Compound **13** (0.08 g, 0.17 mmol) was dissolved in 5 mL of tetrahydrofuran. A solution of lithium diisopropyl amine (0.04 g, 0.33 mmol) in tetrahydrofuran was made and added to the solution of **13**. The resulting solution was stirred for 5 minutes after which, a color change from dark red to orange was seen. The solvent was removed under vacuum and an orange-red residue remained. The residue was extracted with pentane and decanted. The pentane was removed under vacuum and yielded **9** as an orange oil.

3.4.4 Synthesis of $\{[(1,2,3\text{-}\eta^3)\text{-}(\text{CH}_2\text{CHCHCH=NCH})(\text{CMe}_3)]_2\text{Ru}[\text{P}(\text{OMe})_3]_2\}^{2+}$ (O_3SCF_3^-)₂, **14**.

Compound **10** (0.27 g, 0.44 mmol) was dissolved in 10 mL of diethyl ether. A cold 1.33 M solution of triflic acid in diethyl ether (0.06 g, 0.36 mmol) was then added dropwise, causing a red-brown solid to form immediately. The red ether solution was decanted and the solid was washed with diethyl ether and pentane, giving a red-brown solid, **14**. Yield: 0.10 g (94 %).

¹H NMR (acetone-d₆, 22 °C): δ9.74 (d, J_{NH-H4} = 13.2 Hz, 2, NH), 8.23 (dd, 2, H4), 6.32 (m, 2, H2), 3.90 (obscured m, 2, H1), 3.88 (d, J_{P-H} = 10.8 Hz, 9, P(OMe)₃ CH₃'s), 2.94 (m, 2, H3), 2.14 (m, 2, H1), 1.47 (s, 18, *tert*-butyl).

³¹P{¹H} NMR (acetone-d₆, 22 °C): δ145.6 (s, 2, P(OMe)₃).

3.4.5 Synthesis of {[$(1,2,3\text{-}\eta^3)$ -(CH₂CHCHCH=NCH)(CMe₃)₂Ru(PPh₃)(PMe₃)]²⁺

(O₃SCF₃⁻)₂, 15.

Compound **2** (0.10 g, 0.15 mmol) was dissolved in 10 mL of diethyl ether. A cold 1.33 M solution of triflic acid in diethyl ether (0.03 g, 0.21 mmol) was then added dropwise, causing a dark red residue to form immediately. The red ether solution was decanted and the residue was washed with diethyl ether and pentane, giving a dark red residue, **15**. The residue was dissolved in a small quantity of acetone and allowed to sit at room temperature for 48 hours. Yield: 0.07 g (45 %).

¹H NMR (acetone-d₆, 22 °C): δ10.68 (d, J_{NH-H4} = 14.1 Hz, 1, NH), 10.27 (d, J_{NH-H4} = 14.1 Hz, 1, NH'), 8.13 (dd, J_{H4-NH} = 12.0 Hz, J_{H4-H3} = 7.8 Hz, 1, H4), 6.83 (dd, J_{H4-NH} = 15.6 Hz, J_{H4-H3} = 10.5 Hz, 1, H4'), 6.55 (m, 1, H2), 4.39 (m, 1, H2'), 3.91 (m, 1, H1'), 3.70 (m, 1, H1), 3.61 (m, 1, H3'), 3.03 (m, 1, H1), 2.99 (m, 1, H3), 2.88 (m, 1, H1'), 1.46 (s, 9, *tert*-butyl), 1.31 (d, J_{P-H} = 9.6 Hz, 9, PMe₃ CH₃'s), 1.27 (s, 9, *tert*-butyl).

³¹P{¹H} NMR (acetone-d₆, 22 °C): δ54.4 (d, J_{P-P} = 26.6 Hz, PPh₃), 7.83 (d, J_{P-P} = 26.6 Hz, PMe₃).

3.4.6 Synthesis of $\{[(1,2,3\text{-}\eta^3)\text{-}(\text{CH}_2\text{CHCHCH=NCH})(\text{CMe}_3)]_2\text{Ru}(\text{PPh}_3)[\text{P}(\text{OMe})_3]\}^{2+}(\text{O}_3\text{SCF}_3^-)_2$, 16.

$(\text{CH}_2\text{CHCHCH=NCH})(\text{CMe}_3)]_2\text{Ru}(\text{PPh}_3)[\text{P}(\text{OMe})_3]\}^{2+}(\text{O}_3\text{SCF}_3^-)_2$, **16**.

Compound **4** (0.14 g, 0.19 mmol) was dissolved in 10 mL of diethyl ether. A cold 1.33 M solution of triflic acid in diethyl ether (0.03 g, 0.19 mmol) was then added dropwise, causing a dark red residue to form immediately. The red ether solution was decanted and the residue was washed with diethyl ether and pentane, giving a dark red residue, **16**. Yield: 0.02 g (23 %).

Isomer A:

$^{31}\text{P}\{\text{H}\}$ NMR (acetone-d₆, 22 °C): δ 137.3 (d, $J_{\text{P-P}} = 47.2$ Hz, $\text{P}(\text{OMe})_3$), 53.5 (d, $J_{\text{P-P}} = 47.2$ Hz, PPh_3).

Isomer B:

$^{31}\text{P}\{\text{H}\}$ NMR (acetone-d₆, 22 °C): δ 141.1 (d, $J_{\text{P-P}} = 42.6$ Hz, $\text{P}(\text{OMe})_3$), 50.3 (d, $J_{\text{P-P}} = 42.6$ Hz, PPh_3).

3.4.7 Synthesis of $\{[(1,2,3\text{-}\eta^3)\text{-}(\text{CH}_2\text{CHCHCH=NCH})(\text{CMe}_3)]_2\text{Ru}(\text{PPh}_3)(\text{CNCMe}_3)\}^{2+}(\text{O}_3\text{SCF}_3^-)_2$, 17.

$(\text{CH}_2\text{CHCHCH=NCH})(\text{CMe}_3)]_2\text{Ru}(\text{PPh}_3)(\text{CNCMe}_3)\}^{2+}(\text{O}_3\text{SCF}_3^-)_2$, **17**.

Compound **5** (0.02 g, 0.03 mmol) was dissolved in 10 mL of diethyl ether. A cold 1.33 M solution of triflic acid in diethyl ether (0.01 g, 0.09 mmol) was then added dropwise, causing an orange residue to form immediately. The orange ether solution was decanted and the residue was washed with diethyl ether and pentane, giving an orange-yellow residue, **17**. The residue was dissolved in a small quantity of acetone/tetrahydrafuran and allowed to crystallize at -30°C. Yield: 0.02 g (73 %).

Isomer A:

$^{31}\text{P}\{\text{H}\}$ NMR (acetone-d₆, 22 °C): δ 56.3 (s, 1, PPh_3).

Isomer B:

$^{31}\text{P}\{\text{H}\}$ NMR (acetone-d₆, 22 °C): δ53.6 (s, 1, PPh₃).

3.5 References

- (1) Bleeke, J.R.; Anutrasakda, W.; Rath, N.P. *Organometallics*, **2012**, *31*, 2219-2230.
- (2) Bleeke, J.R.; Anutrasakda, W.; Rath, N.P. *Organometallics*, **2013**, *32*, 6410-6426.
- (3) Bleeke, J.R.; Stouffer, M.; Rath, N.P. *J. of Organometallic Chem.*, **2015**, *781*, 11-21.

Chapter 4

Summary and Future Work

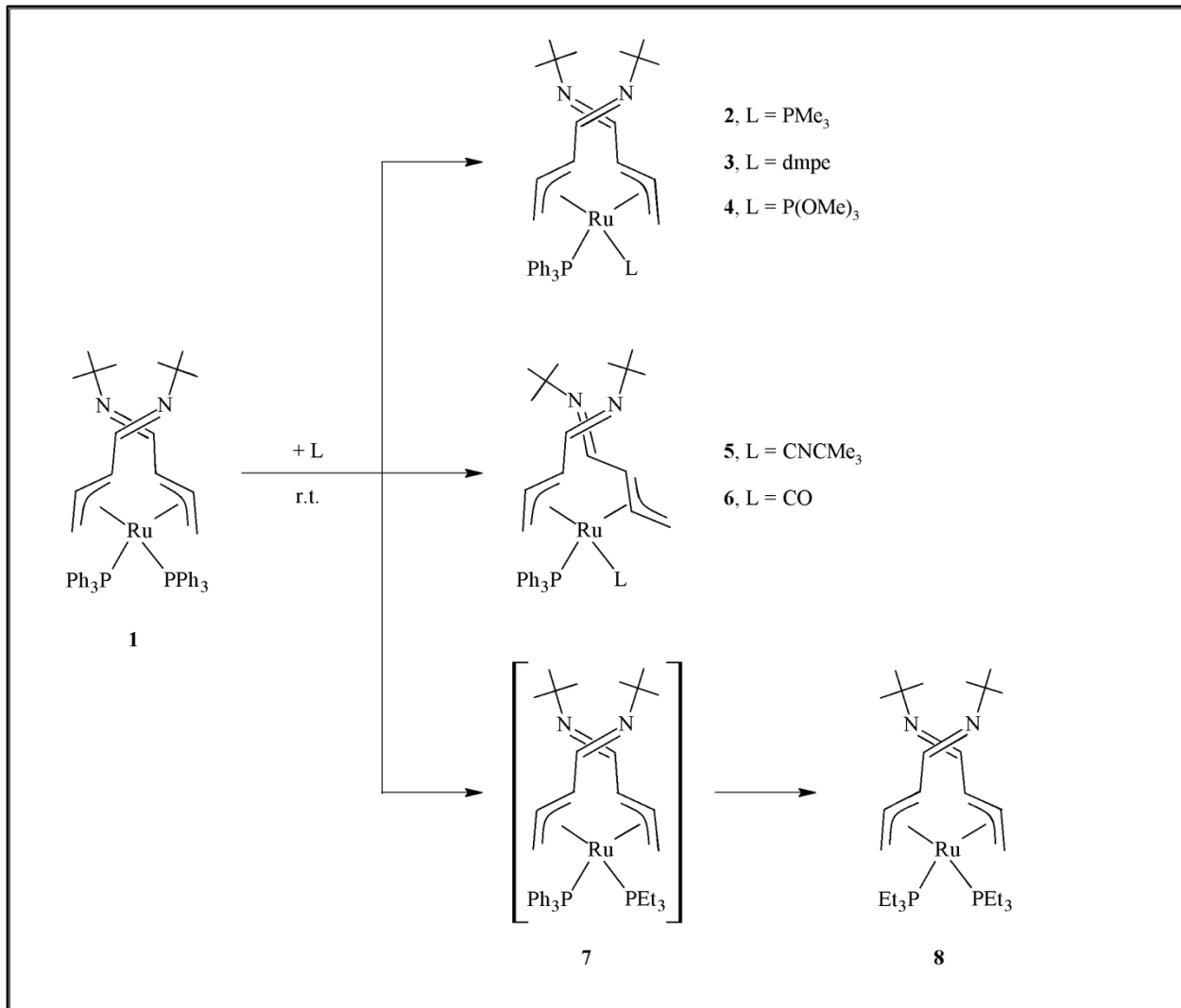
Summary and Future Work

The work described in this dissertation focused on the synthesis of the first *bis*-azapentadienyl-ruthenium-phosphine complexes. Our key synthetic approach involved treating the $\text{Cl}_2\text{Ru}(\text{PPh}_3)_3^1$ precursor with potassium *tert*-butylazapentadienide reagent² to produce $[(1,2,3-\eta^3)-(5\text{-}tert\text{-}butylazapentadienyl})_2\text{Ru}(\text{PPh}_3)_2$ (**1**). The reactivity of this parent compound towards other phosphines and neutral 2e^- donor ligands was studied. These compounds possessed three potential sites of reactivity for electrophiles: the two azapentadienyl nitrogen atoms and the ruthenium metal center. The second focus of this dissertation was the reactivity of the various neutral *bis*-azapentadienyl-ruthenium compounds toward the simplest of electrophiles, H^+ . All of these compounds were characterized by ^1H , ^{13}C , and ^{31}P NMR. Structures of five of the resulting compounds were determined by single-crystal X-ray diffraction studies. This work has recently been published.³

4.1 Summary of Research

Chapter 2 reported the synthesis and characterization of the first example of *bis*-azapentadienyl-ruthenium complexes. The reaction of $\text{Cl}_2\text{Ru}(\text{PPh}_3)_3^1$ with potassium *tert*-butylazapentadienide² produced $[(1,2,3-\eta^3)\text{-}5\text{-}tert\text{-}butylazapentadienyl}]_2\text{Ru}(\text{PPh}_3)_2$ (**1**). Treatment of **1** with 2e^- donor ligands including trimethylphosphine, dmpe, trimethyl phosphite, *tert*-butyl isocyanide, and carbon monoxide at room temperature resulted in ligand replacement reactions and the production of $[(1,2,3-\eta^3)\text{-}5\text{-}tert\text{-}butylazapentadienyl}]_2\text{Ru}(\text{PPh}_3)(\text{L})$ (**2**, $\text{L} = \text{PMe}_3$; **3**, $\text{L} = \text{dmpe}$; **4**, $\text{L} = \text{P}(\text{OMe})_3$; **5**, $\text{L} = \text{CNCMe}_3$; **6**, $\text{L} = \text{CO}$). Treatment of **1** with triethylphosphine, resulted in the replacement of both triphenylphosphine ligands, producing

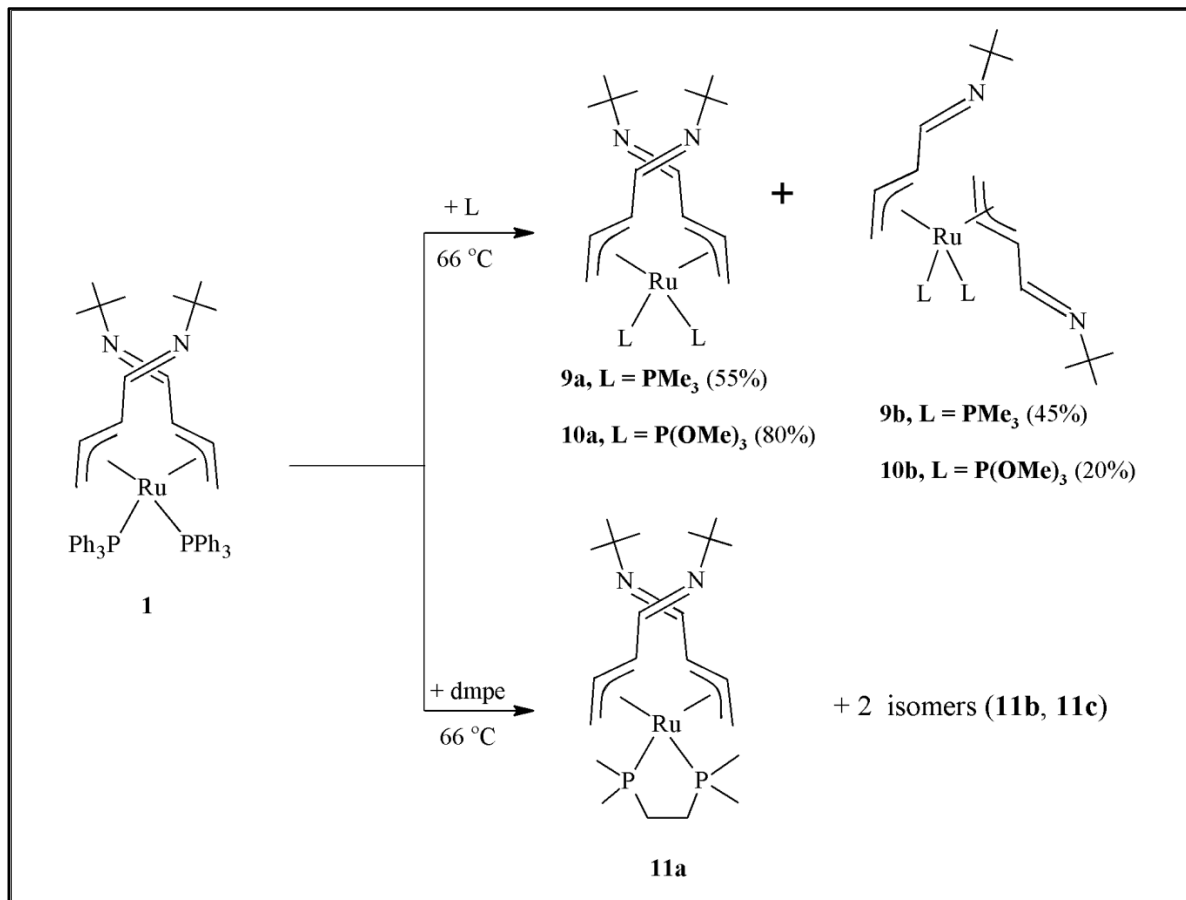
$[(1,2,3\text{-}\eta^3)\text{-}5\text{-}tert\text{-butylazapentadienyl}]_2\text{Ru}(\text{PEt}_3)_2$ (**8**). A summary of the synthesis of compounds **2 – 8** is shown in Scheme 4.1.



Scheme 4.1: Summary of the synthesis of **2 – 8**.

Like **1**, the two azapentadienyl ligands in **2 – 6** and **8** remained coordinated to ruthenium in an η^3 fashion. Also compounds **2 – 4** and **8** retained the mC3/mC3 structure (Figure 2.2) while **5** and **6** exhibited an azapentadienyl ligand rearrangement from mC3/mC3 (**A**) to mC3/bC3 (**B**). According to ¹³C NMR and X-ray crystal structures, compounds **1 – 6** and **8** all possessed ancillary ligands *trans* to the C3 atom of each azapentadienyl ligand.

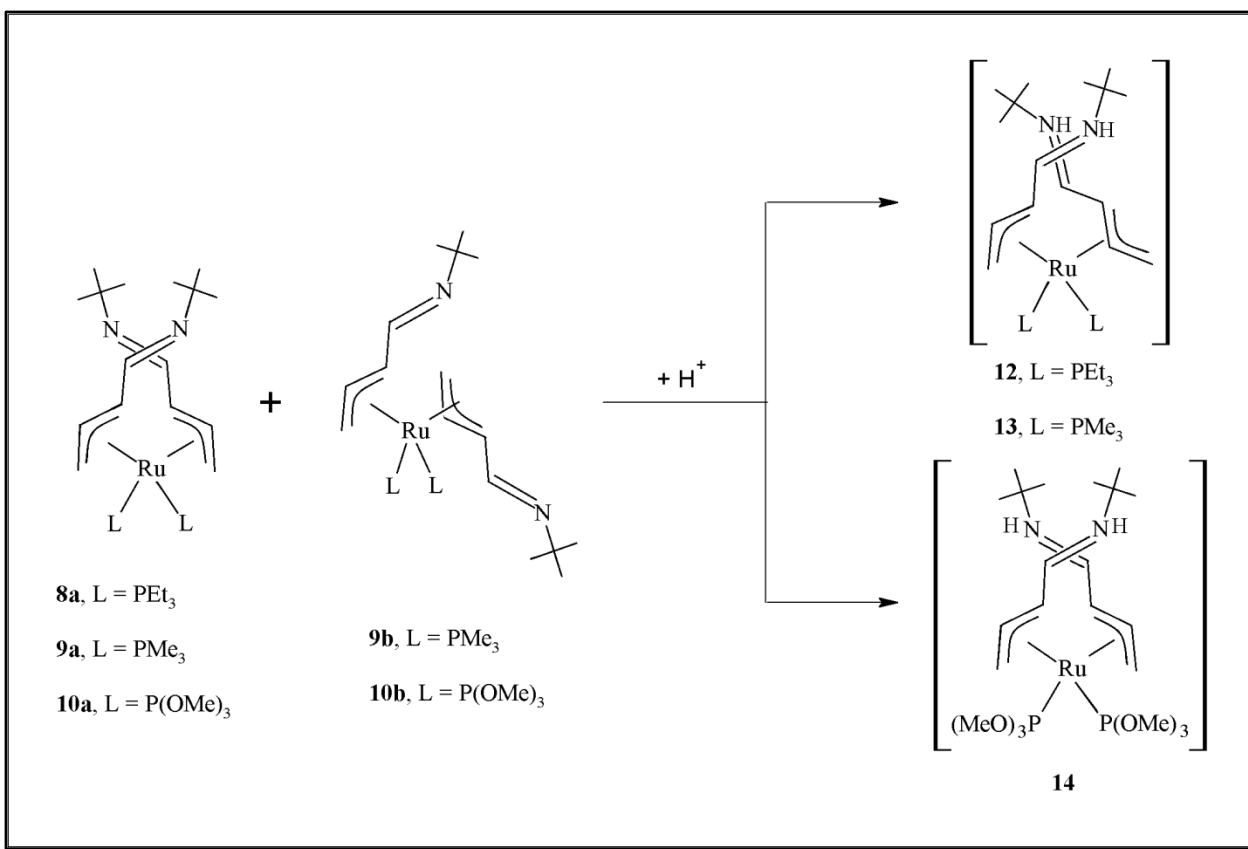
Furthermore, Chapter 2 discussed the reactivity of **1** towards $2e^-$ donor ligands at elevated temperatures. Treatment of **1** with trimethylphosphine, trimethyl phosphite, and dmpe at reflux resulted in ligand substitution of both PPh_3 ligands and the production of $[(1,2,3-\eta^3)-5-tert-butylazapentadienyl]_2\text{Ru}(\text{L})_x$ (**9**, $\text{L} = \text{PMe}_3$, $x = 2$; **10**, $\text{L} = \text{P}(\text{OMe})_3$, $x = 2$; **11**, $\text{L} = \text{dmpe}$, $x = 1$). As in **1**, the η^3 bonding mode of both azapentadienyl ligands is retained. Interestingly, the reactions at elevated temperatures resulted in multiple isomers of **9** - **11**. Compound **9a** and **9b** were seen in a 55:45 ratio of an **A** ($\text{mC3}/\text{mC3}$) and **E** ($\text{mC3}/\text{bC1}$) type structure, while the production of **10** resulted in an 80:20 ratio of **A** (**10a**) and **E** (**10b**). Compound **11** showed a possibility of three isomers whose structures could not be confirmed. A summary of the synthesis of compounds **9** – **11** is shown in Scheme 4.2.



Scheme 4.2: Summary of synthesis of compounds **9** – **11**

In Chapter 3, the reactivity of the neutral compounds **2**, **4**, **5**, and **8 – 10** toward the small electrophile H⁺ (from triflic acid) were discussed. In the case of the “mixed” compounds **2**, **4**, and **5**, where L and L' were not equivalent, multiple diprotonated isomers were observed. Diprotonated Compound **2** isomerized to one isomer (**15**) after 48 hours in solution; however, crystallization attempts proved unsuccessful.

Compounds **8 – 10**, where both L's were equivalent, when reacted with HOTf showed single products (**12 – 14**) with both nitrogen centers protonated. The η^3 coordination of both ligands to ruthenium was retained; however, the **A** (mC3/mC3) type structure was only observed in **14**. Instead, for compounds **12** and **13**, a mC3/bC3 (**B**) structure was seen. This ligand rearrangement could be accomplished via an η^1 intermediate. Compound **10**, when reacted with H⁺, also showed protonation at both nitrogen centers with the retention of the η^3 coordination around the ruthenium metal center. However, upon protonation, the two isomers, **10a** and **10b**, converted to the single **A** type structure isomer (**14**). Compound **14** decomposed quickly, probably due to a possible ligand rearrangement to the preferred mC3/bC3 orientation. A summary of protonation reactions is seen in Scheme 4.3.



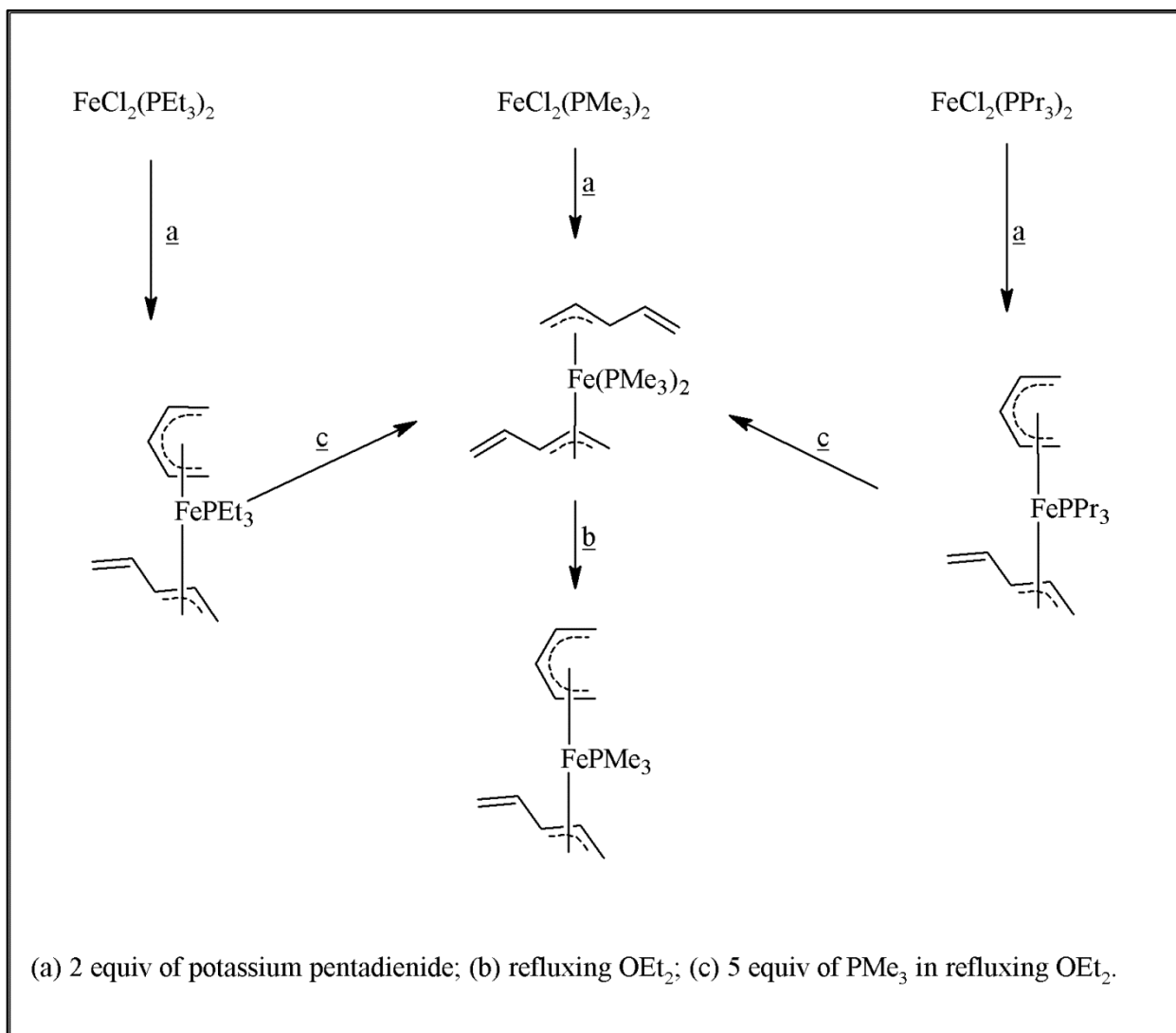
Scheme 4.3: Summary of protonation reactions of **8 – 10**.

4.2 Future Work

4.2.1 Background of *bis*-Pentadienyl-Iron-Phosphine Complexes

Comparison of our ruthenium system to that of the *bis*-pentadienyl-iron-phosphine system^{4,5}, reported earlier by the Bleeeke group, is an important one. It allows us to compare and contrast another series of complexes with a d⁶ metal center (Fe) containing two pentadienyl ligands with our *bis*-azapentadienyl-ruthenium system. Obviously, the major difference in the two systems is that the iron system contains an all carbon pentadienyl ligand while the ruthenium system contains the bulky N(t-Bu) group. A summary of the reactivity of the *bis*-pentadienyl-

iron complexes is seen in Scheme 4.4. The iron system

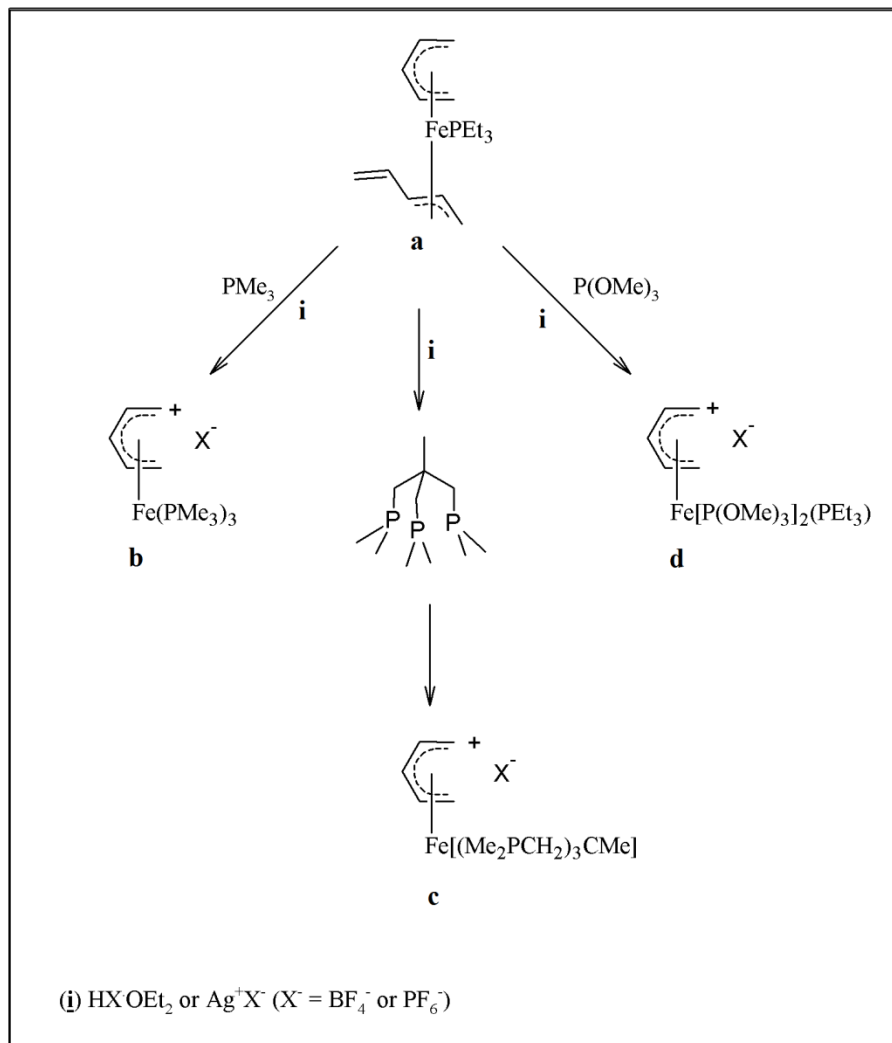


Scheme 4.4: Synthesis of $(\eta^5\text{-Pentadienyl})(\eta^3\text{-pentadienyl})\text{Fe}(\text{PR}_3)$ Complexes.

containing the smaller phosphines (PMe_3), when reacted with two equivalents of potassium pentadienide, resulted in a similar *bis*- η^3 bonding mode as the *tert*-butylazapentadienyl ruthenium system discussed in Chapter 2. The difference lies in the reaction of potassium pentadienide with $\text{FeCl}_2(\text{PR}_3)_2$ where PR_3 is a larger ligand (PEt_3 and PPr_3)⁶. These reactions result in a $(\eta^5\text{-pentadienyl})(\eta^3\text{-pentadienyl})\text{Fe}(\text{PR}_3)$ complex. In contrast, when $\text{Cl}_2\text{Ru}(\text{PPh}_3)_3$ ¹ is reacted with potassium *tert*-butylazapentadienide², a *bis*- η^3 complex is obtained. A mixed $(\eta^5$,

η^3) – complex is never seen. This is most likely due to the increased size of ruthenium compared to iron. Ruthenium can accommodate the two larger PR_3 ligands.

As shown in Scheme 4.5, compound **a** was converted to a series of (η^5 -pentadienyl) FeP_3 complexes by a protonation route.⁵ When **a** was treated with an acid at



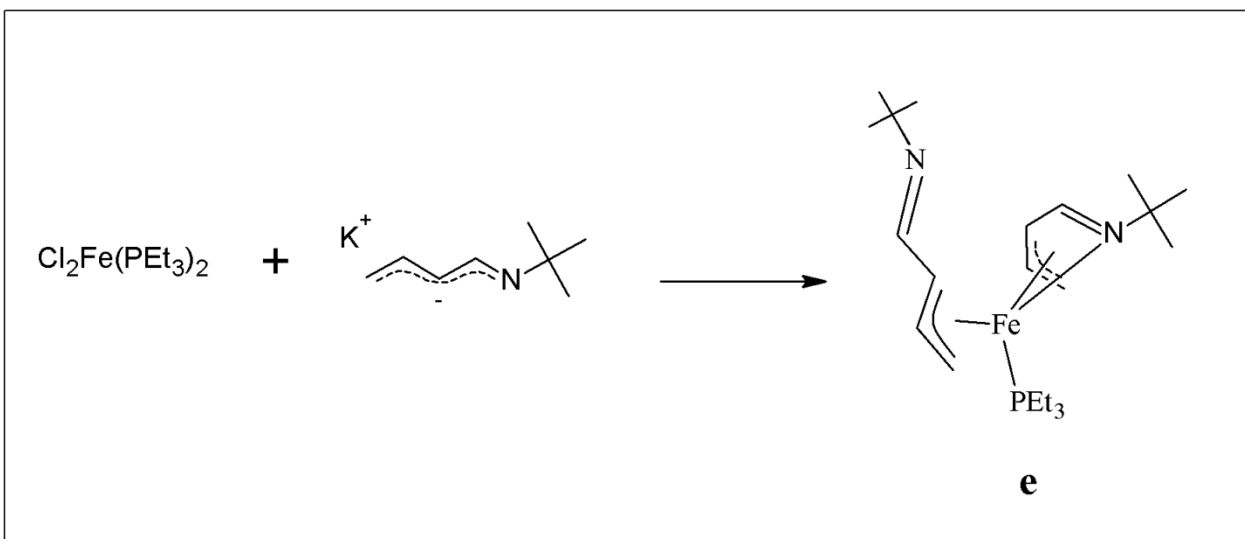
Scheme 4.5: Protonation reactions of (η^5 - pentadienyl)(η^3 - pentadienyl) $\text{Fe}(\text{PEt}_3)$

low temperature in diethyl ether, a salt (**b** - **d**) precipitated out of solution. This reaction most likely proceeded via protonation at iron, followed by rapid migration of the hydride to the

terminal carbon of the η^3 -pentadienyl. As a result, the η^3 -pentadienyl and bulky PEt₃ ligand were displaced by the addition a phosphine.

4.3 Future Direction

The ultimate goal in azapentadienyl-metal chemistry is to create a catalytic cycle utilizing three possible bonding modes (η^1 , η^3 , η^5) (see Scheme 1.4). Converting between these bonding modes opens and closes coordination sites around the metal center. In order to do this, an η^5 -azapentadienyl complex must be synthesized. The most direct way to accomplish this in the *bis*-azapentadienyl systems is to protonate one of the azapentadienyl ligands and introduce a trapping ligand which will help promote dissociation of the protonated azapentadienyl ligand. The *bis*-azapentadienyl-ruthenium complexes prove to be too stable to undergo this protonation route. In order to achieve an η^5 compound, the azapentadienyl ligand must adopt a U-shape instead of a W-shape⁷. The bulkiness created by the presence of two *tert*-butyl groups as well as two ancillary ligands does not allow for the azapentadienyl to take on the required U-shape. Additionally, the ruthenium metal center is large enough to comfortably accommodate the two azapentadienyl ligands and two ancillary ligands. In order to promote dissociation of an azapentadienyl ligand, a smaller metal center might prove helpful. Iron might be a good choice when trying to synthesize an η^5 -azapentadienyl starting material to be used in a catalytic cycle. Scheme 4.6 shows a possible route to obtain an η^5 -azapentadienyl-iron complex. By reacting Cl₂Fe(PEt₃)₂⁸ with potassium *tert*-butylazapentadienide², perhaps (η^5 -*tert*-butylazapentadienyl)(η^3 -*tert*-butylazapentadienyl)FePEt₃ (**e**) could be synthesized.

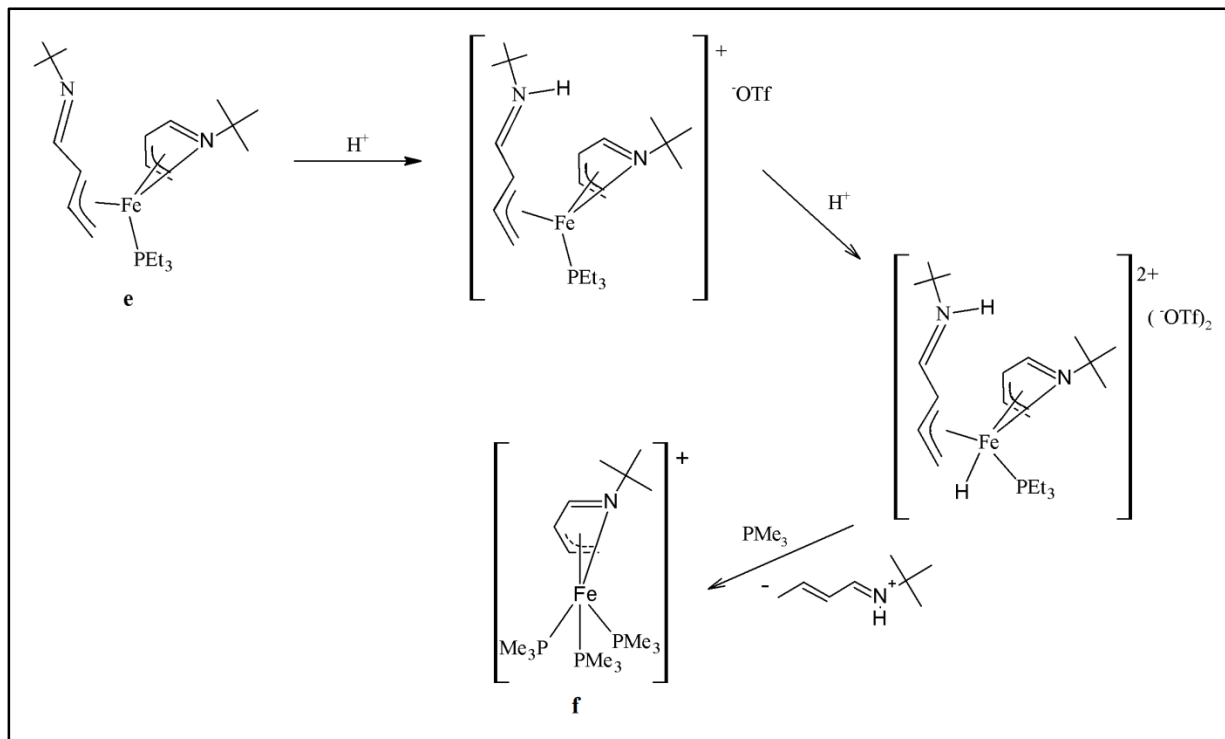


Scheme 4.6: Proposed synthetic route of $(\eta^5\text{-}tert\text{-butylazapentadienyl})(\eta^3\text{-}tert\text{-butylazapentadienyl})\text{Fe}(\text{PEt}_3)$ (**e**).

Based on previous research in the area of pentadienyl-iron chemistry⁵ (see discussion in Section 4.2.1), the introduction of a larger phosphine, such as PEt_3 , may result in $(\eta^5\text{-}tert\text{-butylazapentadienyl})(\eta^3\text{-}tert\text{-butylazapentadienyl})\text{Fe}(\text{PEt}_3)$ (**e**). Theoretically, this reaction would proceed in the azapentadienyl-iron system because the amount of steric interaction of the ligands with respect to the metal center would be reduced. The cone angle sum of two PMe_3 ligands is 236° .⁶ The presence of one PEt_3 would reduce the cone angle total by $\sim 100^\circ$. This reduced steric bulkiness will allow for one of the azapentadienyl ligands to take on a U-shape which is needed to facilitate an η^5 bonding mode. Based on previous azapentadienyl-metal chemistry⁹, an η^3,η^1 bonding mode with bonding through the allyl moiety and the nitrogen lone pair is more likely.

This $\eta^3/\eta^3,\eta^1$ -bis-azapentadienyl-iron compound (**e**) may allow us to dissociate one of the azapentadienyl ligands via the protonation route described previously. Guided by the

protonation chemistry of the azapentadienyl-rhodium system¹⁰, Scheme 4.7 shows the proposed protonation reaction of the *bis*-azapentadienyl-iron compound.



Scheme 4.7: Proposed synthesis of $[(1,2,3-\eta^3,5-\eta^1)-5\text{-}tert\text{-butylazapentadienyl}]\text{Fe}(\text{PMe}_3)_3^+(\text{OTf})$ (**f**).

The proposed scheme shows protonation of the nitrogen center on the η^3 -azapentadienyl ligand of **e**, while retaining the *syn* geometry of the protonated azapentadienyl ligand. The η^4 resonance structure is not a major resonance contributor and because of this, the azapentadienyl remains anionic and difficult to displace. A second protonation at the iron center is most likely required. With the addition of a trapping ligand, PMe_3 , the protonated azapentadienyl ligand can reductively eliminate, resulting in **f**. Protonation of only *one* of the azapentadienyl ligands, more specifically the η^3 -azapentadienyl ligand, is expected because the lone pair on the nitrogen of the η^5 -azapentadienyl ligand is coordinated to the iron metal center

and would not be available for protonation by triflic acid. This change in metal center from ruthenium to iron could help in synthesizing the target *mono*-azapentadienyl compound. This *mono*-azapentadienyl-iron compound has the potential to be used in the catalytic cycle described in Scheme 1.4. As described in Section 2.1.2.1^{9,11} the presence of the azapentadienyl ligand, as opposed to the all carbon pentadienyl ligand, will allow for the opening and closing of coordination sites around the iron metal center. Because an N-Fe bond (in an azapentadienyl complex) is weaker than a (C=C)-Fe bond (in a pentadienyl complex), it can be released from the metal center with the addition of substrate molecules, allowing us to achieve the η^3 and η^1 complexes seen in the catalytic cycle (Scheme 1.4).

4.4 References

- (1) (a) Stephenson, T.A.; Wilkinson, G. *J. Inorg. Nucl. Chem.* **1966**, *28*, 945.
(b) Hallman, P.S.; Stephenson, T.A.; Wilkinson, G. *Inorg. Synth.* **1970**, *12*, 237.
- (2) Bleeke, J.R.; Luaders, S.T.; Robinson, K.D. *Organometallics*, **1994**, *13*, 1592-1600.
- (3) Bleeke, J.R.; Stouffer, M.; Rath, N.P., *J. of Organometallic Chem.*, **2015**,
- (4) Bleeke, J.R.; Hays, M.K. *Organometallics*, **1984**, *3*, 506 – 508.
- (5) Bleeke, J.R.; Hays, M.K.; Wittenbrink, R.J. *Organometallics*, **1988**, *7*, 1417 – 1425.
- (6) Tolman, C.A. *Chem.Rev.*, **1977**, *77*, 313 – 348.
- (7) The E,E (W-shaped) geometry of the lithium salt was established by Wurthwein. The NMR spectra of the potassium salt are identical with those of the lithium salt.
Wolf, G.; Wurthwein, E.-U. *Chem. Ber.* **1991**, *124*, 889 - 896.
- (8) Harris, T.V.; Rathke, J.W.; Muetterties, E.L. *J. Amer. Chem. Soc.* **1978**, *100*, 6966-6977.
- (9) Reyna-Madrigal, A.; Moreno-Gurrola, A.; Perez-Camacho, O.; Navarro-Clemente, M.E.; Juarez-Saavedra, P.; Leyva-Ramirez, M.A.; Arif, A.M.; Ernst, R.D.; Paz-Sandoval, M.A.

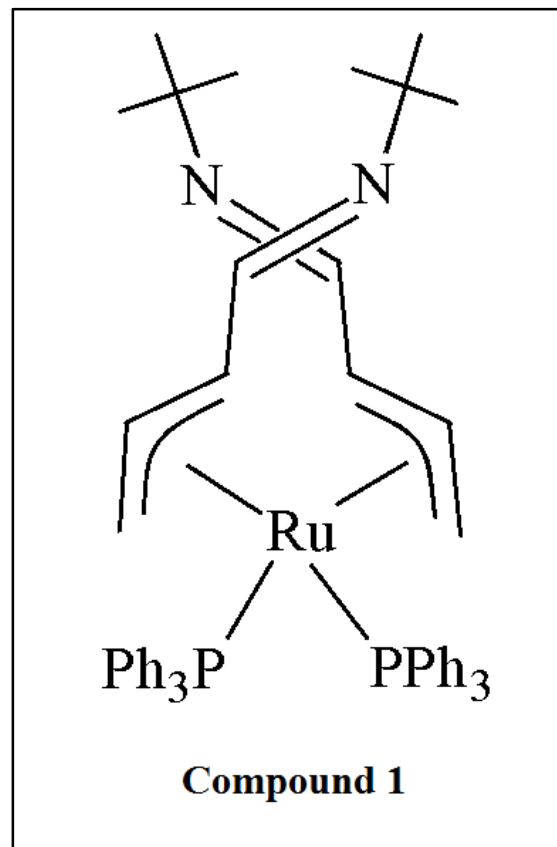
Organometallics **2012**, *31*, 7125-7145.

(10) Bleeke, J.R.; Anutrasakda, w.; Rath, N.P. *Organometallics*, **2013**, *32*, 6410--6426.

(11) Bleeke, J.R.; Rauscher, D. *Organometallics* **1988**, *7*, 2328-2339.

Appendix A

NMR Spectra of Neutral *bis*-Azapentadienyl-Ruthenium-Phosphine Complexes



- ^1H NMR (THF-d₈, 22 °C)
- ^{13}C NMR (THF-d₈, 22 °C)
- DEPT Spectrum (THF-d₈, 22 °C)
- ^{31}P NMR (THF-d₈, 22 °C)
- COSY NMR (THF-d₈, 22 °C)
- HMQC NMR (THF-d₈, 22 °C)

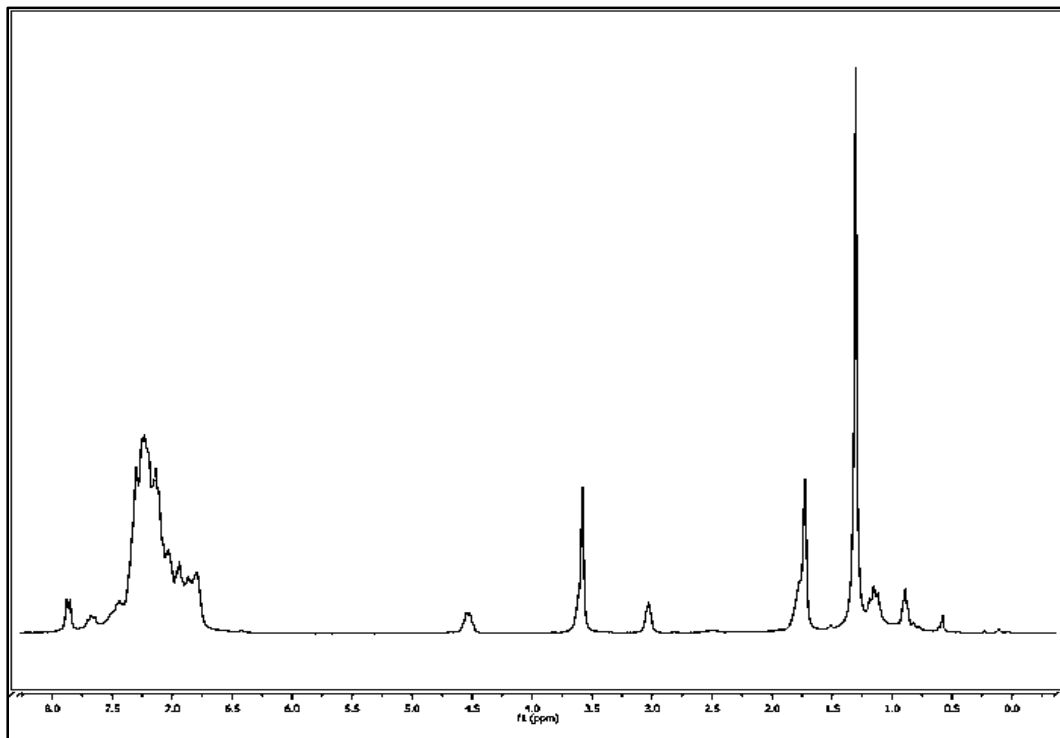


Figure A-1: ^1H NMR Spectrum of **1** ($\text{d}_8\text{-THF}$, 22 °C)

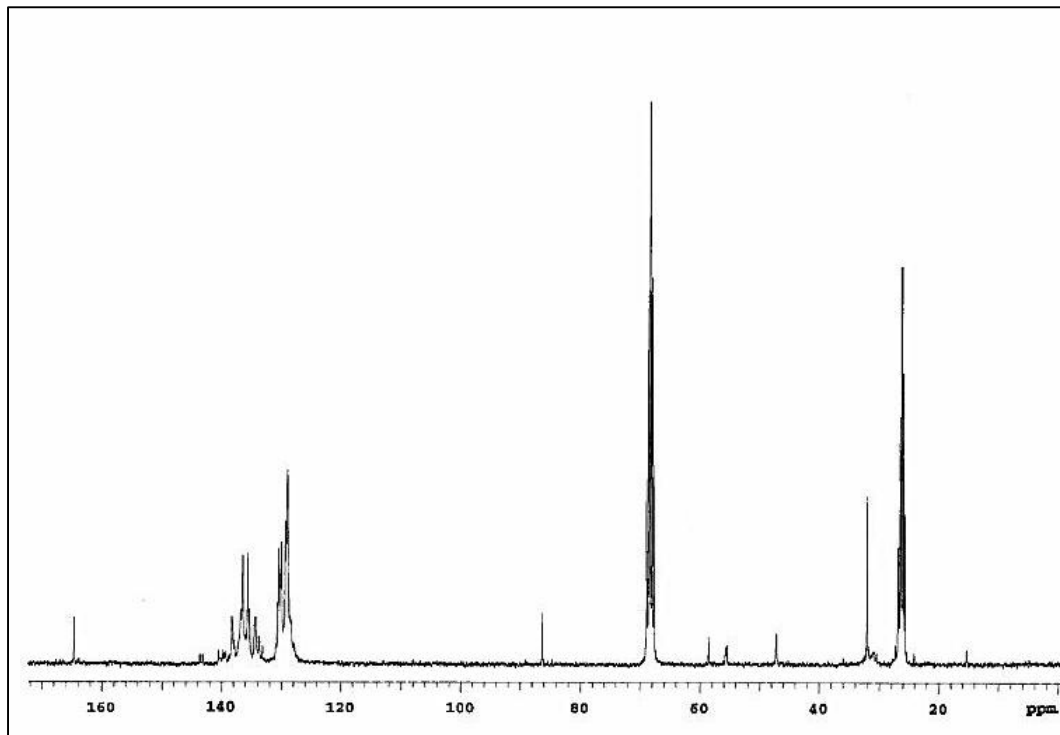


Figure A-2: ^{13}C NMR Spectrum of **1** ($\text{d}_8\text{-THF}$, 22 °C)

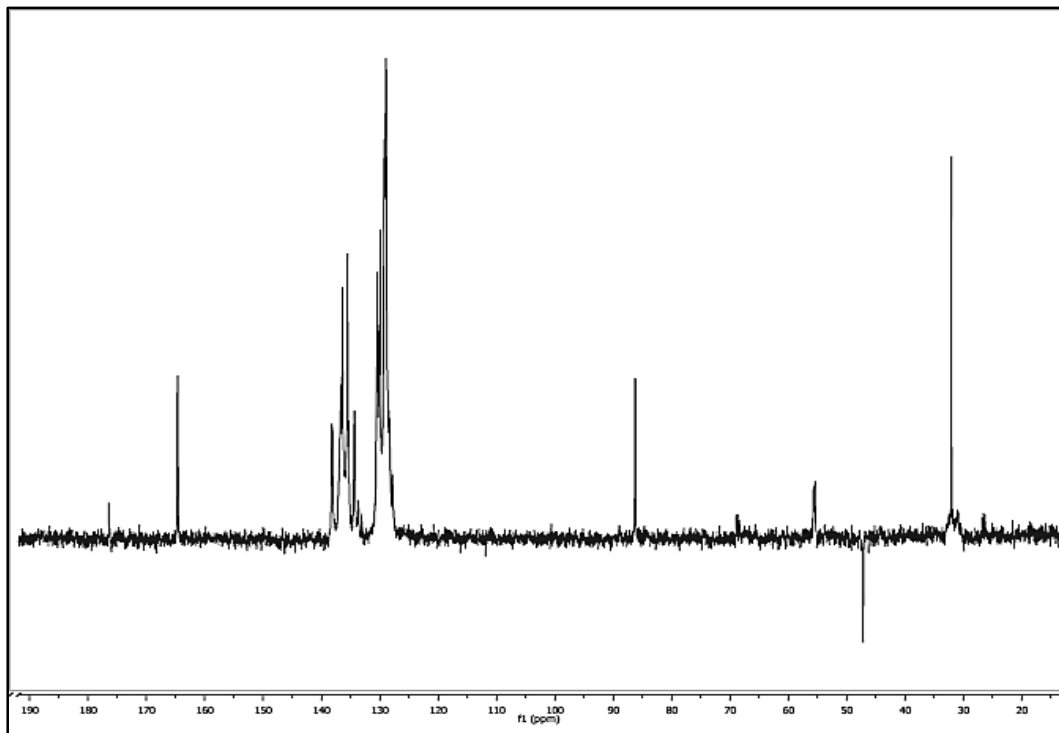


Figure A-3: DEPT NMR Spectrum of **1** (d_8 -THF, 22 °C)

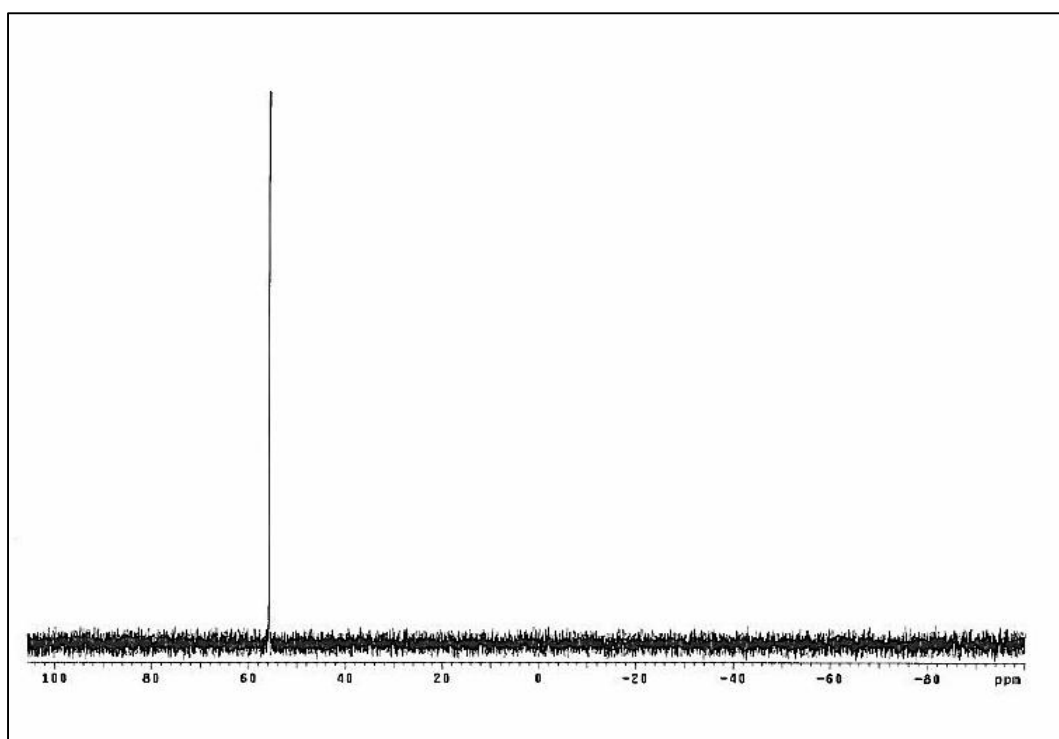


Figure A-4: ^{31}P NMR Spectrum of **1** (d_8 -THF, 22 °C)

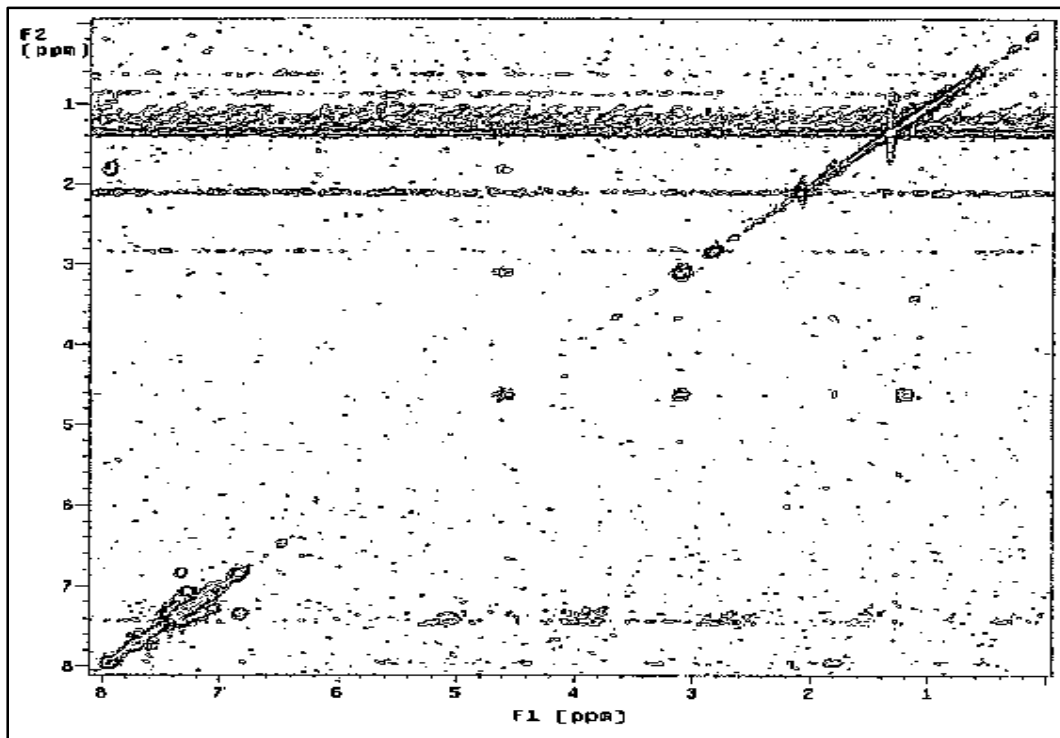


Figure A-5: COSY Spectrum of **1** (d_8 -THF, 22 °C)

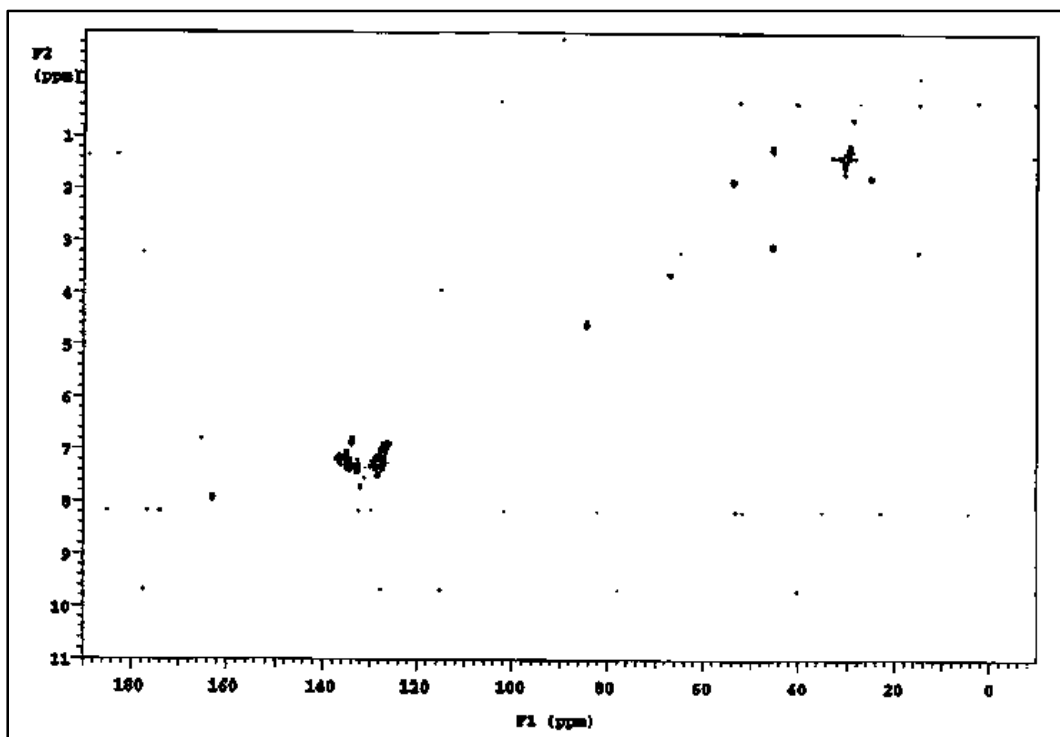
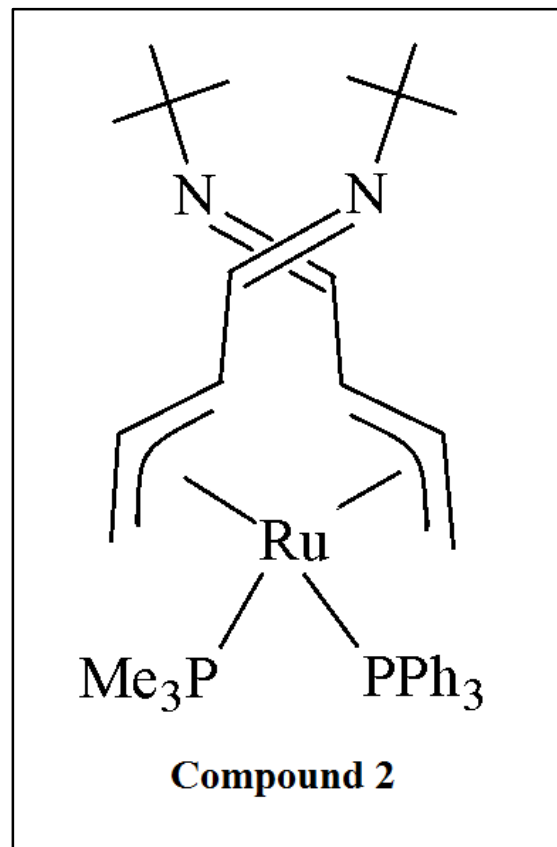


Figure A-6: HMQC Spectrum of **1** (d_8 -THF, 22 °C)



- ¹H NMR (acetone-d₆, 22 °C)
- ¹³C NMR (acetone-d₆, 22 °C)
- DEPT Spectrum (acetone-d₆, 22 °C)
- ³¹P NMR (acetone-d₆, 22 °C)
- COSY NMR (acetone-d₆, 22 °C)
- HMQC NMR (acetone-d₆, 22 °C)

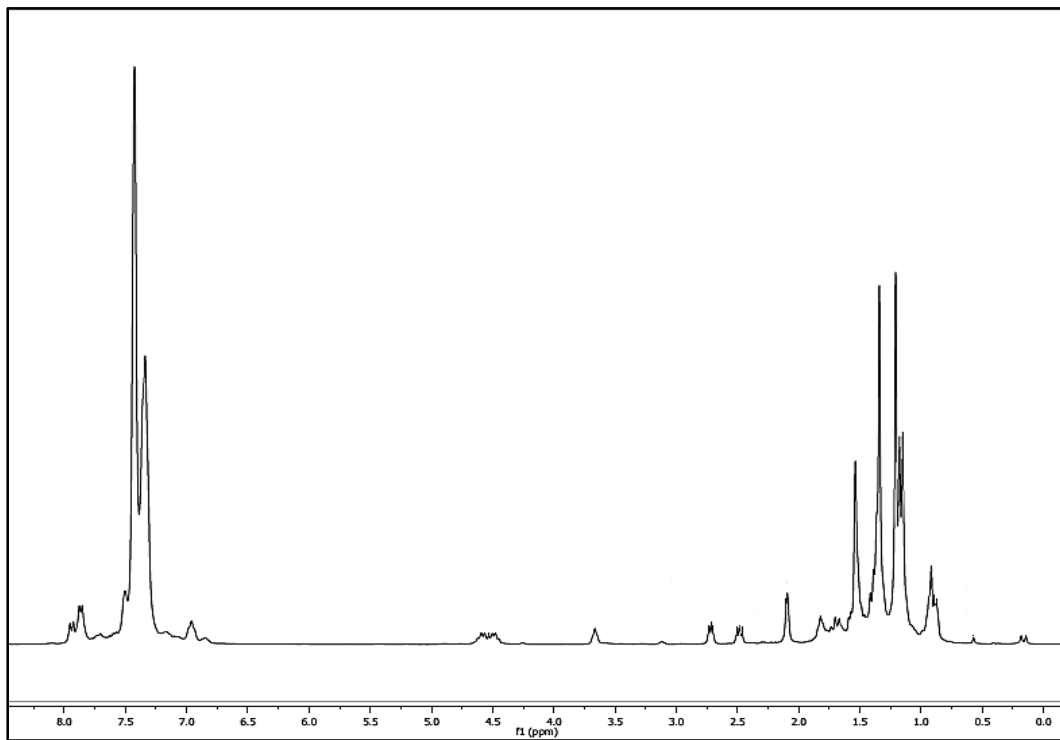


Figure A-7: ¹H NMR Spectrum of **2** (d₆-acetone, 22 °C)

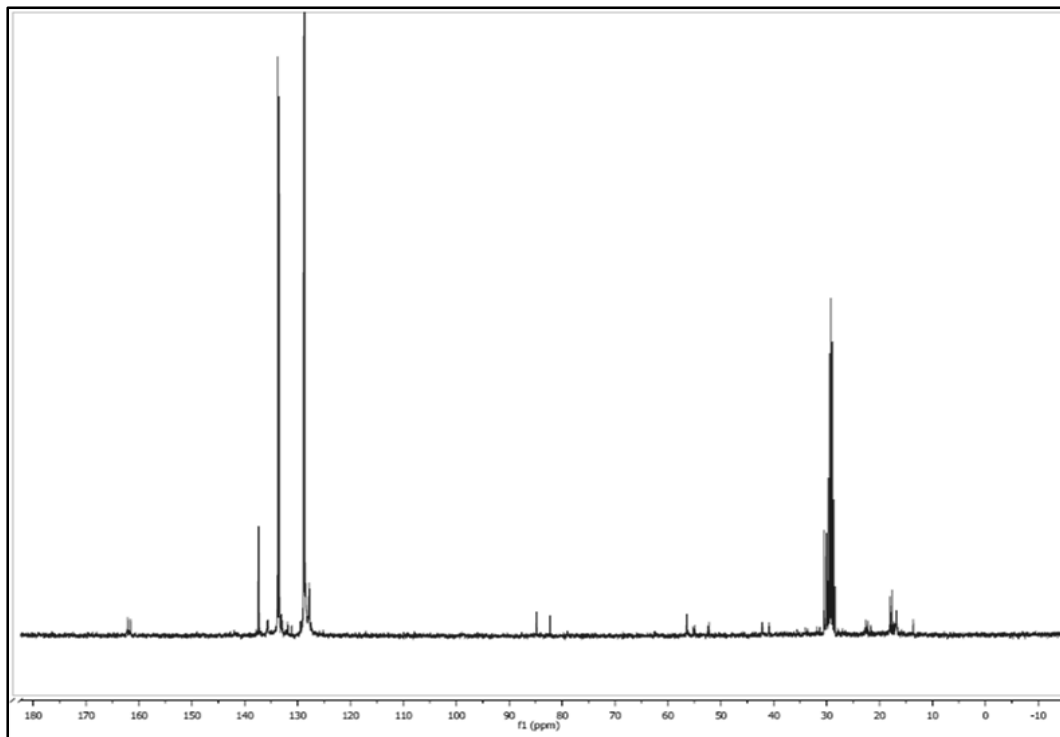


Figure A-8: ¹³C NMR Spectrum of **2** (d₆-acetone, 22 °C)

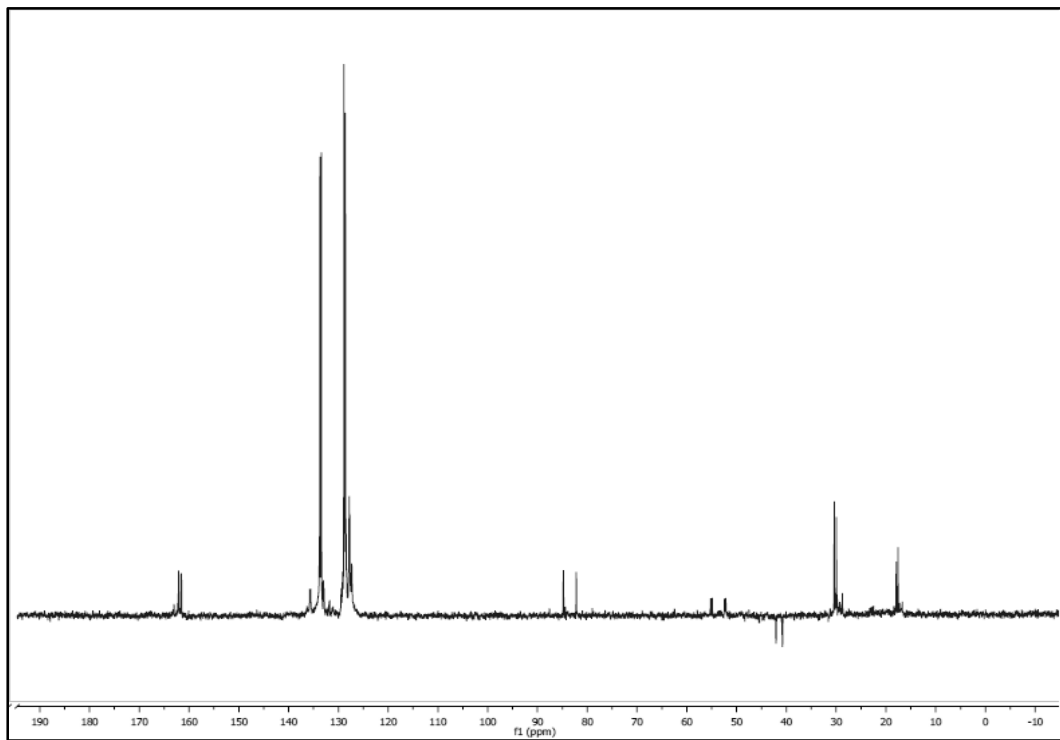


Figure A-9: DEPT Spectrum of **2** (d_6 -acetone, 22 °C)

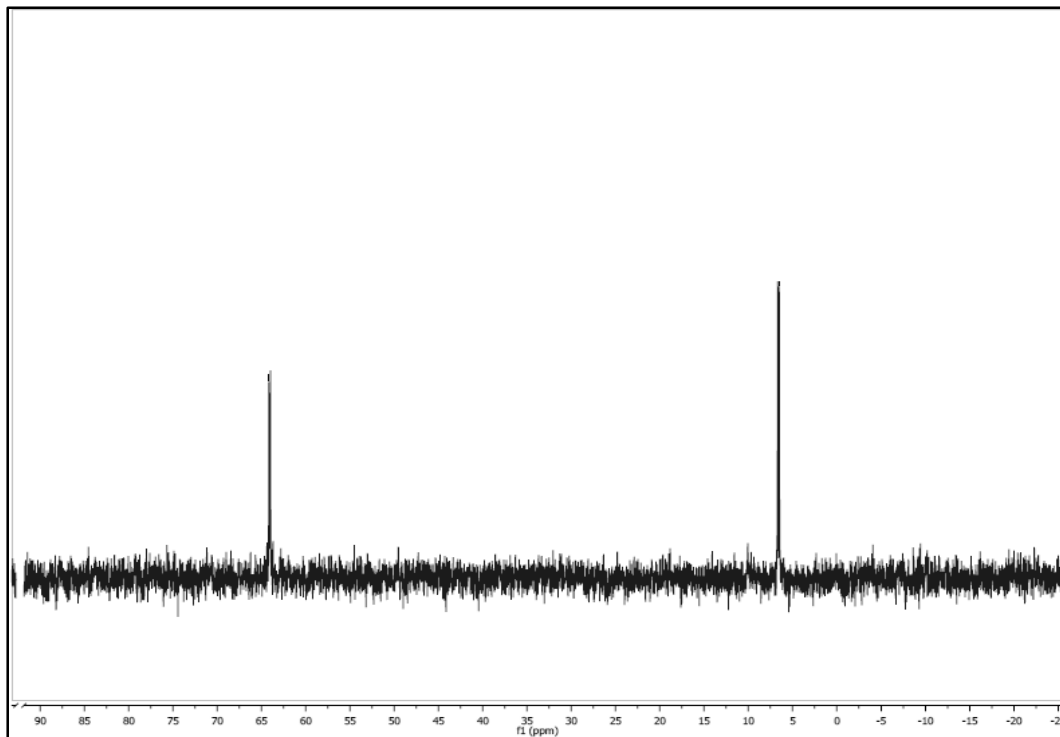


Figure A-10: ^{31}P NMR Spectrum of **2** (d_6 -acetone, 22 °C)

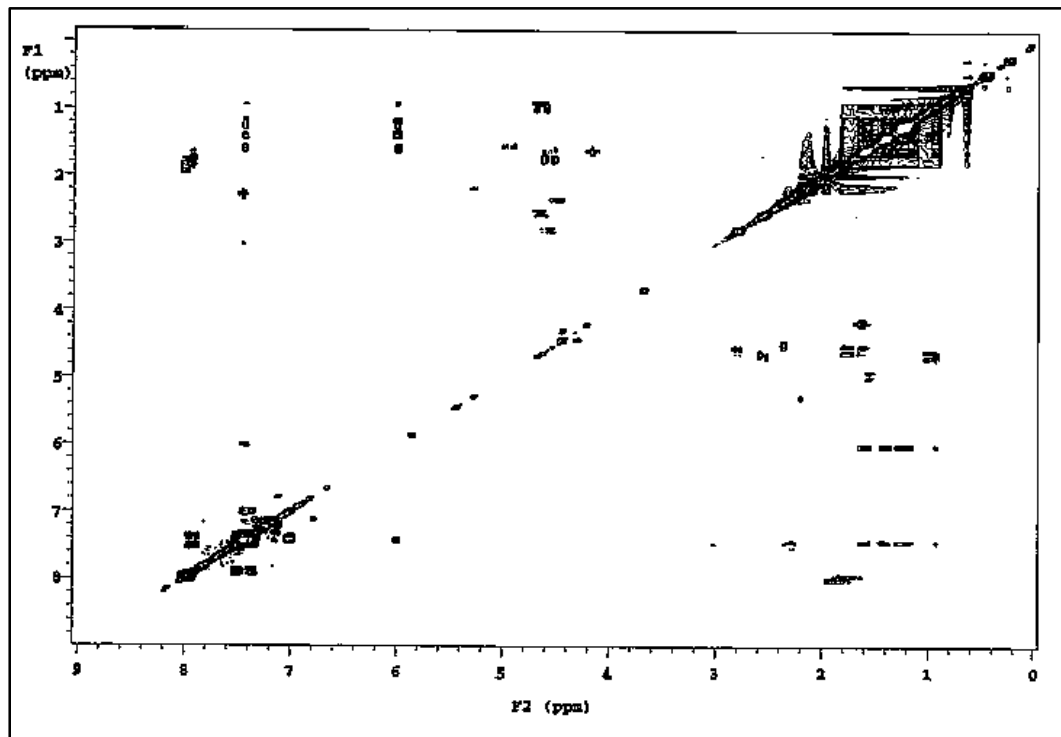


Figure A-11: COSY Spectrum of **2** (d_6 -acetone, 22 °C)

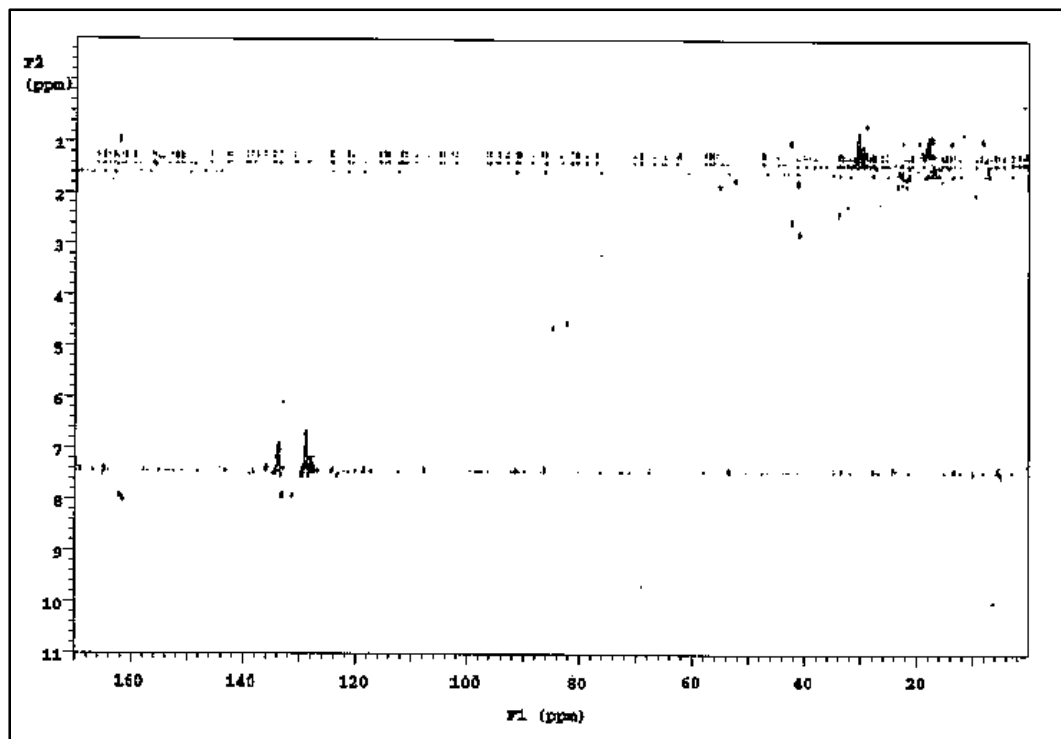
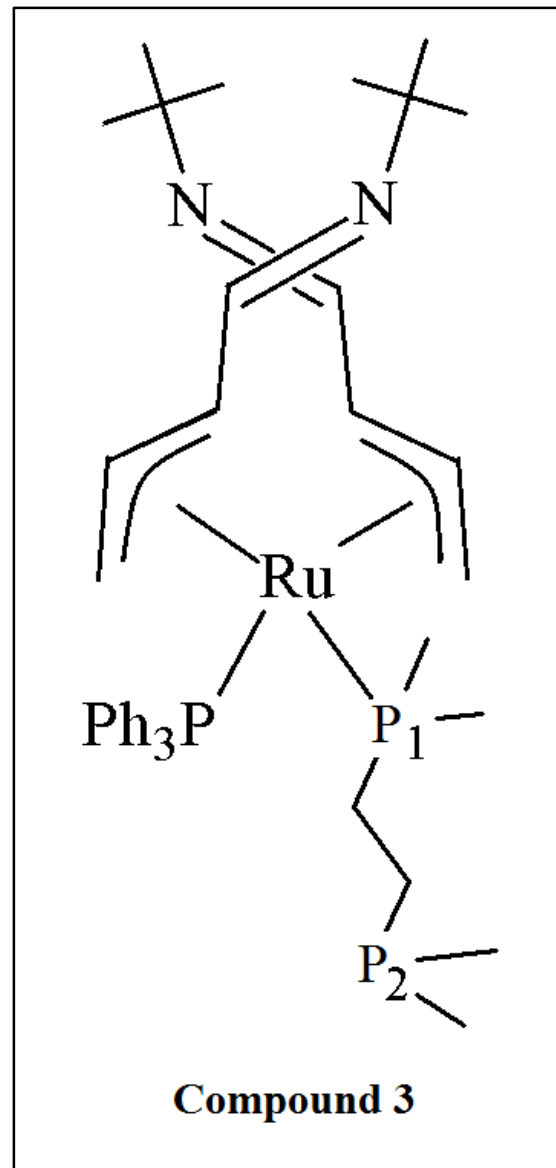


Figure A-12: HMQC Spectrum of **2** (d_6 -acetone, 22 °C)



- ^1H NMR (acetone- d_6 , 22 °C)
- ^{31}P NMR (acetone- d_6 , 22 °C)

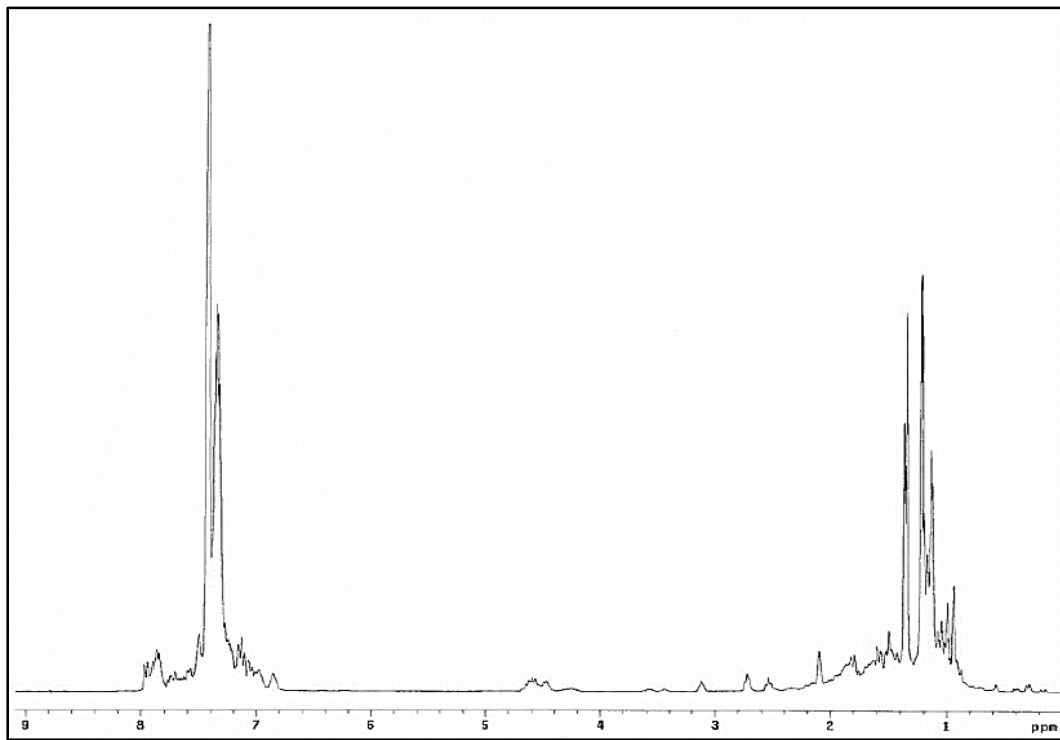


Figure A-13: ¹H NMR Spectrum of **3** (d_6 -acetone, 22 °C)

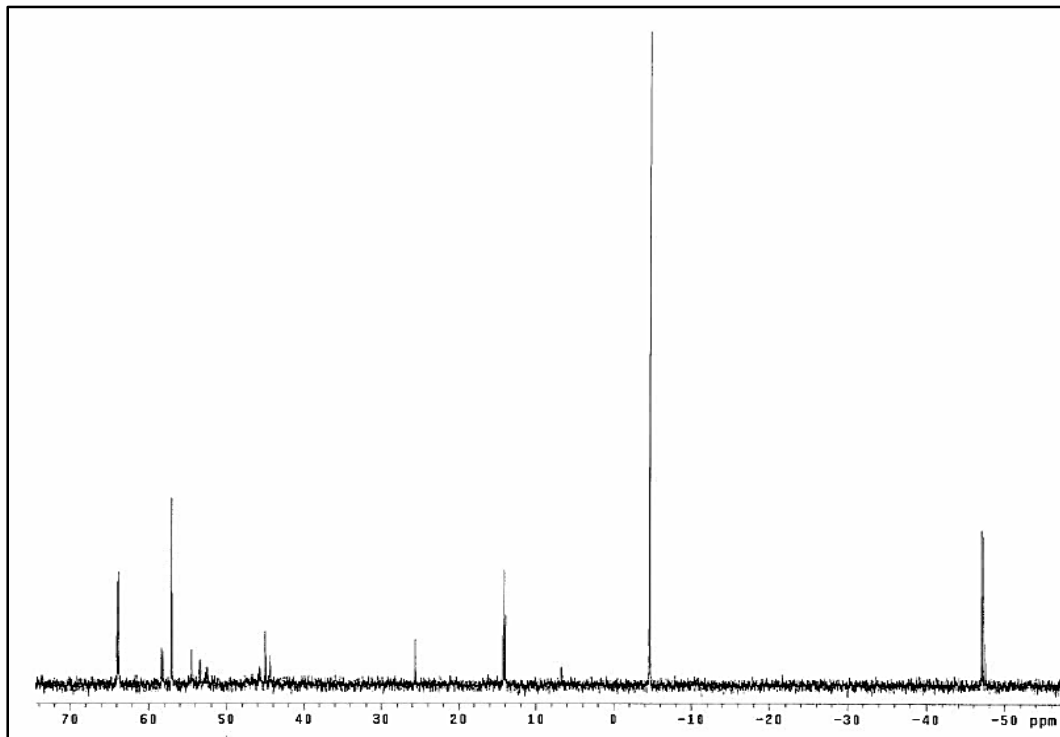
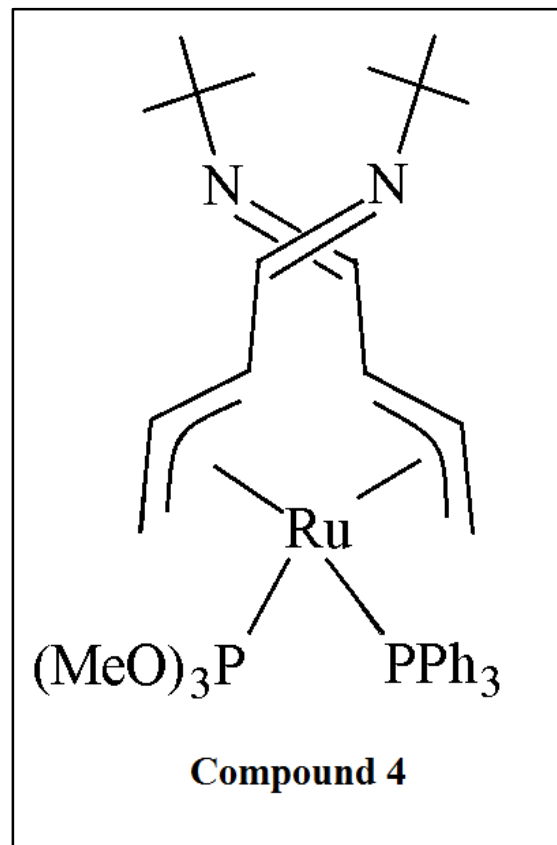


Figure A-14: ³¹P NMR Spectrum of **3** (d_6 -acetone, 22 °C)



- ^1H NMR (acetone- d_6 , 22 °C)
- ^{13}C NMR (acetone- d_6 , 22 °C)
- DEPT Spectrum (acetone- d_6 , 22 °C)
- ^{31}P NMR (acetone- d_6 , 22 °C)
- COSY NMR (acetone- d_6 , 22 °C)
- HMQC NMR (acetone- d_6 , 22 °C)

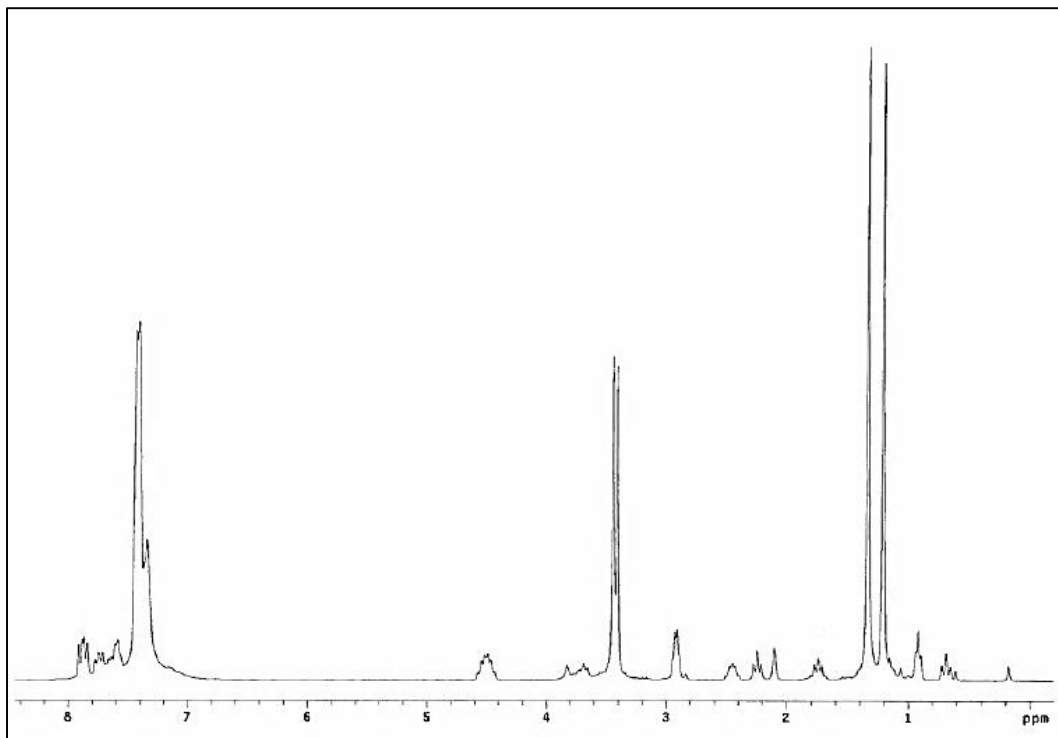


Figure A-15: ¹H NMR Spectrum of **4** (d_6 -acetone, 22 °C)

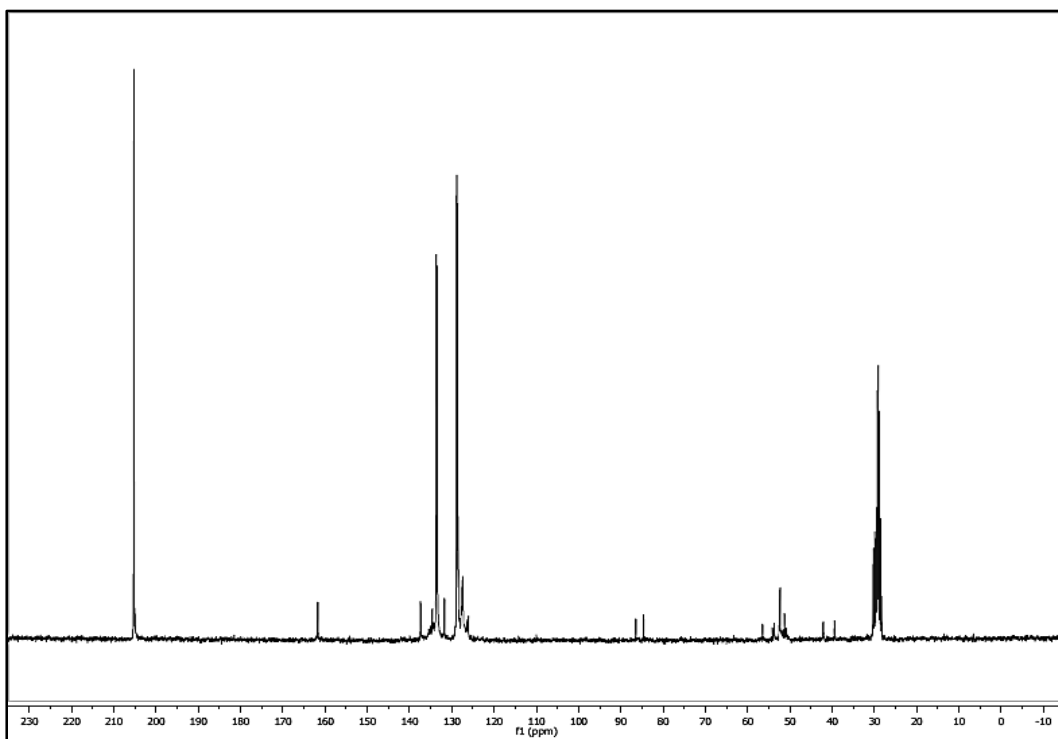


Figure A-16: ¹³C NMR Spectrum of **4** (d_6 -acetone, 22 °C)

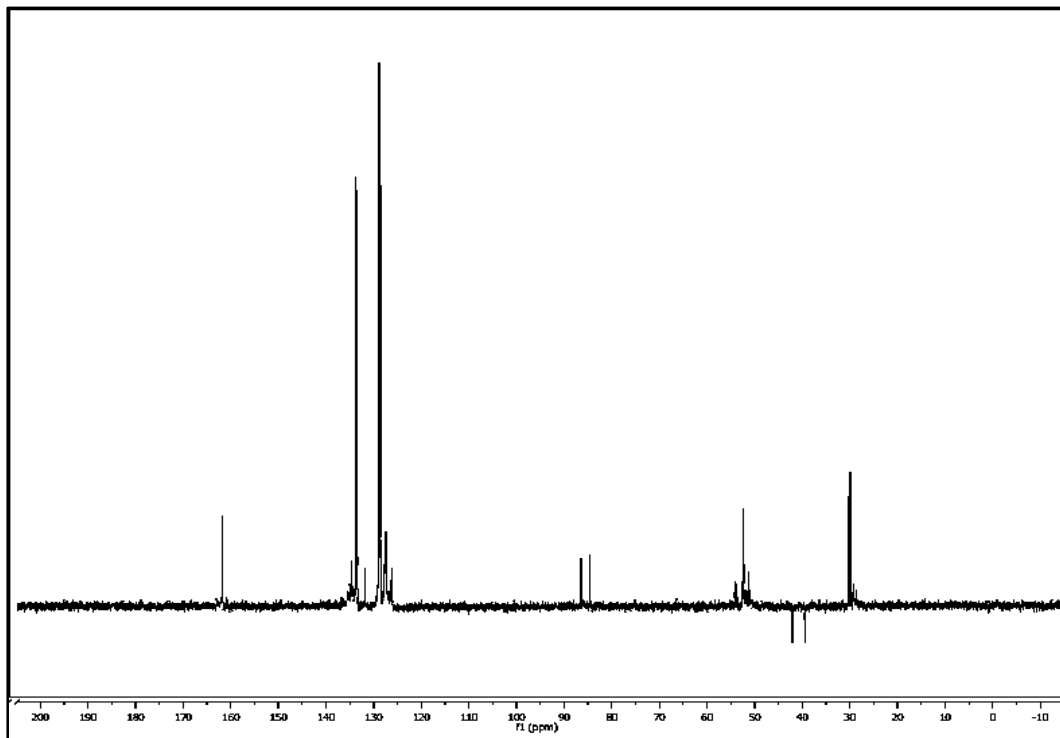


Figure A-17: DEPT Spectrum of **4** (d_6 -acetone, 22 °C)

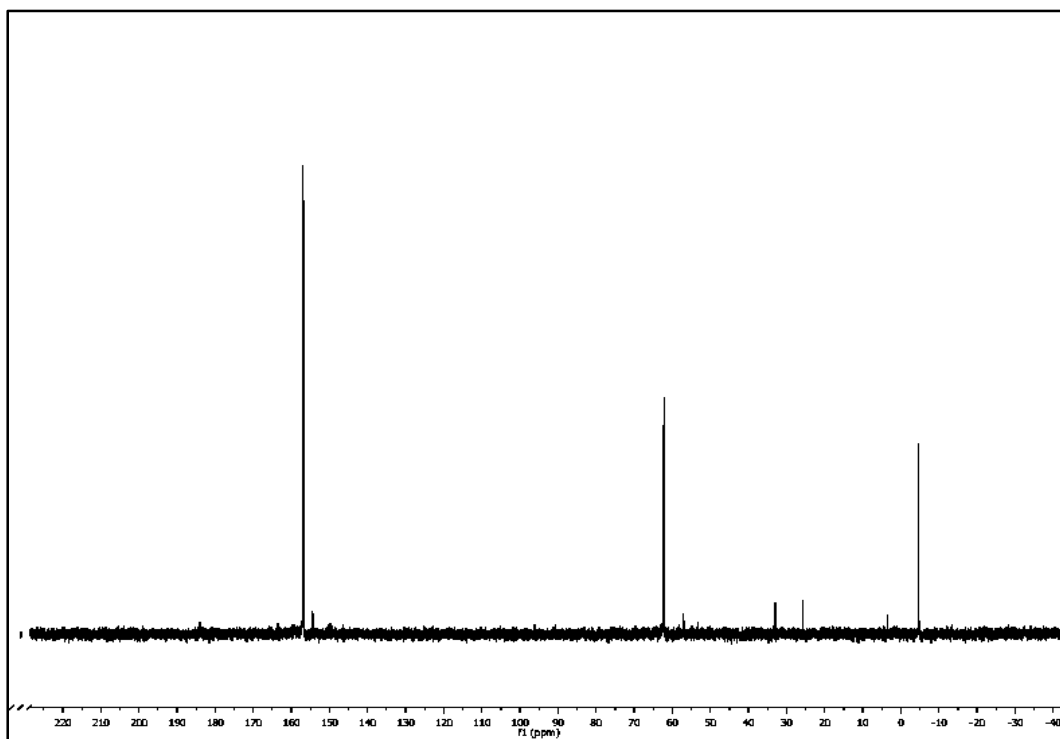


Figure A-18: ³¹P NMR Spectrum of **4** (d_6 -acetone, 22 °C)

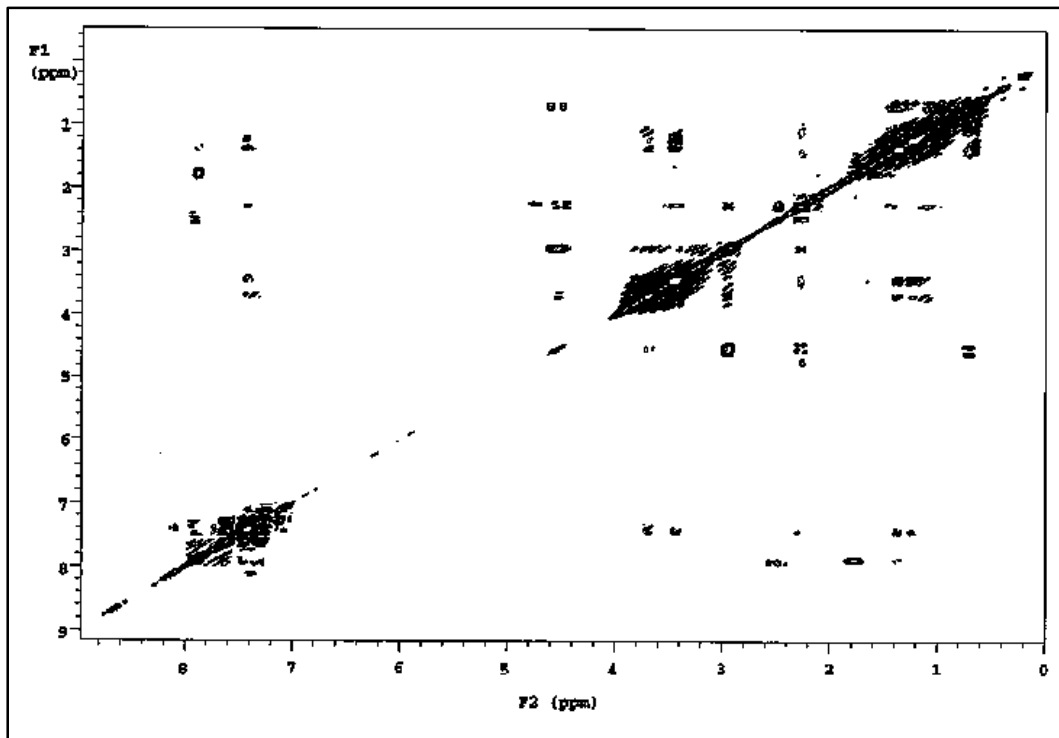


Figure A-19: COSY Spectrum of **4** (d_6 -acetone, 22 °C)

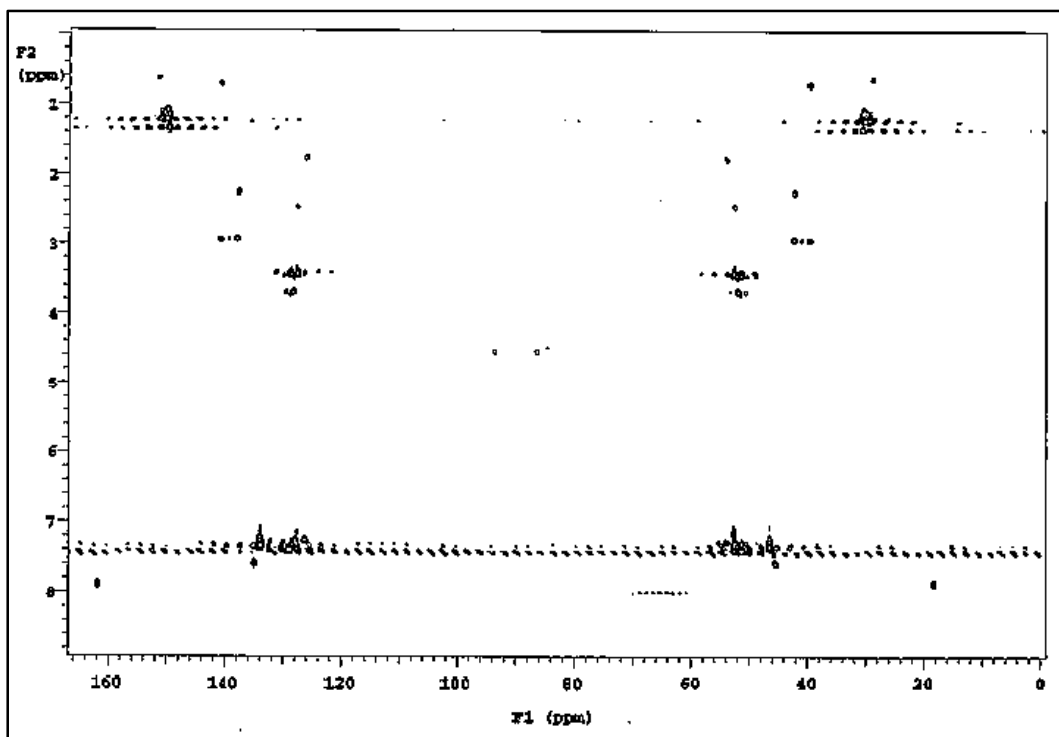
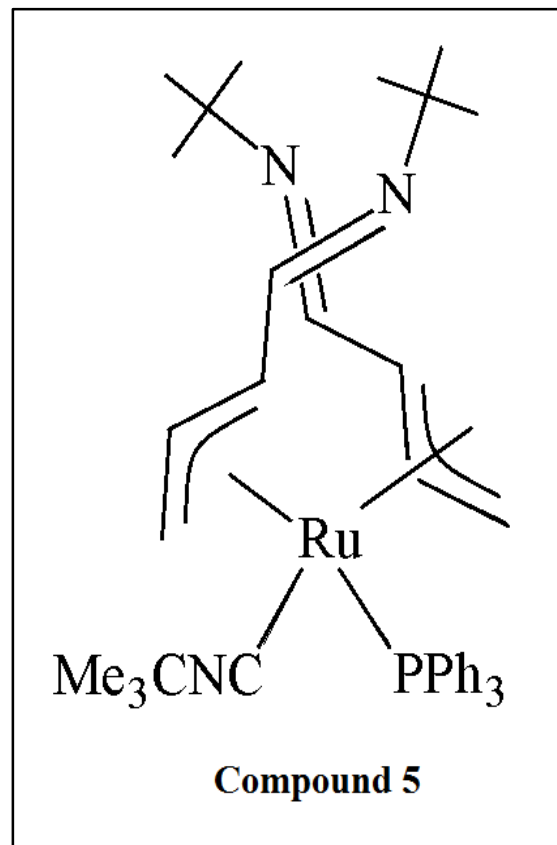


Figure A-20: HMQC Spectrum of **4** (d_6 -acetone, 22 °C)



- ¹H NMR (acetone-d₆, 22 °C)
- ¹³C NMR (acetone-d₆, 22 °C)
- ³¹P NMR (acetone-d₆, 22 °C)
- COSY NMR (acetone-d₆, 22 °C)
- HMQC NMR (acetone-d₆, 22 °C)

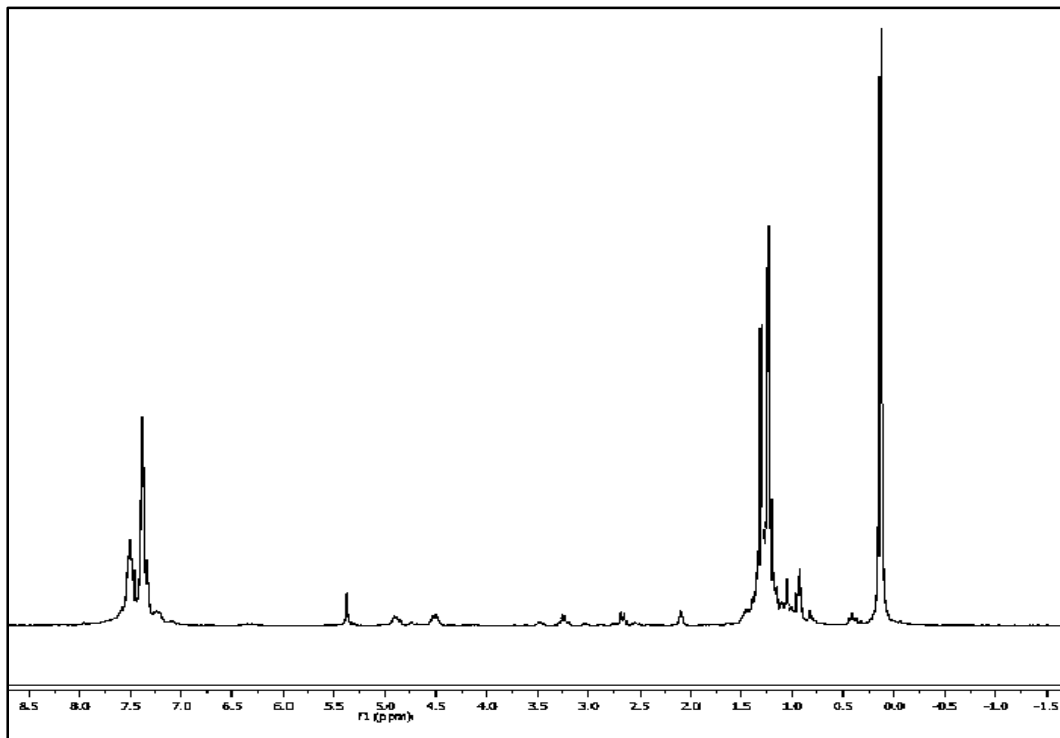


Figure A-21: ¹H NMR Spectrum of **5** (d₂-dichloromethane, 22 °C)

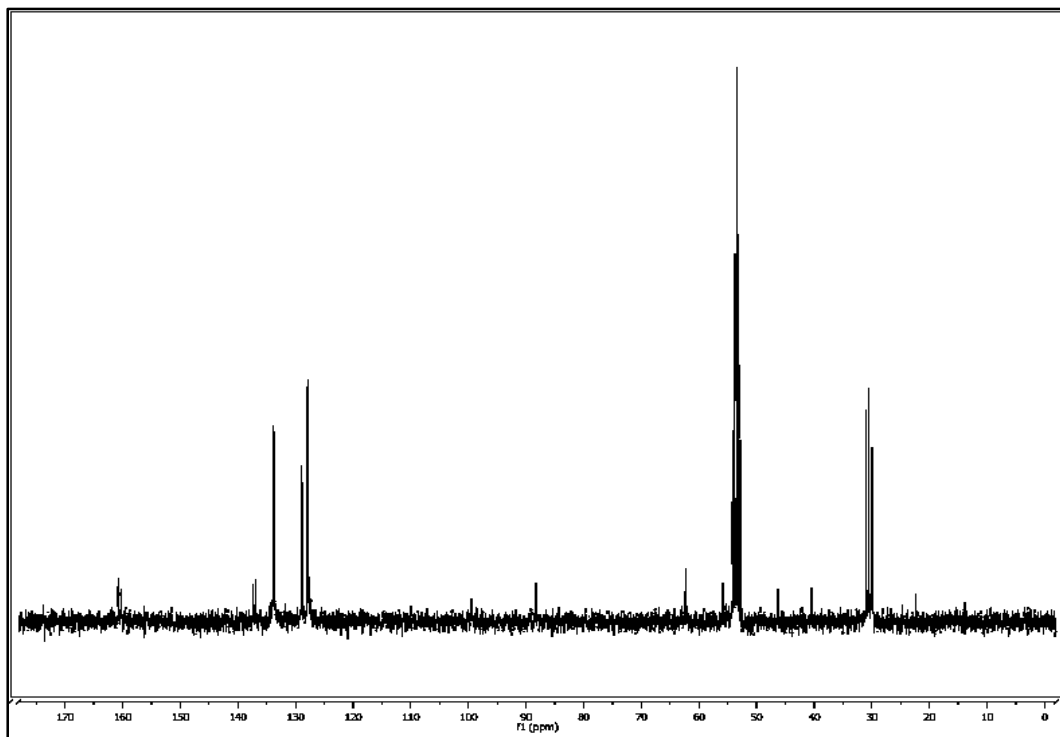


Figure A-22: ¹³C NMR Spectrum of **5** (d₂-dichloromethane, 22 °C)

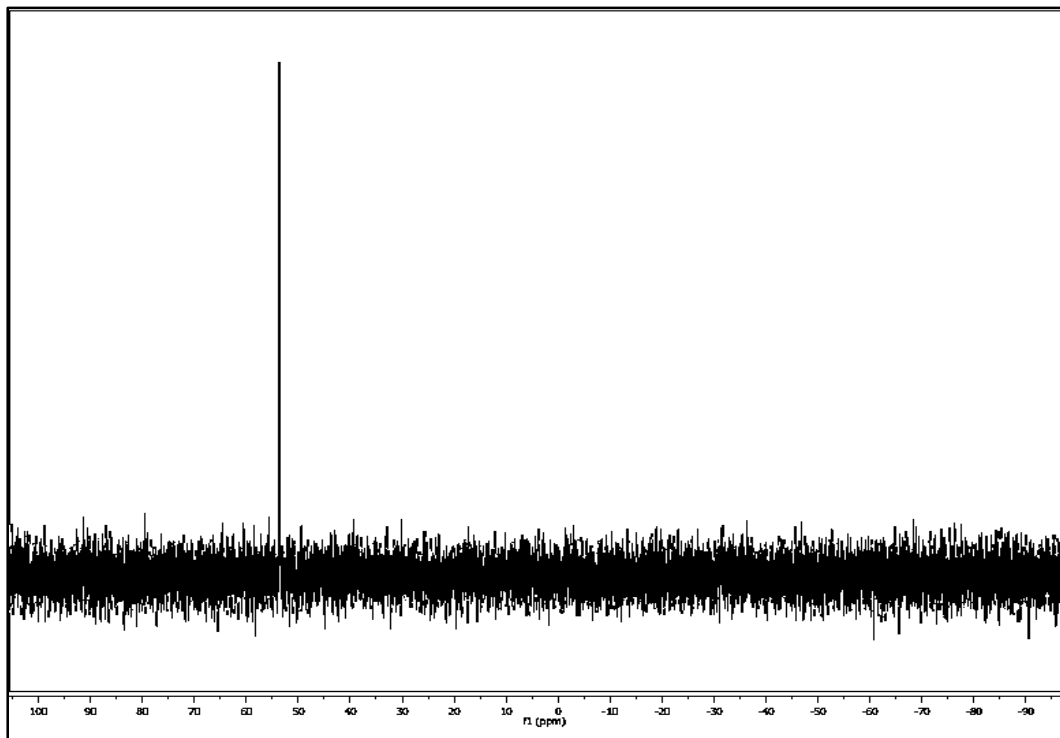


Figure A-23: ^{31}P NMR Spectrum of **5** ($\text{d}_2\text{-dichloromethane}$, 22 °C)

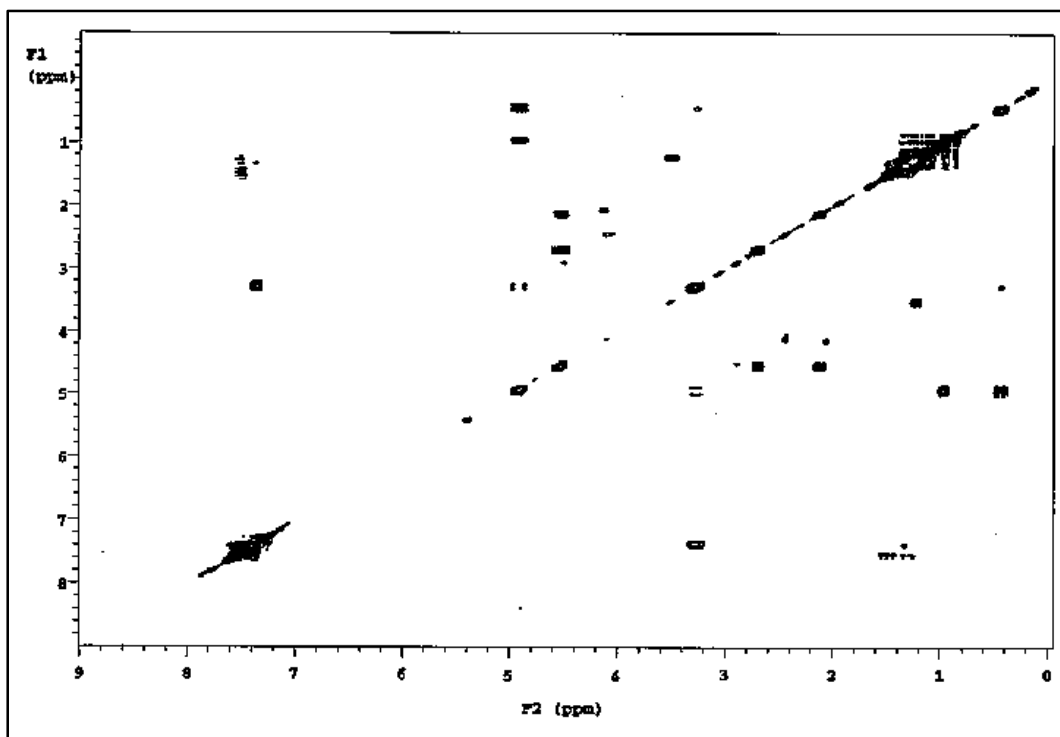


Figure A-24: COSY Spectrum of **5** ($\text{d}_2\text{-dichloromethane}$, 22 °C)

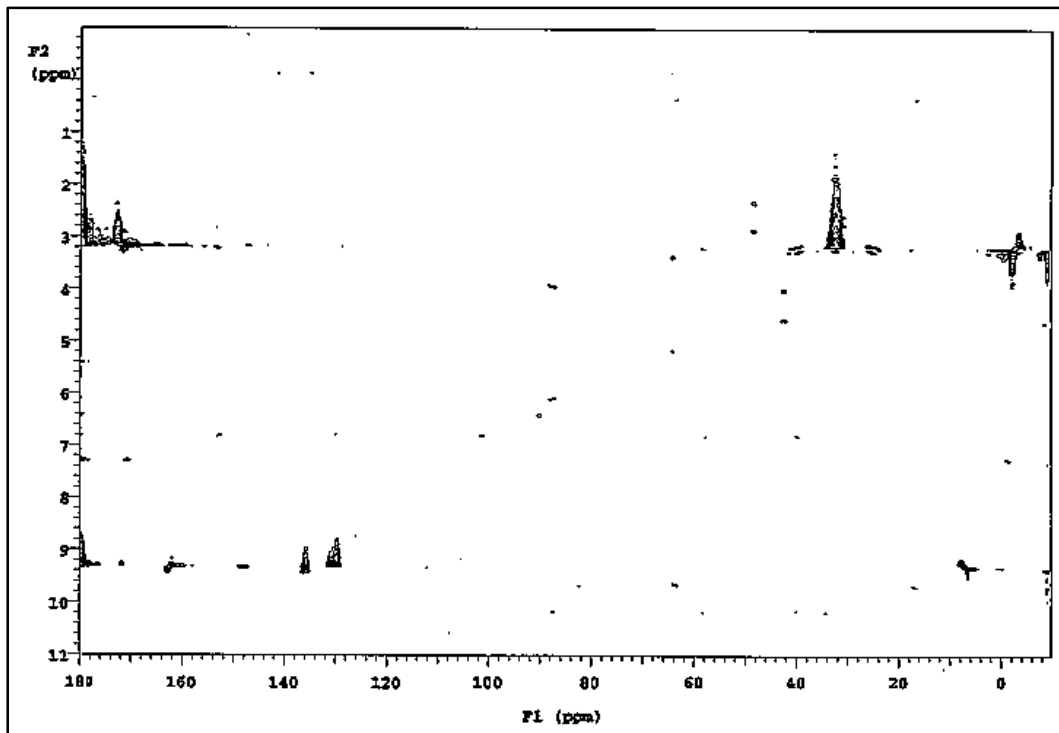
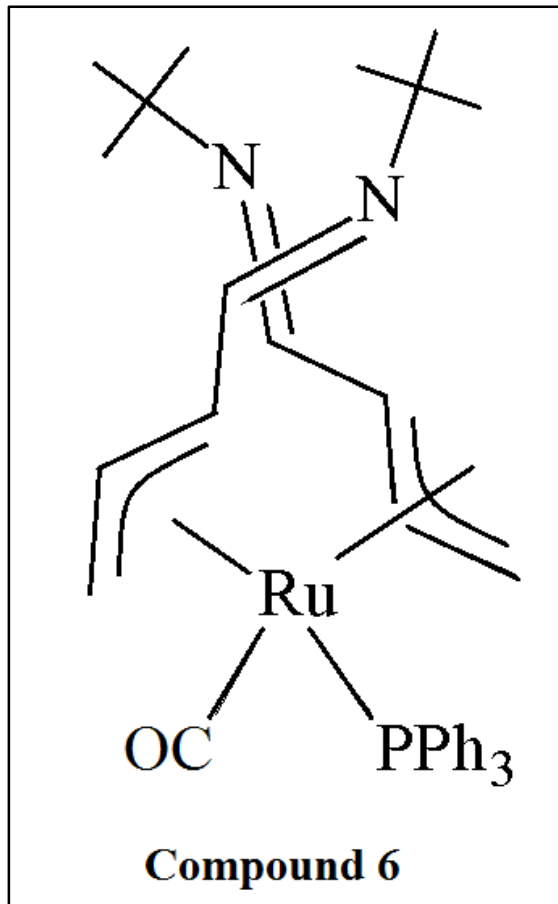


Figure A-25: HMQC Spectrum of **5** (d_2 -dichloromethane, 22 °C)



- ^1H NMR (acetone- d_6 , 22 °C)
- ^{13}C NMR (acetone- d_6 , 22 °C)
- ^{31}P NMR (acetone- d_6 , 22 °C)

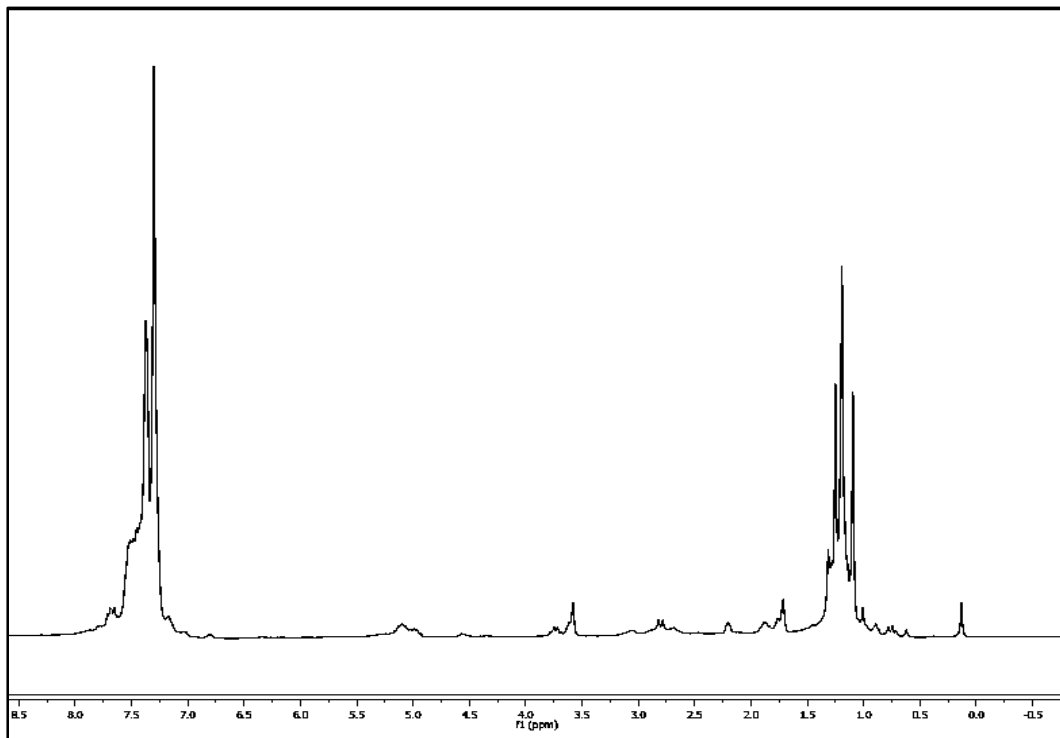


Figure A-26: ^1H NMR Spectrum of **6** (d_6 -acetone, 22 °C)

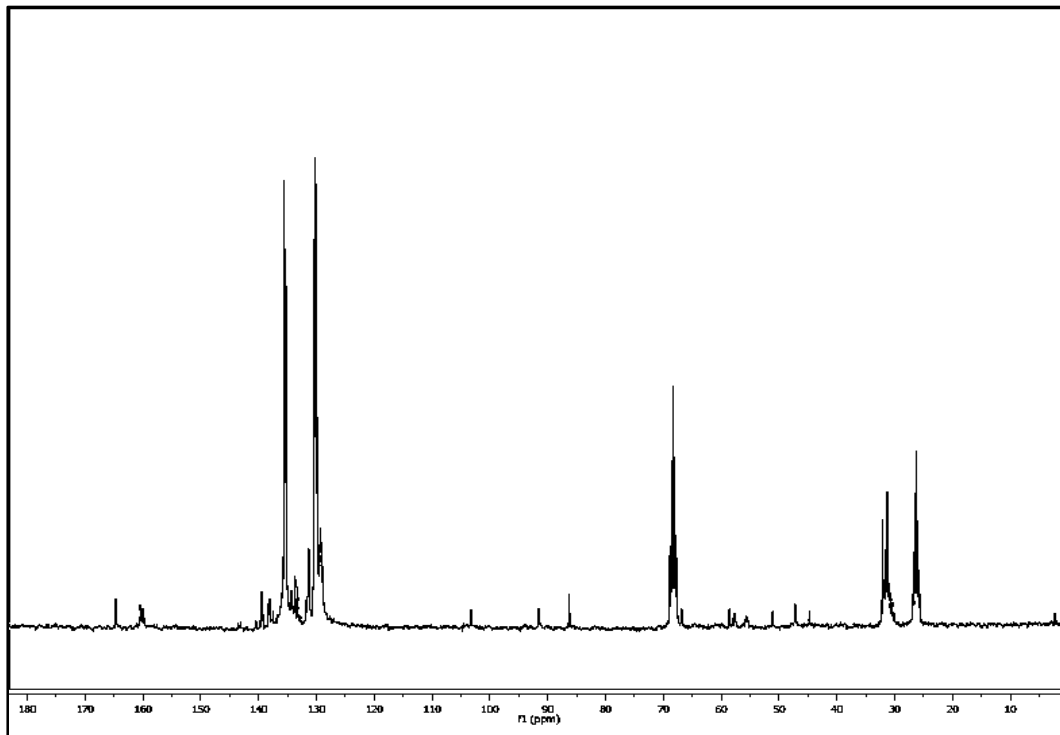


Figure A-27: ^{13}C NMR Spectrum of **6** (d_6 -acetone, 22 °C)

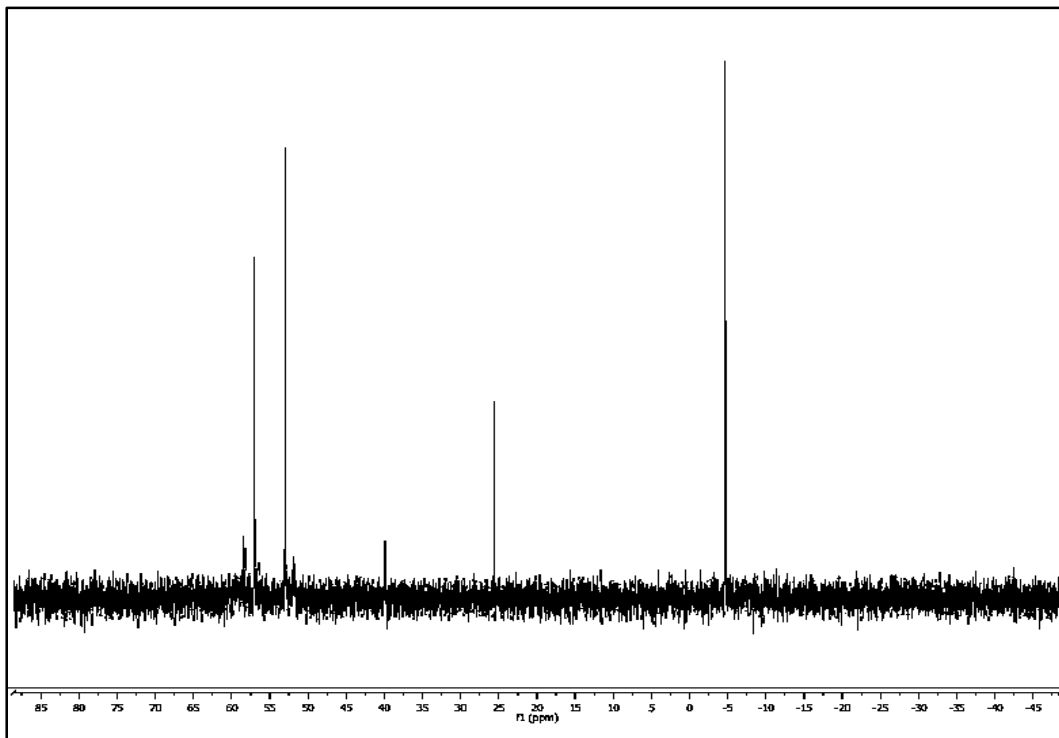
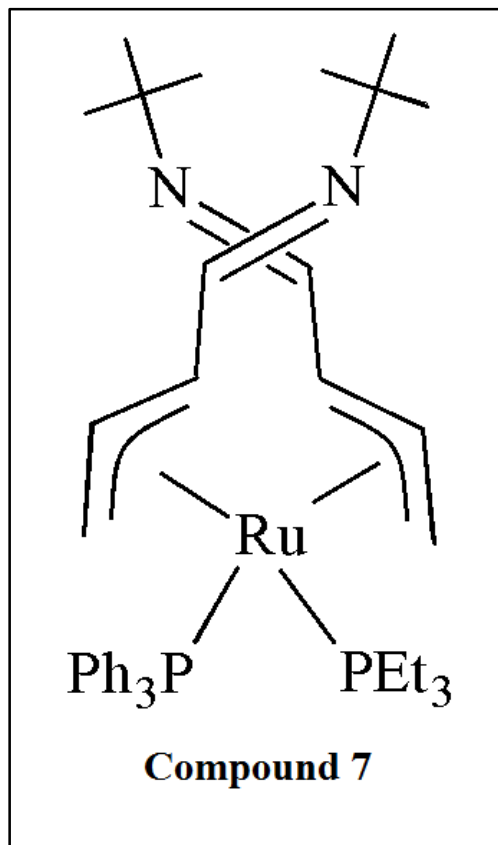


Figure A-28: ^{31}P NMR Spectrum of **6** ($\text{d}_6\text{-acetone}$, 22 °C)



- ${}^{31}\text{P}$ NMR (acetone- d_6 , 22 °C)

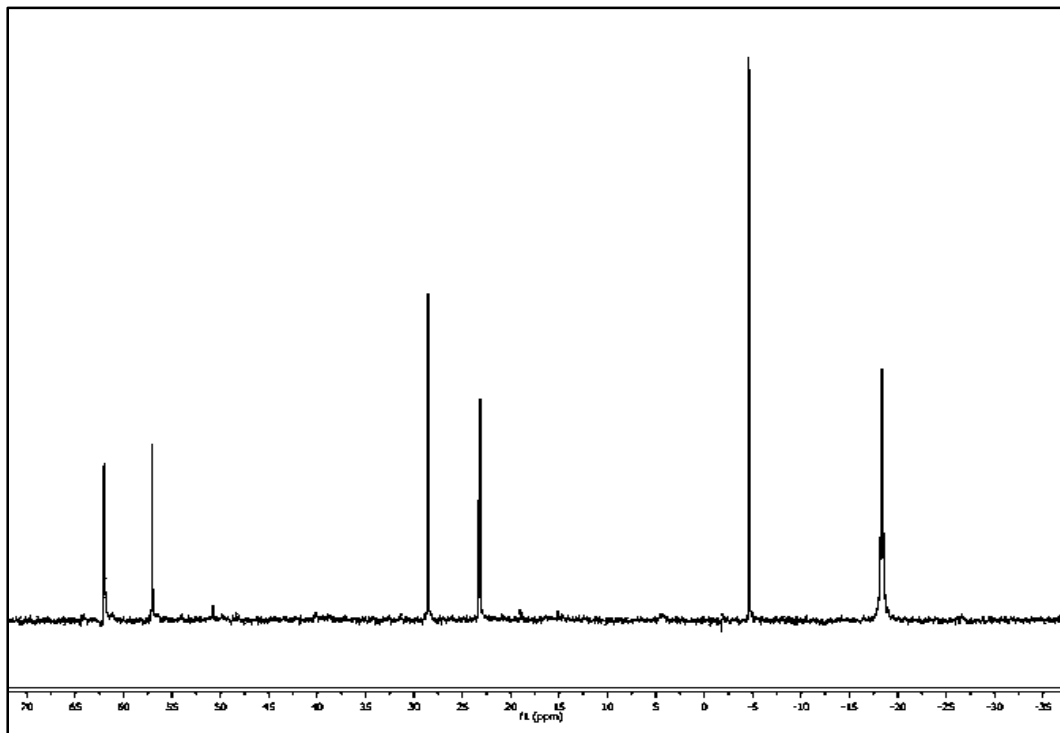
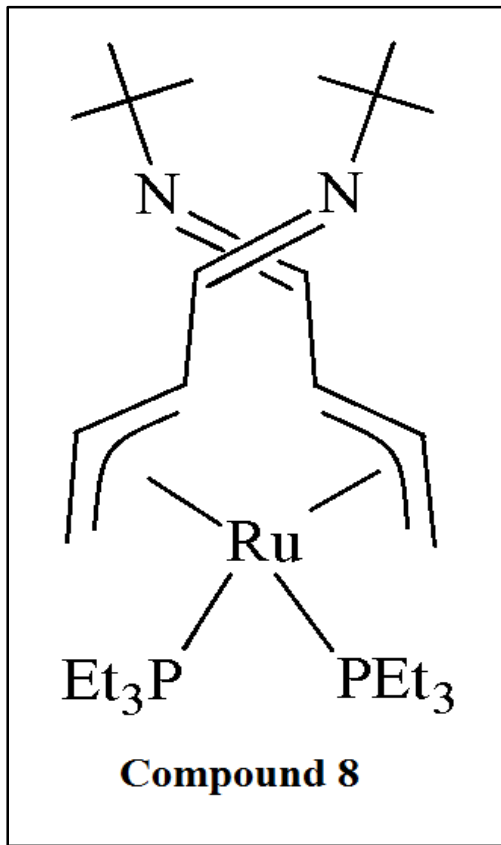


Figure A-29: ^{31}P NMR Spectrum of **7** ($\text{d}_6\text{-acetone}$, 22 °C)



- ^1H NMR (acetone- d_6 , 22 °C)
- ^{13}C NMR (acetone- d_6 , 22 °C)
- DEPT Spectrum (acetone- d_6 , 22 °C)
- ^{31}P NMR (acetone- d_6 , 22 °C)
- COSY NMR (acetone- d_6 , 22 °C)
- HMQC NMR (acetone- d_6 , 22 °C)

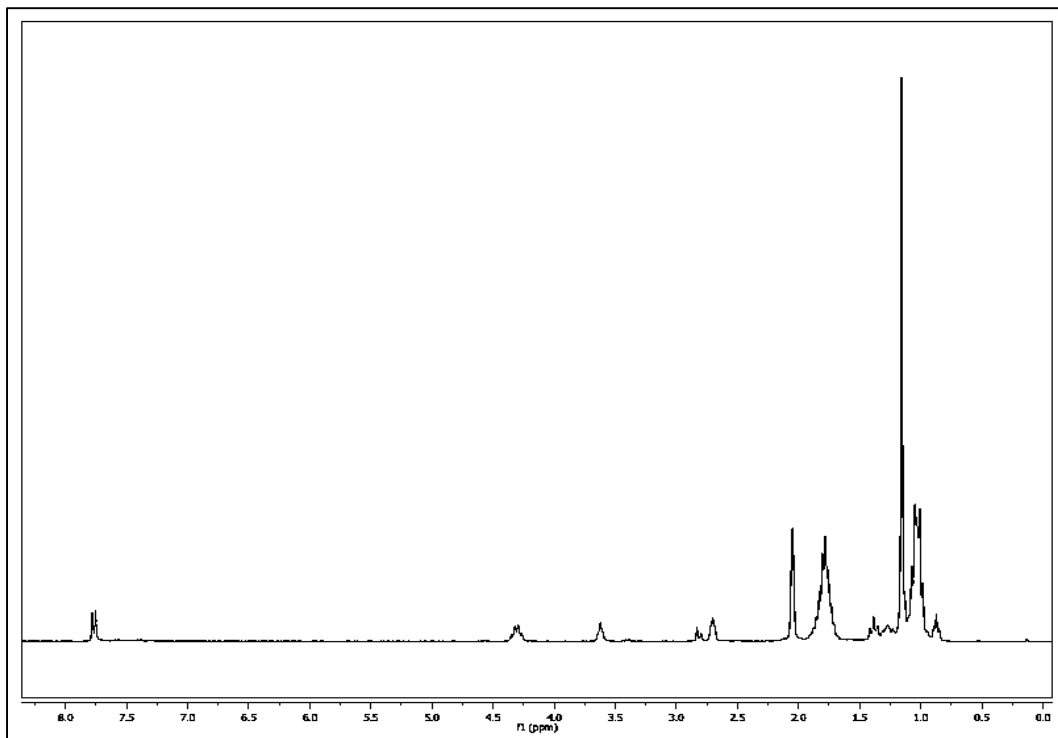


Figure A-30: ¹H NMR Spectrum of **8** (d_6 -acetone, 22 °C)

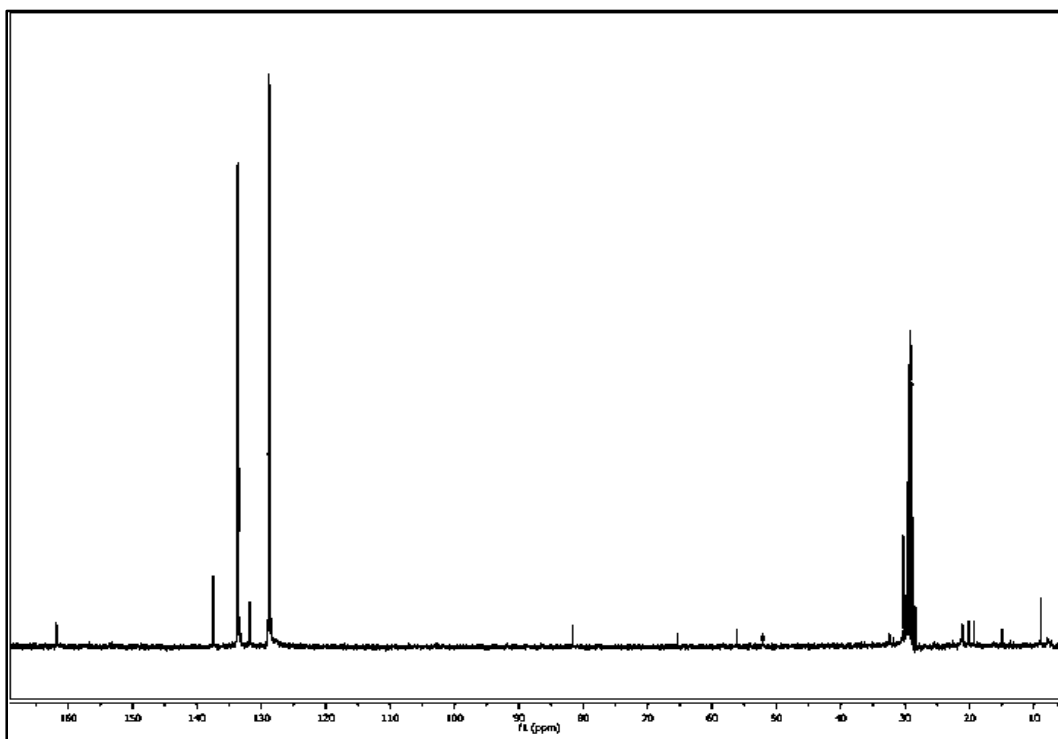


Figure A-31: ¹³C NMR Spectrum of **8** (d_6 -acetone, 22 °C)

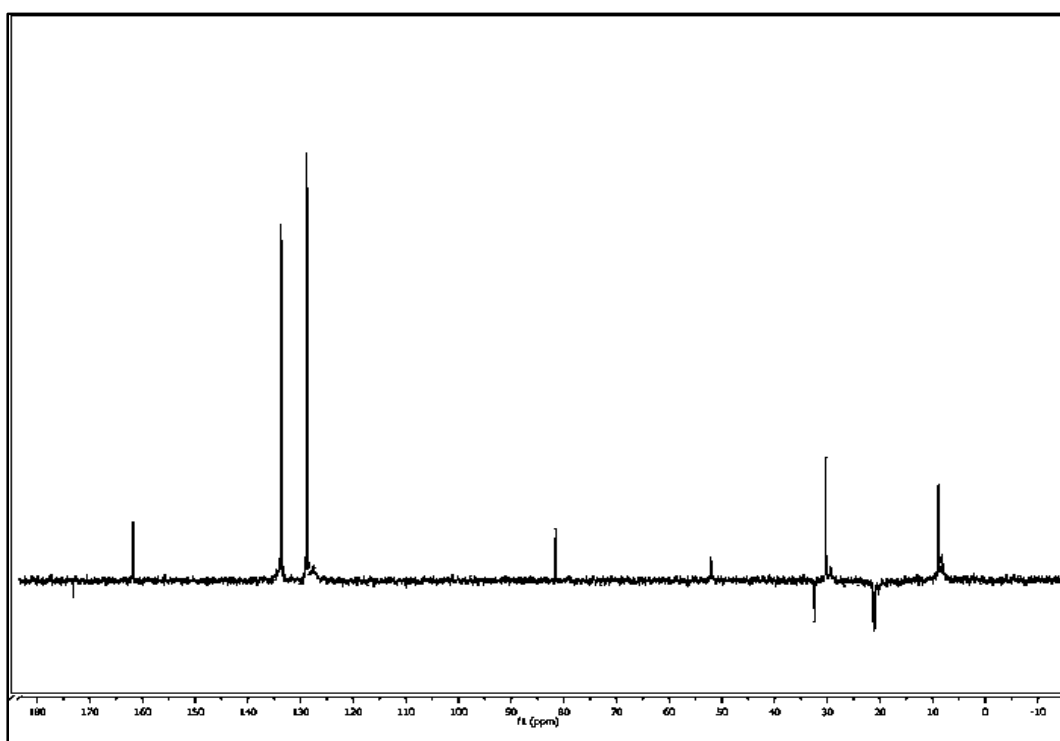


Figure A-32: DEPT Spectrum of **8** (d_6 -acetone, 22 °C)

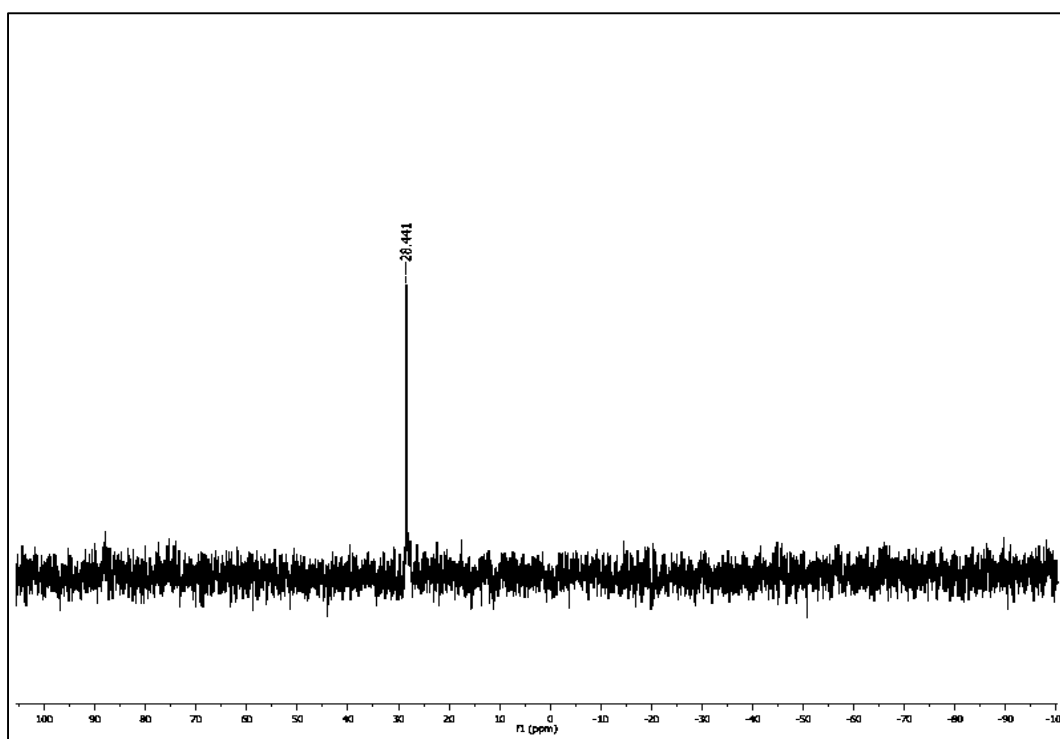


Figure A-33: ³¹P NMR Spectrum of **8** (d_6 -acetone, 22 °C)

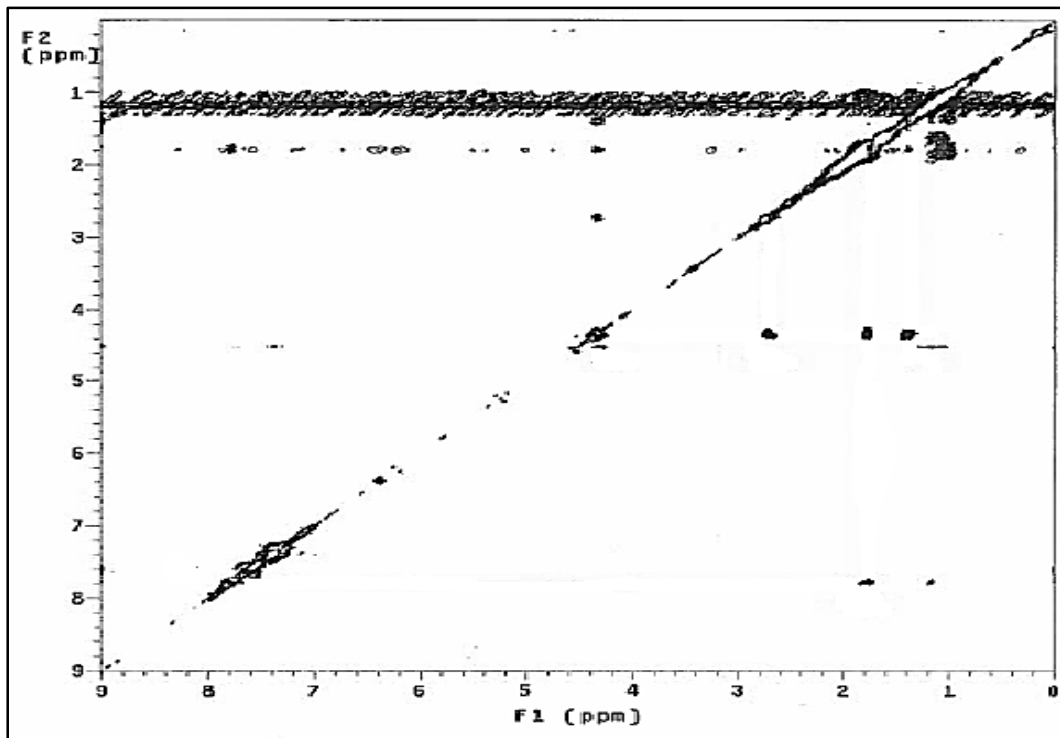


Figure A-34: COSY Spectrum of **8** (d_6 -acetone, 22 °C)

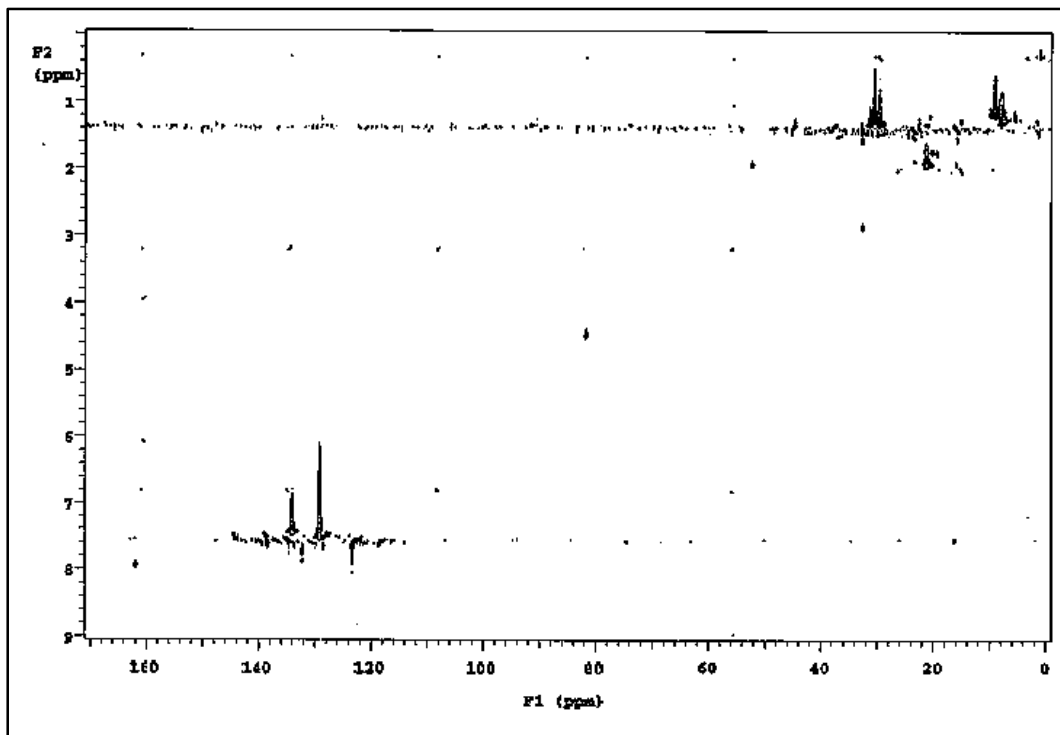
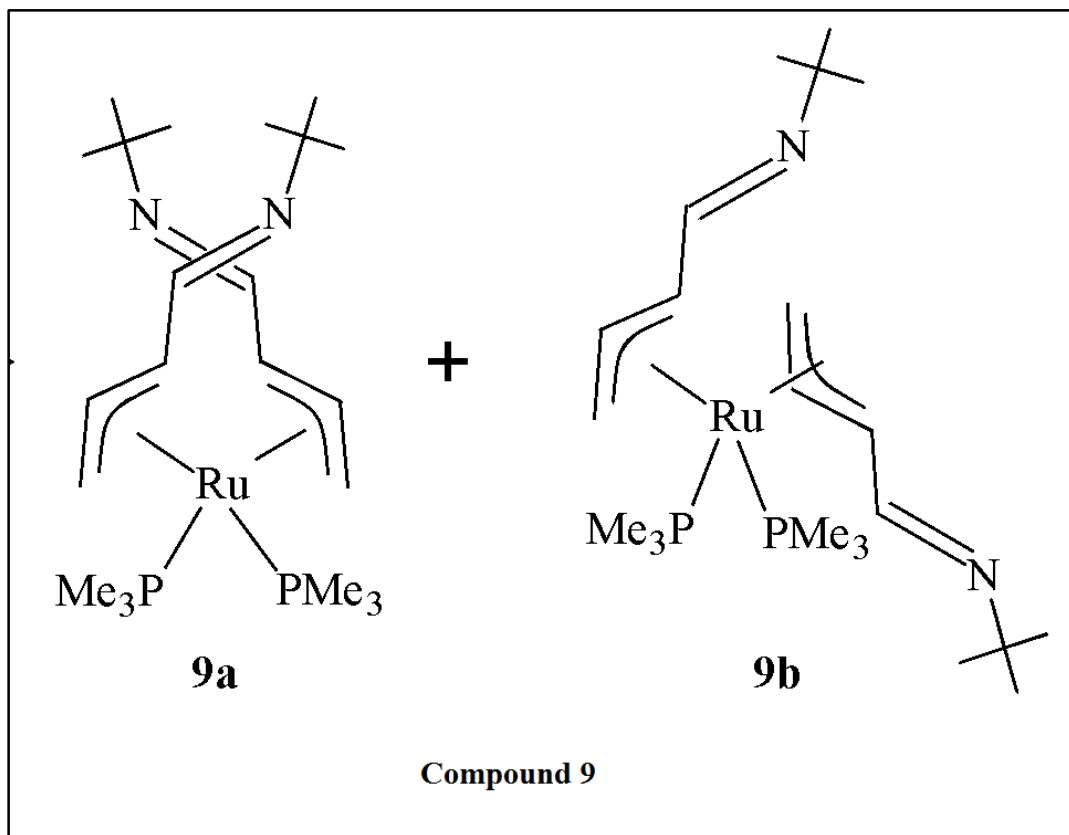


Figure A-35: HMQC Spectrum of **8** (d_6 -acetone, 22 °C)



- ^1H NMR (acetone- d_6 , 22 °C)
- ^{13}C NMR (acetone- d_6 , 22 °C)
- DEPT Spectrum (acetone- d_6 , 22 °C)
- ^{31}P NMR (acetone- d_6 , 22 °C)
- COSY NMR (acetone- d_6 , 22 °C)
- HMQC NMR (acetone- d_6 , 22 °C)

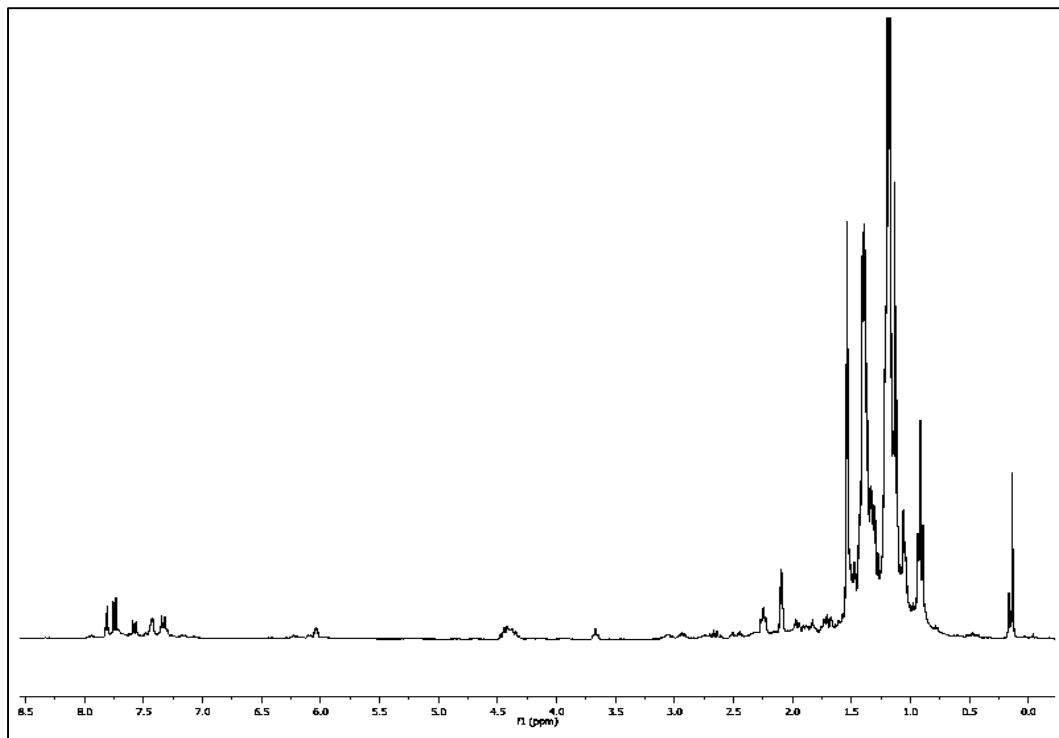


Figure A-36: ^1H NMR Spectrum of **9** (d_6 -acetone, 22 °C)

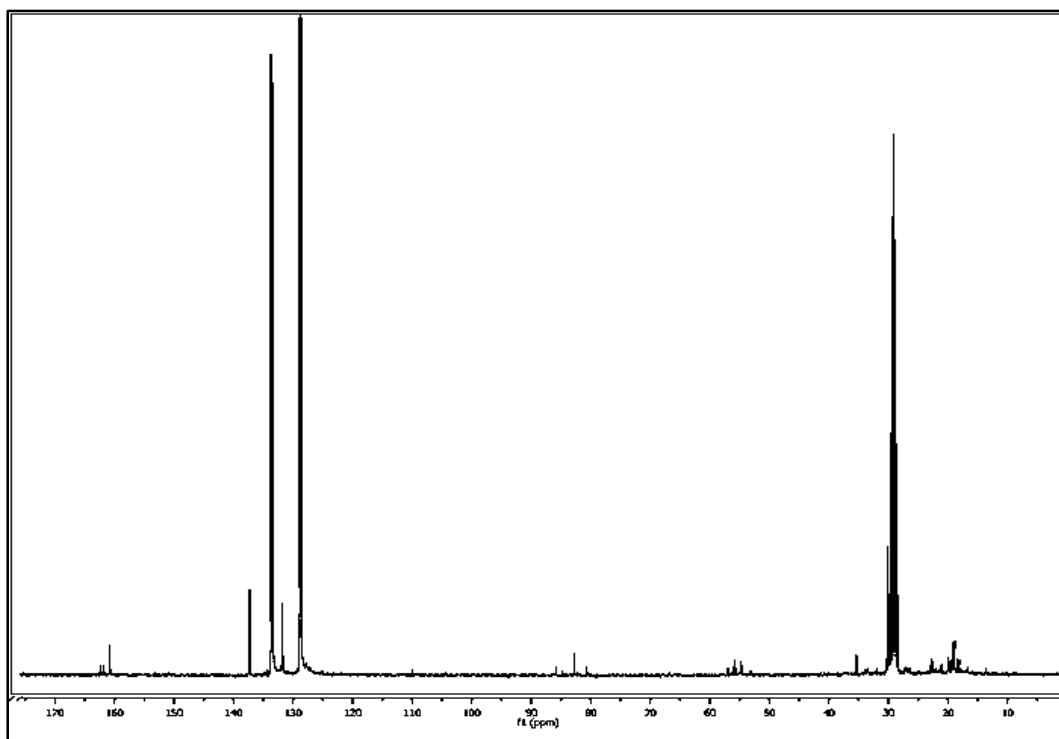


Figure A-37: ^{13}C NMR Spectrum of **9** (d_6 -acetone, 22 °C)

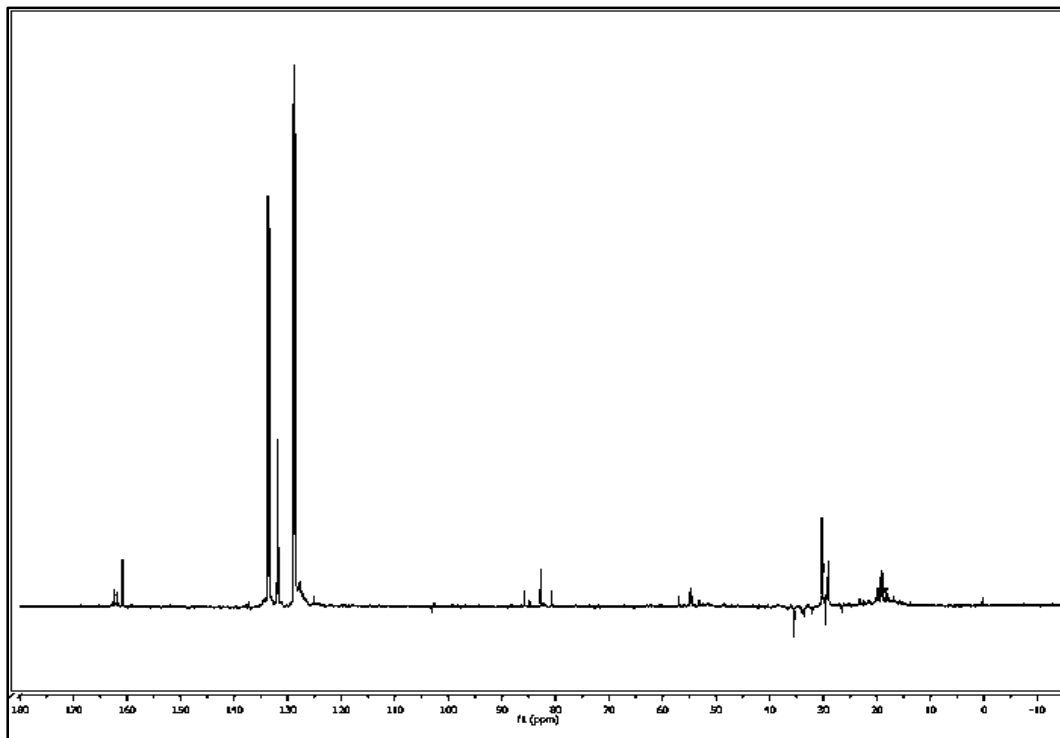


Figure A-38: DEPT Spectrum of **9** (^d₆-acetone, 22 °C)

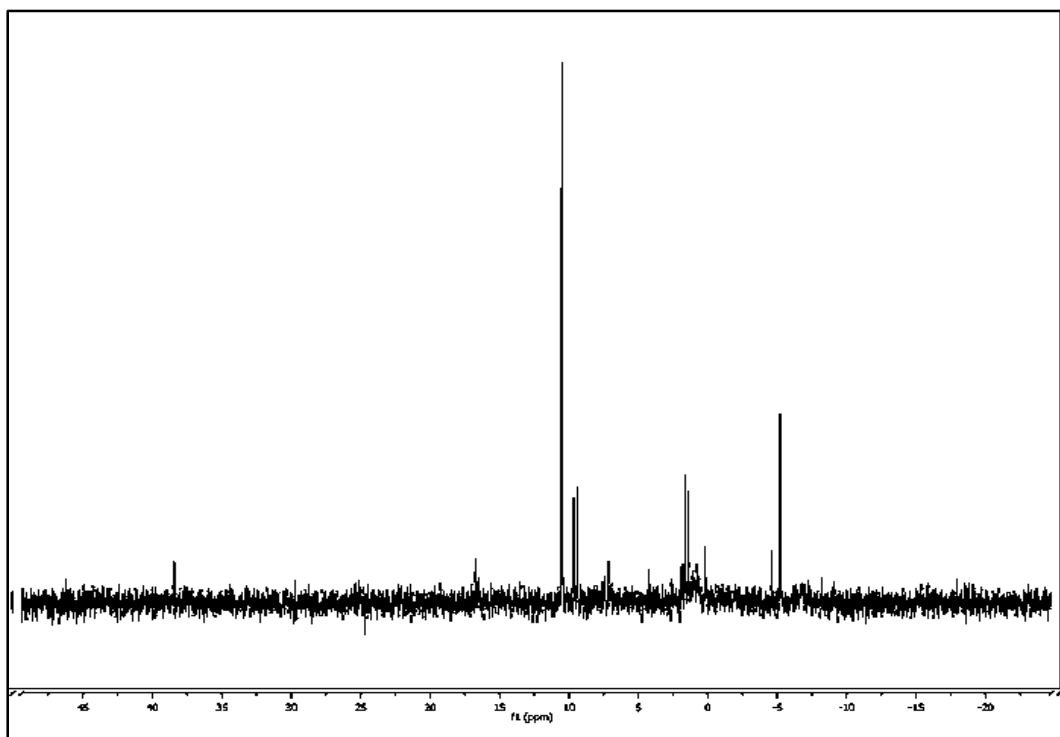


Figure A-39: ³¹P NMR Spectrum of **9** (^d₆-acetone, 22 °C)

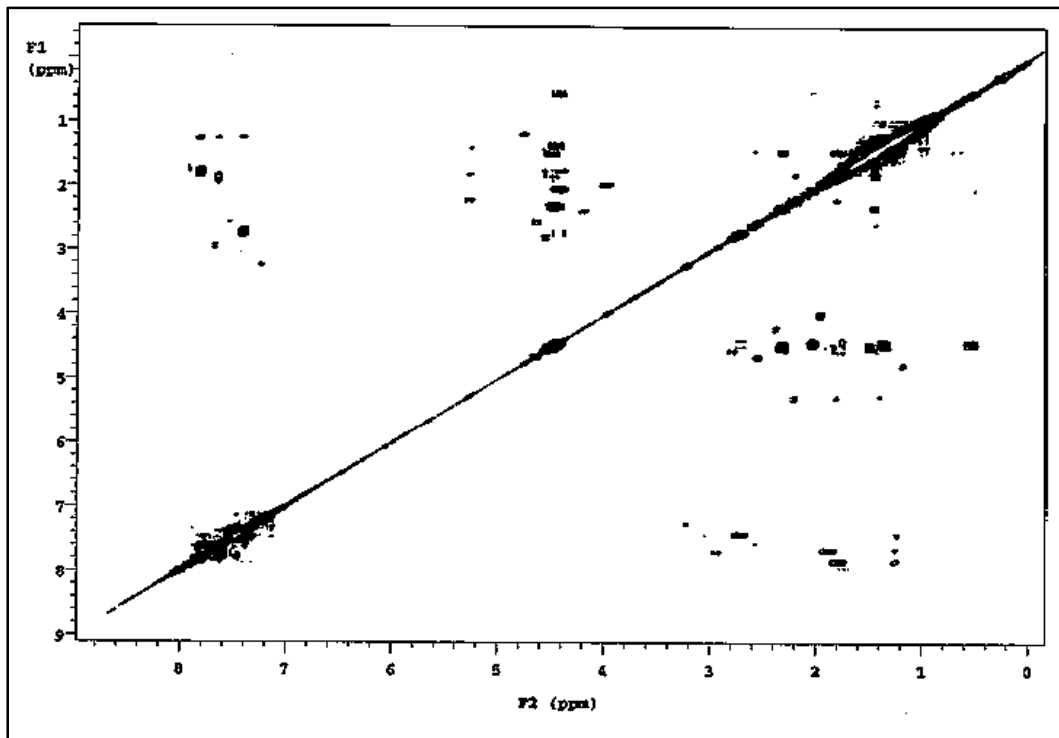


Figure A-40: COSY Spectrum of **9** (d_6 -acetone, 22 °C)

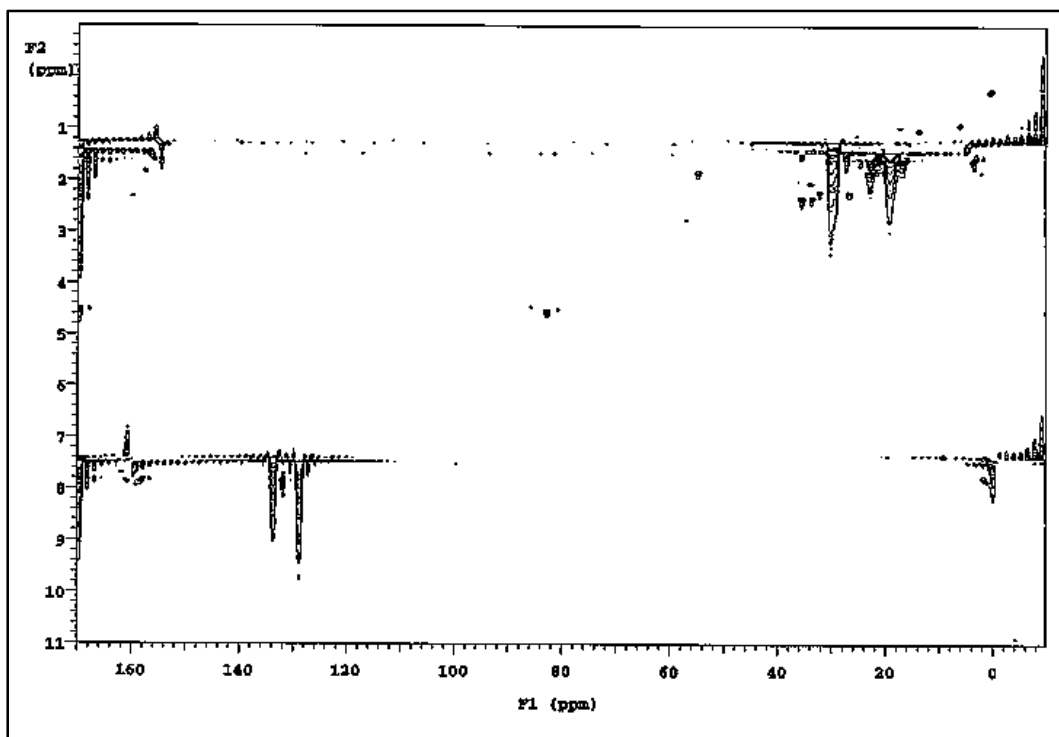
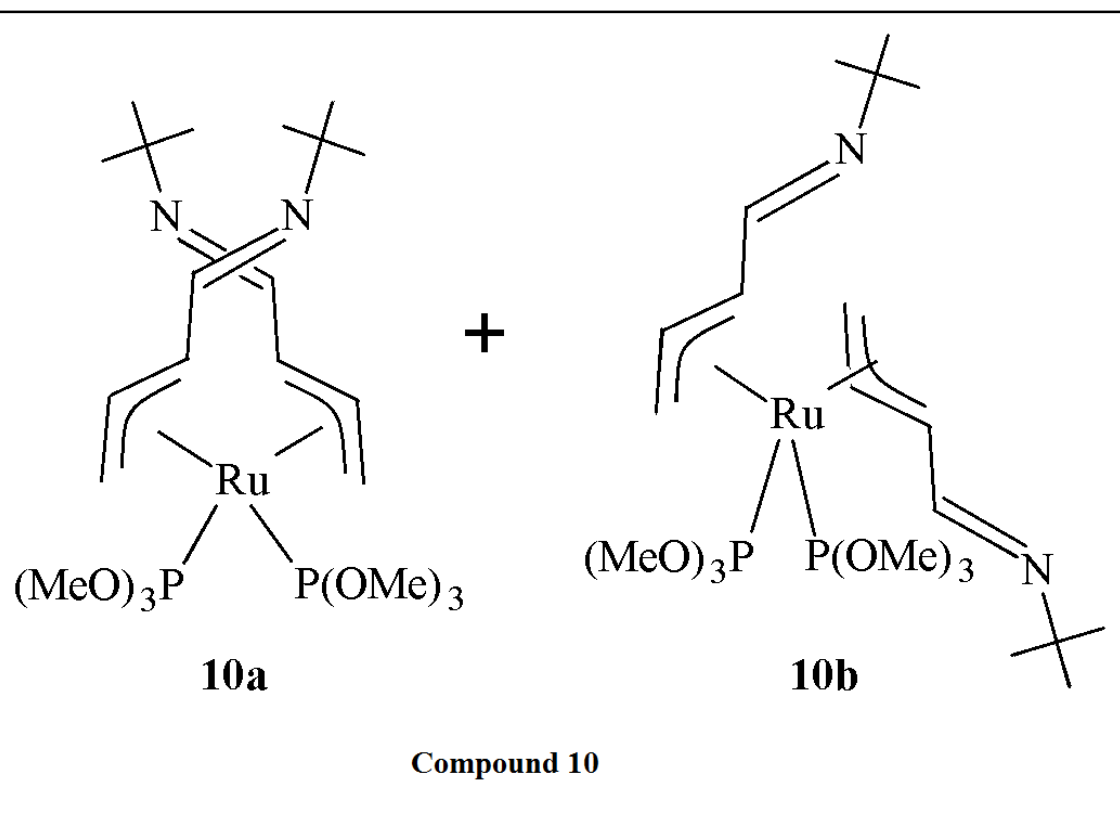


Figure A-41: HMQC Spectrum of **9** (d_6 -acetone, 22 °C)



- ^1H NMR (acetone- d_6 , 22 °C)
- ^{13}C NMR (acetone- d_6 , 22 °C)
- DEPT Spectrum (acetone- d_6 , 22 °C)
- ^{31}P NMR (acetone- d_6 , 22 °C)
- COSY NMR (acetone- d_6 , 22 °C)
- HMQC NMR (acetone- d_6 , 22 °C)

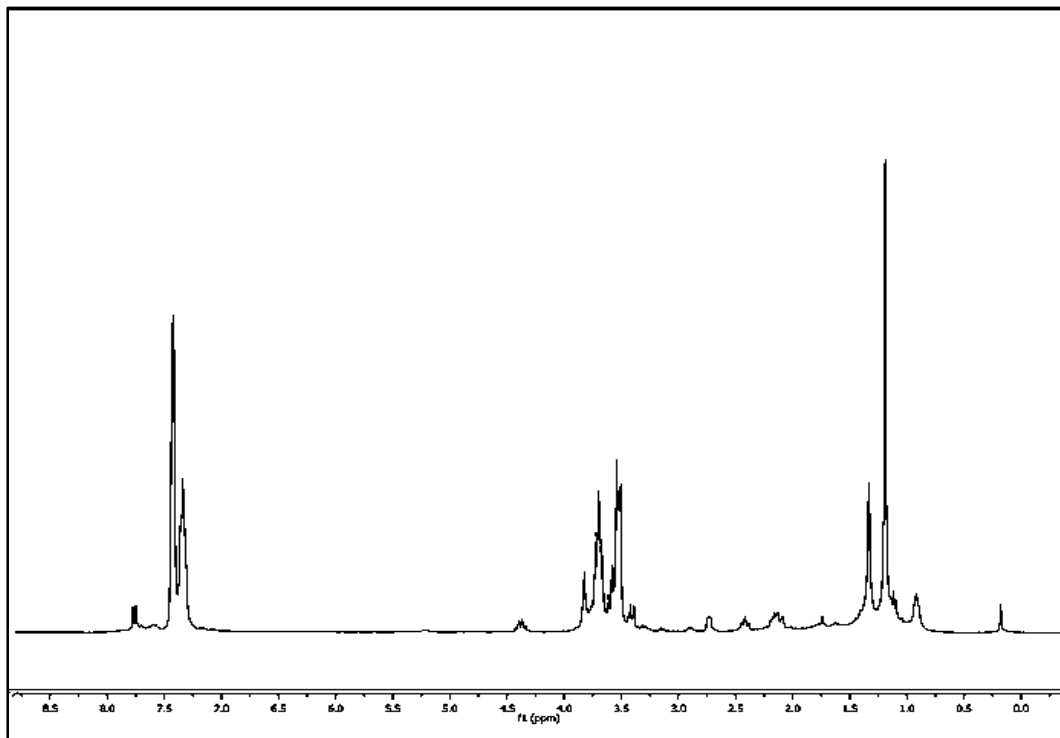


Figure A-42: ¹H NMR Spectrum of **10** (d_6 -acetone, 22 °C)

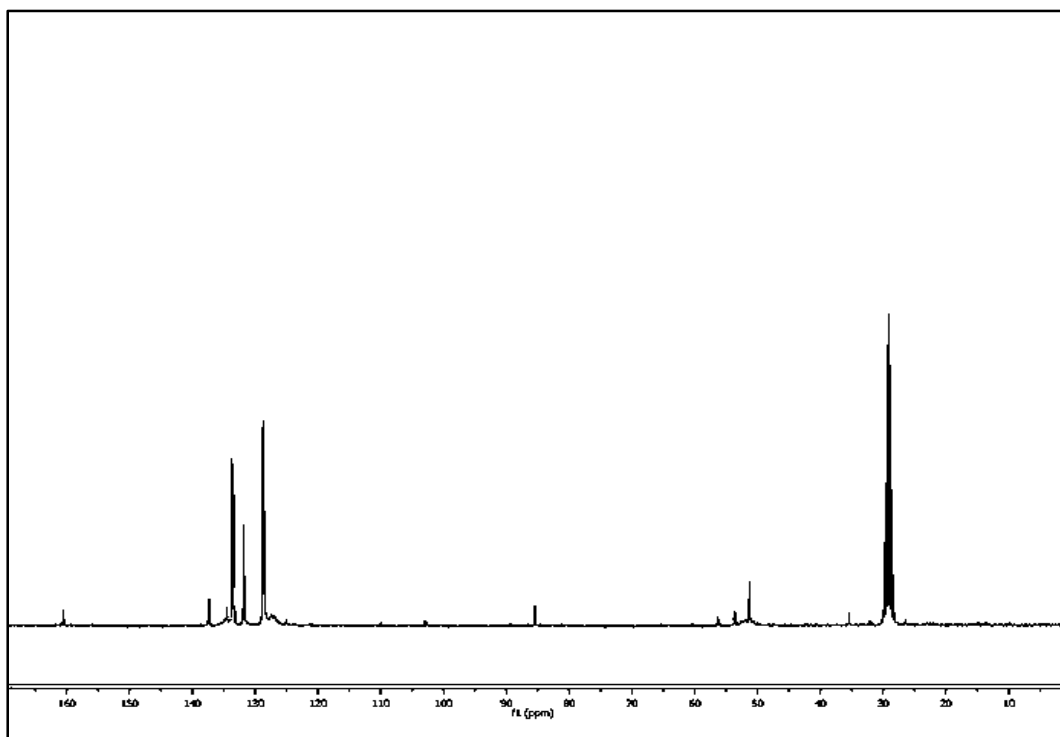


Figure A-43: ¹³C NMR Spectrum of **10** (d_6 -acetone, 22 °C)

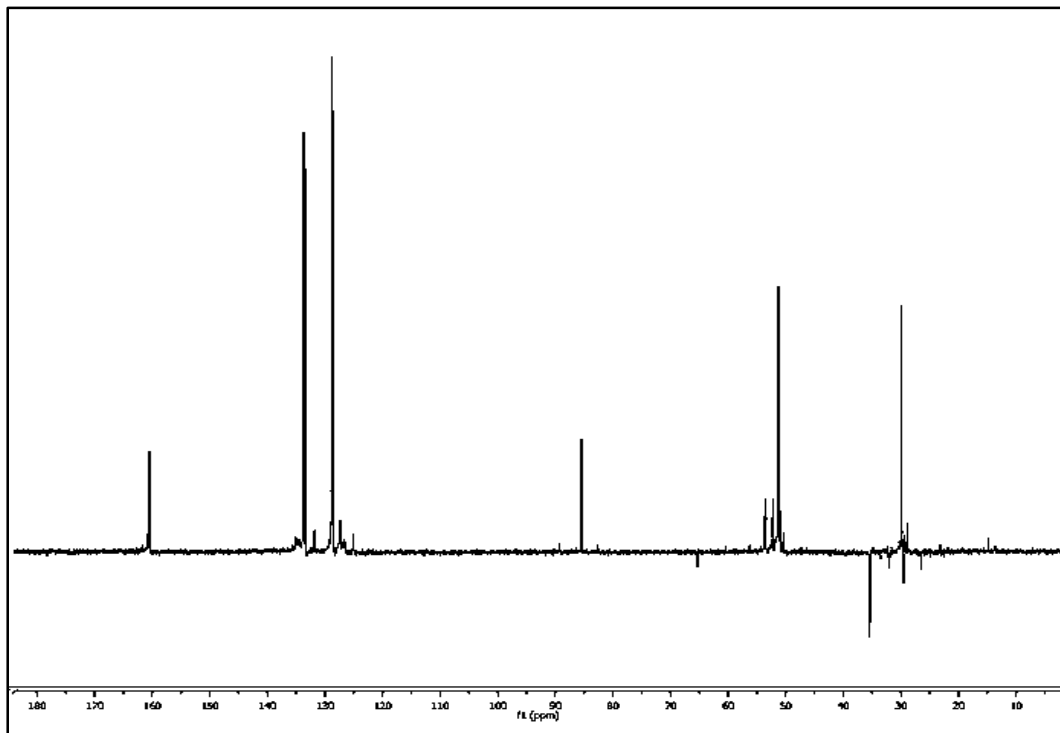


Figure A-44: DEPT Spectrum of **10** (d_6 -acetone, 22 °C)

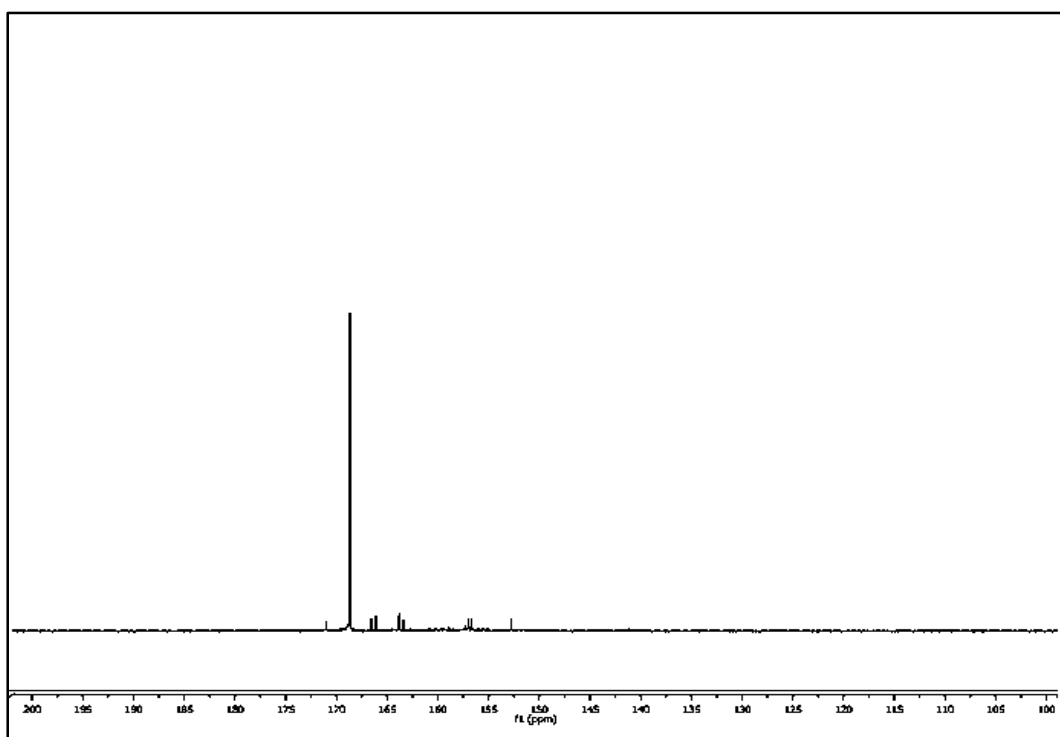


Figure A-45: ^{31}P NMR Spectrum of **10** (d_6 -acetone, 22 °C)

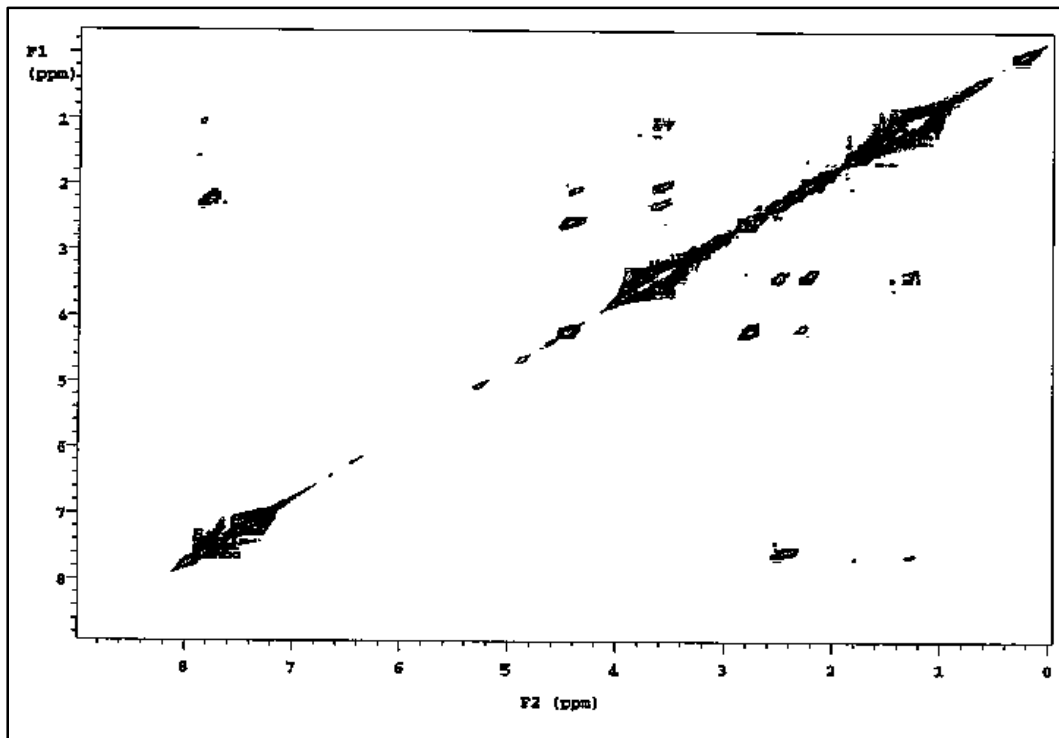


Figure A-46: COSY Spectrum of **10** (d_6 -acetone, 22 °C)

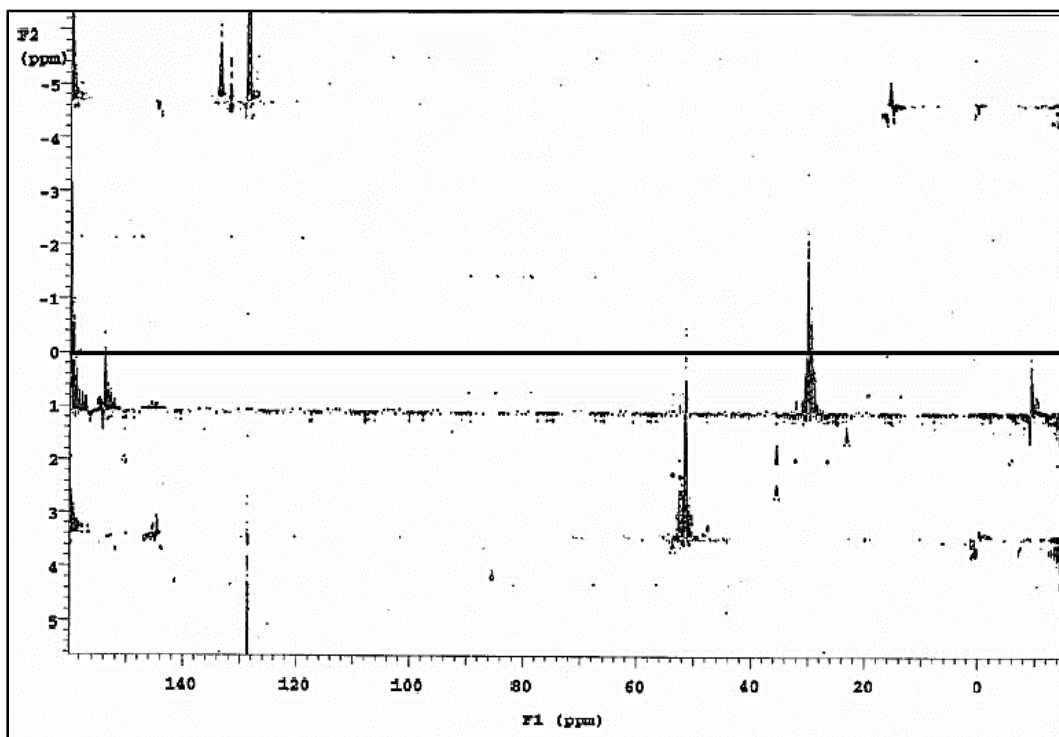
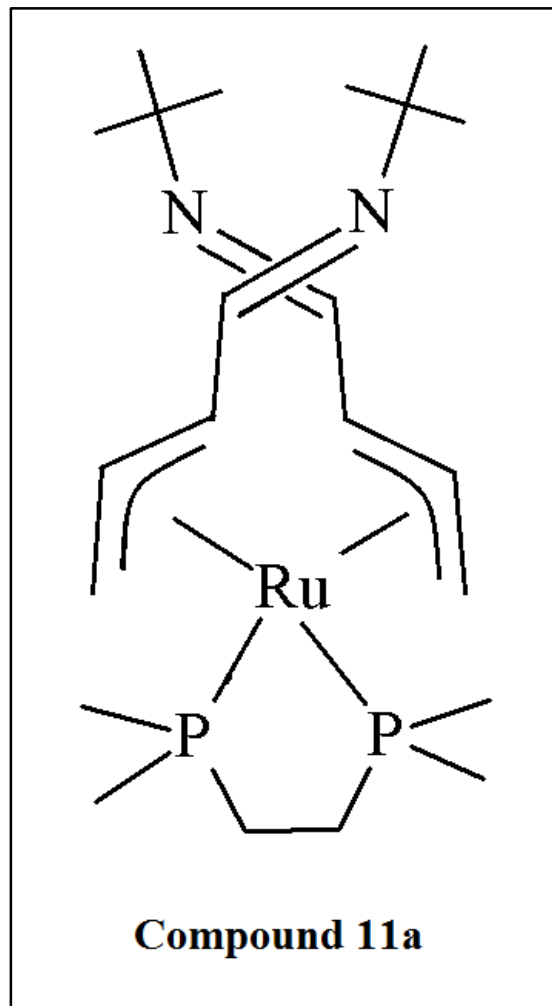


Figure A-47: HMQC Spectrum of **10** (d_6 -acetone, 22 °C)
*spectrum width was not wide enough; folding occurred



- ^{31}P NMR (acetone- d_6 , 22 °C)

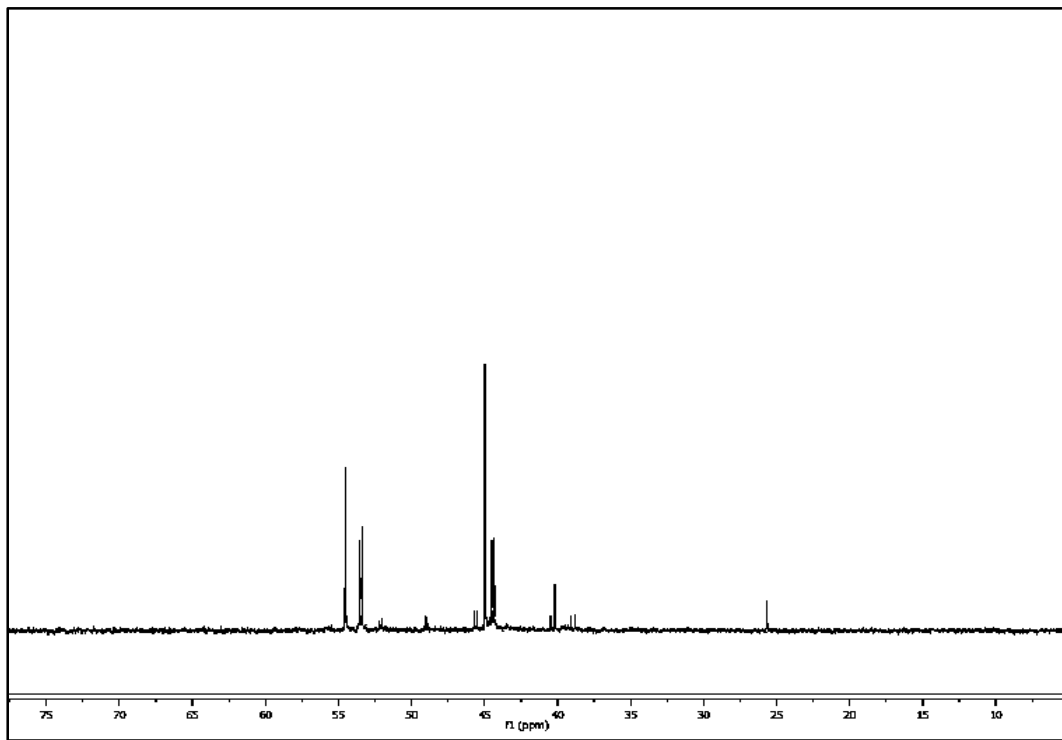
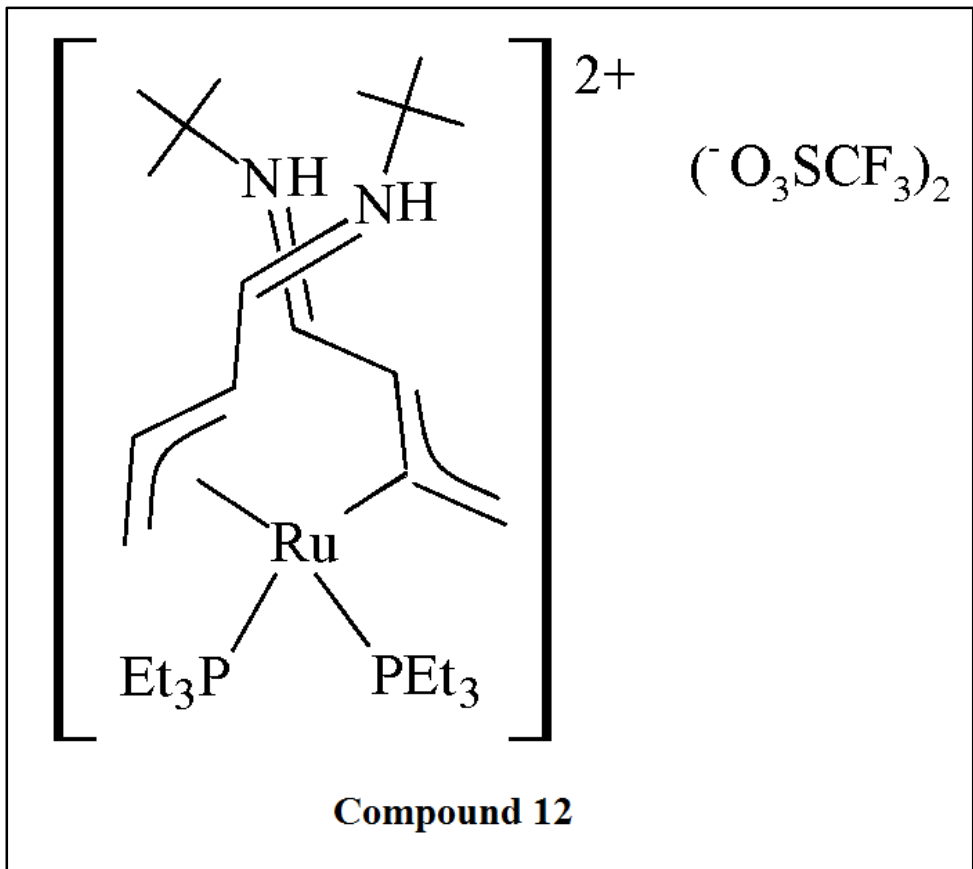


Figure A-48: ^{31}P NMR Spectrum of **11** ($\text{d}_6\text{-acetone}$, 22°C)

Appendix B

NMR Spectra of Protonated *bis*-Azapentadienyl-Ruthenium-Phosphine Complexes



- ¹H NMR (acetone-d₆, 22 °C)
- ¹³C NMR (acetone-d₆, 22 °C)
- DEPT Spectrum (acetone-d₆, 22 °C)
- ³¹P NMR (acetone-d₆, 22 °C)
- COSY NMR (acetone-d₆, 22 °C)
- HMQC NMR (acetone-d₆, 22 °C)

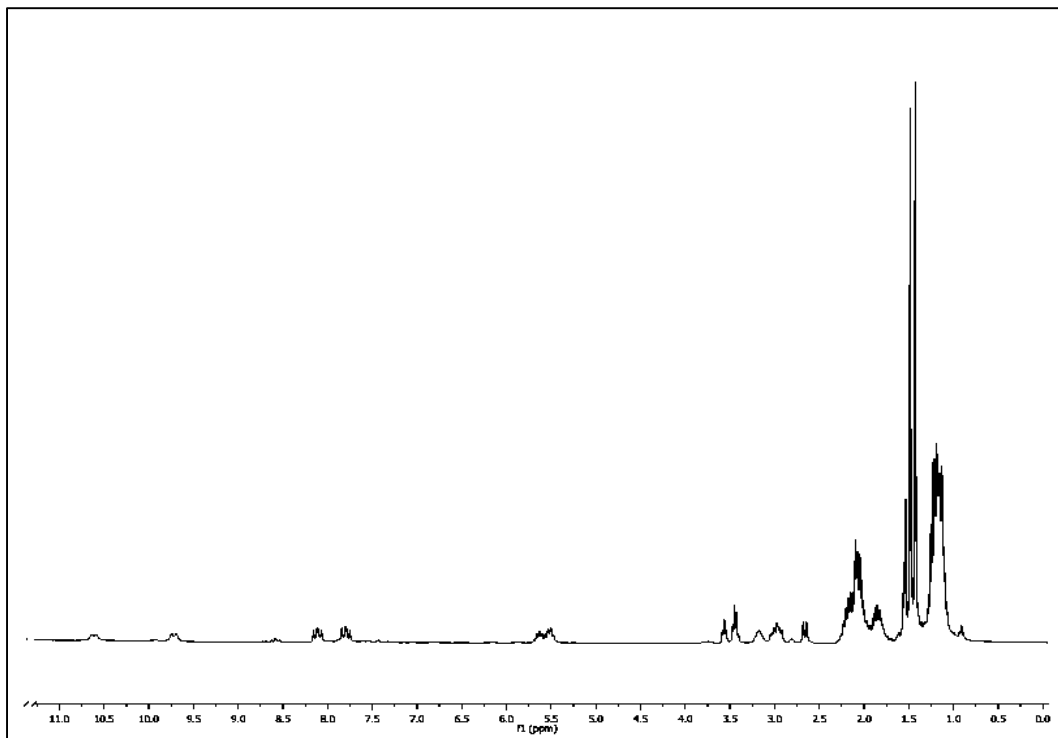


Figure B-1: ¹H NMR spectrum of **12** (acetone-d₆, 22 °C)

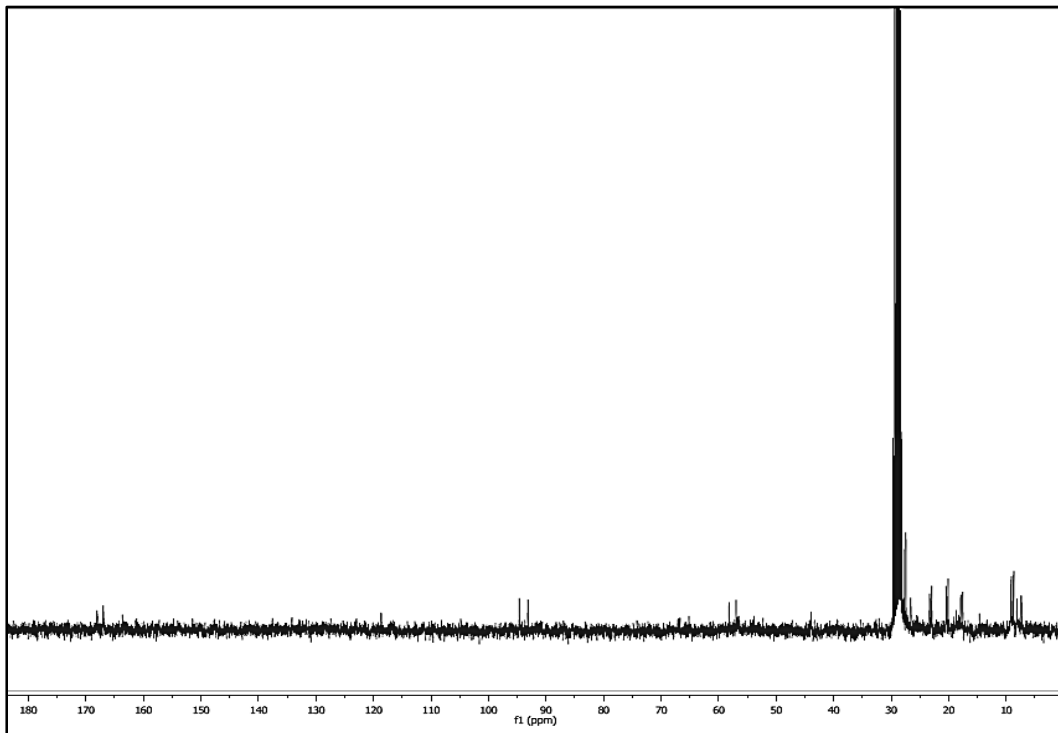


Figure B-2: ¹³C NMR spectrum of **12** (acetone-d₆, 22 °C)

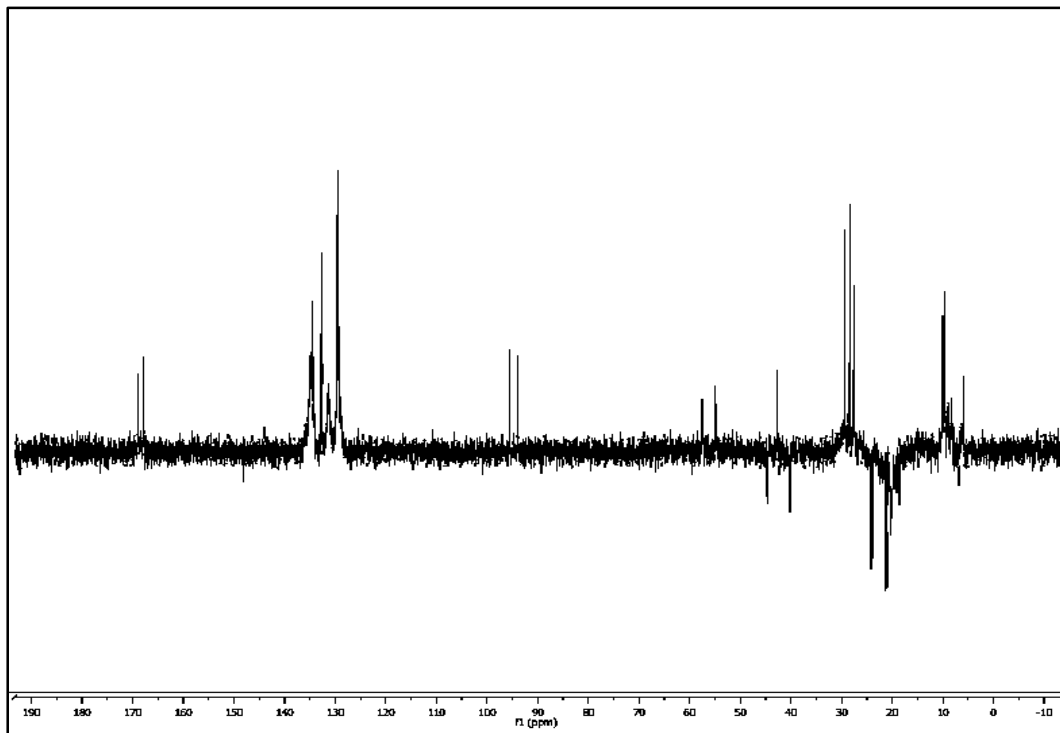


Figure B-3: DEPT spectrum of **12** (acetone-d₆, 22 °C)

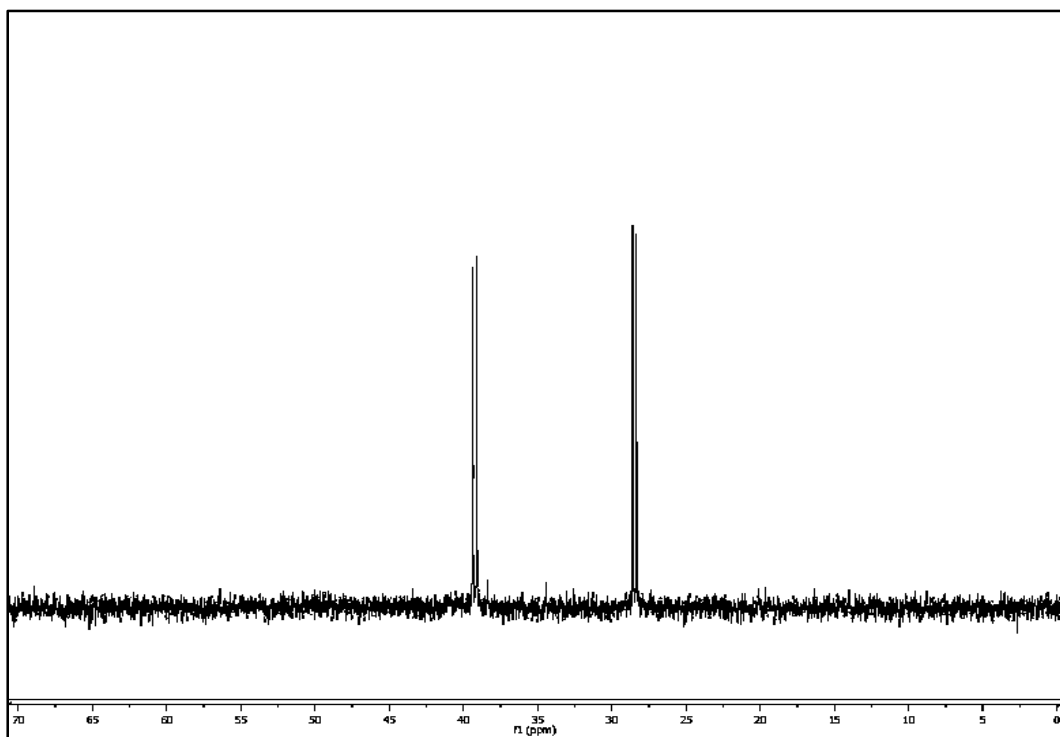


Figure B-4: ³¹P NMR spectrum of **12** (acetone-d₆, 22 °C)

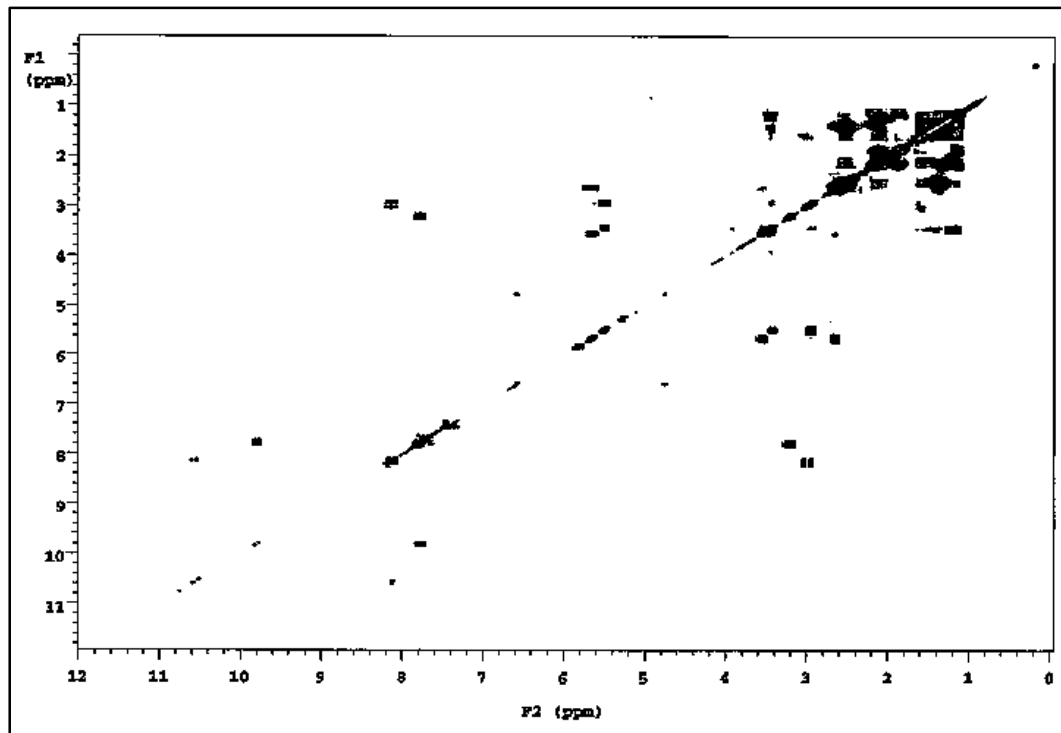


Figure B-5: COSY NMR spectrum of **12** (acetone- d_6 , 22 °C)

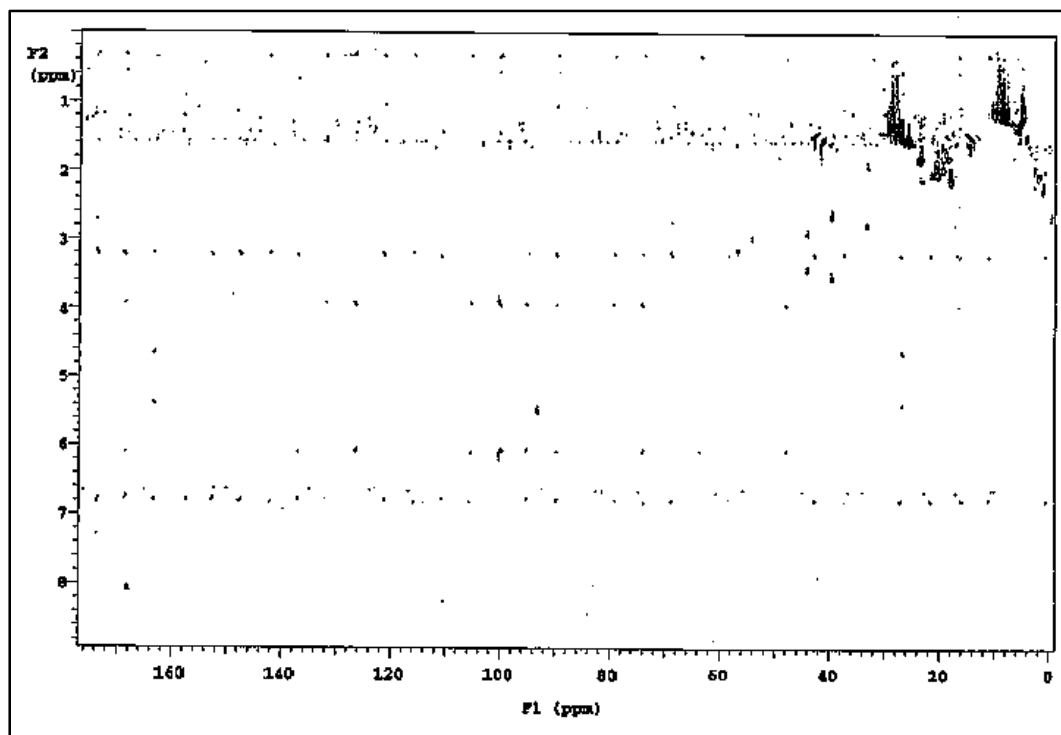
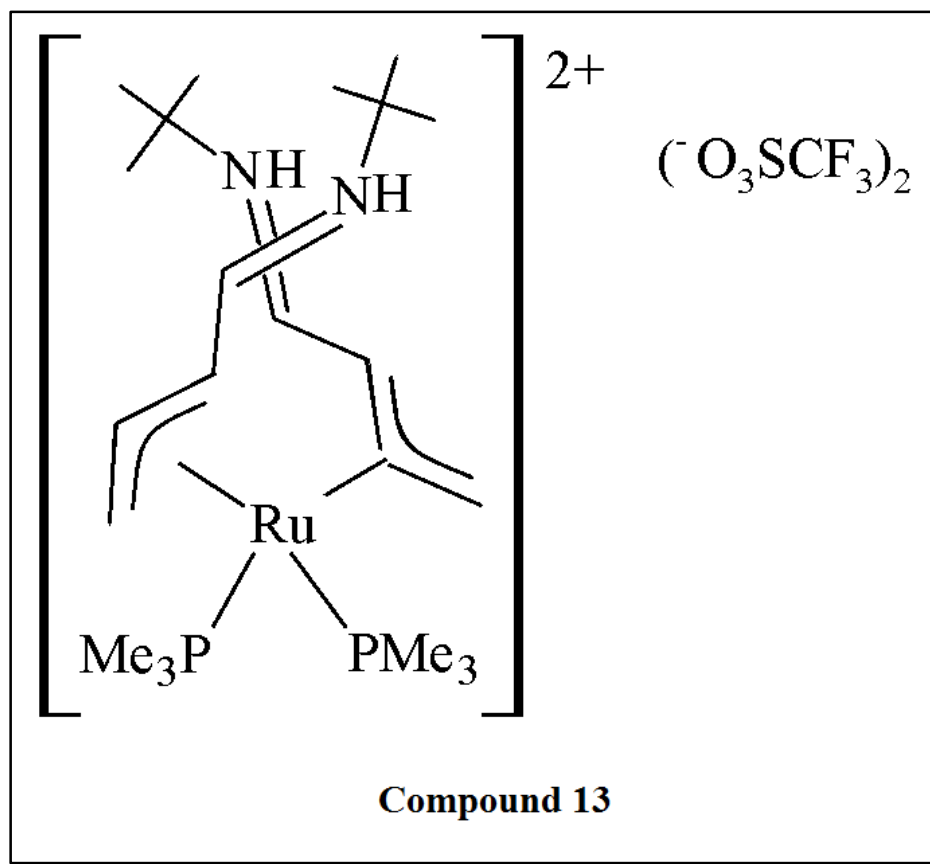


Figure B-6: HMQC NMR spectrum of **12** (acetone- d_6 , 22 °C)



- ^1H NMR (acetone- d_6 , 22 °C)
- ^{13}C NMR (acetone- d_6 , 22 °C)
- DEPT Spectrum (acetone- d_6 , 22 °C)
- ^{31}P NMR (acetone- d_6 , 22 °C)
- COSY NMR (acetone- d_6 , 22 °C)
- HMQC NMR (acetone- d_6 , 22 °C)

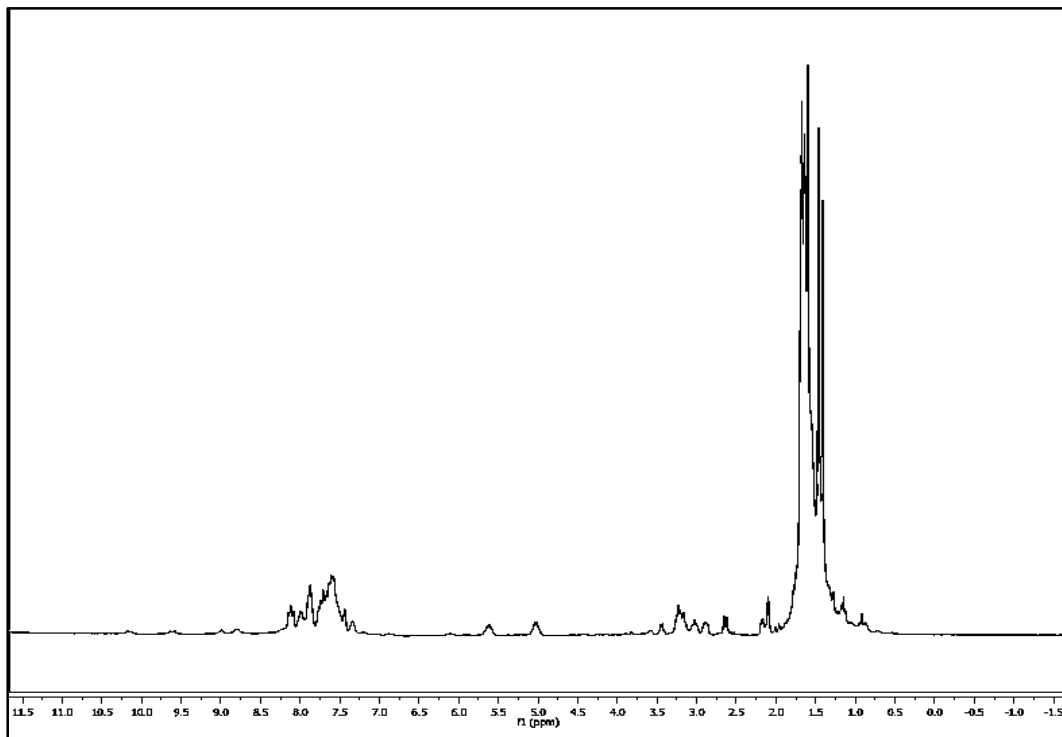


Figure B-7: ¹H NMR spectrum of **13** (acetone-d₆, 22 °C)

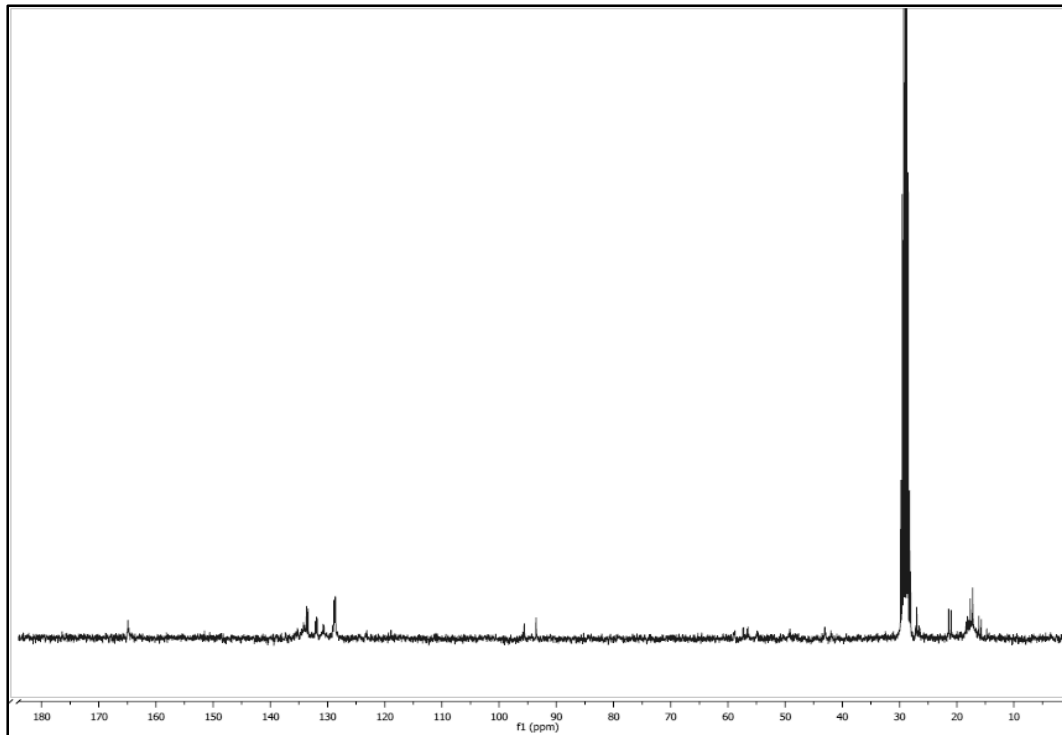


Figure B-8: ¹³C NMR spectrum of **13** (acetone-d₆, 22 °C)

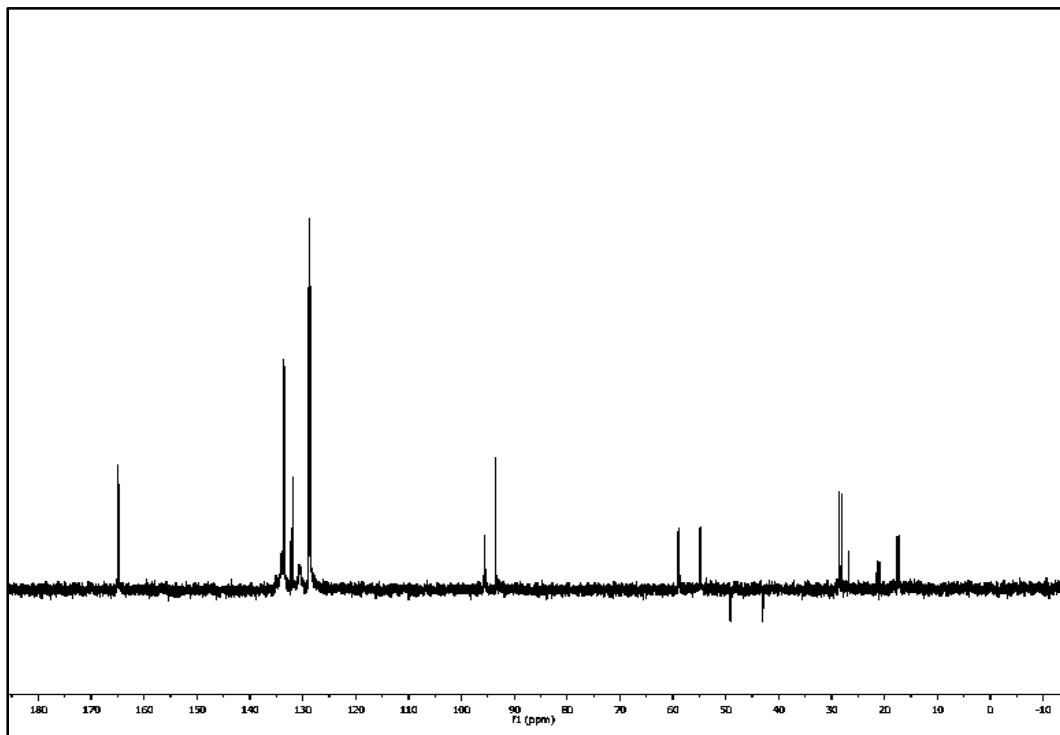


Figure B-9: DEPT spectrum of **13** (acetone-d₆, 22 °C)

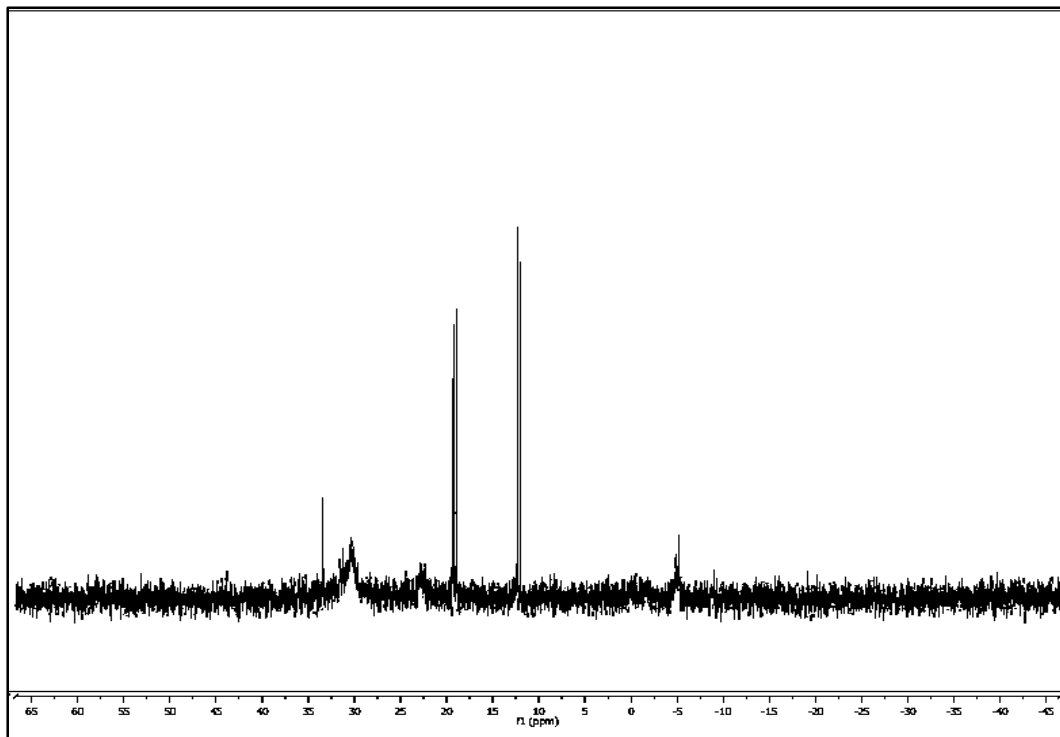


Figure B-10: ³¹P NMR spectrum of **13** (acetone-d₆, 22 °C)

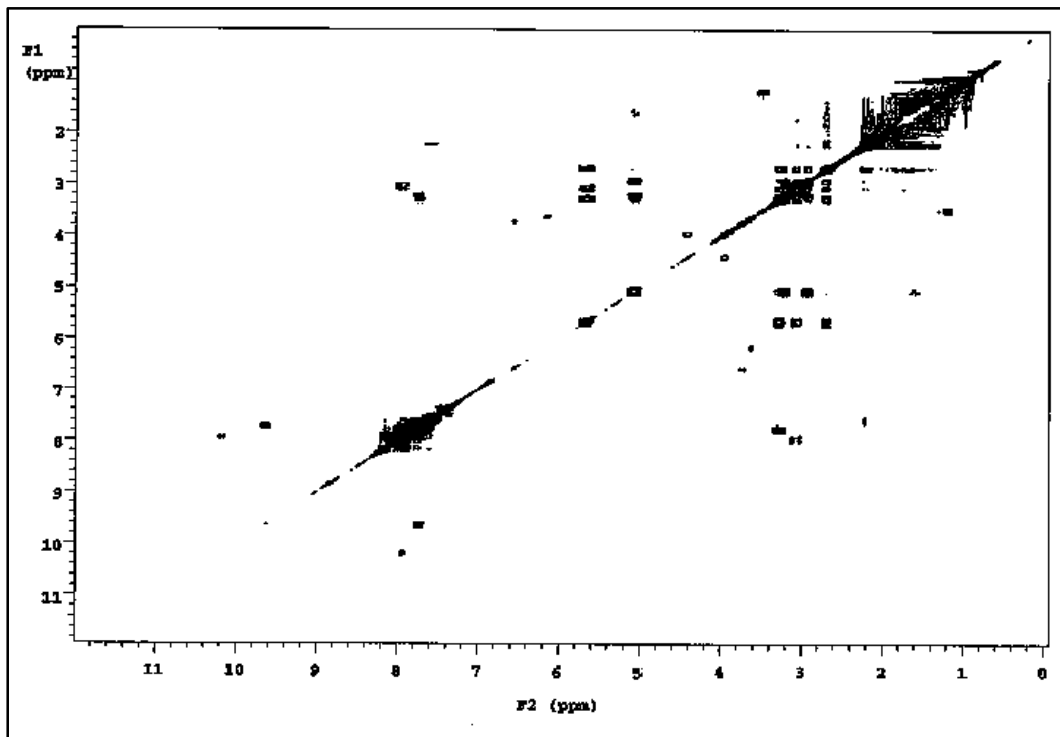


Figure B-11: COSY NMR spectrum of **13** (acetone- d_6 , 22 °C)

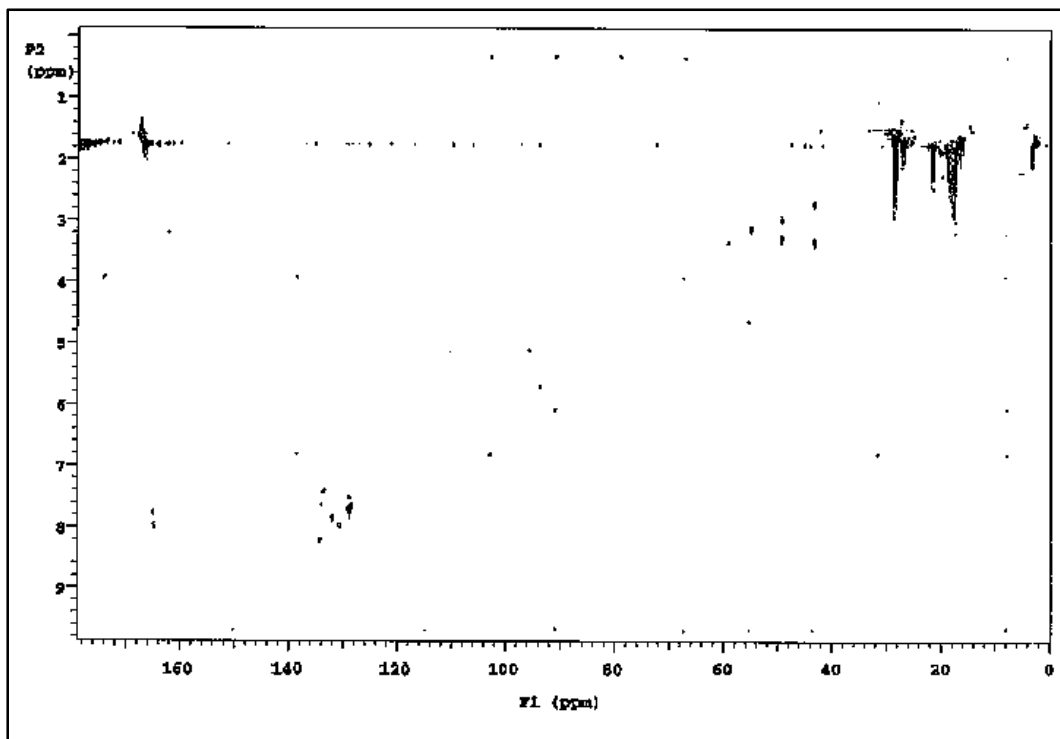
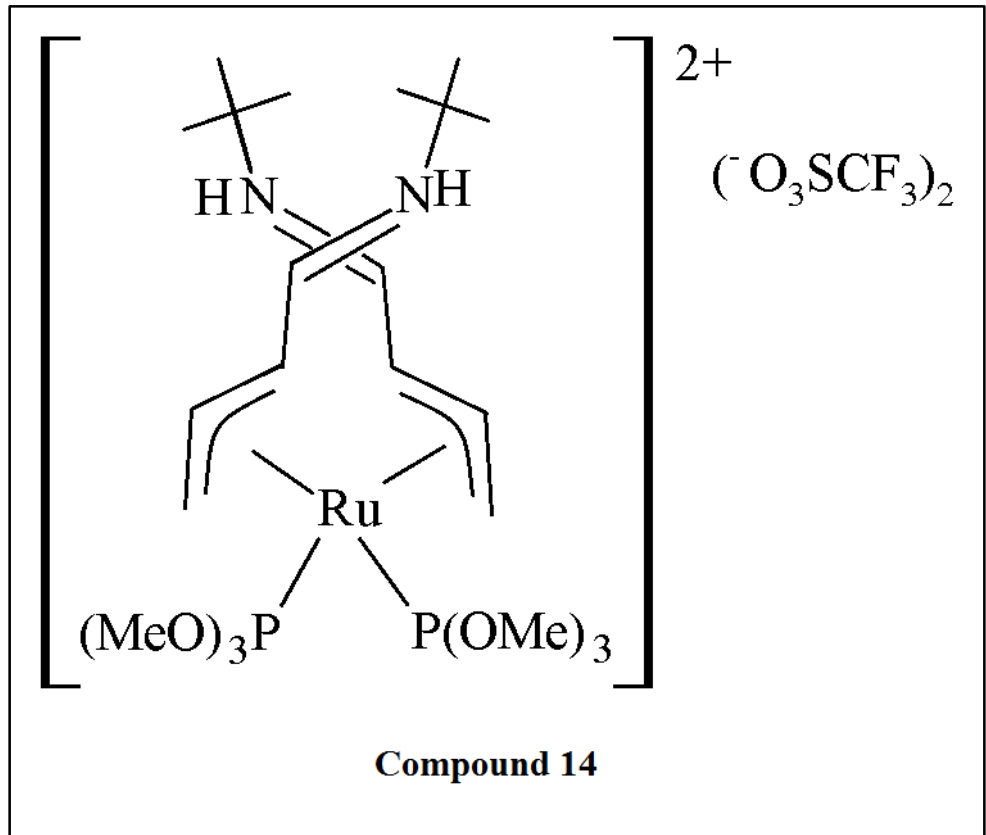


Figure B-12: HMQC NMR spectrum of **13** (acetone- d_6 , 22 °C)



- ^1H NMR (acetone- d_6 , 22 °C)
- ^{31}P NMR (acetone- d_6 , 22 °C)

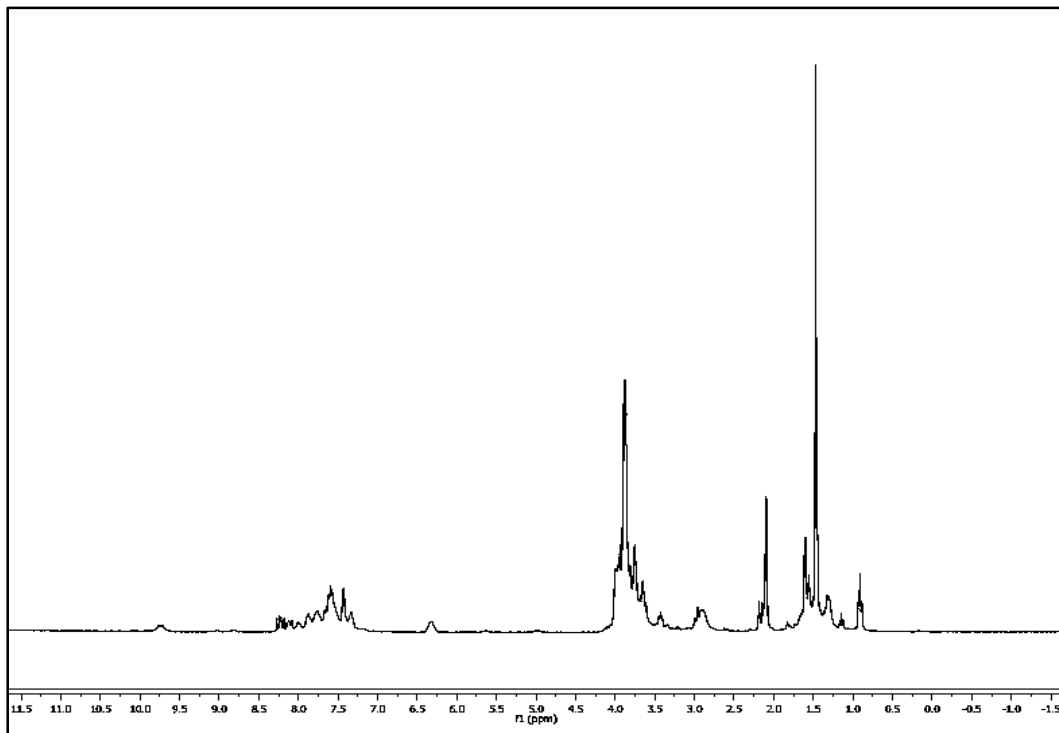


Figure B-13: ¹H NMR spectrum of **14** (acetone-d₆, 22 °C)

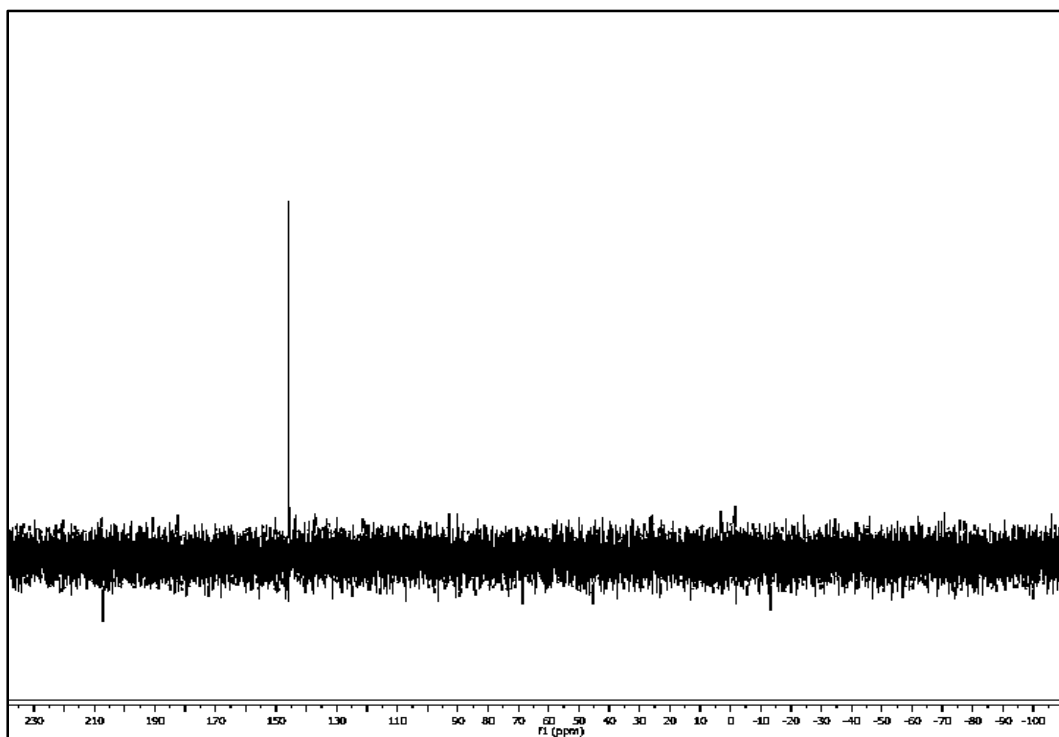
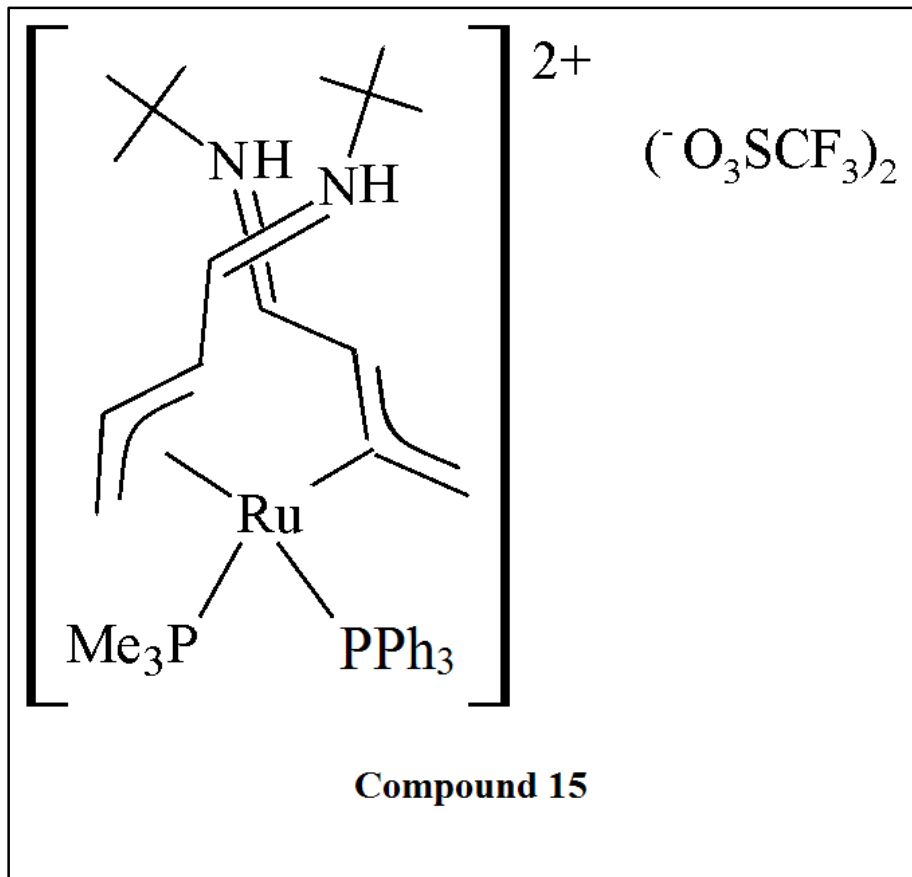


Figure B-14: ³¹P NMR spectrum of **14** (acetone-d₆, 22 °C)



- ^1H NMR (acetone- d_6 , 22 °C)
- ^{31}P NMR (acetone- d_6 , 22 °C)

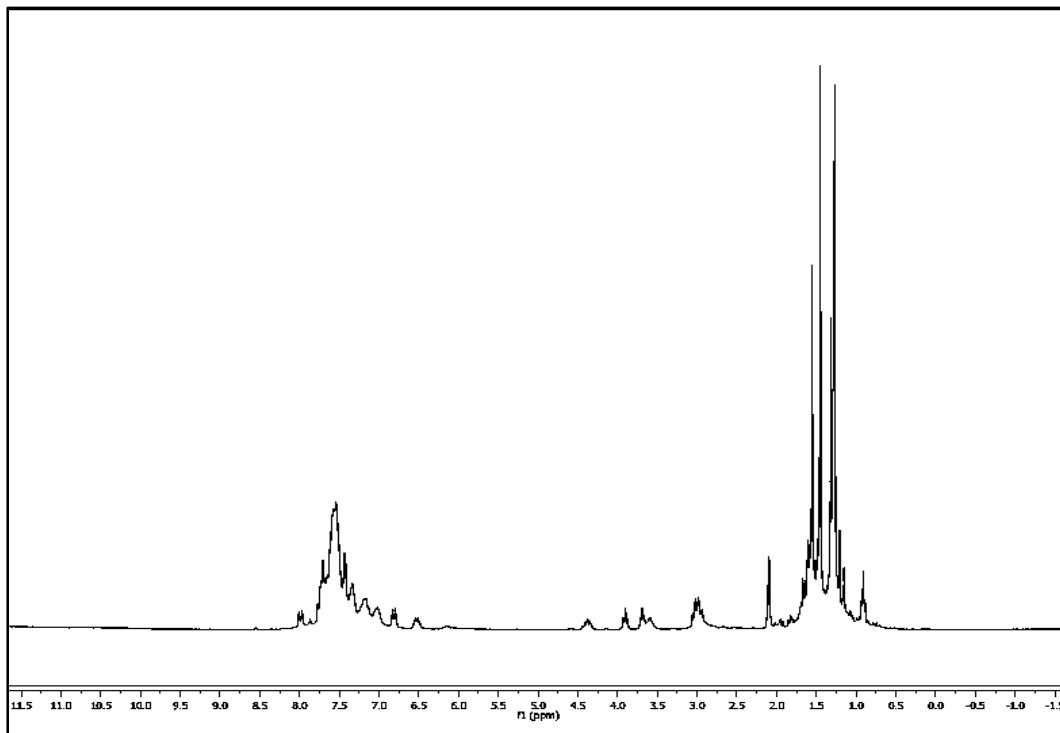


Figure B-15: ¹H NMR spectrum of **15** (acetone-d₆, 22 °C)

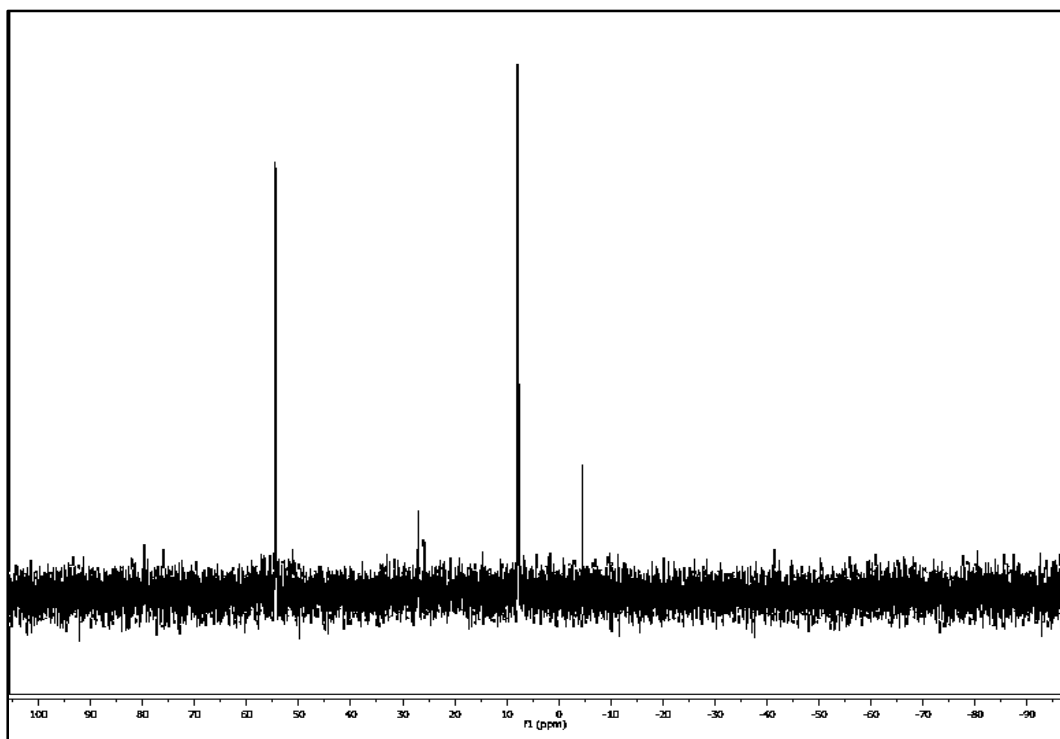


Figure B-16: ³¹P NMR spectrum of **15** (acetone-d₆, 22 °C)

Appendix C

Selected IR/MS Spectra of *bis*-Azapentadienyl-Ruthenium-Phosphine Chemistry

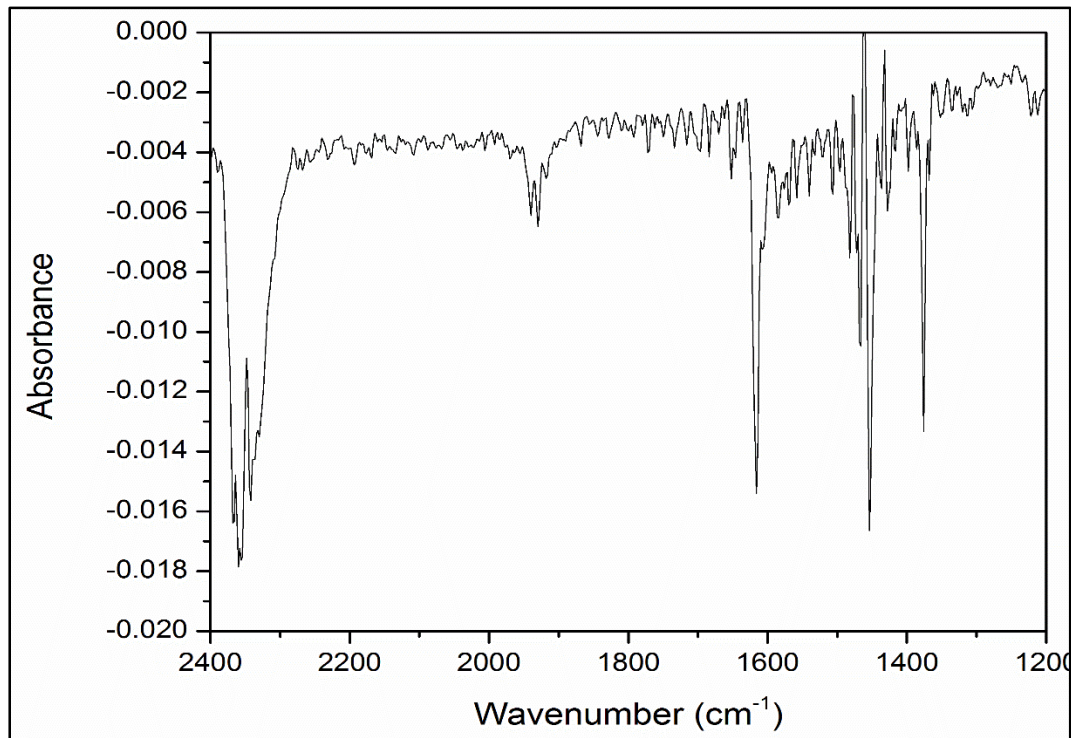


Figure C-1: IR spectrum of **1**.

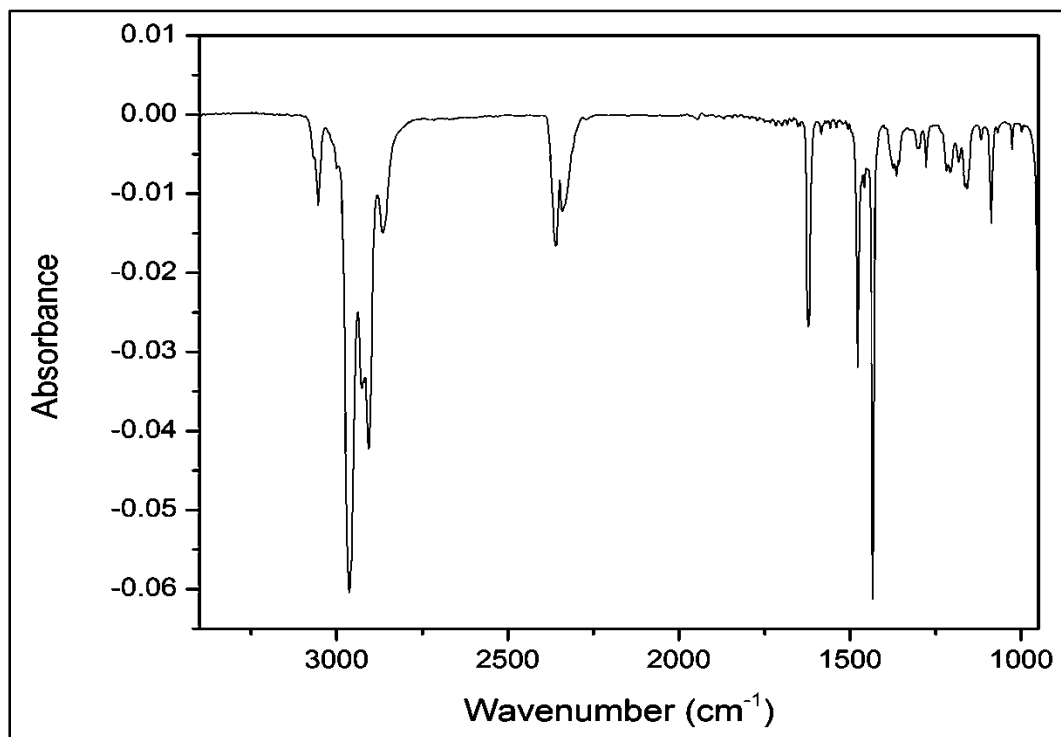


Figure C-2: IR spectrum of **2**.

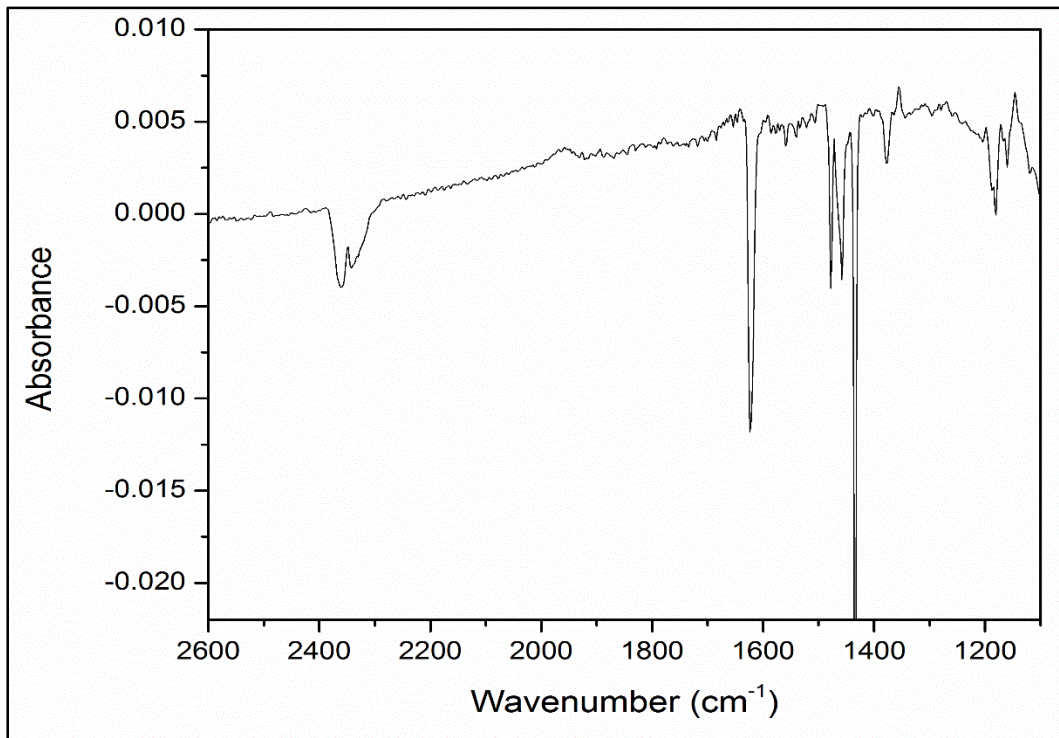


Figure C-3: IR spectrum of **4**.

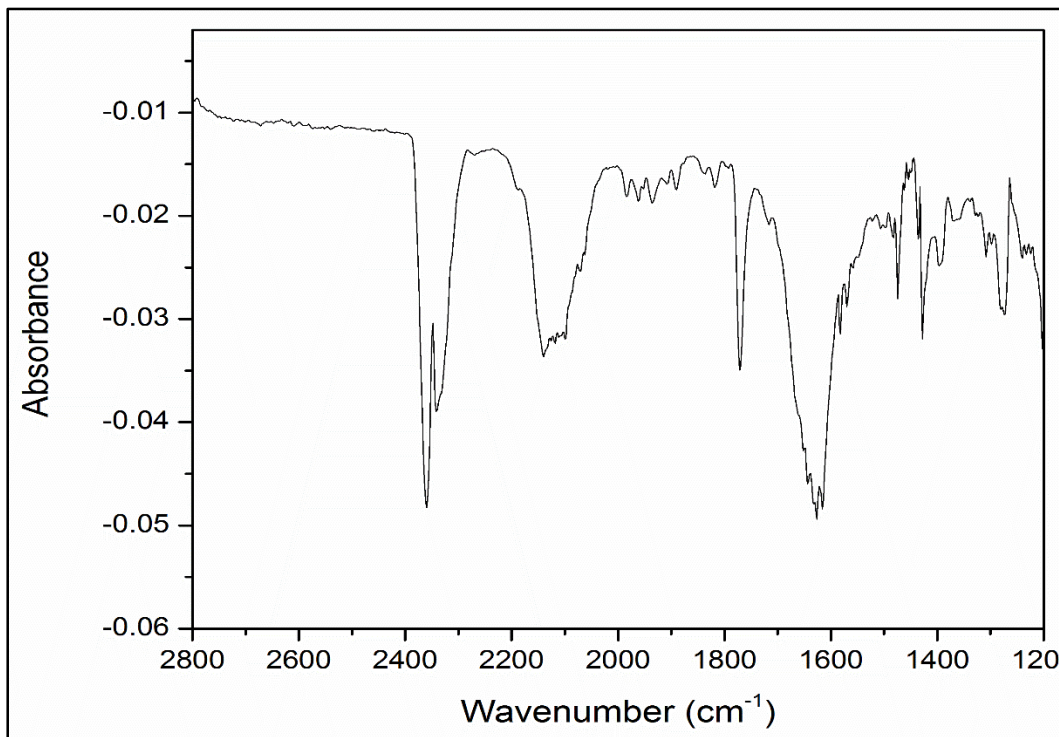


Figure C-4: IR spectrum of **5**.

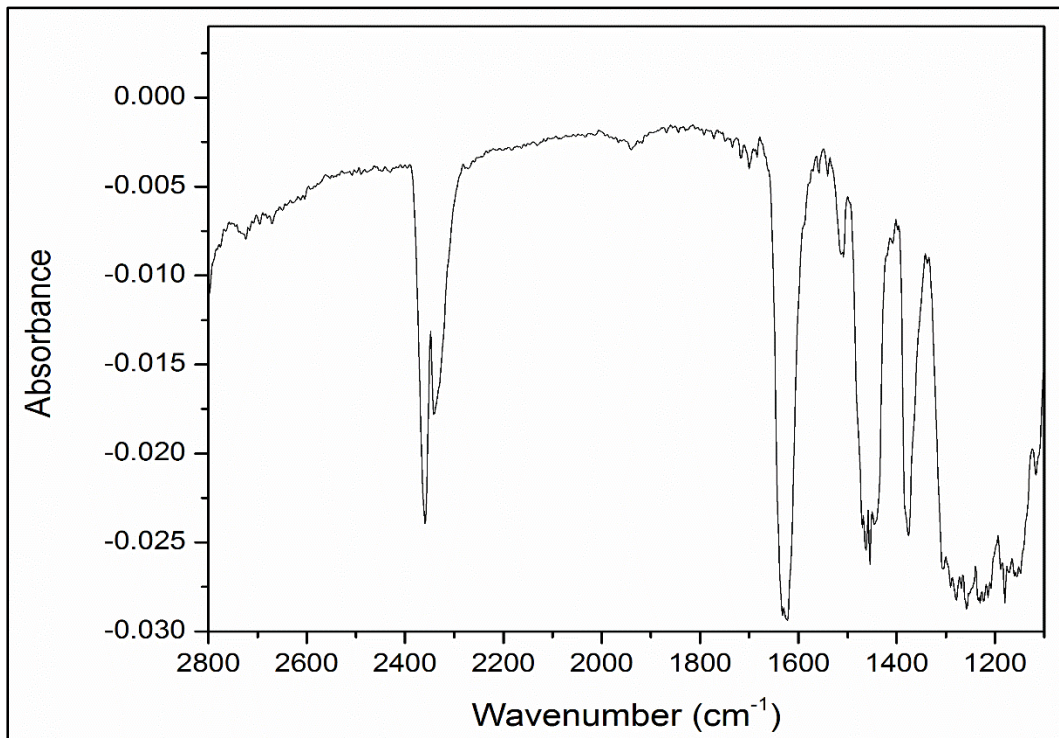


Figure C-5: IR spectrum of **8**.

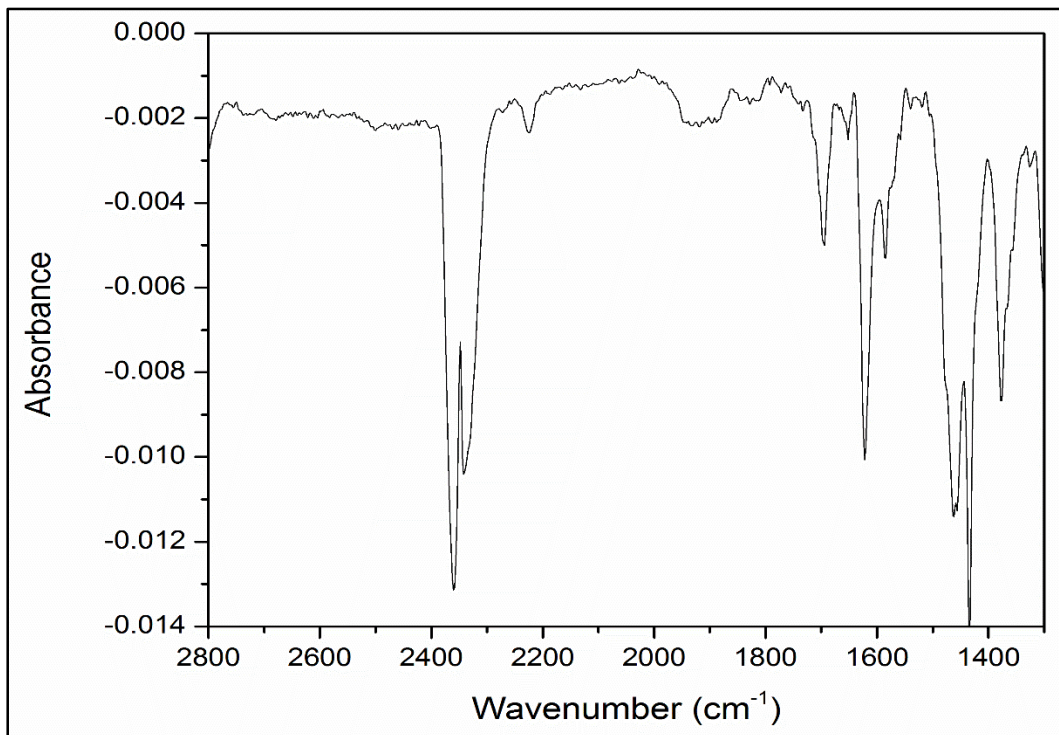


Figure C-6: IR spectrum of **9**

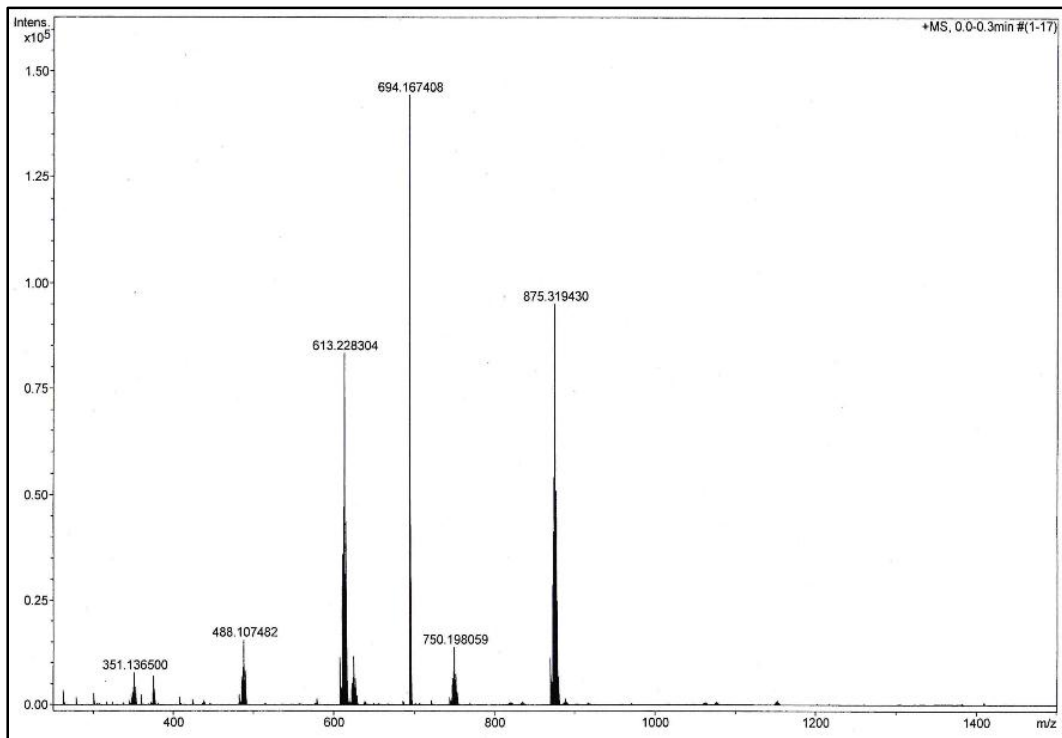


Figure C-7: Full MS spectrum of **1**.

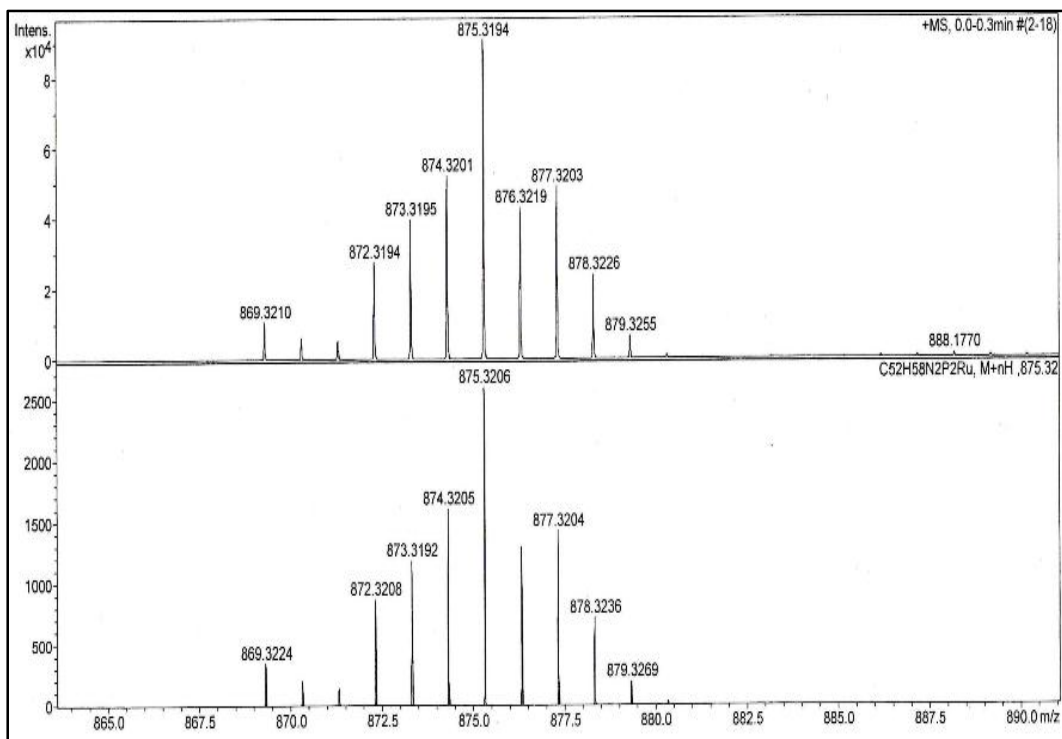


Figure C-8: Partial MS spectrum of **1**.

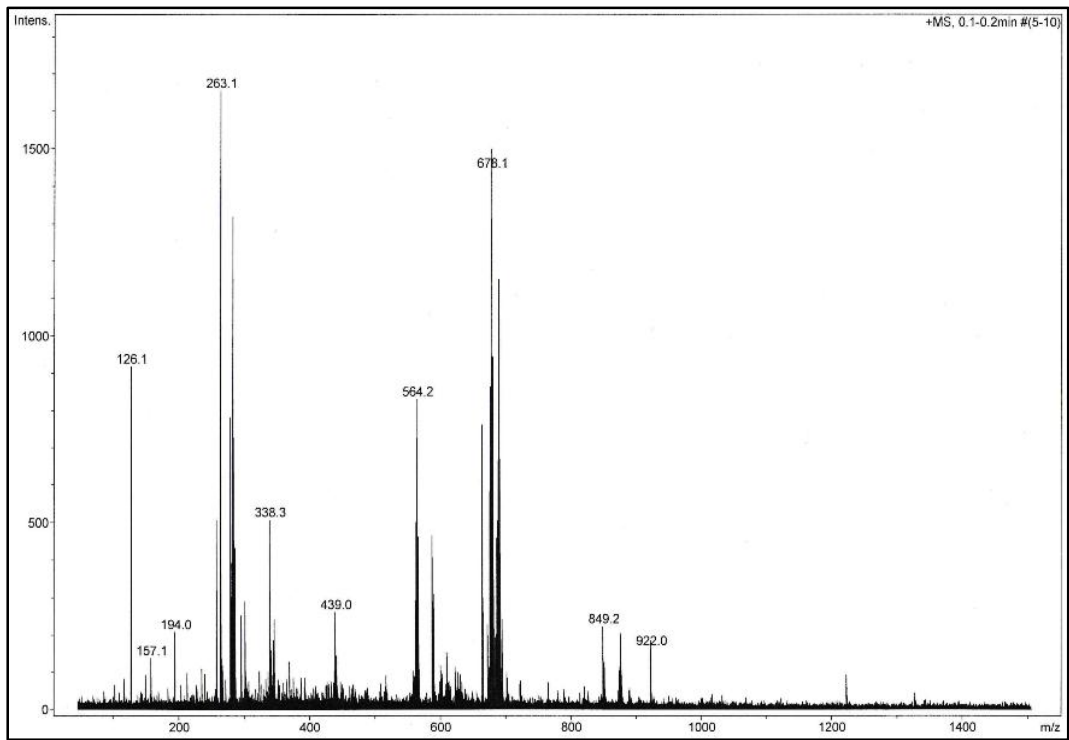


Figure C-9: Full MS spectrum of **2**.

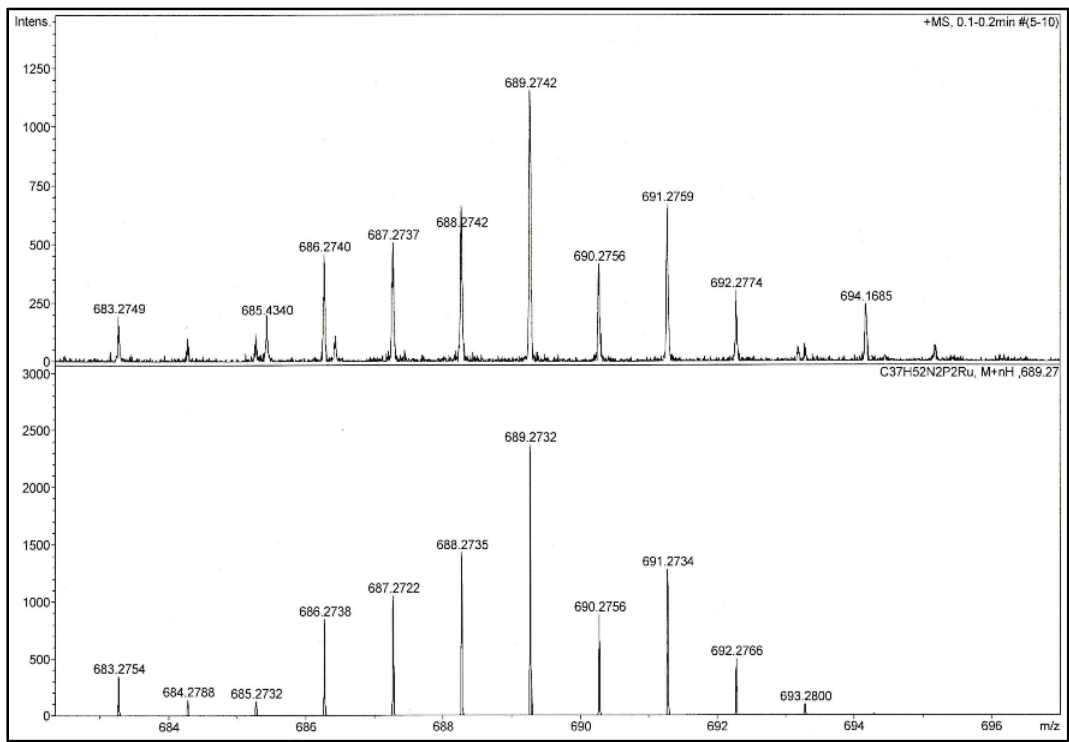


Figure C-10: Partial MS spectrum of **2**.

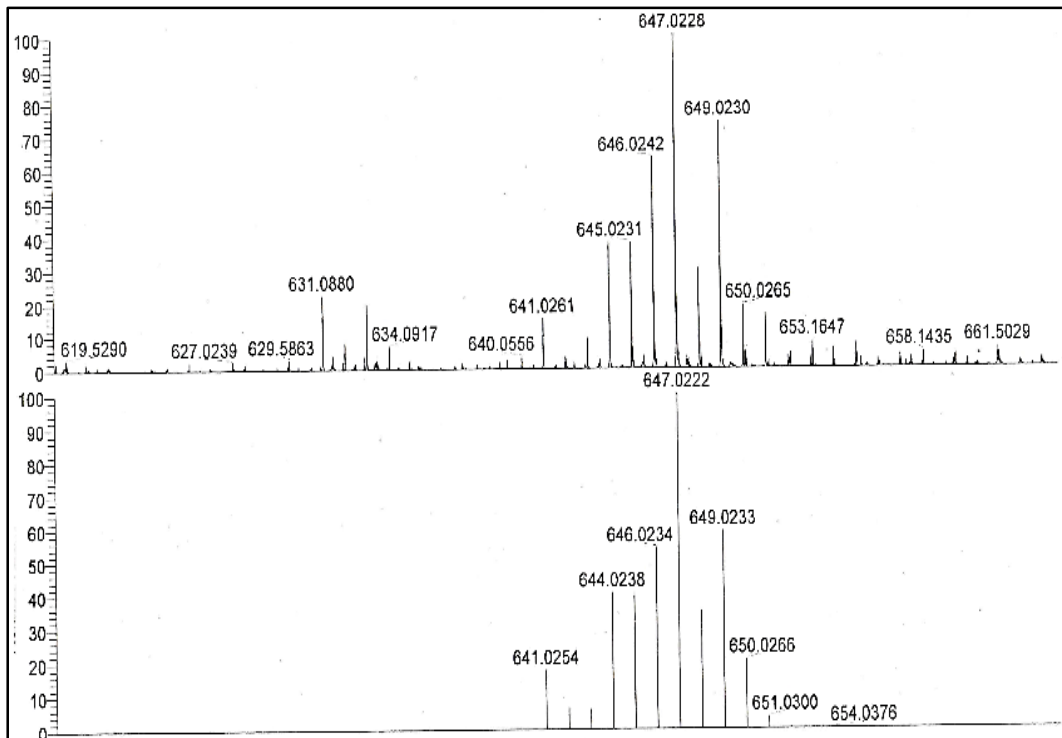


Figure C-11: Partial MS spectrum of 4.

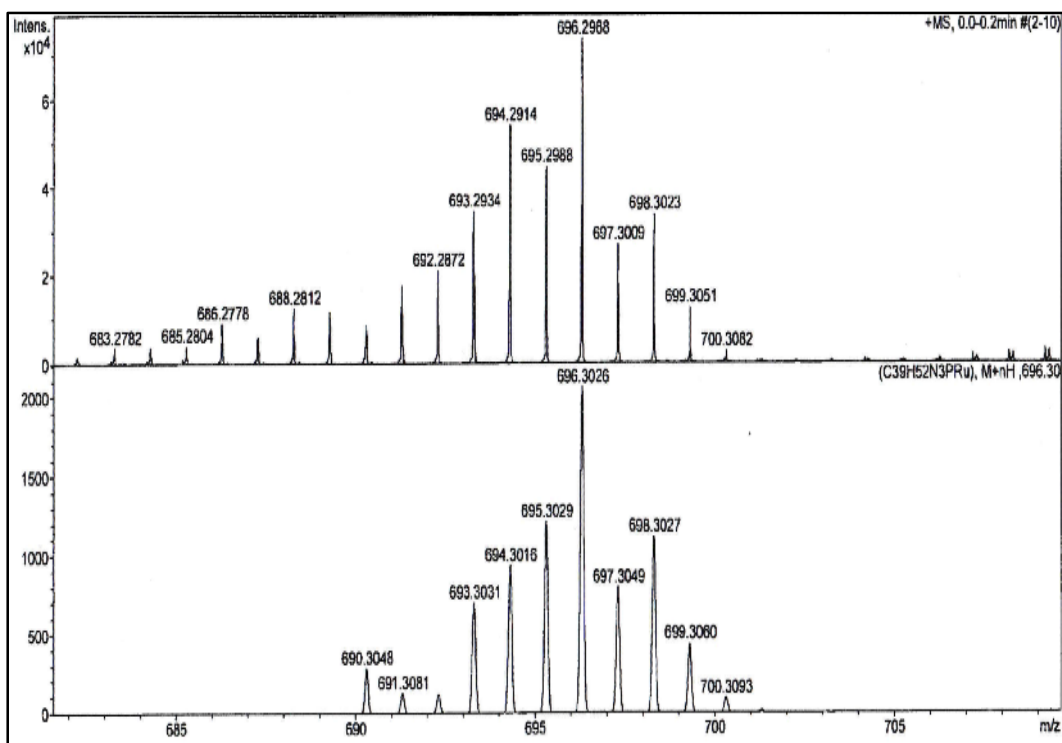


Figure C-12: Partial MS spectrum of 5.

Appendix D

X-Ray Crystallographic Data for *bis*-Azapentadienyl-Ruthenium-Phosphine Complexes

Crystals of X-ray diffraction quality were obtained for compounds **2**, **4**, **5**, **7**, **8**, and **12**.

In all cases crystals of appropriate dimensions were mounted on MiTeGen microloops¹ in random orientations. Preliminary examination and data collection were performed using a Bruker Kappa Apex II charge coupled device (CCD) detector system single crystal X-ray diffractometer equipped with an Oxford Cryostream LT device. All data were collected using graphite monochromated Mo K α radiation ($\lambda=0.71073$) from a fine focus sealed tube X-ray source. Preliminary unit cell constants were determined with a set of 36 narrow frame scans. Typical data sets consisted of combinations of ω and ϕ scan frames with typical scan width of 0.5° and counting time of 15-30 s/frame at a crystal to detector distance of 3.5-4.0 cm. The collected frames were integrated using an orientation matrix determined from the narrow frame scans. Apex II and SAINT software packages² were used for data collection and data integration. Final cell constants were corrected for systematic errors using SADABS or TWINABS.² Crystal data and intensity data collection parameters are listed in the following tables.

Structure solution and refinement were carried out using the SHELXTL-PLUS software package.³ The structures were solved by direct methods and refined with full matrix least-squares refinement by minimizing $\sum w(F_O^2 - F_C^2)^2$. All non-hydrogen atoms were refined anisotropically to convergence, while all H atoms were added in the calculated positions and were refined using appropriate riding models (AFX m3). In **4**, the *tert*-butyl groups on both azapentadienyl ligands (atoms C6-C8) and C14-C16) exhibited twofold rotational disorder, which was successfully modeled. Similarly, one of the phosphite oxygens (O21) showed two-fold disorder and was successfully modeled. In **12**, the oxygen atom of the THF solvent molecule [O(1S)] exhibited a two-fold disorder, which was successfully modeled.

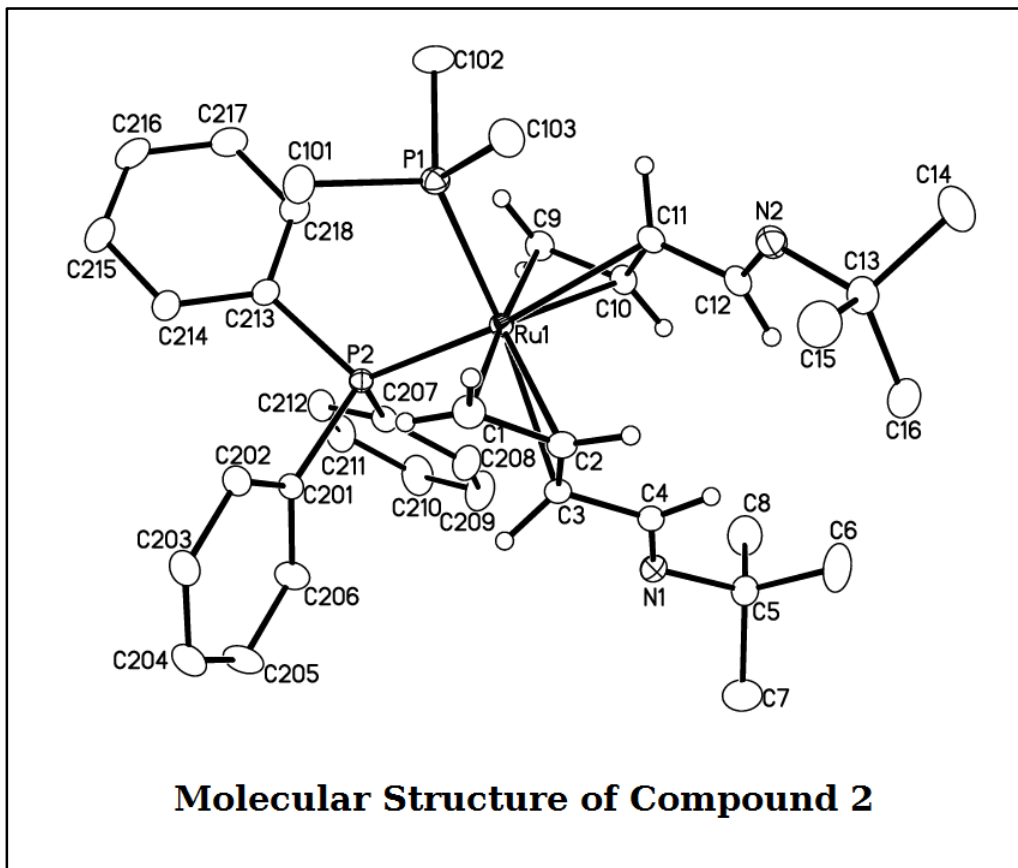
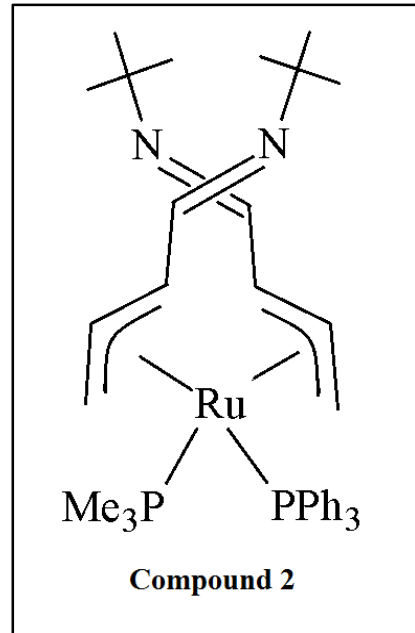


Table D-1.1: Crystal data and structure refinement for Compound 2.

Empirical formula	$C_{37} H_{52} N_2 P_2 Ru$		
Formula weight	687.81		
Temperature	296(2) K		
Wavelength	0.71073 Å		
Crystal system	Triclinic		
Space group	$P \bar{1}$		
Unit cell dimensions	$a = 10.4029(4)$ Å	$\alpha = 102.522(2)^\circ$.	
	$b = 12.9255(5)$ Å	$\beta = 92.908(2)^\circ$.	
	$c = 13.8754(5)$ Å	$\gamma = 100.088(2)^\circ$.	
Volume	$1785.53(12)$ Å ³		
Z	2		
Density (calculated)	1.279 Mg/m ³		
Absorption coefficient	0.555 mm ⁻¹		
F(000)	724		
Crystal size	0.288 x 0.231 x 0.189 mm ³		
Theta range for data collection	1.960 to 36.400°.		
Index ranges	$-17 \leq h \leq 16, -21 \leq k \leq 21, -23 \leq l \leq 22$		
Reflections collected	77008		
Independent reflections	16142 [R(int) = 0.0498]		
Completeness to theta = 25.242°	99.9 %		
Absorption correction	Semi-empirical from equivalents		
Max. and min. transmission	0.7471 and 0.6462		
Refinement method	Full-matrix least-squares on F ²		
Data / restraints / parameters	16142 / 0 / 388		
Goodness-of-fit on F ²	1.021		
Final R indices [I>2sigma(I)]	R1 = 0.0357, wR2 = 0.0733		
R indices (all data)	R1 = 0.0534, wR2 = 0.0798		
Extinction coefficient	n/a		
Largest diff. peak and hole	0.849 and -0.779 e.Å ⁻³		

Table D-1.2: Atomic coordinates ($\times 10^4$) and equivalent isotropic displacement parameters ($\text{\AA}^2 \times 10^3$) for Compound 2. U(eq) is defined as one third of the trace of the orthogonalized U_{ij} tensor.

	x	y	z	U(eq)
Ru(1)	6301(1)	6203(1)	7822(1)	10(1)
P(1)	7199(1)	4923(1)	8404(1)	14(1)
P(2)	7750(1)	7754(1)	8670(1)	11(1)
N(1)	4077(1)	8188(1)	6581(1)	18(1)
N(2)	3495(1)	3575(1)	6480(1)	17(1)
C(1)	5005(1)	6191(1)	9042(1)	16(1)
C(2)	4340(1)	6318(1)	8180(1)	14(1)
C(3)	4696(1)	7263(1)	7814(1)	14(1)
C(4)	3981(1)	7331(1)	6901(1)	15(1)
C(5)	3320(2)	8191(1)	5651(1)	21(1)
C(6)	2279(2)	7180(2)	5224(1)	32(1)
C(7)	2677(2)	9177(2)	5878(1)	38(1)
C(8)	4308(2)	8329(2)	4888(1)	30(1)
C(9)	7496(1)	6142(1)	6538(1)	15(1)
C(10)	6150(1)	5768(1)	6231(1)	15(1)
C(11)	5507(1)	4811(1)	6480(1)	14(1)
C(12)	4089(1)	4445(1)	6286(1)	15(1)
C(13)	2051(1)	3286(1)	6342(1)	18(1)
C(14)	1714(2)	2191(1)	5603(1)	27(1)
C(15)	1609(2)	3168(2)	7353(1)	25(1)
C(16)	1353(2)	4100(1)	5984(1)	21(1)
C(101)	7917(2)	5267(1)	9688(1)	22(1)
C(102)	8470(2)	4296(1)	7783(1)	24(1)
C(103)	5991(2)	3707(1)	8404(1)	20(1)
C(201)	7237(1)	8582(1)	9778(1)	13(1)
C(202)	7020(1)	8154(1)	10614(1)	17(1)
C(203)	6534(2)	8726(1)	11435(1)	20(1)
C(204)	6252(2)	9737(1)	11442(1)	22(1)
C(205)	6473(2)	10168(1)	10624(1)	24(1)
C(206)	6956(2)	9601(1)	9798(1)	19(1)

	x	y	z	U(eq)
C(207)	8238(1)	8764(1)	7934(1)	14(1)
C(208)	7334(2)	8908(1)	7221(1)	20(1)
C(209)	7665(2)	9687(1)	6682(1)	25(1)
C(210)	8910(2)	10318(1)	6827(1)	26(1)
C(211)	9820(2)	10173(1)	7521(1)	23(1)
C(212)	9486(1)	9410(1)	8080(1)	18(1)
C(213)	9382(1)	7599(1)	9105(1)	14(1)
C(214)	9968(1)	8006(1)	10068(1)	17(1)
C(215)	11221(1)	7855(1)	10328(1)	21(1)
C(216)	11911(2)	7316(1)	9625(1)	22(1)
C(217)	11351(2)	6922(1)	8662(1)	22(1)
C(218)	10098(1)	7056(1)	8401(1)	18(1)

Table D-1.3: Bond lengths [Å] for Compound 2.

Ru(1)-C(10)	2.1461(13)	C(7)-H(7B)	0.9600
Ru(1)-C(2)	2.1469(13)	C(7)-H(7C)	0.9600
Ru(1)-C(1)	2.2178(13)	C(8)-H(8A)	0.9600
Ru(1)-C(9)	2.2187(13)	C(8)-H(8B)	0.9600
Ru(1)-C(11)	2.2924(13)	C(8)-H(8C)	0.9600
Ru(1)-P(1)	2.3042(4)	C(9)-C(10)	1.4105(19)
Ru(1)-P(2)	2.3274(4)	C(9)-H(9A)	0.9300
Ru(1)-C(3)	2.3387(13)	C(9)-H(9B)	0.9300
P(1)-C(101)	1.8254(15)	C(10)-C(11)	1.420(2)
P(1)-C(102)	1.8266(15)	C(10)-H(10)	0.9800
P(1)-C(103)	1.8324(15)	C(11)-C(12)	1.4602(19)
P(2)-C(213)	1.8326(13)	C(11)-H(11)	0.9800
P(2)-C(201)	1.8338(13)	C(12)-H(12)	0.9300
P(2)-C(207)	1.8449(14)	C(13)-C(15)	1.528(2)
N(1)-C(4)	1.2711(19)	C(13)-C(14)	1.529(2)
N(1)-C(5)	1.4783(18)	C(13)-C(16)	1.530(2)
N(2)-C(12)	1.2733(19)	C(14)-H(14A)	0.9600
N(2)-C(13)	1.4754(19)	C(14)-H(14B)	0.9600
C(1)-C(2)	1.4054(19)	C(14)-H(14C)	0.9600
C(1)-H(1A)	0.9300	C(15)-H(15A)	0.9600
C(1)-H(1B)	0.9300	C(15)-H(15B)	0.9600
C(2)-C(3)	1.420(2)	C(15)-H(15C)	0.9600
C(2)-H(2)	0.9800	C(16)-H(16A)	0.9600
C(3)-C(4)	1.4630(19)	C(16)-H(16B)	0.9600
C(3)-H(3)	0.9800	C(16)-H(16C)	0.9600
C(4)-H(4)	0.9300	C(101)-H(10A)	0.9600
C(5)-C(7)	1.522(2)	C(101)-H(10B)	0.9600
C(5)-C(6)	1.528(2)	C(101)-H(10C)	0.9600
C(5)-C(8)	1.530(2)	C(102)-H(10D)	0.9600
C(6)-H(6A)	0.9600	C(102)-H(10E)	0.9600
C(6)-H(6B)	0.9600	C(102)-H(10F)	0.9600
C(6)-H(6C)	0.9600	C(103)-H(10G)	0.9600
C(7)-H(7A)	0.9600	C(103)-H(10H)	0.9600
C(103)-H(10I)	0.9600		

C(201)-C(206)	1.393(2)
C(201)-C(202)	1.401(2)
C(202)-C(203)	1.387(2)
C(202)-H(202)	0.9300
C(203)-C(204)	1.387(2)
C(203)-H(203)	0.9300
C(204)-C(205)	1.382(2)
C(204)-H(204)	0.9300
C(205)-C(206)	1.387(2)
C(205)-H(205)	0.9300
C(206)-H(206)	0.9300
C(207)-C(208)	1.3941(19)
C(207)-C(212)	1.394(2)
C(208)-C(209)	1.386(2)
C(208)-H(208)	0.9300
C(209)-C(210)	1.384(2)
C(209)-H(209)	0.9300
C(210)-C(211)	1.381(2)
C(210)-H(210)	0.9300
C(211)-C(212)	1.390(2)
C(211)-H(211)	0.9300
C(212)-H(212)	0.9300
C(213)-C(214)	1.391(2)
C(213)-C(218)	1.400(2)
C(214)-C(215)	1.392(2)
C(214)-H(214)	0.9300
C(215)-C(216)	1.380(2)
C(215)-H(215)	0.9300
C(216)-C(217)	1.381(2)
C(216)-H(216)	0.9300
C(217)-C(218)	1.385(2)
C(217)-H(217)	0.9300
C(218)-H(218)	0.9300

Table D-1.4: Bond angles [°] for Compound 2.

C(10)-Ru(1)-C(2)	104.48(5)	C(103)-P(1)-Ru(1)	112.94(5)
C(10)-Ru(1)-C(1)	138.91(5)	C(213)-P(2)-C(201)	102.36(6)
C(2)-Ru(1)-C(1)	37.52(5)	C(213)-P(2)-C(207)	99.02(6)
C(10)-Ru(1)-C(9)	37.66(5)	C(201)-P(2)-C(207)	101.65(6)
C(2)-Ru(1)-C(9)	139.94(5)	C(213)-P(2)-Ru(1)	117.43(5)
C(1)-Ru(1)-C(9)	176.40(5)	C(201)-P(2)-Ru(1)	118.38(5)
C(10)-Ru(1)-C(11)	37.13(5)	C(207)-P(2)-Ru(1)	115.04(4)
C(2)-Ru(1)-C(11)	90.58(5)	C(4)-N(1)-C(5)	120.38(13)
C(1)-Ru(1)-C(11)	111.21(5)	C(12)-N(2)-C(13)	120.43(13)
C(9)-Ru(1)-C(11)	65.29(5)	C(2)-C(1)-Ru(1)	68.50(7)
C(10)-Ru(1)-P(1)	108.10(4)	C(2)-C(1)-H(1A)	120.0
C(2)-Ru(1)-P(1)	115.81(4)	Ru(1)-C(1)-H(1A)	81.9
C(1)-Ru(1)-P(1)	86.28(4)	C(2)-C(1)-H(1B)	120.0
C(9)-Ru(1)-P(1)	94.11(4)	Ru(1)-C(1)-H(1B)	120.5
C(11)-Ru(1)-P(1)	84.30(4)	H(1A)-C(1)-H(1B)	120.0
C(10)-Ru(1)-P(2)	119.71(4)	C(1)-C(2)-C(3)	121.04(13)
C(2)-Ru(1)-P(2)	109.69(4)	C(1)-C(2)-Ru(1)	73.98(8)
C(1)-Ru(1)-P(2)	94.16(4)	C(3)-C(2)-Ru(1)	79.07(8)
C(9)-Ru(1)-P(2)	89.31(4)	C(1)-C(2)-H(2)	119.5
C(11)-Ru(1)-P(2)	154.56(4)	C(3)-C(2)-H(2)	119.5
P(1)-Ru(1)-P(2)	99.617(13)	Ru(1)-C(2)-H(2)	119.5
C(10)-Ru(1)-C(3)	91.64(5)	C(2)-C(3)-C(4)	118.10(12)
C(2)-Ru(1)-C(3)	36.60(5)	C(2)-C(3)-Ru(1)	64.33(7)
C(1)-Ru(1)-C(3)	65.28(5)	C(4)-C(3)-Ru(1)	122.71(9)
C(9)-Ru(1)-C(3)	113.96(5)	C(2)-C(3)-H(3)	114.2
C(11)-Ru(1)-C(3)	100.79(5)	C(4)-C(3)-H(3)	114.2
P(1)-Ru(1)-C(3)	151.12(4)	Ru(1)-C(3)-H(3)	114.2
P(2)-Ru(1)-C(3)	87.91(4)	N(1)-C(4)-C(3)	123.66(13)
C(101)-P(1)-C(102)	100.28(8)	N(1)-C(4)-H(4)	118.2
C(101)-P(1)-C(103)	100.61(7)	C(3)-C(4)-H(4)	118.2
C(102)-P(1)-C(103)	99.46(8)	N(1)-C(5)-C(7)	106.14(12)
C(101)-P(1)-Ru(1)	118.26(5)	N(1)-C(5)-C(6)	115.55(13)
C(102)-P(1)-Ru(1)	121.75(6)	C(103)-P(1)-Ru(1)	112.94(5)
C(7)-C(5)-C(6)	109.84(15)	C(10)-C(11)-Ru(1)	65.83(7)

N(1)-C(5)-C(8)	106.87(13)	C(12)-C(11)-Ru(1)	118.38(9)
C(7)-C(5)-C(8)	109.45(15)	C(10)-C(11)-H(11)	114.2
C(6)-C(5)-C(8)	108.83(14)	C(12)-C(11)-H(11)	114.2
C(5)-C(6)-H(6A)	109.5	Ru(1)-C(11)-H(11)	114.2
C(5)-C(6)-H(6B)	109.5	N(2)-C(12)-C(11)	122.65(13)
H(6A)-C(6)-H(6B)	109.5	N(2)-C(12)-H(12)	118.7
C(5)-C(6)-H(6C)	109.5	C(11)-C(12)-H(12)	118.7
H(6A)-C(6)-H(6C)	109.5	N(2)-C(13)-C(15)	105.96(12)
H(6B)-C(6)-H(6C)	109.5	N(2)-C(13)-C(14)	106.27(12)
C(5)-C(7)-H(7A)	109.5	C(15)-C(13)-C(14)	109.70(13)
C(5)-C(7)-H(7B)	109.5	N(2)-C(13)-C(16)	115.70(12)
H(7A)-C(7)-H(7B)	109.5	C(15)-C(13)-C(16)	108.90(13)
C(5)-C(7)-H(7C)	109.5	C(14)-C(13)-C(16)	110.13(13)
H(7A)-C(7)-H(7C)	109.5	C(13)-C(14)-H(14A)	109.5
H(7B)-C(7)-H(7C)	109.5	C(13)-C(14)-H(14B)	109.5
C(5)-C(8)-H(8A)	109.5	H(14A)-C(14)-H(14B)	109.5
C(5)-C(8)-H(8B)	109.5	C(13)-C(14)-H(14C)	109.5
H(8A)-C(8)-H(8B)	109.5	H(14A)-C(14)-H(14C)	109.5
C(5)-C(8)-H(8C)	109.5	H(14B)-C(14)-H(14C)	109.5
H(8A)-C(8)-H(8C)	109.5	C(13)-C(15)-H(15A)	109.5
H(8B)-C(8)-H(8C)	109.5	C(13)-C(15)-H(15B)	109.5
C(10)-C(9)-Ru(1)	68.38(7)	H(15A)-C(15)-H(15B)	109.5
C(10)-C(9)-H(9A)	120.0	C(13)-C(15)-H(15C)	109.5
Ru(1)-C(9)-H(9A)	81.0	H(15A)-C(15)-H(15C)	109.5
C(10)-C(9)-H(9B)	120.0	H(15B)-C(15)-H(15C)	109.5
Ru(1)-C(9)-H(9B)	121.6	C(13)-C(16)-H(16A)	109.5
H(9A)-C(9)-H(9B)	120.0	C(13)-C(16)-H(16B)	109.5
C(9)-C(10)-C(11)	118.64(13)	H(16A)-C(16)-H(16B)	109.5
C(9)-C(10)-Ru(1)	73.96(8)	C(13)-C(16)-H(16C)	109.5
C(11)-C(10)-Ru(1)	77.04(8)	H(16A)-C(16)-H(16C)	109.5
C(9)-C(10)-H(10)	120.7	H(16B)-C(16)-H(16C)	109.5
C(11)-C(10)-H(10)	120.7	P(1)-C(101)-H(10A)	109.5
Ru(1)-C(10)-H(10)	120.7	P(1)-C(101)-H(10B)	109.5
C(10)-C(11)-C(12)	121.53(13)	H(10A)-C(101)-H(10B)	109.5
P(1)-C(101)-H(10C)	109.5	C(212)-C(207)-P(2)	121.94(11)
H(10A)-C(101)-H(10C)	109.5	C(209)-C(208)-C(207)	120.65(14)

H(10B)-C(101)-H(10C)	109.5	C(209)-C(208)-H(208)	119.7
P(1)-C(102)-H(10D)	109.5	C(207)-C(208)-H(208)	119.7
P(1)-C(102)-H(10E)	109.5	C(210)-C(209)-C(208)	120.49(15)
H(10D)-C(102)-H(10E)	109.5	C(210)-C(209)-H(209)	119.8
P(1)-C(102)-H(10F)	109.5	C(208)-C(209)-H(209)	119.8
H(10D)-C(102)-H(10F)	109.5	C(211)-C(210)-C(209)	119.40(15)
H(10E)-C(102)-H(10F)	109.5	C(211)-C(210)-H(210)	120.3
P(1)-C(103)-H(10G)	109.5	C(209)-C(210)-H(210)	120.3
P(1)-C(103)-H(10H)	109.5	C(210)-C(211)-C(212)	120.43(14)
H(10G)-C(103)-H(10H)	109.5	C(210)-C(211)-H(211)	119.8
P(1)-C(103)-H(10I)	109.5	C(212)-C(211)-H(211)	119.8
H(10G)-C(103)-H(10I)	109.5	C(211)-C(212)-C(207)	120.60(14)
H(10H)-C(103)-H(10I)	109.5	C(211)-C(212)-H(212)	119.7
C(206)-C(201)-C(202)	118.01(13)	C(207)-C(212)-H(212)	119.7
C(206)-C(201)-P(2)	122.26(11)	C(214)-C(213)-C(218)	118.21(13)
C(202)-C(201)-P(2)	119.55(10)	C(214)-C(213)-P(2)	124.82(11)
C(203)-C(202)-C(201)	121.00(14)	C(218)-C(213)-P(2)	116.94(10)
C(203)-C(202)-H(202)	119.5	C(213)-C(214)-C(215)	120.72(14)
C(201)-C(202)-H(202)	119.5	C(213)-C(214)-H(214)	119.6
C(204)-C(203)-C(202)	120.32(15)	C(215)-C(214)-H(214)	119.6
C(204)-C(203)-H(203)	119.8	C(216)-C(215)-C(214)	120.28(14)
C(202)-C(203)-H(203)	119.8	C(216)-C(215)-H(215)	119.9
C(205)-C(204)-C(203)	119.03(14)	C(214)-C(215)-H(215)	119.9
C(205)-C(204)-H(204)	120.5	C(215)-C(216)-C(217)	119.64(14)
C(203)-C(204)-H(204)	120.5	C(215)-C(216)-H(216)	120.2
C(204)-C(205)-C(206)	121.03(15)	C(217)-C(216)-H(216)	120.2
C(204)-C(205)-H(205)	119.5	C(216)-C(217)-C(218)	120.41(15)
C(206)-C(205)-H(205)	119.5	C(216)-C(217)-H(217)	119.8
C(205)-C(206)-C(201)	120.61(14)	C(218)-C(217)-H(217)	119.8
C(205)-C(206)-H(206)	119.7	C(217)-C(218)-C(213)	120.73(14)
C(201)-C(206)-H(206)	119.7	C(217)-C(218)-H(218)	119.6
C(208)-C(207)-C(212)	118.41(13)	C(213)-C(218)-H(218)	119.6
C(208)-C(207)-P(2)	119.64(10)		

Table D-1.5: Anisotropic displacement parameters ($\text{\AA}^2 \times 10^3$) for Compound 2. The anisotropic displacement factor exponent takes the form: $-2\pi^2 [h^2 a^{*2} U_{11} + \dots + 2 h k a^{*} b^{*} U_{12}]$

	U ₁₁	U ₂₂	U ₃₃	U ₂₃	U ₁₃	U ₁₂
Ru(1)	10(1)	11(1)	9(1)	2(1)	2(1)	2(1)
P(1)	16(1)	13(1)	14(1)	4(1)	1(1)	4(1)
P(2)	10(1)	12(1)	11(1)	2(1)	1(1)	2(1)
N(1)	18(1)	18(1)	17(1)	2(1)	-3(1)	7(1)
N(2)	16(1)	16(1)	17(1)	2(1)	1(1)	2(1)
C(1)	14(1)	20(1)	16(1)	5(1)	5(1)	2(1)
C(2)	10(1)	17(1)	15(1)	2(1)	4(1)	3(1)
C(3)	13(1)	15(1)	14(1)	1(1)	1(1)	5(1)
C(4)	13(1)	14(1)	17(1)	0(1)	0(1)	4(1)
C(5)	23(1)	21(1)	18(1)	2(1)	-5(1)	7(1)
C(6)	29(1)	39(1)	26(1)	9(1)	-11(1)	-2(1)
C(7)	50(1)	41(1)	26(1)	3(1)	-7(1)	31(1)
C(8)	32(1)	35(1)	23(1)	8(1)	0(1)	5(1)
C(9)	16(1)	19(1)	11(1)	4(1)	5(1)	3(1)
C(10)	17(1)	19(1)	9(1)	2(1)	3(1)	4(1)
C(11)	16(1)	15(1)	12(1)	0(1)	2(1)	4(1)
C(12)	17(1)	16(1)	11(1)	0(1)	1(1)	3(1)
C(13)	17(1)	19(1)	16(1)	4(1)	1(1)	0(1)
C(14)	28(1)	20(1)	26(1)	0(1)	0(1)	-4(1)
C(15)	25(1)	31(1)	22(1)	10(1)	6(1)	4(1)
C(16)	17(1)	25(1)	20(1)	6(1)	0(1)	2(1)
C(101)	28(1)	17(1)	20(1)	7(1)	-6(1)	2(1)
C(102)	24(1)	21(1)	30(1)	7(1)	7(1)	12(1)
C(103)	25(1)	16(1)	19(1)	6(1)	1(1)	0(1)
C(201)	12(1)	14(1)	13(1)	1(1)	1(1)	3(1)
C(202)	19(1)	17(1)	14(1)	2(1)	0(1)	5(1)
C(203)	21(1)	25(1)	13(1)	1(1)	2(1)	5(1)
C(204)	22(1)	22(1)	19(1)	-3(1)	4(1)	5(1)
C(205)	29(1)	16(1)	26(1)	0(1)	8(1)	8(1)
C(206)	21(1)	15(1)	21(1)	3(1)	6(1)	5(1)

	U^{11}	U^{22}	U^{33}	U^{23}	U^{13}	U^{12}
C(207)	15(1)	13(1)	13(1)	3(1)	2(1)	2(1)
C(208)	18(1)	21(1)	21(1)	10(1)	-1(1)	-1(1)
C(209)	26(1)	26(1)	25(1)	15(1)	-5(1)	-2(1)
C(210)	32(1)	23(1)	21(1)	12(1)	2(1)	-6(1)
C(211)	21(1)	22(1)	23(1)	6(1)	2(1)	-6(1)
C(212)	18(1)	17(1)	17(1)	4(1)	1(1)	-1(1)
C(213)	12(1)	13(1)	18(1)	5(1)	1(1)	2(1)
C(214)	15(1)	18(1)	18(1)	4(1)	-1(1)	3(1)
C(215)	16(1)	22(1)	25(1)	9(1)	-4(1)	1(1)
C(216)	14(1)	21(1)	33(1)	11(1)	-2(1)	4(1)
C(217)	15(1)	22(1)	31(1)	6(1)	6(1)	6(1)
C(218)	14(1)	20(1)	20(1)	3(1)	2(1)	4(1)

Table D-1.6. Hydrogen coordinates ($\times 10^4$) and isotropic displacement parameters ($\text{\AA}^2 \times 10^3$) for Compound 2.

	x	y	z	U(eq)
H(1A)	5690	6730	9381	20
H(1B)	4760	5567	9272	20
H(2)	3605	5754	7836	17
H(3)	4872	7936	8327	17
H(4)	3425	6712	6534	18
H(6A)	2695	6567	5047	49
H(6B)	1809	7273	4645	49
H(6C)	1679	7065	5711	49
H(7A)	2043	9084	6347	56
H(7B)	2248	9261	5279	56
H(7C)	3334	9808	6153	56
H(8A)	4947	8978	5139	45
H(8B)	3859	8375	4281	45
H(8C)	4740	7721	4764	45
H(9A)	7944	5764	6896	18
H(9B)	7936	6768	6383	18
H(10)	5674	6151	5840	18
H(11)	6008	4227	6383	17
H(12)	3600	4863	6009	18
H(14A)	2058	2256	4985	40
H(14B)	779	1960	5498	40
H(14C)	2095	1671	5861	40
H(15A)	2052	2666	7589	38
H(15B)	680	2906	7291	38
H(15C)	1818	3857	7814	38
H(16A)	1588	4789	6444	31
H(16B)	422	3854	5938	31
H(16C)	1613	4170	5343	31
H(10A)	8669	5838	9769	32
H(10B)	8179	4644	9849	32

	x	y	z	U(eq)
H(10C)	7281	5500	10121	32
H(10D)	8162	3974	7102	35
H(10E)	8673	3750	8105	35
H(10F)	9244	4835	7816	35
H(10G)	5373	3883	8875	30
H(10H)	6430	3171	8581	30
H(10I)	5537	3428	7754	30
H(202)	7204	7476	10618	20
H(203)	6396	8429	11984	24
H(204)	5920	10120	11990	27
H(205)	6294	10849	10626	28
H(206)	7093	9904	9253	23
H(208)	6501	8477	7105	24
H(209)	7046	9786	6221	30
H(210)	9133	10835	6460	31
H(211)	10662	10588	7616	28
H(212)	10101	9330	8555	22
H(214)	9518	8384	10544	21
H(215)	11593	8118	10978	25
H(216)	12750	7219	9799	27
H(217)	11817	6564	8186	27
H(218)	9728	6782	7752	22

Table D-1.7. Torsion angles [°] for Compound 2.

Ru(1)-C(1)-C(2)-C(3)	-66.23(11)
C(1)-C(2)-C(3)-C(4)	178.64(12)
Ru(1)-C(2)-C(3)-C(4)	115.03(11)
C(1)-C(2)-C(3)-Ru(1)	63.62(11)
C(5)-N(1)-C(4)-C(3)	-179.95(13)
C(2)-C(3)-C(4)-N(1)	169.41(13)
Ru(1)-C(3)-C(4)-N(1)	-114.52(14)
C(4)-N(1)-C(5)-C(7)	131.96(16)
C(4)-N(1)-C(5)-C(6)	10.0(2)
C(4)-N(1)-C(5)-C(8)	-111.30(16)
Ru(1)-C(9)-C(10)-C(11)	-64.98(11)
C(9)-C(10)-C(11)-C(12)	172.96(12)
Ru(1)-C(10)-C(11)-C(12)	109.63(12)
C(9)-C(10)-C(11)-Ru(1)	63.34(11)
C(13)-N(2)-C(12)-C(11)	175.15(12)
C(10)-C(11)-C(12)-N(2)	178.22(13)
Ru(1)-C(11)-C(12)-N(2)	-104.16(14)
C(12)-N(2)-C(13)-C(15)	-122.05(15)
C(12)-N(2)-C(13)-C(14)	121.28(15)
C(12)-N(2)-C(13)-C(16)	-1.29(19)
C(213)-P(2)-C(201)-C(206)	118.92(12)
C(207)-P(2)-C(201)-C(206)	16.86(13)
Ru(1)-P(2)-C(201)-C(206)	-110.20(11)
C(213)-P(2)-C(201)-C(202)	-66.07(12)
C(207)-P(2)-C(201)-C(202)	-168.14(11)
Ru(1)-P(2)-C(201)-C(202)	64.81(12)
C(206)-C(201)-C(202)-C(203)	0.3(2)
P(2)-C(201)-C(202)-C(203)	-174.94(11)
C(201)-C(202)-C(203)-C(204)	0.0(2)
C(202)-C(203)-C(204)-C(205)	-0.5(2)
C(203)-C(204)-C(205)-C(206)	0.6(2)
C(204)-C(205)-C(206)-C(201)	-0.3(2)
C(202)-C(201)-C(206)-C(205)	-0.1(2)
P(2)-C(201)-C(206)-C(205)	174.93(12)

C(213)-P(2)-C(207)-C(208)	161.09(12)
C(201)-P(2)-C(207)-C(208)	-94.19(12)
Ru(1)-P(2)-C(207)-C(208)	35.01(13)
C(213)-P(2)-C(207)-C(212)	-20.07(13)
C(201)-P(2)-C(207)-C(212)	84.65(13)
Ru(1)-P(2)-C(207)-C(212)	-146.16(11)
C(212)-C(207)-C(208)-C(209)	-1.1(2)
P(2)-C(207)-C(208)-C(209)	177.82(13)
C(207)-C(208)-C(209)-C(210)	1.6(3)
C(208)-C(209)-C(210)-C(211)	-0.7(3)
C(209)-C(210)-C(211)-C(212)	-0.8(3)
C(210)-C(211)-C(212)-C(207)	1.4(2)
C(208)-C(207)-C(212)-C(211)	-0.4(2)
P(2)-C(207)-C(212)-C(211)	-179.27(12)
C(201)-P(2)-C(213)-C(214)	2.32(14)
C(207)-P(2)-C(213)-C(214)	106.45(13)
Ru(1)-P(2)-C(213)-C(214)	-129.14(12)
C(201)-P(2)-C(213)-C(218)	-175.72(11)
C(207)-P(2)-C(213)-C(218)	-71.58(12)
Ru(1)-P(2)-C(213)-C(218)	52.83(12)
C(218)-C(213)-C(214)-C(215)	-1.4(2)
P(2)-C(213)-C(214)-C(215)	-179.44(12)
C(213)-C(214)-C(215)-C(216)	1.4(2)
C(214)-C(215)-C(216)-C(217)	-0.3(2)
C(215)-C(216)-C(217)-C(218)	-0.6(2)
C(216)-C(217)-C(218)-C(213)	0.5(2)
C(214)-C(213)-C(218)-C(217)	0.5(2)
P(2)-C(213)-C(218)-C(217)	178.67(12)

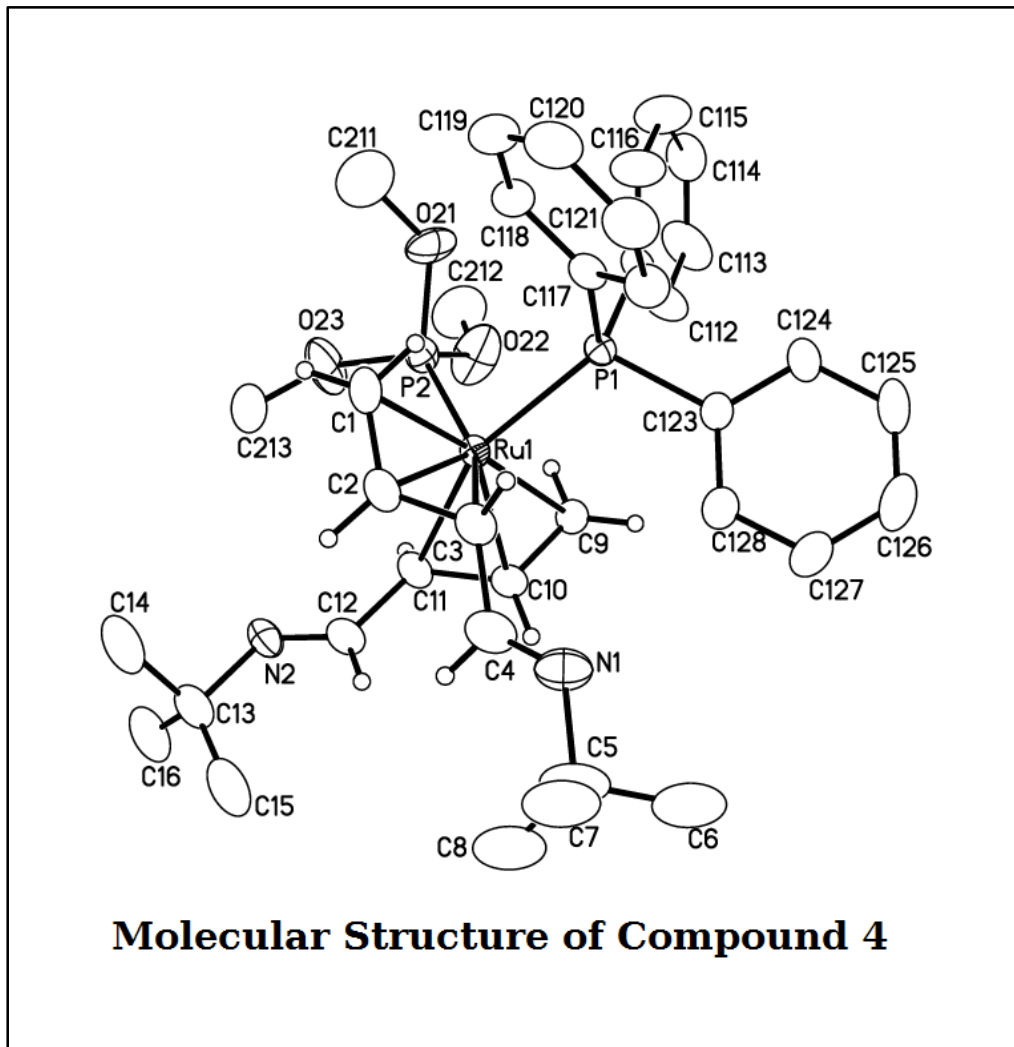
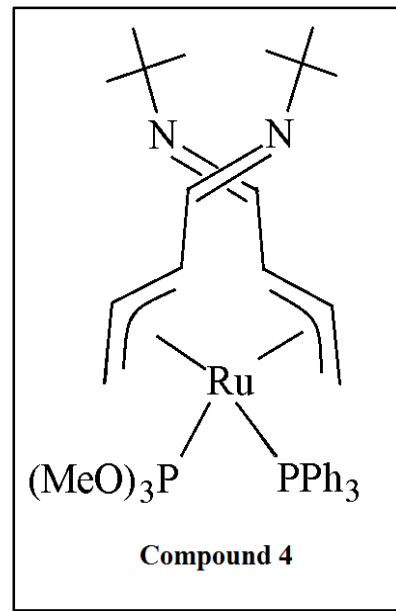


Table D-2.1: Crystal data and structure refinement for Compound 4.

Empirical formula	$C_{37} H_{52} N_2 O_3 P_2 Ru$		
Formula weight	735.81		
Temperature	250(2) K		
Wavelength	0.71073 Å		
Crystal system	Orthorhombic		
Space group	$P\bar{n}\bar{a}\bar{2}_1$		
Unit cell dimensions	$a = 18.7815(5)$ Å	$\alpha = 90^\circ$.	
	$b = 20.2151(6)$ Å	$\beta = 90^\circ$.	
	$c = 10.1211(3)$ Å	$\gamma = 90^\circ$.	
Volume	$3842.68(19)$ Å ³		
Z	4		
Density (calculated)	1.272 Mg/m ³		
Absorption coefficient	0.526 mm ⁻¹		
F(000)	1544		
Crystal size	$0.406 \times 0.153 \times 0.149$ mm ³		
Theta range for data collection	2.015 to 27.530°.		
Index ranges	$-24 \leq h \leq 24, -26 \leq k \leq 26, -13 \leq l \leq 13$		
Reflections collected	74975		
Independent reflections	8849 [R(int) = 0.0482]		
Completeness to theta = 25.242°	100.0 %		
Absorption correction	Semi-empirical from equivalents		
Max. and min. transmission	0.7456 and 0.7030		
Refinement method	Full-matrix least-squares on F^2		
Data / restraints / parameters	8849 / 380 / 415		
Goodness-of-fit on F^2	1.047		
Final R indices [I>2sigma(I)]	$R_1 = 0.0329, wR_2 = 0.0748$		
R indices (all data)	$R_1 = 0.0430, wR_2 = 0.0807$		
Absolute structure parameter	-0.005(11)		
Extinction coefficient	n/a		
Largest diff. peak and hole	0.425 and -0.415 e.Å ⁻³		

Table D-2.2: Atomic coordinates ($\times 10^4$) and equivalent isotropic displacement parameters ($\text{\AA}^2 \times 10^3$) for Compound 4. U(eq) is defined as one third of the trace of the orthogonalized \mathbf{U}^{ij} tensor.

	x	y	z	U(eq)
Ru(1)	13917(1)	7461(1)	5029(1)	31(1)
P(1)	13704(1)	8539(1)	4297(1)	33(1)
P(2)	13167(1)	7001(1)	3587(1)	44(1)
O(21)	12476(4)	7356(8)	2995(17)	71(3)
O(21')	12437(4)	7401(4)	3662(16)	71(3)
O(22)	13451(3)	6923(3)	2132(4)	101(2)
O(23)	12885(3)	6269(2)	3760(5)	94(2)
N(1)	15302(3)	8237(3)	8091(4)	67(1)
N(2)	14397(2)	5539(2)	6430(4)	54(1)
C(1)	13044(3)	7463(2)	6516(5)	51(1)
C(2)	13704(3)	7375(2)	7114(5)	47(1)
C(3)	14216(3)	7888(2)	7118(4)	46(1)
C(4)	14894(3)	7779(3)	7770(5)	58(1)
C(5)	15971(4)	8115(4)	8821(6)	91(2)
C(6)	16525(6)	8554(6)	8148(13)	117(3)
C(7)	15837(6)	8441(8)	10157(10)	117(3)
C(8)	16222(7)	7427(5)	8911(16)	117(3)
C(6')	16532(17)	8644(16)	8680(40)	117(3)
C(7')	15804(18)	7970(20)	10244(17)	117(3)
C(8')	16290(20)	7486(13)	8210(40)	117(3)
C(9)	14834(2)	7413(2)	3614(5)	41(1)
C(10)	14964(2)	7048(2)	4765(4)	41(1)
C(11)	14547(2)	6485(2)	5045(6)	43(1)
C(12)	14667(3)	6104(2)	6246(5)	46(1)
C(13)	14515(3)	5190(3)	7700(6)	68(2)
C(14)	13789(6)	5231(7)	8347(13)	100(2)
C(15)	15083(8)	5462(7)	8562(13)	100(2)
C(16)	14619(9)	4485(5)	7280(13)	100(2)
C(14')	14131(11)	5512(8)	8850(15)	100(2)

	x	y	z	U(eq)
C(15')	15298(6)	5178(10)	8070(20)	100(2)
C(16')	14277(11)	4477(6)	7650(20)	100(2)
C(111)	13374(2)	8647(2)	2593(4)	39(1)
C(112)	13791(3)	8402(3)	1599(5)	64(2)
C(113)	13563(4)	8438(3)	280(5)	78(2)
C(114)	12945(3)	8722(3)	-22(7)	69(1)
C(115)	12526(4)	8980(4)	940(7)	88(2)
C(116)	12747(3)	8941(4)	2253(6)	73(2)
C(117)	13095(2)	9053(2)	5271(4)	39(1)
C(118)	12382(2)	8872(2)	5359(4)	47(1)
C(119)	11914(3)	9229(3)	6157(6)	59(1)
C(120)	12156(3)	9763(3)	6854(6)	66(2)
C(121)	12856(3)	9938(3)	6792(6)	64(2)
C(122)	13329(3)	9591(2)	6000(5)	50(1)
C(123)	14500(2)	9070(2)	4237(5)	39(1)
C(124)	14508(3)	9634(3)	3444(6)	61(2)
C(125)	15097(4)	10047(3)	3452(8)	78(2)
C(126)	15662(3)	9914(3)	4233(7)	74(2)
C(127)	15659(3)	9365(3)	5012(8)	65(1)
C(128)	15079(2)	8939(2)	5011(6)	50(1)
C(211)	11770(4)	7247(5)	3256(9)	114(2)
C(212)	13138(4)	6632(5)	1048(8)	114(2)
C(213)	12839(3)	5902(3)	4907(7)	68(2)

Table D-2.3: Bond lengths [Å] for Compound 4.

Ru(1)-C(10)	2.154(4)	C(5)-C(6')	1.508(12)
Ru(1)-C(2)	2.155(5)	C(5)-C(7)	1.525(9)
Ru(1)-C(1)	2.226(5)	C(5)-C(6)	1.527(9)
Ru(1)-P(2)	2.2312(13)	C(5)-C(8')	1.533(12)
Ru(1)-C(9)	2.242(4)	C(6)-H(6A)	0.9700
Ru(1)-C(11)	2.302(4)	C(6)-H(6B)	0.9700
Ru(1)-P(1)	2.3353(11)	C(6)-H(6C)	0.9700
Ru(1)-C(3)	2.352(5)	C(7)-H(7A)	0.9700
P(1)-C(117)	1.834(4)	C(7)-H(7B)	0.9700
P(1)-C(123)	1.841(4)	C(7)-H(7C)	0.9700
P(1)-C(111)	1.846(4)	C(8)-H(8A)	0.9700
P(2)-O(22)	1.575(5)	C(8)-H(8B)	0.9700
P(2)-O(23)	1.581(4)	C(8)-H(8C)	0.9700
P(2)-O(21')	1.594(7)	C(6')-H(6'1)	0.9700
P(2)-O(21)	1.600(9)	C(6')-H(6'2)	0.9700
O(21)-C(211)	1.370(10)	C(6')-H(6'3)	0.9700
O(21')-C(211)	1.355(9)	C(7')-H(7'1)	0.9700
O(22)-C(212)	1.377(7)	C(7')-H(7'2)	0.9700
O(23)-C(213)	1.381(7)	C(7')-H(7'3)	0.9700
N(1)-C(4)	1.246(7)	C(8')-H(8'1)	0.9700
N(1)-C(5)	1.479(8)	C(8')-H(8'2)	0.9700
N(2)-C(12)	1.262(6)	C(8')-H(8'3)	0.9700
N(2)-C(13)	1.484(7)	C(9)-C(10)	1.400(6)
C(1)-C(2)	1.391(8)	C(9)-H(9A)	0.9400
C(1)-H(1A)	0.9400	C(9)-H(9B)	0.9400
C(1)-H(1B)	0.9400	C(10)-C(11)	1.410(6)
C(2)-C(3)	1.415(7)	C(10)-H(10)	0.9900
C(2)-H(2)	0.9900	C(11)-C(12)	1.456(7)
C(3)-C(4)	1.450(7)	C(11)-H(11)	0.9900
C(3)-H(3)	0.9900	C(12)-H(12)	0.9400
C(4)-H(4)	0.9400	C(13)-C(15)	1.485(9)
C(5)-C(8)	1.472(9)	C(13)-C(16)	1.499(9)
C(5)-C(7')	1.504(12)	C(13)-C(16')	1.509(10)

C(13)-C(14)	1.515(9)	C(118)-H(118)	0.9400
C(13)-C(14')	1.516(10)	C(119)-C(120)	1.367(8)
C(13)-C(15')	1.519(10)	C(119)-H(119)	0.9400
C(14)-H(14A)	0.9700	C(120)-C(121)	1.363(9)
C(14)-H(14B)	0.9700	C(120)-H(120)	0.9400
C(14)-H(14C)	0.9700	C(121)-C(122)	1.387(7)
C(15)-H(15A)	0.9700	C(121)-H(121)	0.9400
C(15)-H(15B)	0.9700	C(122)-H(122)	0.9400
C(15)-H(15C)	0.9700	C(123)-C(128)	1.366(7)
C(16)-H(16A)	0.9700	C(123)-C(124)	1.394(6)
C(16)-H(16B)	0.9700	C(124)-C(125)	1.385(8)
C(16)-H(16C)	0.9700	C(124)-H(124)	0.9400
C(14')-H(14D)	0.9700	C(125)-C(126)	1.350(10)
C(14')-H(14E)	0.9700	C(125)-H(125)	0.9400
C(14')-H(14F)	0.9700	C(126)-C(127)	1.363(9)
C(15')-H(15D)	0.9700	C(126)-H(126)	0.9400
C(15')-H(15E)	0.9700	C(127)-C(128)	1.387(6)
C(15')-H(15F)	0.9700	C(127)-H(127)	0.9400
C(16')-H(16D)	0.9700	C(128)-H(128)	0.9400
C(16')-H(16E)	0.9700	C(211)-H(21A)	0.9700
C(16')-H(16F)	0.9700	C(211)-H(21B)	0.9700
C(111)-C(116)	1.363(7)	C(211)-H(21C)	0.9700
C(111)-C(112)	1.367(7)	C(212)-H(21D)	0.9700
C(112)-C(113)	1.404(8)	C(212)-H(21E)	0.9700
C(112)-H(112)	0.9400	C(212)-H(21F)	0.9700
C(113)-C(114)	1.330(8)	C(213)-H(21G)	0.9700
C(113)-H(113)	0.9400	C(213)-H(21H)	0.9700
C(114)-C(115)	1.357(9)	C(213)-H(21I)	0.9700
C(114)-H(114)	0.9400		
C(115)-C(116)	1.394(8)		
C(115)-H(115)	0.9400		
C(116)-H(116)	0.9400		
C(117)-C(122)	1.385(6)		
C(117)-C(118)	1.390(6)		
C(118)-C(119)	1.395(6)		

Table D-2.4: Bond angles [°] for Compound 4.

C(10)-Ru(1)-C(2)	105.06(18)	C(111)-P(1)-Ru(1)	117.65(14)
C(10)-Ru(1)-C(1)	139.22(19)	O(22)-P(2)-O(23)	97.1(3)
C(2)-Ru(1)-C(1)	37.0(2)	O(22)-P(2)-O(21')	112.8(7)
C(10)-Ru(1)-P(2)	109.48(13)	O(23)-P(2)-O(21')	100.4(4)
C(2)-Ru(1)-P(2)	119.29(15)	O(22)-P(2)-O(21)	88.3(6)
C(1)-Ru(1)-P(2)	88.73(16)	O(23)-P(2)-O(21)	100.9(6)
C(10)-Ru(1)-C(9)	37.06(16)	O(22)-P(2)-Ru(1)	116.07(17)
C(2)-Ru(1)-C(9)	139.9(2)	O(23)-P(2)-Ru(1)	121.98(18)
C(1)-Ru(1)-C(9)	176.28(19)	O(21')-P(2)-Ru(1)	107.5(4)
P(2)-Ru(1)-C(9)	92.82(13)	O(21)-P(2)-Ru(1)	124.7(6)
C(10)-Ru(1)-C(11)	36.72(15)	C(211)-O(21)-P(2)	129.9(11)
C(2)-Ru(1)-C(11)	91.1(2)	C(211)-O(21')-P(2)	131.7(7)
C(1)-Ru(1)-C(11)	112.05(18)	C(212)-O(22)-P(2)	130.0(5)
P(2)-Ru(1)-C(11)	88.38(13)	C(213)-O(23)-P(2)	128.0(4)
C(9)-Ru(1)-C(11)	64.64(16)	C(4)-N(1)-C(5)	122.0(6)
C(10)-Ru(1)-P(1)	118.59(12)	C(12)-N(2)-C(13)	119.9(5)
C(2)-Ru(1)-P(1)	110.74(13)	C(2)-C(1)-Ru(1)	68.7(3)
C(1)-Ru(1)-P(1)	95.00(13)	C(2)-C(1)-H(1A)	120.0
P(2)-Ru(1)-P(1)	94.26(5)	Ru(1)-C(1)-H(1A)	82.3
C(9)-Ru(1)-P(1)	88.27(11)	C(2)-C(1)-H(1B)	120.0
C(11)-Ru(1)-P(1)	152.89(13)	Ru(1)-C(1)-H(1B)	119.7
C(10)-Ru(1)-C(3)	92.03(17)	H(1A)-C(1)-H(1B)	120.0
C(2)-Ru(1)-C(3)	36.26(19)	C(1)-C(2)-C(3)	120.9(5)
C(1)-Ru(1)-C(3)	64.4(2)	C(1)-C(2)-Ru(1)	74.3(3)
P(2)-Ru(1)-C(3)	153.10(13)	C(3)-C(2)-Ru(1)	79.5(3)
C(9)-Ru(1)-C(3)	113.99(18)	C(1)-C(2)-H(2)	119.5
C(11)-Ru(1)-C(3)	100.66(19)	C(3)-C(2)-H(2)	119.5
P(1)-Ru(1)-C(3)	89.06(12)	Ru(1)-C(2)-H(2)	119.5
C(117)-P(1)-C(123)	101.2(2)	C(2)-C(3)-C(4)	119.1(5)
C(117)-P(1)-C(111)	103.0(2)	C(2)-C(3)-Ru(1)	64.3(3)
C(123)-P(1)-C(111)	100.0(2)	C(4)-C(3)-Ru(1)	124.2(3)
C(117)-P(1)-Ru(1)	117.70(14)	C(2)-C(3)-H(3)	113.5
C(123)-P(1)-Ru(1)	114.56(15)	C(4)-C(3)-H(3)	113.5
Ru(1)-C(3)-H(3)	113.5	C(5)-C(6')-H(6'2)	109.5

N(1)-C(4)-C(3)	123.0(5)	H(6'1)-C(6')-H(6'2)	109.5
N(1)-C(4)-H(4)	118.5	C(5)-C(6')-H(6'3)	109.5
C(3)-C(4)-H(4)	118.5	H(6'1)-C(6')-H(6'3)	109.5
C(8)-C(5)-N(1)	117.4(7)	H(6'2)-C(6')-H(6'3)	109.5
N(1)-C(5)-C(7')	109.5(14)	C(5)-C(7')-H(7'1)	109.5
N(1)-C(5)-C(6')	115.3(17)	C(5)-C(7')-H(7'2)	109.5
C(7')-C(5)-C(6')	112.3(13)	H(7'1)-C(7')-H(7'2)	109.5
C(8)-C(5)-C(7)	113.9(8)	C(5)-C(7')-H(7'3)	109.5
N(1)-C(5)-C(7)	103.3(6)	H(7'1)-C(7')-H(7'3)	109.5
C(8)-C(5)-C(6)	111.0(8)	H(7'2)-C(7')-H(7'3)	109.5
N(1)-C(5)-C(6)	105.1(6)	C(5)-C(8')-H(8'1)	109.5
C(7)-C(5)-C(6)	104.9(7)	C(5)-C(8')-H(8'2)	109.5
N(1)-C(5)-C(8')	105.5(16)	H(8'1)-C(8')-H(8'2)	109.5
C(7')-C(5)-C(8')	107.5(13)	C(5)-C(8')-H(8'3)	109.5
C(6')-C(5)-C(8')	106.2(13)	H(8'1)-C(8')-H(8'3)	109.5
C(5)-C(6)-H(6A)	109.5	H(8'2)-C(8')-H(8'3)	109.5
C(5)-C(6)-H(6B)	109.5	C(10)-C(9)-Ru(1)	68.1(2)
H(6A)-C(6)-H(6B)	109.5	C(10)-C(9)-H(9A)	120.0
C(5)-C(6)-H(6C)	109.5	Ru(1)-C(9)-H(9A)	81.6
H(6A)-C(6)-H(6C)	109.5	C(10)-C(9)-H(9B)	120.0
H(6B)-C(6)-H(6C)	109.5	Ru(1)-C(9)-H(9B)	121.4
C(5)-C(7)-H(7A)	109.5	H(9A)-C(9)-H(9B)	120.0
C(5)-C(7)-H(7B)	109.5	C(9)-C(10)-C(11)	119.7(4)
H(7A)-C(7)-H(7B)	109.5	C(9)-C(10)-Ru(1)	74.9(2)
C(5)-C(7)-H(7C)	109.5	C(11)-C(10)-Ru(1)	77.3(2)
H(7A)-C(7)-H(7C)	109.5	C(9)-C(10)-H(10)	120.1
H(7B)-C(7)-H(7C)	109.5	C(11)-C(10)-H(10)	120.1
C(5)-C(8)-H(8A)	109.5	Ru(1)-C(10)-H(10)	120.1
C(5)-C(8)-H(8B)	109.5	C(10)-C(11)-C(12)	120.7(5)
H(8A)-C(8)-H(8B)	109.5	C(10)-C(11)-Ru(1)	65.9(2)
C(5)-C(8)-H(8C)	109.5	C(12)-C(11)-Ru(1)	122.6(3)
H(8A)-C(8)-H(8C)	109.5	C(10)-C(11)-H(11)	113.2
H(8B)-C(8)-H(8C)	109.5	C(12)-C(11)-H(11)	113.2
N(2)-C(12)-C(11)	122.7(5)	H(14D)-C(14')-H(14E)	109.5
N(2)-C(12)-H(12)	118.6	H(14D)-C(14')-H(14F)	109.5
C(11)-C(12)-H(12)	118.6	H(14E)-C(14')-H(14F)	109.5

N(2)-C(13)-C(15)	116.0(6)	C(13)-C(15')-H(15D)	109.5
N(2)-C(13)-C(16)	103.1(6)	C(13)-C(15')-H(15E)	109.5
C(15)-C(13)-C(16)	115.2(8)	H(15D)-C(15')-H(15E)	109.5
N(2)-C(13)-C(16')	112.6(9)	C(13)-C(15')-H(15F)	109.5
N(2)-C(13)-C(14)	102.3(6)	H(15D)-C(15')-H(15F)	109.5
C(15)-C(13)-C(14)	111.9(8)	H(15E)-C(15')-H(15F)	109.5
C(16)-C(13)-C(14)	107.0(7)	C(13)-C(16')-H(16D)	109.5
N(2)-C(13)-C(14')	112.9(8)	C(13)-C(16')-H(16E)	109.5
C(16')-C(13)-C(14')	107.1(9)	H(16D)-C(16')-H(16E)	109.5
N(2)-C(13)-C(15')	111.4(8)	C(13)-C(16')-H(16F)	109.5
C(16')-C(13)-C(15')	106.2(9)	H(16D)-C(16')-H(16F)	109.5
C(14')-C(13)-C(15')	106.1(10)	H(16E)-C(16')-H(16F)	109.5
C(13)-C(14)-H(14A)	109.5	C(116)-C(111)-C(112)	117.8(5)
C(13)-C(14)-H(14B)	109.5	C(116)-C(111)-P(1)	125.3(4)
H(14A)-C(14)-H(14B)	109.5	C(112)-C(111)-P(1)	116.9(4)
C(13)-C(14)-H(14C)	109.5	C(111)-C(112)-C(113)	120.4(5)
H(14A)-C(14)-H(14C)	109.5	C(111)-C(112)-H(112)	119.8
H(14B)-C(14)-H(14C)	109.5	C(113)-C(112)-H(112)	119.8
C(13)-C(15)-H(15A)	109.5	C(114)-C(113)-C(112)	120.5(6)
C(13)-C(15)-H(15B)	109.5	C(114)-C(113)-H(113)	119.8
H(15A)-C(15)-H(15B)	109.5	C(112)-C(113)-H(113)	119.8
C(13)-C(15)-H(15C)	109.5	C(113)-C(114)-C(115)	120.5(6)
H(15A)-C(15)-H(15C)	109.5	C(113)-C(114)-H(114)	119.8
H(15B)-C(15)-H(15C)	109.5	C(115)-C(114)-H(114)	119.8
C(13)-C(16)-H(16A)	109.5	C(114)-C(115)-C(116)	119.3(6)
C(13)-C(16)-H(16B)	109.5	C(114)-C(115)-H(115)	120.3
H(16A)-C(16)-H(16B)	109.5	C(116)-C(115)-H(115)	120.3
C(13)-C(16)-H(16C)	109.5	C(111)-C(116)-C(115)	121.5(6)
H(16A)-C(16)-H(16C)	109.5	C(111)-C(116)-H(116)	119.3
H(16B)-C(16)-H(16C)	109.5	C(115)-C(116)-H(116)	119.3
C(13)-C(14')-H(14D)	109.5	C(122)-C(117)-P(1)	122.2(4)
C(13)-C(14')-H(14F)	109.5	C(118)-C(117)-P(1)	119.1(3)
C(117)-C(118)-C(119)	120.6(5)	C(117)-C(118)-H(118)	119.7
C(119)-C(118)-H(118)	119.7	O(22)-C(212)-H(21D)	109.5
C(120)-C(119)-C(118)	119.8(5)	O(22)-C(212)-H(21E)	109.5
C(120)-C(119)-H(119)	120.1	H(21D)-C(212)-H(21E)	109.5

C(118)-C(119)-H(119)	120.1	O(22)-C(212)-H(21F)	109.5
C(121)-C(120)-C(119)	120.1(5)	H(21D)-C(212)-H(21F)	109.5
C(121)-C(120)-H(120)	119.9	H(21E)-C(212)-H(21F)	109.5
C(119)-C(120)-H(120)	119.9	O(23)-C(213)-H(21G)	109.5
C(120)-C(121)-C(122)	120.9(5)	O(23)-C(213)-H(21H)	109.5
C(120)-C(121)-H(121)	119.6	H(21G)-C(213)-H(21H)	109.5
C(122)-C(121)-H(121)	119.6	O(23)-C(213)-H(21I)	109.5
C(117)-C(122)-C(121)	120.1(5)	H(21G)-C(213)-H(21I)	109.5
C(117)-C(122)-H(122)	120.0	H(21H)-C(213)-H(21I)	109.5
C(121)-C(122)-H(122)	120.0		
C(128)-C(123)-C(124)	118.7(4)		
C(128)-C(123)-P(1)	120.9(3)		
C(124)-C(123)-P(1)	120.3(4)		
C(125)-C(124)-C(123)	119.9(6)		
C(125)-C(124)-H(124)	120.1		
C(123)-C(124)-H(124)	120.1		
C(126)-C(125)-C(124)	120.7(6)		
C(126)-C(125)-H(125)	119.6		
C(124)-C(125)-H(125)	119.6		
C(125)-C(126)-C(127)	119.8(5)		
C(125)-C(126)-H(126)	120.1		
C(127)-C(126)-H(126)	120.1		
C(126)-C(127)-C(128)	120.6(6)		
C(126)-C(127)-H(127)	119.7		
C(128)-C(127)-H(127)	119.7		
C(123)-C(128)-C(127)	120.3(5)		
C(123)-C(128)-H(128)	119.9		
C(127)-C(128)-H(128)	119.9		
O(21)-C(211)-H(21A)	109.5		
H(21A)-C(211)-H(21C)	109.5		
H(21B)-C(211)-H(21C)	109.5		

Table D-2.5: Anisotropic displacement parameters ($\text{\AA}^2 \times 10^3$) for Compound 4. The anisotropic displacement factor exponent takes the form: $-2\pi^2 [h^2 a^{*2} U^{11} + \dots + 2 h k a^{*} b^{*} U^{12}]$

	U ¹¹	U ²²	U ³³	U ²³	U ¹³	U ¹²
Ru(1)	36(1)	30(1)	28(1)	-1(1)	5(1)	3(1)
P(1)	36(1)	30(1)	32(1)	-2(1)	2(1)	3(1)
P(2)	50(1)	39(1)	44(1)	-2(1)	-4(1)	-4(1)
O(21)	47(2)	60(3)	107(9)	-28(5)	-29(4)	-2(2)
O(21')	47(2)	60(3)	107(9)	-28(5)	-29(4)	-2(2)
O(22)	107(4)	153(5)	45(2)	-27(3)	-1(2)	-53(3)
O(23)	151(5)	50(2)	81(3)	12(2)	-45(3)	-43(3)
N(1)	68(3)	82(3)	51(3)	-14(2)	-15(2)	13(3)
N(2)	65(3)	41(2)	55(3)	12(2)	1(2)	6(2)
C(1)	60(3)	45(3)	47(3)	5(2)	22(3)	-2(2)
C(2)	62(3)	48(3)	31(2)	5(2)	14(2)	8(2)
C(3)	60(3)	47(3)	30(2)	-5(2)	5(2)	6(2)
C(4)	71(4)	66(3)	36(3)	-9(2)	-2(3)	18(3)
C(5)	79(5)	126(7)	68(4)	-9(4)	-26(4)	33(4)
C(6)	98(4)	154(6)	98(5)	-2(5)	-48(4)	15(4)
C(7)	98(4)	154(6)	98(5)	-2(5)	-48(4)	15(4)
C(8)	98(4)	154(6)	98(5)	-2(5)	-48(4)	15(4)
C(6')	98(4)	154(6)	98(5)	-2(5)	-48(4)	15(4)
C(7')	98(4)	154(6)	98(5)	-2(5)	-48(4)	15(4)
C(8')	98(4)	154(6)	98(5)	-2(5)	-48(4)	15(4)
C(9)	38(2)	46(3)	39(2)	3(2)	12(2)	4(2)
C(10)	41(2)	43(2)	39(3)	-1(2)	6(2)	12(2)
C(11)	55(2)	35(2)	40(2)	2(3)	8(3)	12(2)
C(12)	55(3)	44(3)	40(3)	0(2)	5(2)	15(2)
C(13)	82(4)	62(4)	61(4)	23(3)	3(3)	8(3)
C(14)	135(7)	90(4)	76(5)	38(4)	2(4)	-9(4)
C(15)	135(7)	90(4)	76(5)	38(4)	2(4)	-9(4)
C(16)	135(7)	90(4)	76(5)	38(4)	2(4)	-9(4)
C(14')	135(7)	90(4)	76(5)	38(4)	2(4)	-9(4)

	U^{11}	U^{22}	U^{33}	U^{23}	U^{13}	U^{12}
C(15')	135(7)	90(4)	76(5)	38(4)	2(4)	-9(4)
C(16')	135(7)	90(4)	76(5)	38(4)	2(4)	-9(4)
C(111)	50(2)	32(2)	35(2)	0(2)	-2(2)	3(2)
C(112)	83(4)	72(4)	36(3)	9(3)	11(3)	32(3)
C(113)	128(6)	76(4)	30(3)	1(2)	8(3)	27(4)
C(114)	93(4)	76(3)	37(3)	6(3)	-13(4)	-18(3)
C(115)	64(4)	141(7)	59(4)	14(4)	-16(3)	16(4)
C(116)	63(4)	115(5)	41(3)	5(3)	-4(3)	26(3)
C(117)	48(2)	36(2)	31(3)	-1(2)	3(2)	10(2)
C(118)	46(2)	49(3)	46(3)	-6(2)	2(2)	8(2)
C(119)	48(3)	70(3)	58(3)	-6(3)	10(2)	18(2)
C(120)	75(4)	65(4)	57(3)	-15(3)	13(3)	31(3)
C(121)	82(4)	55(3)	55(3)	-23(3)	5(3)	17(3)
C(122)	58(3)	45(3)	47(3)	-12(2)	2(2)	5(2)
C(123)	42(2)	36(2)	39(2)	-3(2)	5(2)	-3(2)
C(124)	63(3)	48(3)	74(4)	18(3)	-3(3)	-10(2)
C(125)	89(5)	54(3)	92(5)	19(3)	3(4)	-27(3)
C(126)	69(4)	68(4)	84(4)	-8(3)	20(4)	-28(3)
C(127)	51(3)	75(3)	70(3)	-4(4)	-5(4)	-17(2)
C(128)	49(2)	48(2)	51(2)	-3(3)	5(3)	-6(2)
C(211)	103(5)	141(5)	99(4)	-14(4)	-18(4)	-21(4)
C(212)	103(5)	141(5)	99(4)	-14(4)	-18(4)	-21(4)
C(213)	81(4)	55(3)	68(4)	1(4)	-3(4)	-26(3)

Table D-2.6. Hydrogen coordinates ($\times 10^4$) and isotropic displacement parameters ($\text{\AA}^2 \times 10^3$) for Compound 4.

	x	y	z	U(eq)
H(1A)	12933	7868	6107	61
H(1B)	12708	7118	6521	61
H(2)	13809	6954	7573	56
H(3)	14011	8331	7292	55
H(4)	15031	7342	7958	69
H(6A)	16554	8440	7219	175
H(6B)	16986	8486	8561	175
H(6C)	16387	9014	8239	175
H(7A)	15694	8897	10025	175
H(7B)	16269	8427	10680	175
H(7C)	15461	8205	10616	175
H(8A)	15943	7191	9566	175
H(8B)	16720	7423	9168	175
H(8C)	16169	7213	8059	175
H(6'1)	16430	8910	7902	175
H(6'2)	16996	8439	8579	175
H(6'3)	16531	8924	9455	175
H(7'1)	15399	8231	10523	175
H(7'2)	16213	8074	10788	175
H(7'3)	15691	7502	10339	175
H(8'1)	16122	7103	8701	175
H(8'2)	16803	7506	8254	175
H(8'3)	16138	7450	7298	175
H(9A)	14470	7282	3033	49
H(9B)	15111	7788	3423	49
H(10)	15357	7177	5365	49
H(11)	14456	6206	4260	52
H(12)	14957	6285	6910	56
H(14A)	13717	5673	8695	151

	x	y	z	U(eq)
H(14B)	13761	4913	9062	151
H(14C)	13423	5135	7698	151
H(15A)	15505	5549	8037	151
H(15B)	15197	5145	9249	151
H(15C)	14920	5871	8962	151
H(16A)	14267	4372	6616	151
H(16B)	14564	4197	8038	151
H(16C)	15092	4432	6913	151
H(14D)	14366	5924	9076	151
H(14E)	14140	5217	9606	151
H(14F)	13641	5601	8603	151
H(15D)	15555	4898	7456	151
H(15E)	15351	5006	8959	151
H(15F)	15489	5624	8032	151
H(16D)	13762	4457	7695	151
H(16E)	14478	4239	8397	151
H(16F)	14439	4276	6836	151
H(112)	14233	8209	1800	76
H(113)	13848	8260	-394	94
H(114)	12798	8745	-909	83
H(115)	12091	9183	724	105
H(116)	12457	9122	2919	88
H(118)	12215	8507	4877	57
H(119)	11433	9103	6215	70
H(120)	11839	10010	7376	79
H(121)	13021	10298	7293	77
H(122)	13809	9721	5958	60
H(124)	14115	9734	2906	74
H(125)	15103	10423	2907	94
H(126)	16056	10201	4239	88
H(127)	16053	9273	5555	78
H(128)	15085	8559	5546	59
H(21A)	11704	6793	3543	172

	x	y	z	U(eq)
H(21B)	11493	7325	2462	172
H(21C)	11613	7546	3948	172
H(21D)	12827	6277	1336	172
H(21E)	13504	6454	472	172
H(21F)	12862	6960	571	172
H(21G)	13244	6001	5469	102
H(21H)	12838	5435	4691	102
H(21I)	12402	6014	5368	102

Table D-2.7. Torsion angles [°] for Compound 4.

O(22)-P(2)-O(21)-C(211)	131.9(16)
O(23)-P(2)-O(21)-C(211)	35.0(17)
O(21')-P(2)-O(21)-C(211)	-56.3(15)
Ru(1)-P(2)-O(21)-C(211)	-107.2(15)
O(22)-P(2)-O(21')-C(211)	68.6(17)
O(23)-P(2)-O(21')-C(211)	-33.7(18)
O(21)-P(2)-O(21')-C(211)	59.8(14)
Ru(1)-P(2)-O(21')-C(211)	-162.2(15)
O(23)-P(2)-O(22)-C(212)	45.3(9)
O(21')-P(2)-O(22)-C(212)	-59.1(9)
O(21)-P(2)-O(22)-C(212)	-55.4(10)
Ru(1)-P(2)-O(22)-C(212)	176.3(7)
O(22)-P(2)-O(23)-C(213)	150.3(6)
O(21')-P(2)-O(23)-C(213)	-94.9(8)
O(21)-P(2)-O(23)-C(213)	-120.1(9)
Ru(1)-P(2)-O(23)-C(213)	23.4(7)
Ru(1)-C(1)-C(2)-C(3)	67.1(4)
C(1)-C(2)-C(3)-C(4)	179.1(5)
Ru(1)-C(2)-C(3)-C(4)	-116.5(4)
C(1)-C(2)-C(3)-Ru(1)	-64.4(4)
C(5)-N(1)-C(4)-C(3)	176.6(5)
C(2)-C(3)-C(4)-N(1)	-162.7(5)
Ru(1)-C(3)-C(4)-N(1)	120.1(5)
C(4)-N(1)-C(5)-C(8)	12.9(11)
C(4)-N(1)-C(5)-C(7')	-75(2)
C(4)-N(1)-C(5)-C(6')	156.9(19)
C(4)-N(1)-C(5)-C(7)	-113.5(8)
C(4)-N(1)-C(5)-C(6)	136.8(8)
C(4)-N(1)-C(5)-C(8')	40(2)
Ru(1)-C(9)-C(10)-C(11)	65.5(3)
C(9)-C(10)-C(11)-C(12)	-179.1(4)
Ru(1)-C(10)-C(11)-C(12)	-115.0(4)
C(9)-C(10)-C(11)-Ru(1)	-64.2(3)
C(13)-N(2)-C(12)-C(11)	-177.4(4)

C(10)-C(11)-C(12)-N(2)	-167.5(4)
Ru(1)-C(11)-C(12)-N(2)	113.1(5)
C(12)-N(2)-C(13)-C(15)	-13.6(10)
C(12)-N(2)-C(13)-C(16)	-140.5(8)
C(12)-N(2)-C(13)-C(16')	-168.9(10)
C(12)-N(2)-C(13)-C(14)	108.5(8)
C(12)-N(2)-C(13)-C(14')	69.6(11)
C(12)-N(2)-C(13)-C(15')	-49.7(11)
C(117)-P(1)-C(111)-C(116)	-10.8(5)
C(123)-P(1)-C(111)-C(116)	-114.9(5)
Ru(1)-P(1)-C(111)-C(116)	120.5(5)
C(117)-P(1)-C(111)-C(112)	170.1(4)
C(123)-P(1)-C(111)-C(112)	66.1(4)
Ru(1)-P(1)-C(111)-C(112)	-58.6(5)
C(116)-C(111)-C(112)-C(113)	-2.0(9)
P(1)-C(111)-C(112)-C(113)	177.2(5)
C(111)-C(112)-C(113)-C(114)	1.4(11)
C(112)-C(113)-C(114)-C(115)	-0.2(11)
C(113)-C(114)-C(115)-C(116)	-0.3(11)
C(112)-C(111)-C(116)-C(115)	1.5(10)
P(1)-C(111)-C(116)-C(115)	-177.6(6)
C(114)-C(115)-C(116)-C(111)	-0.3(12)
C(123)-P(1)-C(117)-C(122)	-15.2(4)
C(111)-P(1)-C(117)-C(122)	-118.3(4)
Ru(1)-P(1)-C(117)-C(122)	110.4(4)
C(123)-P(1)-C(117)-C(118)	169.4(4)
C(111)-P(1)-C(117)-C(118)	66.3(4)
Ru(1)-P(1)-C(117)-C(118)	-65.0(4)
C(122)-C(117)-C(118)-C(119)	0.5(7)
P(1)-C(117)-C(118)-C(119)	176.1(4)
C(117)-C(118)-C(119)-C(120)	0.3(8)
C(118)-C(119)-C(120)-C(121)	-1.4(9)
C(119)-C(120)-C(121)-C(122)	1.7(10)
C(118)-C(117)-C(122)-C(121)	-0.2(7)
P(1)-C(117)-C(122)-C(121)	-175.6(4)
C(120)-C(121)-C(122)-C(117)	-0.9(9)

C(117)-P(1)-C(123)-C(128)	103.6(4)
C(111)-P(1)-C(123)-C(128)	-150.8(4)
Ru(1)-P(1)-C(123)-C(128)	-24.1(5)
C(117)-P(1)-C(123)-C(124)	-73.1(4)
C(111)-P(1)-C(123)-C(124)	32.4(4)
Ru(1)-P(1)-C(123)-C(124)	159.2(4)
C(128)-C(123)-C(124)-C(125)	0.2(9)
P(1)-C(123)-C(124)-C(125)	177.0(5)
C(123)-C(124)-C(125)-C(126)	-0.9(10)
C(124)-C(125)-C(126)-C(127)	0.8(11)
C(125)-C(126)-C(127)-C(128)	0.0(10)
C(124)-C(123)-C(128)-C(127)	0.6(8)
P(1)-C(123)-C(128)-C(127)	-176.3(4)
C(126)-C(127)-C(128)-C(123)	-0.6(9)
P(2)-O(21')-C(211)-O(21)	-60.3(14)
P(2)-O(21)-C(211)-O(21')	57.5(15)

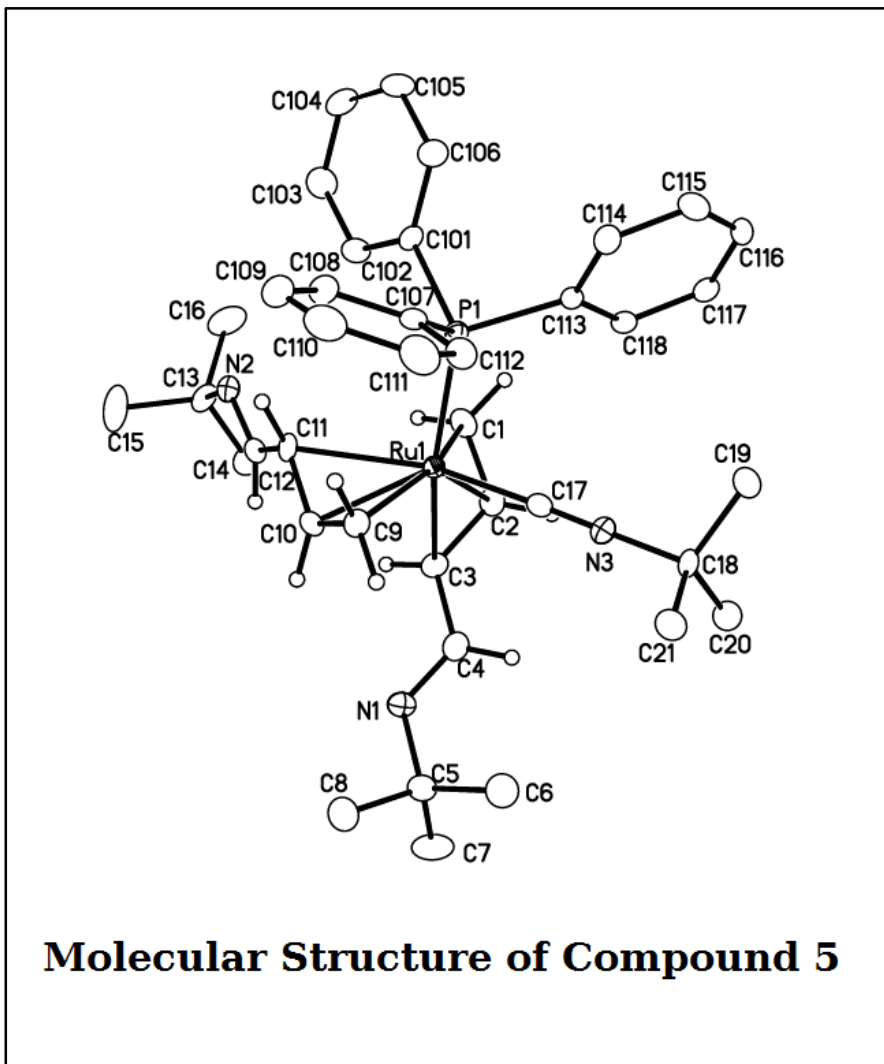
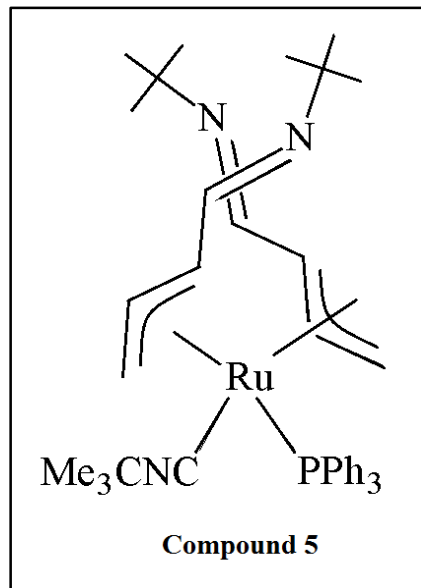


Table D-3.1: Crystal data and structure refinement for Compound 5.

Empirical formula	$C_{39} H_{52} N_3 P Ru$		
Formula weight	694.87		
Temperature	100(2) K		
Wavelength	0.71073 Å		
Crystal system	Monoclinic		
Space group	$P 2_1/c$		
Unit cell dimensions	$a = 19.5838(11)$ Å	$\alpha = 90^\circ$.	
	$b = 9.4921(6)$ Å	$\beta = 90.432(3)^\circ$.	
	$c = 19.3271(12)$ Å	$\gamma = 90^\circ$.	
Volume	$3592.6(4)$ Å ³		
Z	4		
Density (calculated)	1.285 Mg/m ³		
Absorption coefficient	0.511 mm ⁻¹		
F(000)	1464		
Crystal size	$0.183 \times 0.124 \times 0.098$ mm ³		
Theta range for data collection	2.080 to 27.119°.		
Index ranges	$-25 \leq h \leq 24, -7 \leq k \leq 12, -24 \leq l \leq 24$		
Reflections collected	43440		
Independent reflections	7921 [R(int) = 0.0727]		
Completeness to theta = 25.242°	100.0 %		
Absorption correction	Semi-empirical from equivalents		
Max. and min. transmission	0.8620 and 0.7868		
Refinement method	Full-matrix least-squares on F ²		
Data / restraints / parameters	7921 / 37 / 415		
Goodness-of-fit on F ²	1.023		
Final R indices [I>2sigma(I)]	$R_1 = 0.0369, wR_2 = 0.0686$		
R indices (all data)	$R_1 = 0.0598, wR_2 = 0.0777$		
Extinction coefficient	n/a		
Largest diff. peak and hole	0.579 and -0.489 e.Å ⁻³		

Table D-3.2: Atomic coordinates ($\times 10^4$) and equivalent isotropic displacement parameters ($\text{\AA}^2 \times 10^3$) for Compound 5. U(eq) is defined as one third of the trace of the orthogonalized U^{ij} tensor.

	x	y	z	U(eq)
Ru(1)	2510(1)	613(1)	5147(1)	12(1)
P(1)	2025(1)	905(1)	6237(1)	13(1)
N(1)	3745(1)	179(2)	3560(1)	18(1)
N(2)	1340(1)	-2939(2)	4677(1)	17(1)
N(3)	3345(1)	3307(2)	5448(1)	19(1)
C(1)	1555(1)	1164(3)	4555(1)	18(1)
C(2)	2141(1)	1683(3)	4234(1)	17(1)
C(3)	2639(1)	704(3)	3999(1)	16(1)
C(4)	3335(1)	1079(3)	3820(1)	17(1)
C(5)	4474(1)	538(3)	3450(2)	21(1)
C(6)	4735(1)	1821(3)	3852(2)	30(1)
C(7)	4562(1)	769(4)	2677(2)	33(1)
C(8)	4876(1)	-756(3)	3681(2)	28(1)
C(9)	3398(1)	-640(3)	5539(1)	17(1)
C(10)	3024(1)	-1382(3)	5034(1)	16(1)
C(11)	2344(1)	-1823(3)	5150(1)	15(1)
C(12)	1934(1)	-2419(3)	4592(1)	17(1)
C(13)	938(1)	-3443(3)	4073(1)	19(1)
C(14)	1085(1)	-2671(3)	3403(2)	24(1)
C(15)	1029(5)	-5024(4)	4012(4)	35(2)
C(16)	188(2)	-3101(11)	4246(4)	31(1)
C(15')	1283(16)	-4860(20)	3933(18)	35(2)
C(16')	210(7)	-3640(40)	4297(16)	31(1)
C(17)	3014(1)	2321(3)	5323(1)	16(1)
C(18)	3723(1)	4612(3)	5550(2)	17(1)
C(19)	3373(1)	5446(3)	6120(2)	23(1)
C(20)	3713(1)	5394(3)	4860(2)	26(1)
C(21)	4453(1)	4211(3)	5759(2)	24(1)
C(101)	1173(1)	144(3)	6402(1)	15(1)

	x	y	z	U(eq)
C(102)	878(1)	-767(3)	5925(2)	19(1)
C(103)	244(1)	-1380(3)	6059(2)	25(1)
C(104)	-102(1)	-1061(3)	6655(2)	23(1)
C(105)	182(1)	-129(3)	7126(2)	22(1)
C(106)	818(1)	463(3)	7003(1)	20(1)
C(107)	2533(1)	170(3)	6953(1)	14(1)
C(108)	2436(1)	-1227(3)	7149(2)	20(1)
C(109)	2882(1)	-1890(3)	7610(2)	25(1)
C(110)	3424(1)	-1151(3)	7884(2)	27(1)
C(111)	3533(1)	235(3)	7691(2)	27(1)
C(112)	3098(1)	885(3)	7219(1)	20(1)
C(113)	1869(1)	2743(3)	6498(1)	13(1)
C(114)	1883(1)	3198(3)	7183(1)	18(1)
C(115)	1675(1)	4549(3)	7354(2)	20(1)
C(116)	1442(1)	5463(3)	6848(1)	18(1)
C(117)	1441(1)	5041(3)	6163(2)	17(1)
C(118)	1658(1)	3694(3)	5992(1)	14(1)

Table D-3.3: Bond lengths [Å] for Compound 5.

Ru(1)-C(17)	1.927(3)	C(7)-H(7C)	0.9800
Ru(1)-C(10)	2.156(2)	C(8)-H(8A)	0.9800
Ru(1)-C(2)	2.156(3)	C(8)-H(8B)	0.9800
Ru(1)-C(9)	2.233(2)	C(8)-H(8C)	0.9800
Ru(1)-C(3)	2.236(3)	C(9)-C(10)	1.404(4)
Ru(1)-C(1)	2.248(2)	C(9)-H(9A)	0.9900
Ru(1)-P(1)	2.3343(7)	C(9)-H(9B)	0.9900
Ru(1)-C(11)	2.335(2)	C(10)-C(11)	1.416(3)
P(1)-C(107)	1.837(3)	C(10)-H(10)	1.0000
P(1)-C(113)	1.842(3)	C(11)-C(12)	1.454(3)
P(1)-C(101)	1.848(2)	C(11)-H(11)	1.0000
N(1)-C(4)	1.279(3)	C(12)-H(12)	0.9500
N(1)-C(5)	1.484(3)	C(13)-C(16')	1.505(9)
N(2)-C(12)	1.276(3)	C(13)-C(15)	1.516(4)
N(2)-C(13)	1.484(3)	C(13)-C(14)	1.517(4)
N(3)-C(17)	1.163(3)	C(13)-C(15')	1.530(10)
N(3)-C(18)	1.455(3)	C(13)-C(16)	1.543(5)
C(1)-C(2)	1.399(4)	C(14)-H(14A)	0.9800
C(1)-H(1A)	0.9900	C(14)-H(14B)	0.9800
C(1)-H(1B)	0.9900	C(14)-H(14C)	0.9800
C(2)-C(3)	1.425(3)	C(15)-H(15A)	0.9800
C(2)-H(2)	1.0000	C(15)-H(15B)	0.9800
C(3)-C(4)	1.452(3)	C(15)-H(15C)	0.9800
C(3)-H(3)	1.0000	C(16)-H(16A)	0.9800
C(4)-H(4)	0.9500	C(16)-H(16B)	0.9800
C(5)-C(7)	1.521(4)	C(16)-H(16C)	0.9800
C(5)-C(8)	1.523(4)	C(15')-H(15D)	0.9800
C(5)-C(6)	1.530(4)	C(15')-H(15E)	0.9800
C(6)-H(6A)	0.9800	C(15')-H(15F)	0.9800
C(6)-H(6B)	0.9800	C(16')-H(16D)	0.9800
C(6)-H(6C)	0.9800	C(16')-H(16E)	0.9800
C(7)-H(7A)	0.9800	C(16')-H(16F)	0.9800
C(7)-H(7B)	0.9800	C(18)-C(19)	1.524(4)
C(18)-C(20)	1.527(4)	C(113)-C(118)	1.391(3)

C(18)-C(21)	1.530(3)	C(113)-C(114)	1.393(4)
C(19)-H(19A)	0.9800	C(114)-C(115)	1.386(4)
C(19)-H(19B)	0.9800	C(114)-H(114)	0.9500
C(19)-H(19C)	0.9800	C(115)-C(116)	1.384(4)
C(20)-H(20A)	0.9800	C(115)-H(115)	0.9500
C(20)-H(20B)	0.9800	C(116)-C(117)	1.382(4)
C(20)-H(20C)	0.9800	C(116)-H(116)	0.9500
C(21)-H(21A)	0.9800	C(117)-C(118)	1.388(3)
C(21)-H(21B)	0.9800	C(117)-H(117)	0.9500
C(21)-H(21C)	0.9800	C(118)-H(118)	0.9500
C(101)-C(102)	1.387(4)		
C(101)-C(106)	1.393(4)		
C(102)-C(103)	1.397(3)		
C(102)-H(102)	0.9500		
C(103)-C(104)	1.375(4)		
C(103)-H(103)	0.9500		
C(104)-C(105)	1.383(4)		
C(104)-H(104)	0.9500		
C(105)-C(106)	1.388(3)		
C(105)-H(105)	0.9500		
C(106)-H(106)	0.9500		
C(107)-C(108)	1.393(4)		
C(107)-C(112)	1.394(3)		
C(108)-C(109)	1.394(4)		
C(108)-H(108)	0.9500		
C(109)-C(110)	1.374(4)		
C(109)-H(109)	0.9500		
C(110)-C(111)	1.384(4)		
C(110)-H(110)	0.9500		
C(111)-C(112)	1.388(4)		
C(111)-H(111)	0.9500		
C(112)-H(112)	0.9500		
C(18)-C(20)	1.527(4)		
C(18)-C(21)	1.530(3)		

Table D-3.4: Bond angles [°] for Compound 5.

C(17)-Ru(1)-C(10)	121.23(10)	C(101)-P(1)-Ru(1)	118.96(9)
C(17)-Ru(1)-C(2)	85.23(11)	C(4)-N(1)-C(5)	120.7(2)
C(10)-Ru(1)-C(2)	119.02(10)	C(17)-N(3)-C(18)	174.4(3)
C(17)-Ru(1)-C(9)	89.57(10)	C(2)-C(1)-Ru(1)	67.95(14)
C(10)-Ru(1)-C(9)	37.25(9)	C(2)-C(1)-H(1A)	116.9
C(2)-Ru(1)-C(9)	141.63(10)	Ru(1)-C(1)-H(1A)	116.9
C(17)-Ru(1)-C(3)	94.70(10)	C(2)-C(1)-H(1B)	116.9
C(10)-Ru(1)-C(3)	82.97(10)	Ru(1)-C(1)-H(1B)	116.9
C(2)-Ru(1)-C(3)	37.79(9)	H(1A)-C(1)-H(1B)	113.9
C(9)-Ru(1)-C(3)	105.29(9)	C(1)-C(2)-C(3)	118.6(2)
C(17)-Ru(1)-C(1)	108.49(10)	C(1)-C(2)-Ru(1)	75.09(15)
C(10)-Ru(1)-C(1)	122.72(10)	C(3)-C(2)-Ru(1)	74.17(15)
C(2)-Ru(1)-C(1)	36.96(9)	C(1)-C(2)-H(2)	120.7
C(9)-Ru(1)-C(1)	159.93(9)	C(3)-C(2)-H(2)	120.7
C(3)-Ru(1)-C(1)	65.55(9)	Ru(1)-C(2)-H(2)	120.7
C(17)-Ru(1)-P(1)	87.21(8)	C(2)-C(3)-C(4)	124.2(2)
C(10)-Ru(1)-P(1)	112.90(8)	C(2)-C(3)-Ru(1)	68.04(15)
C(2)-Ru(1)-P(1)	123.08(7)	C(4)-C(3)-Ru(1)	111.00(17)
C(9)-Ru(1)-P(1)	94.50(7)	C(2)-C(3)-H(3)	114.8
C(3)-Ru(1)-P(1)	160.11(6)	C(4)-C(3)-H(3)	114.8
C(1)-Ru(1)-P(1)	95.05(7)	Ru(1)-C(3)-H(3)	114.8
C(17)-Ru(1)-C(11)	154.71(9)	N(1)-C(4)-C(3)	121.5(2)
C(10)-Ru(1)-C(11)	36.50(9)	N(1)-C(4)-H(4)	119.2
C(2)-Ru(1)-C(11)	115.01(10)	C(3)-C(4)-H(4)	119.2
C(9)-Ru(1)-C(11)	65.17(9)	N(1)-C(5)-C(7)	106.8(2)
C(3)-Ru(1)-C(11)	93.33(10)	N(1)-C(5)-C(8)	105.6(2)
C(1)-Ru(1)-C(11)	96.67(9)	C(7)-C(5)-C(8)	110.0(2)
P(1)-Ru(1)-C(11)	93.27(7)	N(1)-C(5)-C(6)	115.3(2)
C(107)-P(1)-C(113)	104.07(12)	C(7)-C(5)-C(6)	110.1(3)
C(107)-P(1)-C(101)	101.87(11)	C(8)-C(5)-C(6)	108.9(2)
C(113)-P(1)-C(101)	99.88(11)	C(5)-C(6)-H(6A)	109.5
C(107)-P(1)-Ru(1)	114.36(8)	C(5)-C(6)-H(6B)	109.5
C(113)-P(1)-Ru(1)	115.42(9)	H(6A)-C(6)-H(6B)	109.5
C(5)-C(6)-H(6C)	109.5	C(11)-C(12)-H(12)	118.2

H(6A)-C(6)-H(6C)	109.5	N(2)-C(13)-C(16')	108.1(13)
H(6B)-C(6)-H(6C)	109.5	N(2)-C(13)-C(15)	108.5(3)
C(5)-C(7)-H(7A)	109.5	N(2)-C(13)-C(14)	114.4(2)
C(5)-C(7)-H(7B)	109.5	C(16')-C(13)-C(14)	119.5(13)
H(7A)-C(7)-H(7B)	109.5	C(15)-C(13)-C(14)	113.0(4)
C(5)-C(7)-H(7C)	109.5	N(2)-C(13)-C(15')	100.9(12)
H(7A)-C(7)-H(7C)	109.5	C(16')-C(13)-C(15')	111.2(12)
H(7B)-C(7)-H(7C)	109.5	C(14)-C(13)-C(15')	100.8(14)
C(5)-C(8)-H(8A)	109.5	N(2)-C(13)-C(16)	105.1(3)
C(5)-C(8)-H(8B)	109.5	C(15)-C(13)-C(16)	109.7(3)
H(8A)-C(8)-H(8B)	109.5	C(14)-C(13)-C(16)	105.7(4)
C(5)-C(8)-H(8C)	109.5	C(13)-C(14)-H(14A)	109.5
H(8A)-C(8)-H(8C)	109.5	C(13)-C(14)-H(14B)	109.5
H(8B)-C(8)-H(8C)	109.5	H(14A)-C(14)-H(14B)	109.5
C(10)-C(9)-Ru(1)	68.38(14)	C(13)-C(14)-H(14C)	109.5
C(10)-C(9)-H(9A)	116.8	H(14A)-C(14)-H(14C)	109.5
Ru(1)-C(9)-H(9A)	116.8	H(14B)-C(14)-H(14C)	109.5
C(10)-C(9)-H(9B)	116.8	C(13)-C(15)-H(15A)	109.5
Ru(1)-C(9)-H(9B)	116.8	C(13)-C(15)-H(15B)	109.5
H(9A)-C(9)-H(9B)	113.8	H(15A)-C(15)-H(15B)	109.5
C(9)-C(10)-C(11)	121.6(2)	C(13)-C(15)-H(15C)	109.5
C(9)-C(10)-Ru(1)	74.37(15)	H(15A)-C(15)-H(15C)	109.5
C(11)-C(10)-Ru(1)	78.64(14)	H(15B)-C(15)-H(15C)	109.5
C(9)-C(10)-H(10)	119.2	C(13)-C(16)-H(16A)	109.5
C(11)-C(10)-H(10)	119.2	C(13)-C(16)-H(16B)	109.5
Ru(1)-C(10)-H(10)	119.2	H(16A)-C(16)-H(16B)	109.5
C(10)-C(11)-C(12)	120.8(2)	C(13)-C(16)-H(16C)	109.5
C(10)-C(11)-Ru(1)	64.86(14)	H(16A)-C(16)-H(16C)	109.5
C(12)-C(11)-Ru(1)	117.36(17)	H(16B)-C(16)-H(16C)	109.5
C(10)-C(11)-H(11)	114.9	C(13)-C(15')-H(15D)	109.5
C(12)-C(11)-H(11)	114.9	C(13)-C(15')-H(15E)	109.5
Ru(1)-C(11)-H(11)	114.9	H(15D)-C(15')-H(15E)	109.5
N(2)-C(12)-C(11)	123.6(3)	C(13)-C(15')-H(15F)	109.5
N(2)-C(12)-H(12)	118.2	H(15D)-C(15')-H(15F)	109.5
H(15E)-C(15')-H(15F)	109.5	C(101)-C(102)-C(103)	120.2(3)
C(13)-C(16')-H(16D)	109.5	C(101)-C(102)-H(102)	119.9

C(13)-C(16')-H(16E)	109.5	C(103)-C(102)-H(102)	119.9
H(16D)-C(16')-H(16E)	109.5	C(104)-C(103)-C(102)	120.5(3)
C(13)-C(16')-H(16F)	109.5	C(104)-C(103)-H(103)	119.8
H(16D)-C(16')-H(16F)	109.5	C(102)-C(103)-H(103)	119.8
H(16E)-C(16')-H(16F)	109.5	C(103)-C(104)-C(105)	119.7(2)
N(3)-C(17)-Ru(1)	176.2(2)	C(103)-C(104)-H(104)	120.1
N(3)-C(18)-C(19)	108.0(2)	C(105)-C(104)-H(104)	120.1
N(3)-C(18)-C(20)	107.0(2)	C(104)-C(105)-C(106)	120.2(3)
C(19)-C(18)-C(20)	112.1(2)	C(104)-C(105)-H(105)	119.9
N(3)-C(18)-C(21)	107.3(2)	C(106)-C(105)-H(105)	119.9
C(19)-C(18)-C(21)	111.3(2)	C(105)-C(106)-C(101)	120.6(3)
C(20)-C(18)-C(21)	110.9(2)	C(105)-C(106)-H(106)	119.7
C(18)-C(19)-H(19A)	109.5	C(101)-C(106)-H(106)	119.7
C(18)-C(19)-H(19B)	109.5	C(108)-C(107)-C(112)	118.3(2)
H(19A)-C(19)-H(19B)	109.5	C(108)-C(107)-P(1)	119.5(2)
C(18)-C(19)-H(19C)	109.5	C(112)-C(107)-P(1)	121.2(2)
H(19A)-C(19)-H(19C)	109.5	C(107)-C(108)-C(109)	121.1(3)
H(19B)-C(19)-H(19C)	109.5	C(107)-C(108)-H(108)	119.4
C(18)-C(20)-H(20A)	109.5	C(109)-C(108)-H(108)	119.4
C(18)-C(20)-H(20B)	109.5	C(110)-C(109)-C(108)	119.7(3)
H(20A)-C(20)-H(20B)	109.5	C(110)-C(109)-H(109)	120.2
C(18)-C(20)-H(20C)	109.5	C(108)-C(109)-H(109)	120.2
H(20A)-C(20)-H(20C)	109.5	C(109)-C(110)-C(111)	120.1(3)
H(20B)-C(20)-H(20C)	109.5	C(109)-C(110)-H(110)	120.0
C(18)-C(21)-H(21A)	109.5	C(111)-C(110)-H(110)	120.0
C(18)-C(21)-H(21B)	109.5	C(110)-C(111)-C(112)	120.3(3)
H(21A)-C(21)-H(21B)	109.5	C(110)-C(111)-H(111)	119.8
C(18)-C(21)-H(21C)	109.5	C(112)-C(111)-H(111)	119.8
H(21A)-C(21)-H(21C)	109.5	C(111)-C(112)-C(107)	120.5(3)
H(21B)-C(21)-H(21C)	109.5	C(111)-C(112)-H(112)	119.8
C(102)-C(101)-C(106)	118.8(2)	C(107)-C(112)-H(112)	119.8
C(102)-C(101)-P(1)	120.1(2)	C(118)-C(113)-C(114)	118.0(2)
C(106)-C(101)-P(1)	121.2(2)	C(118)-C(113)-P(1)	118.1(2)
C(114)-C(113)-P(1)	123.5(2)		
C(115)-C(114)-C(113)	120.7(3)		
C(115)-C(114)-H(114)	119.7		

C(113)-C(114)-H(114)	119.7
C(116)-C(115)-C(114)	120.5(3)
C(116)-C(115)-H(115)	119.8
C(114)-C(115)-H(115)	119.8
C(117)-C(116)-C(115)	119.6(2)
C(117)-C(116)-H(116)	120.2
C(115)-C(116)-H(116)	120.2
C(116)-C(117)-C(118)	119.7(3)
C(116)-C(117)-H(117)	120.1
C(118)-C(117)-H(117)	120.1
C(117)-C(118)-C(113)	121.4(3)
C(117)-C(118)-H(118)	119.3
C(113)-C(118)-H(118)	119.3

Table D-3.5: Anisotropic displacement parameters ($\text{\AA}^2 \times 10^3$) for Compound 5. The anisotropic displacement factor exponent takes the form: $-2\pi^2 [h^2 a^{*2} U^{11} + \dots + 2 h k a^{*} b^{*} U^{12}]$

	U^{11}	U^{22}	U^{33}	U^{23}	U^{13}	U^{12}
Ru(1)	10(1)	12(1)	13(1)	-1(1)	-1(1)	0(1)
P(1)	11(1)	13(1)	14(1)	0(1)	0(1)	0(1)
N(1)	16(1)	22(1)	16(1)	-2(1)	0(1)	-1(1)
N(2)	19(1)	14(1)	17(1)	0(1)	-1(1)	-1(1)
N(3)	18(1)	15(1)	24(1)	-1(1)	4(1)	-3(1)
C(1)	17(1)	20(1)	16(2)	-4(1)	-7(1)	4(1)
C(2)	19(1)	18(1)	15(2)	2(1)	-5(1)	2(1)
C(3)	18(1)	20(1)	10(1)	2(1)	-2(1)	-1(1)
C(4)	23(1)	18(1)	10(1)	2(1)	-4(1)	-1(1)
C(5)	17(1)	22(1)	23(2)	-2(1)	1(1)	0(1)
C(6)	20(2)	28(2)	43(2)	-4(2)	-3(1)	-1(1)
C(7)	22(2)	49(2)	28(2)	6(2)	7(1)	1(1)
C(8)	23(2)	24(2)	38(2)	-1(2)	-1(1)	2(1)
C(9)	13(1)	16(1)	21(2)	4(1)	-3(1)	1(1)
C(10)	15(1)	15(1)	19(2)	0(1)	2(1)	5(1)
C(11)	20(1)	9(1)	16(2)	3(1)	-3(1)	0(1)
C(12)	20(1)	13(1)	18(2)	-1(1)	2(1)	3(1)
C(13)	23(1)	18(1)	16(2)	2(1)	-4(1)	-8(1)
C(14)	24(2)	27(2)	21(2)	0(1)	-5(1)	-6(1)
C(15)	56(4)	16(2)	33(3)	-1(2)	-20(3)	-8(2)
C(16)	22(2)	45(4)	25(2)	3(3)	-3(1)	-14(2)
C(15')	56(4)	16(2)	33(3)	-1(2)	-20(3)	-8(2)
C(16')	22(2)	45(4)	25(2)	3(3)	-3(1)	-14(2)
C(17)	17(1)	16(1)	14(2)	2(1)	3(1)	4(1)
C(18)	16(1)	10(1)	25(2)	-2(1)	1(1)	-4(1)
C(19)	21(1)	19(2)	28(2)	-7(1)	2(1)	-1(1)
C(20)	29(2)	19(2)	31(2)	4(1)	9(1)	3(1)
C(21)	18(1)	23(2)	32(2)	-4(1)	2(1)	1(1)
C(101)	9(1)	14(1)	21(2)	6(1)	-1(1)	1(1)

	U^{11}	U^{22}	U^{33}	U^{23}	U^{13}	U^{12}
C(102)	15(1)	23(2)	20(2)	-1(1)	2(1)	1(1)
C(103)	17(1)	26(2)	32(2)	-6(1)	-2(1)	-3(1)
C(104)	9(1)	27(2)	32(2)	9(1)	1(1)	-2(1)
C(105)	15(1)	31(2)	18(2)	4(1)	4(1)	3(1)
C(106)	17(1)	23(2)	19(2)	0(1)	-1(1)	-2(1)
C(107)	14(1)	18(1)	10(1)	-1(1)	2(1)	0(1)
C(108)	19(1)	20(1)	22(2)	2(1)	2(1)	-1(1)
C(109)	26(2)	22(2)	25(2)	9(1)	4(1)	4(1)
C(110)	23(2)	38(2)	19(2)	5(1)	-4(1)	12(1)
C(111)	18(1)	34(2)	28(2)	-6(1)	-9(1)	3(1)
C(112)	19(1)	21(2)	20(2)	-2(1)	-2(1)	1(1)
C(113)	11(1)	13(1)	15(2)	-1(1)	1(1)	-2(1)
C(114)	19(1)	17(1)	18(2)	1(1)	-1(1)	-1(1)
C(115)	19(1)	25(2)	16(2)	-5(1)	0(1)	0(1)
C(116)	16(1)	12(1)	24(2)	-2(1)	3(1)	-1(1)
C(117)	14(1)	16(1)	21(2)	4(1)	2(1)	0(1)
C(118)	14(1)	18(1)	12(2)	-1(1)	1(1)	-2(1)

Table D-3.6: Hydrogen coordinates ($\times 10^4$) and isotropic displacement parameters ($\text{\AA}^2 \times 10^3$) for Compound 5.

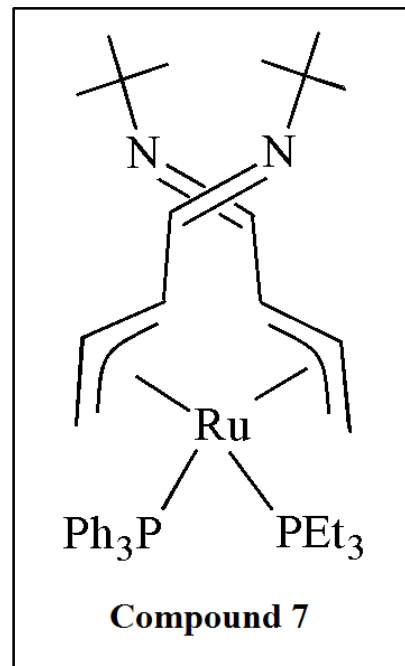
	x	y	z	U(eq)
H(1A)	1313	381	4320	21
H(1B)	1247	1865	4768	21
H(2)	2211	2719	4175	21
H(3)	2450	-124	3741	19
H(4)	3489	2015	3899	20
H(6A)	4511	2673	3676	45
H(6B)	5230	1906	3793	45
H(6C)	4631	1706	4344	45
H(7A)	4426	-86	2427	50
H(7B)	5041	984	2580	50
H(7C)	4274	1558	2526	50
H(8A)	4815	-899	4179	43
H(8B)	5361	-615	3583	43
H(8C)	4710	-1585	3429	43
H(9A)	3858	-309	5407	20
H(9B)	3371	-993	6020	20
H(10)	3246	-1615	4584	20
H(11)	2260	-2243	5617	18
H(12)	2119	-2422	4139	20
H(14A)	1040	-1654	3478	36
H(14B)	759	-2973	3046	36
H(14C)	1550	-2886	3254	36
H(15A)	1496	-5234	3867	53
H(15B)	705	-5397	3669	53
H(15C)	944	-5465	4462	53
H(16A)	64	-3570	4679	46
H(16B)	-110	-3435	3872	46
H(16C)	135	-2080	4299	46
H(15D)	1739	-4698	3742	53

	x	y	z	U(eq)
H(15E)	1008	-5399	3601	53
H(15F)	1324	-5389	4366	53
H(16D)	199	-4253	4705	46
H(16E)	-54	-4074	3921	46
H(16F)	11	-2724	4412	46
H(19A)	2904	5668	5977	34
H(19B)	3624	6323	6204	34
H(19C)	3365	4884	6545	34
H(20A)	3920	4802	4503	40
H(20B)	3972	6273	4905	40
H(20C)	3240	5610	4729	40
H(21A)	4444	3659	6187	37
H(21B)	4722	5068	5833	37
H(21C)	4659	3649	5390	37
H(102)	1107	-974	5506	23
H(103)	50	-2021	5735	30
H(104)	-533	-1479	6743	27
H(105)	-60	107	7535	26
H(106)	1012	1092	7332	23
H(108)	2059	-1738	6965	24
H(109)	2813	-2848	7734	29
H(110)	3723	-1591	8208	32
H(111)	3908	742	7882	32
H(112)	3186	1826	7077	24
H(114)	2035	2576	7537	22
H(115)	1693	4850	7823	24
H(116)	1284	6375	6969	21
H(117)	1293	5671	5811	20
H(118)	1662	3415	5520	17

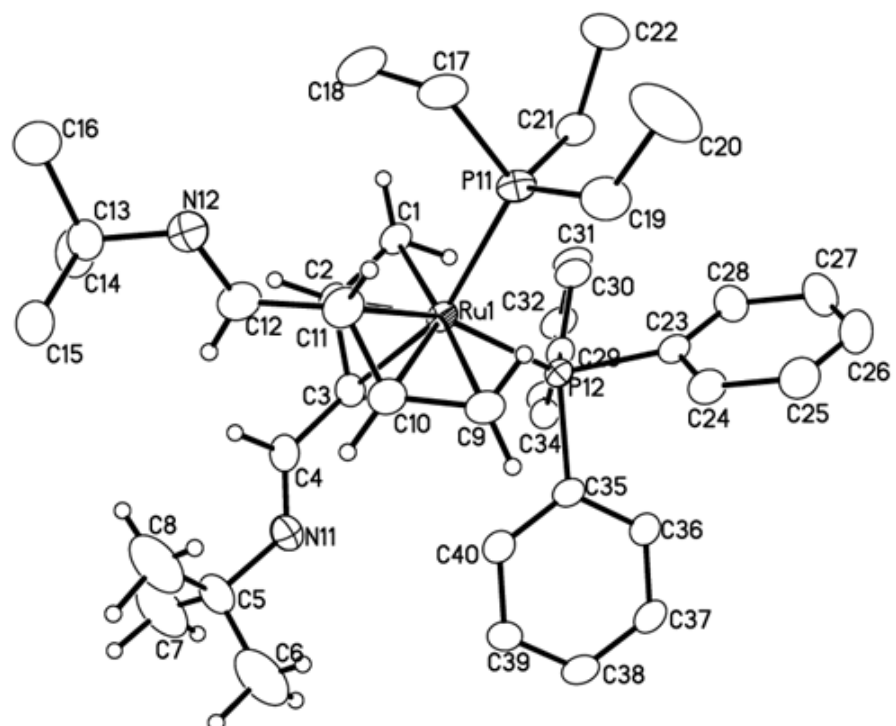
Table D-3.7: Torsion angles [°] for Compound 5.

Ru(1)-C(1)-C(2)-C(3)	62.2(2)
C(1)-C(2)-C(3)-C(4)	-163.8(2)
Ru(1)-C(2)-C(3)-C(4)	-101.1(2)
C(1)-C(2)-C(3)-Ru(1)	-62.7(2)
C(5)-N(1)-C(4)-C(3)	-173.4(2)
C(2)-C(3)-C(4)-N(1)	-174.3(3)
Ru(1)-C(3)-C(4)-N(1)	108.6(3)
C(4)-N(1)-C(5)-C(7)	-105.4(3)
C(4)-N(1)-C(5)-C(8)	137.5(3)
C(4)-N(1)-C(5)-C(6)	17.3(4)
Ru(1)-C(9)-C(10)-C(11)	-65.7(2)
C(9)-C(10)-C(11)-C(12)	171.6(2)
Ru(1)-C(10)-C(11)-C(12)	108.1(2)
C(9)-C(10)-C(11)-Ru(1)	63.5(2)
C(13)-N(2)-C(12)-C(11)	176.1(2)
C(10)-C(11)-C(12)-N(2)	174.1(2)
Ru(1)-C(11)-C(12)-N(2)	-110.3(3)
C(12)-N(2)-C(13)-C(16')	-165.6(15)
C(12)-N(2)-C(13)-C(15)	97.4(5)
C(12)-N(2)-C(13)-C(14)	-29.7(3)
C(12)-N(2)-C(13)-C(15')	77.6(15)
C(12)-N(2)-C(13)-C(16)	-145.3(4)
C(107)-P(1)-C(101)-C(102)	-116.8(2)
C(113)-P(1)-C(101)-C(102)	136.4(2)
Ru(1)-P(1)-C(101)-C(102)	9.9(2)
C(107)-P(1)-C(101)-C(106)	63.0(2)
C(113)-P(1)-C(101)-C(106)	-43.8(2)
Ru(1)-P(1)-C(101)-C(106)	-170.26(18)
C(106)-C(101)-C(102)-C(103)	-1.9(4)
P(1)-C(101)-C(102)-C(103)	177.9(2)
C(101)-C(102)-C(103)-C(104)	1.7(4)
C(102)-C(103)-C(104)-C(105)	-0.1(4)
C(103)-C(104)-C(105)-C(106)	-1.2(4)
C(104)-C(105)-C(106)-C(101)	0.9(4)

C(102)-C(101)-C(106)-C(105)	0.6(4)
P(1)-C(101)-C(106)-C(105)	-179.2(2)
C(113)-P(1)-C(107)-C(108)	144.1(2)
C(101)-P(1)-C(107)-C(108)	40.6(2)
Ru(1)-P(1)-C(107)-C(108)	-89.0(2)
C(113)-P(1)-C(107)-C(112)	-47.9(2)
C(101)-P(1)-C(107)-C(112)	-151.4(2)
Ru(1)-P(1)-C(107)-C(112)	78.9(2)
C(112)-C(107)-C(108)-C(109)	1.3(4)
P(1)-C(107)-C(108)-C(109)	169.6(2)
C(107)-C(108)-C(109)-C(110)	0.9(4)
C(108)-C(109)-C(110)-C(111)	-1.5(4)
C(109)-C(110)-C(111)-C(112)	0.0(4)
C(110)-C(111)-C(112)-C(107)	2.2(4)
C(108)-C(107)-C(112)-C(111)	-2.8(4)
P(1)-C(107)-C(112)-C(111)	-170.9(2)
C(107)-P(1)-C(113)-C(118)	163.00(19)
C(101)-P(1)-C(113)-C(118)	-92.0(2)
Ru(1)-P(1)-C(113)-C(118)	36.8(2)
C(107)-P(1)-C(113)-C(114)	-24.0(2)
C(101)-P(1)-C(113)-C(114)	81.1(2)
Ru(1)-P(1)-C(113)-C(114)	-150.11(18)
C(118)-C(113)-C(114)-C(115)	1.5(4)
P(1)-C(113)-C(114)-C(115)	-171.56(19)
C(113)-C(114)-C(115)-C(116)	0.9(4)
C(114)-C(115)-C(116)-C(117)	-2.5(4)
C(115)-C(116)-C(117)-C(118)	1.6(4)
C(116)-C(117)-C(118)-C(113)	0.8(4)
C(114)-C(113)-C(118)-C(117)	-2.4(4)
P(1)-C(113)-C(118)-C(117)	171.07(18)



Compound 7



Molecular Structure of Compound 7

Table D-4.1. Crystal data and structure refinement for Compound 7.

Empirical formula	$C_{183} H_{261} N_8 O P_9 Ru_4$		
Formula weight	3271.99		
Temperature	100(2) K		
Wavelength	0.71073 Å		
Crystal system	Triclinic		
Space group	$P \bar{1}$		
Unit cell dimensions	$a = 12.9476(5)$ Å	$\alpha = 101.868(2)^\circ$.	
	$b = 18.7814(8)$ Å	$\beta = 100.642(2)^\circ$.	
	$c = 20.8624(9)$ Å	$\gamma = 105.467(2)^\circ$.	
Volume	$4628.1(3)$ Å ³		
Z	1		
Density (calculated)	1.174 Mg/m ³		
Absorption coefficient	0.447 mm ⁻¹		
F(000)	1734		
Crystal size	$0.471 \times 0.287 \times 0.062$ mm ³		
Theta range for data collection	1.947 to 26.486°.		
Index ranges	$-15 \leq h \leq 16, -23 \leq k \leq 23, -26 \leq l \leq 26$		
Reflections collected	131786		
Independent reflections	18994 [R(int) = 0.0547]		
Completeness to theta = 25.000°	99.6 %		
Absorption correction	Semi-empirical from equivalents		
Max. and min. transmission	0.5624 and 0.4881		
Refinement method	Full-matrix least-squares on F ²		
Data / restraints / parameters	18994 / 1118 / 1040		
Goodness-of-fit on F ²	1.038		
Final R indices [I>2sigma(I)]	R1 = 0.0490, wR2 = 0.1303		
R indices (all data)	R1 = 0.0697, wR2 = 0.1479		
Extinction coefficient	n/a		
Largest diff. peak and hole	1.222 and -1.081 e.Å ⁻³		

Table D-4.2: Atomic coordinates ($\times 10^4$) and equivalent isotropic displacement parameters ($\text{\AA}^2 \times 10^3$) for Compound 7. U(eq) is defined as one third of the trace of the orthogonalized U_{ij} tensor.

	x	y	z	U(eq)
Ru(1)	7333(1)	3756(1)	159(1)	19(1)
P(11)	7337(1)	4074(1)	-864(1)	24(1)
P(12)	6974(1)	2448(1)	-258(1)	18(1)
N(11)	7441(3)	3470(2)	2153(2)	31(1)
N(12)	8145(3)	6176(2)	1158(2)	30(1)
C(1)	5536(3)	3654(2)	-16(2)	23(1)
C(2)	6085(3)	3947(2)	676(2)	24(1)
C(3)	6534(3)	3496(2)	1045(2)	23(1)
C(4)	7147(3)	3840(2)	1749(2)	27(1)
C(5)	8095(4)	3881(2)	2851(2)	41(1)
C(6)	9009(6)	3547(4)	2990(3)	84(1)
C(7)	7339(6)	3756(4)	3313(3)	84(1)
C(8)	8665(6)	4738(4)	2978(3)	84(1)
C(9)	9137(3)	3880(2)	401(2)	26(1)
C(10)	8886(3)	4410(2)	875(2)	25(1)
C(11)	8505(3)	4999(2)	689(2)	28(1)
C(12)	8261(3)	5545(2)	1216(2)	29(1)
C(13)	7904(3)	6633(2)	1742(2)	30(1)
C(14)	6837(3)	6193(2)	1891(2)	40(1)
C(15)	8868(4)	6891(2)	2371(2)	37(1)
C(16)	7730(4)	7335(3)	1533(2)	45(1)
C(17)	7286(3)	5040(2)	-877(2)	35(1)
C(18)	6390(3)	5275(2)	-599(2)	41(1)
C(19)	8549(4)	4069(3)	-1205(2)	41(1)
C(20)	8619(4)	4238(5)	-1873(3)	76(2)
C(21)	6134(3)	3448(2)	-1556(2)	28(1)
C(22)	5808(3)	3689(3)	-2194(2)	37(1)
C(23)	7422(3)	2095(2)	-1021(2)	24(1)
C(24)	8567(3)	2296(2)	-950(2)	34(1)
C(25)	8986(4)	2014(3)	-1471(2)	46(1)

	x	y	z	U(eq)
C(26)	8284(5)	1528(3)	-2070(3)	53(1)
C(27)	7168(5)	1340(3)	-2154(2)	46(1)
C(28)	6729(4)	1620(2)	-1629(2)	32(1)
C(29)	5545(3)	1797(2)	-440(2)	21(1)
C(30)	4719(3)	1807(2)	-969(2)	27(1)
C(31)	3637(3)	1325(2)	-1105(2)	31(1)
C(32)	3361(3)	841(2)	-705(2)	30(1)
C(33)	4156(3)	842(2)	-167(2)	28(1)
C(34)	5244(3)	1316(2)	-36(2)	23(1)
C(35)	7686(3)	1988(2)	301(2)	20(1)
C(36)	7751(3)	1257(2)	36(2)	23(1)
C(37)	8196(3)	878(2)	460(2)	25(1)
C(38)	8566(3)	1210(2)	1150(2)	26(1)
C(39)	8526(3)	1936(2)	1415(2)	25(1)
C(40)	8092(3)	2325(2)	989(2)	23(1)
Ru(2)	7248(1)	7786(1)	6956(1)	27(1)
P(21)	6698(1)	6545(1)	7063(1)	38(1)
P(22)	7364(1)	8477(1)	8042(1)	19(1)
N(21)	8123(3)	9942(2)	6413(2)	40(1)
N(22)	7185(5)	6681(3)	4955(2)	68(1)
C(1A)	5457(3)	7693(3)	6594(2)	36(1)
C(2A)	6128(4)	8103(3)	6254(2)	37(1)
C(3A)	6921(3)	8824(2)	6596(2)	35(1)
C(4A)	7579(4)	9237(3)	6209(2)	37(1)
C(5A)	8713(5)	10316(3)	5968(3)	50(1)
C(6A)	8208(8)	10946(5)	5867(4)	103(3)
C(7A)	8614(6)	9804(4)	5274(3)	73(2)
C(8A)	9903(5)	10671(4)	6353(3)	77(2)
C(9A)	9050(3)	7919(2)	7281(2)	32(1)
C(10A)	8735(3)	7951(3)	6611(2)	37(1)
C(11A)	7997(4)	7286(3)	6119(2)	41(1)
C(12A)	7645(5)	7294(3)	5419(2)	49(1)
C(13A)	6822(7)	6703(3)	4249(3)	92(2)

	x	y	z	U(eq)
C(14A)	7263(9)	7487(4)	4113(3)	123(4)
C(15A)	7215(8)	6111(4)	3830(3)	112(3)
C(16A)	5567(8)	6444(4)	4088(3)	111(3)
C(17A)	6034(4)	5777(3)	6264(3)	63(2)
C(18A)	5027(5)	5826(3)	5805(3)	70(2)
C(19A)	7652(5)	6115(3)	7430(4)	94(2)
C(20A)	8477(8)	6376(6)	8096(4)	62(3)
C(20B)	8365(9)	5731(6)	7101(7)	94(2)
C(21A)	5657(4)	6366(2)	7548(2)	40(1)
C(22A)	5161(5)	5557(2)	7606(3)	60(1)
C(23A)	7679(3)	8059(2)	8755(2)	20(1)
C(24A)	8718(3)	7965(3)	8904(2)	35(1)
C(25A)	9027(3)	7642(3)	9416(2)	40(1)
C(26A)	8296(3)	7392(2)	9788(2)	28(1)
C(27A)	7270(3)	7496(2)	9656(2)	28(1)
C(28A)	6967(3)	7833(2)	9151(2)	26(1)
C(29A)	6188(3)	8794(2)	8210(2)	20(1)
C(30A)	5175(3)	8241(2)	8138(2)	23(1)
C(31A)	4256(3)	8443(2)	8243(2)	24(1)
C(32A)	4325(3)	9211(2)	8425(2)	28(1)
C(33A)	5315(3)	9766(2)	8483(2)	29(1)
C(34A)	6241(3)	9561(2)	8375(2)	23(1)
C(35A)	8535(3)	9385(2)	8361(2)	22(1)
C(36A)	8873(3)	9764(2)	9049(2)	25(1)
C(37A)	9777(3)	10429(2)	9299(2)	27(1)
C(38A)	10362(3)	10713(2)	8870(2)	28(1)
C(39A)	10024(3)	10344(2)	8187(2)	29(1)
C(40A)	9114(3)	9687(2)	7933(2)	26(1)
O(1S)	2010(30)	9488(19)	7139(13)	161(9)
O(2S)	2480(30)	6467(19)	3983(13)	161(9)
P(3)	946(5)	7057(3)	4602(3)	112(2)
C(41)	2102(13)	7331(10)	4228(7)	121(5)
C(42)	3181(13)	7785(11)	4562(9)	183(11)

	x	y	z	U(eq)
C(43)	3954(14)	8043(13)	4218(12)	203(11)
C(44)	3776(18)	7837(15)	3526(12)	203(12)
C(45)	2671(19)	7425(11)	3202(9)	173(9)
C(46)	1867(16)	7115(10)	3524(7)	137(6)
C(47)	1385(13)	7623(8)	5451(7)	112(5)
C(48)	836(11)	8142(9)	5611(8)	126(6)
C(49)	1225(11)	8677(9)	6226(8)	116(5)
C(50)	2054(13)	8735(7)	6763(6)	91(4)
C(51)	2668(16)	8256(11)	6569(8)	150(9)
C(52)	2317(15)	7690(10)	5947(7)	129(7)
C(53)	1147(13)	6179(8)	4721(8)	106(4)
C(54)	2048(14)	5953(10)	4600(8)	150(7)
C(55)	2096(15)	5252(10)	4680(8)	145(9)
C(56)	1350(18)	4734(10)	4882(10)	184(12)
C(57)	434(19)	4963(11)	4976(15)	151(9)
C(58)	336(14)	5675(10)	4914(10)	146(7)
C(59)	6546(17)	8744(10)	3037(7)	160(10)
C(60)	5950(17)	9204(12)	3143(6)	330(30)
C(61)	5854(9)	9678(7)	3656(6)	122(6)
C(62)	5199(10)	10057(12)	3859(10)	270(20)
C(63)	5159(18)	10584(12)	4365(10)	151(9)
C(63')	5574(18)	10759(10)	4251(14)	151(9)

Table D-4.3. Bond lengths [Å] for Compound 7.

Ru(1)-C(10)	2.146(3)	C(7)-H(7B)	0.9800
Ru(1)-C(2)	2.167(3)	C(7)-H(7C)	0.9800
Ru(1)-C(9)	2.234(3)	C(8)-H(8A)	0.9800
Ru(1)-C(1)	2.237(3)	C(8)-H(8B)	0.9800
Ru(1)-P(12)	2.3162(9)	C(8)-H(8C)	0.9800
Ru(1)-C(11)	2.326(3)	C(9)-C(10)	1.400(5)
Ru(1)-P(11)	2.3322(10)	C(9)-H(9A)	0.9500
Ru(1)-C(3)	2.352(3)	C(9)-H(9B)	0.9500
P(11)-C(19)	1.839(4)	C(10)-C(11)	1.420(5)
P(11)-C(17)	1.840(4)	C(10)-H(10)	1.0000
P(11)-C(21)	1.840(4)	C(11)-C(12)	1.484(6)
P(12)-C(35)	1.845(3)	C(11)-H(11)	1.0000
P(12)-C(29)	1.845(3)	C(12)-H(12)	0.9500
P(12)-C(23)	1.850(4)	C(13)-C(15)	1.524(5)
N(11)-C(4)	1.265(5)	C(13)-C(16)	1.530(5)
N(11)-C(5)	1.473(5)	C(13)-C(14)	1.531(5)
N(12)-C(12)	1.259(5)	C(14)-H(14D)	0.9800
N(12)-C(13)	1.474(5)	C(14)-H(14E)	0.9800
C(1)-C(2)	1.405(5)	C(14)-H(14F)	0.9800
C(1)-H(1A)	0.9500	C(15)-H(15D)	0.9800
C(1)-H(1B)	0.9500	C(15)-H(15E)	0.9800
C(2)-C(3)	1.420(5)	C(15)-H(15F)	0.9800
C(2)-H(2)	1.0000	C(16)-H(16D)	0.9800
C(3)-C(4)	1.453(5)	C(16)-H(16E)	0.9800
C(3)-H(3)	1.0000	C(16)-H(16F)	0.9800
C(4)-H(4)	0.9500	C(17)-C(18)	1.513(6)
C(5)-C(6)	1.492(7)	C(17)-H(17C)	0.9900
C(5)-C(7)	1.503(8)	C(17)-H(17D)	0.9900
C(5)-C(8)	1.525(8)	C(18)-H(18D)	0.9800
C(6)-H(6A)	0.9800	C(18)-H(18E)	0.9800
C(6)-H(6B)	0.9800	C(18)-H(18F)	0.9800
C(6)-H(6C)	0.9800	C(19)-C(20)	1.505(6)
C(7)-H(7A)	0.9800	C(19)-H(19A)	0.9900
C(19)-H(19B)	0.9900	C(36)-H(36)	0.9500

C(20)-H(20G)	0.9800	C(37)-C(38)	1.381(5)
C(20)-H(20H)	0.9800	C(37)-H(37)	0.9500
C(20)-H(20I)	0.9800	C(38)-C(39)	1.379(5)
C(21)-C(22)	1.515(5)	C(38)-H(38)	0.9500
C(21)-H(21C)	0.9900	C(39)-C(40)	1.394(5)
C(21)-H(21D)	0.9900	C(39)-H(39)	0.9500
C(22)-H(22D)	0.9800	C(40)-H(40)	0.9500
C(22)-H(22E)	0.9800	Ru(2)-C(10A)	2.146(4)
C(22)-H(22F)	0.9800	Ru(2)-C(2A)	2.154(4)
C(23)-C(28)	1.377(5)	Ru(2)-C(9A)	2.236(4)
C(23)-C(24)	1.400(5)	Ru(2)-C(1A)	2.249(4)
C(24)-C(25)	1.375(6)	Ru(2)-C(11A)	2.304(4)
C(24)-H(24)	0.9500	Ru(2)-P(21)	2.3186(12)
C(25)-C(26)	1.374(8)	Ru(2)-P(22)	2.3228(9)
C(25)-H(25)	0.9500	Ru(2)-C(3A)	2.339(4)
C(26)-C(27)	1.360(7)	P(21)-C(19A)	1.789(6)
C(26)-H(26)	0.9500	P(21)-C(21A)	1.831(5)
C(27)-C(28)	1.398(6)	P(21)-C(17A)	1.849(5)
C(27)-H(27)	0.9500	P(22)-C(29A)	1.840(3)
C(28)-H(28)	0.9500	P(22)-C(23A)	1.852(3)
C(29)-C(34)	1.387(5)	P(22)-C(35A)	1.853(4)
C(29)-C(30)	1.395(5)	N(21)-C(4A)	1.260(6)
C(30)-C(31)	1.391(5)	N(21)-C(5A)	1.479(6)
C(30)-H(30)	0.9500	N(22)-C(12A)	1.256(6)
C(31)-C(32)	1.377(5)	N(22)-C(13A)	1.472(7)
C(31)-H(31)	0.9500	C(1A)-C(2A)	1.397(6)
C(32)-C(33)	1.375(5)	C(1A)-H(1AA)	0.9500
C(32)-H(32)	0.9500	C(1A)-H(1AB)	0.9500
C(33)-C(34)	1.393(5)	C(2A)-C(3A)	1.410(6)
C(33)-H(33)	0.9500	C(2A)-H(2A)	1.0000
C(34)-H(34)	0.9500	C(3A)-C(4A)	1.462(6)
C(35)-C(40)	1.380(5)	C(3A)-H(3A)	1.0000
C(35)-C(36)	1.402(5)	C(4A)-H(4A)	0.9500
C(36)-C(37)	1.381(5)	C(5A)-C(8A)	1.496(8)
C(5A)-C(7A)	1.525(7)	C(18A)-H(18B)	0.9800
C(5A)-C(6A)	1.528(8)	C(18A)-H(18C)	0.9800

C(6A)-H(6AA)	0.9800	C(19A)-C(20A)	1.485(4)
C(6A)-H(6AB)	0.9800	C(19A)-C(20B)	1.493(4)
C(6A)-H(6AC)	0.9800	C(19A)-H(19C)	0.9900
C(7A)-H(7AA)	0.9800	C(19A)-H(19D)	0.9900
C(7A)-H(7AB)	0.9800	C(20A)-H(20A)	0.9800
C(7A)-H(7AC)	0.9800	C(20A)-H(20B)	0.9800
C(8A)-H(8AA)	0.9800	C(20A)-H(20C)	0.9800
C(8A)-H(8AB)	0.9800	C(20B)-H(20D)	0.9800
C(8A)-H(8AC)	0.9800	C(20B)-H(20E)	0.9800
C(9A)-C(10A)	1.400(6)	C(20B)-H(20F)	0.9800
C(9A)-H(9AA)	0.9500	C(21A)-C(22A)	1.524(5)
C(9A)-H(9AB)	0.9500	C(21A)-H(21A)	0.9900
C(10A)-C(11A)	1.414(6)	C(21A)-H(21B)	0.9900
C(10A)-H(10A)	1.0000	C(22A)-H(22A)	0.9800
C(11A)-C(12A)	1.452(6)	C(22A)-H(22B)	0.9800
C(11A)-H(11A)	1.0000	C(22A)-H(22C)	0.9800
C(12A)-H(12A)	0.9500	C(23A)-C(28A)	1.389(5)
C(13A)-C(16A)	1.517(10)	C(23A)-C(24A)	1.390(5)
C(13A)-C(15A)	1.526(9)	C(24A)-C(25A)	1.381(6)
C(13A)-C(14A)	1.534(8)	C(24A)-H(24A)	0.9500
C(14A)-H(14A)	0.9800	C(25A)-C(26A)	1.378(6)
C(14A)-H(14B)	0.9800	C(25A)-H(25A)	0.9500
C(14A)-H(14C)	0.9800	C(26A)-C(27A)	1.381(5)
C(15A)-H(15A)	0.9800	C(26A)-H(26A)	0.9500
C(15A)-H(15B)	0.9800	C(27A)-C(28A)	1.384(5)
C(15A)-H(15C)	0.9800	C(27A)-H(27A)	0.9500
C(16A)-H(16A)	0.9800	C(28A)-H(28A)	0.9500
C(16A)-H(16B)	0.9800	C(29A)-C(34A)	1.392(5)
C(16A)-H(16C)	0.9800	C(29A)-C(30A)	1.400(5)
C(17A)-C(18A)	1.505(6)	C(30A)-C(31A)	1.381(5)
C(17A)-H(17A)	0.9900	C(30A)-H(30A)	0.9500
C(17A)-H(17B)	0.9900	C(31A)-C(32A)	1.388(5)
C(18A)-H(18A)	0.9800	C(31A)-H(31A)	0.9500
C(32A)-C(33A)	1.387(5)	C(48)-H(48)	0.9500
C(32A)-H(32A)	0.9500	C(49)-C(50)	1.365(7)
C(33A)-C(34A)	1.394(5)	C(49)-H(49)	0.9500

C(33A)-H(33A)	0.9500	C(50)-C(51)	1.399(7)
C(34A)-H(34A)	0.9500	C(50)-H(50)	0.9500
C(35A)-C(40A)	1.381(5)	C(51)-C(52)	1.407(7)
C(35A)-C(36A)	1.393(5)	C(51)-H(51)	0.9500
C(36A)-C(37A)	1.388(5)	C(52)-H(52)	0.9500
C(36A)-H(36A)	0.9500	C(53)-C(54)	1.390(7)
C(37A)-C(38A)	1.376(5)	C(53)-C(58)	1.393(8)
C(37A)-H(37A)	0.9500	C(54)-C(55)	1.377(7)
C(38A)-C(39A)	1.380(6)	C(54)-H(54)	0.9500
C(38A)-H(38A)	0.9500	C(55)-C(56)	1.369(7)
C(39A)-C(40A)	1.384(5)	C(55)-H(55)	0.9500
C(39A)-H(39A)	0.9500	C(56)-C(57)	1.398(7)
C(40A)-H(40A)	0.9500	C(56)-H(56)	0.9500
O(1S)-H(1SA)	0.9324	C(57)-C(58)	1.408(7)
O(1S)-H(1SB)	1.1630	C(57)-H(57)	0.9500
P(3)-C(47)	1.767(14)	C(58)-H(58)	0.9500
P(3)-C(53)	1.795(14)	C(59)-C(60)	1.3163
P(3)-C(41)	1.816(16)	C(59)-H(59A)	0.9800
C(41)-C(42)	1.387(7)	C(59)-H(59B)	0.9800
C(41)-C(46)	1.392(8)	C(59)-H(59C)	0.9800
C(42)-C(43)	1.379(7)	C(60)-C(61)	1.2918
C(42)-H(42)	0.9500	C(60)-H(60A)	0.9900
C(43)-C(44)	1.375(7)	C(60)-H(60B)	0.9900
C(43)-H(43)	0.9500	C(61)-C(62)	1.3162
C(44)-C(45)	1.393(7)	C(61)-H(61A)	0.9900
C(44)-H(44)	0.9500	C(61)-H(61B)	0.9900
C(45)-C(46)	1.404(7)	C(62)-C(63')	1.3085
C(45)-H(45)	0.9500	C(62)-C(63)	1.3096
C(46)-H(46)	0.9500	C(62)-H(62A)	0.9900
C(47)-C(48)	1.374(7)	C(62)-H(62B)	0.9900
C(47)-C(52)	1.395(10)	C(63)-H(63A)	0.9800
C(48)-C(49)	1.369(7)	C(63)-H(63B)	0.9800
C(63)-H(63C)	0.9800		
C(63')-H(63D)	0.9800		
C(63')-H(63E)	0.9800		
C(63')-H(63F)	0.9800		

Table D-4.4. Bond angles [°] for Compound 7.

C(10)-Ru(1)-C(2)	104.94(14)	C(21)-P(11)-Ru(1)	112.90(12)
C(10)-Ru(1)-C(9)	37.20(14)	C(35)-P(12)-C(29)	98.91(15)
C(2)-Ru(1)-C(9)	139.35(14)	C(35)-P(12)-C(23)	97.22(15)
C(10)-Ru(1)-C(1)	139.79(13)	C(29)-P(12)-C(23)	102.74(16)
C(2)-Ru(1)-C(1)	37.18(13)	C(35)-P(12)-Ru(1)	115.76(11)
C(9)-Ru(1)-C(1)	176.52(13)	C(29)-P(12)-Ru(1)	119.25(11)
C(10)-Ru(1)-P(12)	118.33(10)	C(23)-P(12)-Ru(1)	119.02(11)
C(2)-Ru(1)-P(12)	109.12(10)	C(4)-N(11)-C(5)	120.0(3)
C(9)-Ru(1)-P(12)	88.07(9)	C(12)-N(12)-C(13)	115.4(3)
C(1)-Ru(1)-P(12)	93.38(9)	C(2)-C(1)-Ru(1)	68.69(19)
C(10)-Ru(1)-C(11)	36.74(13)	C(2)-C(1)-H(1A)	120.0
C(2)-Ru(1)-C(11)	91.51(13)	Ru(1)-C(1)-H(1A)	81.5
C(9)-Ru(1)-C(11)	65.10(13)	C(2)-C(1)-H(1B)	120.0
C(1)-Ru(1)-C(11)	113.30(13)	Ru(1)-C(1)-H(1B)	120.7
P(12)-Ru(1)-C(11)	153.09(9)	H(1A)-C(1)-H(1B)	120.0
C(10)-Ru(1)-P(11)	108.83(10)	C(1)-C(2)-C(3)	121.5(3)
C(2)-Ru(1)-P(11)	119.01(10)	C(1)-C(2)-Ru(1)	74.1(2)
C(9)-Ru(1)-P(11)	93.68(10)	C(3)-C(2)-Ru(1)	78.9(2)
C(1)-Ru(1)-P(11)	89.28(10)	C(1)-C(2)-H(2)	119.3
P(12)-Ru(1)-P(11)	97.28(3)	C(3)-C(2)-H(2)	119.3
C(11)-Ru(1)-P(11)	86.95(10)	Ru(1)-C(2)-H(2)	119.3
C(10)-Ru(1)-C(3)	90.44(13)	C(2)-C(3)-C(4)	119.2(3)
C(2)-Ru(1)-C(3)	36.35(13)	C(2)-C(3)-Ru(1)	64.70(19)
C(9)-Ru(1)-C(3)	111.99(13)	C(4)-C(3)-Ru(1)	121.2(2)
C(1)-Ru(1)-C(3)	64.93(13)	C(2)-C(3)-H(3)	114.3
P(12)-Ru(1)-C(3)	88.22(9)	C(4)-C(3)-H(3)	114.3
C(11)-Ru(1)-C(3)	99.59(13)	Ru(1)-C(3)-H(3)	114.3
P(11)-Ru(1)-C(3)	153.96(9)	N(11)-C(4)-C(3)	124.6(3)
C(19)-P(11)-C(17)	100.2(2)	N(11)-C(4)-H(4)	117.7
C(19)-P(11)-C(21)	105.1(2)	C(3)-C(4)-H(4)	117.7
C(17)-P(11)-C(21)	102.77(17)	N(11)-C(5)-C(6)	106.3(4)
C(19)-P(11)-Ru(1)	117.41(14)	N(11)-C(5)-C(7)	107.8(4)
C(17)-P(11)-Ru(1)	116.62(15)	C(6)-C(5)-C(7)	112.0(5)
N(11)-C(5)-C(8)	115.7(4)	C(12)-C(11)-Ru(1)	123.6(2)

C(6)-C(5)-C(8)	105.4(5)	C(10)-C(11)-H(11)	113.8
C(7)-C(5)-C(8)	109.6(5)	C(12)-C(11)-H(11)	113.8
C(5)-C(6)-H(6A)	109.5	Ru(1)-C(11)-H(11)	113.8
C(5)-C(6)-H(6B)	109.5	N(12)-C(12)-C(11)	124.1(4)
H(6A)-C(6)-H(6B)	109.5	N(12)-C(12)-H(12)	117.9
C(5)-C(6)-H(6C)	109.5	C(11)-C(12)-H(12)	117.9
H(6A)-C(6)-H(6C)	109.5	N(12)-C(13)-C(15)	111.4(3)
H(6B)-C(6)-H(6C)	109.5	N(12)-C(13)-C(16)	105.5(3)
C(5)-C(7)-H(7A)	109.5	C(15)-C(13)-C(16)	109.6(3)
C(5)-C(7)-H(7B)	109.5	N(12)-C(13)-C(14)	111.6(3)
H(7A)-C(7)-H(7B)	109.5	C(15)-C(13)-C(14)	110.2(3)
C(5)-C(7)-H(7C)	109.5	C(16)-C(13)-C(14)	108.2(4)
H(7A)-C(7)-H(7C)	109.5	C(13)-C(14)-H(14D)	109.5
H(7B)-C(7)-H(7C)	109.5	C(13)-C(14)-H(14E)	109.5
C(5)-C(8)-H(8A)	109.5	H(14D)-C(14)-H(14E)	109.5
C(5)-C(8)-H(8B)	109.5	C(13)-C(14)-H(14F)	109.5
H(8A)-C(8)-H(8B)	109.5	H(14D)-C(14)-H(14F)	109.5
C(5)-C(8)-H(8C)	109.5	H(14E)-C(14)-H(14F)	109.5
H(8A)-C(8)-H(8C)	109.5	C(13)-C(15)-H(15D)	109.5
H(8B)-C(8)-H(8C)	109.5	C(13)-C(15)-H(15E)	109.5
C(10)-C(9)-Ru(1)	68.0(2)	H(15D)-C(15)-H(15E)	109.5
C(10)-C(9)-H(9A)	120.0	C(13)-C(15)-H(15F)	109.5
Ru(1)-C(9)-H(9A)	82.2	H(15D)-C(15)-H(15F)	109.5
C(10)-C(9)-H(9B)	120.0	H(15E)-C(15)-H(15F)	109.5
Ru(1)-C(9)-H(9B)	120.8	C(13)-C(16)-H(16D)	109.5
H(9A)-C(9)-H(9B)	120.0	C(13)-C(16)-H(16E)	109.5
C(9)-C(10)-C(11)	121.1(4)	H(16D)-C(16)-H(16E)	109.5
C(9)-C(10)-Ru(1)	74.8(2)	C(13)-C(16)-H(16F)	109.5
C(11)-C(10)-Ru(1)	78.5(2)	H(16D)-C(16)-H(16F)	109.5
C(9)-C(10)-H(10)	119.5	H(16E)-C(16)-H(16F)	109.5
C(11)-C(10)-H(10)	119.5	C(18)-C(17)-P(11)	116.0(3)
Ru(1)-C(10)-H(10)	119.5	C(18)-C(17)-H(17C)	108.3
C(10)-C(11)-C(12)	118.3(4)	P(11)-C(17)-H(17C)	108.3
C(10)-C(11)-Ru(1)	64.72(19)	C(18)-C(17)-H(17D)	108.3
P(11)-C(17)-H(17D)	108.3	C(25)-C(24)-C(23)	120.6(4)
H(17C)-C(17)-H(17D)	107.4	C(25)-C(24)-H(24)	119.7

C(17)-C(18)-H(18D)	109.5	C(23)-C(24)-H(24)	119.7
C(17)-C(18)-H(18E)	109.5	C(26)-C(25)-C(24)	120.3(5)
H(18D)-C(18)-H(18E)	109.5	C(26)-C(25)-H(25)	119.8
C(17)-C(18)-H(18F)	109.5	C(24)-C(25)-H(25)	119.8
H(18D)-C(18)-H(18F)	109.5	C(27)-C(26)-C(25)	119.9(4)
H(18E)-C(18)-H(18F)	109.5	C(27)-C(26)-H(26)	120.0
C(20)-C(19)-P(11)	121.8(3)	C(25)-C(26)-H(26)	120.0
C(20)-C(19)-H(19A)	106.9	C(26)-C(27)-C(28)	120.4(5)
P(11)-C(19)-H(19A)	106.9	C(26)-C(27)-H(27)	119.8
C(20)-C(19)-H(19B)	106.9	C(28)-C(27)-H(27)	119.8
P(11)-C(19)-H(19B)	106.9	C(23)-C(28)-C(27)	120.3(4)
H(19A)-C(19)-H(19B)	106.7	C(23)-C(28)-H(28)	119.8
C(19)-C(20)-H(20G)	109.5	C(27)-C(28)-H(28)	119.8
C(19)-C(20)-H(20H)	109.5	C(34)-C(29)-C(30)	118.0(3)
H(20G)-C(20)-H(20H)	109.5	C(34)-C(29)-P(12)	121.4(3)
C(19)-C(20)-H(20I)	109.5	C(30)-C(29)-P(12)	120.5(3)
H(20G)-C(20)-H(20I)	109.5	C(31)-C(30)-C(29)	120.9(3)
H(20H)-C(20)-H(20I)	109.5	C(31)-C(30)-H(30)	119.6
C(22)-C(21)-P(11)	120.7(3)	C(29)-C(30)-H(30)	119.6
C(22)-C(21)-H(21C)	107.2	C(32)-C(31)-C(30)	120.1(3)
P(11)-C(21)-H(21C)	107.2	C(32)-C(31)-H(31)	119.9
C(22)-C(21)-H(21D)	107.2	C(30)-C(31)-H(31)	119.9
P(11)-C(21)-H(21D)	107.2	C(33)-C(32)-C(31)	119.8(3)
H(21C)-C(21)-H(21D)	106.8	C(33)-C(32)-H(32)	120.1
C(21)-C(22)-H(22D)	109.5	C(31)-C(32)-H(32)	120.1
C(21)-C(22)-H(22E)	109.5	C(32)-C(33)-C(34)	120.2(3)
H(22D)-C(22)-H(22E)	109.5	C(32)-C(33)-H(33)	119.9
C(21)-C(22)-H(22F)	109.5	C(34)-C(33)-H(33)	119.9
H(22D)-C(22)-H(22F)	109.5	C(29)-C(34)-C(33)	121.0(3)
H(22E)-C(22)-H(22F)	109.5	C(29)-C(34)-H(34)	119.5
C(28)-C(23)-C(24)	118.3(4)	C(33)-C(34)-H(34)	119.5
C(28)-C(23)-P(12)	125.4(3)	C(40)-C(35)-C(36)	118.7(3)
C(24)-C(23)-P(12)	116.2(3)	C(40)-C(35)-P(12)	121.3(3)
C(36)-C(35)-P(12)	119.8(3)	C(11A)-Ru(2)-P(22)	153.25(12)
C(37)-C(36)-C(35)	120.4(3)	P(21)-Ru(2)-P(22)	100.36(4)
C(37)-C(36)-H(36)	119.8	C(10A)-Ru(2)-C(3A)	91.04(16)

C(35)-C(36)-H(36)	119.8	C(2A)-Ru(2)-C(3A)	36.27(16)
C(38)-C(37)-C(36)	120.3(3)	C(9A)-Ru(2)-C(3A)	113.12(15)
C(38)-C(37)-H(37)	119.8	C(1A)-Ru(2)-C(3A)	64.22(15)
C(36)-C(37)-H(37)	119.8	C(11A)-Ru(2)-C(3A)	100.54(16)
C(39)-C(38)-C(37)	119.8(3)	P(21)-Ru(2)-C(3A)	153.04(11)
C(39)-C(38)-H(38)	120.1	P(22)-Ru(2)-C(3A)	86.59(10)
C(37)-C(38)-H(38)	120.1	C(19A)-P(21)-C(21A)	100.9(3)
C(38)-C(39)-C(40)	120.0(3)	C(19A)-P(21)-C(17A)	97.4(3)
C(38)-C(39)-H(39)	120.0	C(21A)-P(21)-C(17A)	102.1(2)
C(40)-C(39)-H(39)	120.0	C(19A)-P(21)-Ru(2)	122.7(2)
C(35)-C(40)-C(39)	120.6(3)	C(21A)-P(21)-Ru(2)	114.45(13)
C(35)-C(40)-H(40)	119.7	C(17A)-P(21)-Ru(2)	116.0(2)
C(39)-C(40)-H(40)	119.7	C(29A)-P(22)-C(23A)	101.56(15)
C(10A)-Ru(2)-C(2A)	105.42(17)	C(29A)-P(22)-C(35A)	102.25(15)
C(10A)-Ru(2)-C(9A)	37.18(15)	C(23A)-P(22)-C(35A)	98.02(15)
C(2A)-Ru(2)-C(9A)	140.13(16)	C(29A)-P(22)-Ru(2)	119.40(11)
C(10A)-Ru(2)-C(1A)	140.26(16)	C(23A)-P(22)-Ru(2)	118.61(11)
C(2A)-Ru(2)-C(1A)	36.91(16)	C(35A)-P(22)-Ru(2)	113.72(12)
C(9A)-Ru(2)-C(1A)	177.03(15)	C(4A)-N(21)-C(5A)	119.6(4)
C(10A)-Ru(2)-C(11A)	36.83(16)	C(12A)-N(22)-C(13A)	120.3(5)
C(2A)-Ru(2)-C(11A)	92.28(16)	C(2A)-C(1A)-Ru(2)	67.8(2)
C(9A)-Ru(2)-C(11A)	64.51(15)	C(2A)-C(1A)-H(1AA)	120.0
C(1A)-Ru(2)-C(11A)	114.18(16)	Ru(2)-C(1A)-H(1AA)	83.1
C(10A)-Ru(2)-P(21)	107.90(13)	C(2A)-C(1A)-H(1AB)	120.0
C(2A)-Ru(2)-P(21)	117.85(12)	Ru(2)-C(1A)-H(1AB)	119.9
C(9A)-Ru(2)-P(21)	93.17(12)	H(1AA)-C(1A)-H(1AB)	120.0
C(1A)-Ru(2)-P(21)	89.34(12)	C(1A)-C(2A)-C(3A)	120.8(4)
C(11A)-Ru(2)-P(21)	84.97(13)	C(1A)-C(2A)-Ru(2)	75.3(2)
C(10A)-Ru(2)-P(22)	118.20(12)	C(3A)-C(2A)-Ru(2)	79.0(2)
C(2A)-Ru(2)-P(22)	107.75(12)	C(1A)-C(2A)-H(2A)	119.6
C(9A)-Ru(2)-P(22)	88.92(10)	C(3A)-C(2A)-H(2A)	119.6
C(1A)-Ru(2)-P(22)	92.20(11)	Ru(2)-C(2A)-H(2A)	119.6
C(2A)-C(3A)-C(4A)	118.4(4)	Ru(2)-C(9A)-H(9AA)	82.2
C(2A)-C(3A)-Ru(2)	64.7(2)	C(10A)-C(9A)-H(9AB)	120.0
C(4A)-C(3A)-Ru(2)	123.8(3)	Ru(2)-C(9A)-H(9AB)	120.7
C(2A)-C(3A)-H(3A)	113.7	H(9AA)-C(9A)-H(9AB)	120.0

C(4A)-C(3A)-H(3A)	113.7	C(9A)-C(10A)-C(11A)	119.0(4)
Ru(2)-C(3A)-H(3A)	113.7	C(9A)-C(10A)-Ru(2)	74.9(2)
N(21)-C(4A)-C(3A)	123.8(4)	C(11A)-C(10A)-Ru(2)	77.7(3)
N(21)-C(4A)-H(4A)	118.1	C(9A)-C(10A)-H(10A)	120.5
C(3A)-C(4A)-H(4A)	118.1	C(11A)-C(10A)-H(10A)	120.5
N(21)-C(5A)-C(8A)	106.7(4)	Ru(2)-C(10A)-H(10A)	120.5
N(21)-C(5A)-C(7A)	116.3(4)	C(10A)-C(11A)-C(12A)	120.9(4)
C(8A)-C(5A)-C(7A)	110.5(5)	C(10A)-C(11A)-Ru(2)	65.5(2)
N(21)-C(5A)-C(6A)	104.9(4)	C(12A)-C(11A)-Ru(2)	122.9(3)
C(8A)-C(5A)-C(6A)	109.6(6)	C(10A)-C(11A)-H(11A)	113.2
C(7A)-C(5A)-C(6A)	108.7(5)	C(12A)-C(11A)-H(11A)	113.2
C(5A)-C(6A)-H(6AA)	109.5	Ru(2)-C(11A)-H(11A)	113.2
C(5A)-C(6A)-H(6AB)	109.5	N(22)-C(12A)-C(11A)	121.3(5)
H(6AA)-C(6A)-H(6AB)	109.5	N(22)-C(12A)-H(12A)	119.3
C(5A)-C(6A)-H(6AC)	109.5	C(11A)-C(12A)-H(12A)	119.3
H(6AA)-C(6A)-H(6AC)	109.5	N(22)-C(13A)-C(16A)	105.1(5)
H(6AB)-C(6A)-H(6AC)	109.5	N(22)-C(13A)-C(15A)	105.2(5)
C(5A)-C(7A)-H(7AA)	109.5	C(16A)-C(13A)-C(15A)	110.3(6)
C(5A)-C(7A)-H(7AB)	109.5	N(22)-C(13A)-C(14A)	115.4(5)
H(7AA)-C(7A)-H(7AB)	109.5	C(16A)-C(13A)-C(14A)	110.5(7)
C(5A)-C(7A)-H(7AC)	109.5	C(15A)-C(13A)-C(14A)	110.2(6)
H(7AA)-C(7A)-H(7AC)	109.5	C(13A)-C(14A)-H(14A)	109.5
H(7AB)-C(7A)-H(7AC)	109.5	C(13A)-C(14A)-H(14B)	109.5
C(5A)-C(8A)-H(8AA)	109.5	H(14A)-C(14A)-H(14B)	109.5
C(5A)-C(8A)-H(8AB)	109.5	C(13A)-C(14A)-H(14C)	109.5
H(8AA)-C(8A)-H(8AB)	109.5	H(14A)-C(14A)-H(14C)	109.5
C(5A)-C(8A)-H(8AC)	109.5	H(14B)-C(14A)-H(14C)	109.5
H(8AA)-C(8A)-H(8AC)	109.5	C(13A)-C(15A)-H(15A)	109.5
H(8AB)-C(8A)-H(8AC)	109.5	C(13A)-C(15A)-H(15B)	109.5
C(10A)-C(9A)-Ru(2)	67.9(2)	H(15A)-C(15A)-H(15B)	109.5
C(10A)-C(9A)-H(9AA)	120.0	C(13A)-C(15A)-H(15C)	109.5
H(15A)-C(15A)-H(15C)	109.5	H(20D)-C(20B)-H(20E)	109.5
H(15B)-C(15A)-H(15C)	109.5	C(19A)-C(20B)-H(20F)	109.5
C(13A)-C(16A)-H(16A)	109.5	H(20D)-C(20B)-H(20F)	109.5
C(13A)-C(16A)-H(16B)	109.5	H(20E)-C(20B)-H(20F)	109.5
H(16A)-C(16A)-H(16B)	109.5	C(22A)-C(21A)-P(21)	119.4(4)

C(13A)-C(16A)-H(16C)	109.5	C(22A)-C(21A)-H(21A)	107.5
H(16A)-C(16A)-H(16C)	109.5	P(21)-C(21A)-H(21A)	107.5
H(16B)-C(16A)-H(16C)	109.5	C(22A)-C(21A)-H(21B)	107.5
C(18A)-C(17A)-P(21)	117.7(4)	P(21)-C(21A)-H(21B)	107.5
C(18A)-C(17A)-H(17A)	107.9	H(21A)-C(21A)-H(21B)	107.0
P(21)-C(17A)-H(17A)	107.9	C(21A)-C(22A)-H(22A)	109.5
C(18A)-C(17A)-H(17B)	107.9	C(21A)-C(22A)-H(22B)	109.5
P(21)-C(17A)-H(17B)	107.9	H(22A)-C(22A)-H(22B)	109.5
H(17A)-C(17A)-H(17B)	107.2	C(21A)-C(22A)-H(22C)	109.5
C(17A)-C(18A)-H(18A)	109.5	H(22A)-C(22A)-H(22C)	109.5
C(17A)-C(18A)-H(18B)	109.5	H(22B)-C(22A)-H(22C)	109.5
H(18A)-C(18A)-H(18B)	109.5	C(28A)-C(23A)-C(24A)	117.7(3)
C(17A)-C(18A)-H(18C)	109.5	C(28A)-C(23A)-P(22)	125.5(3)
H(18A)-C(18A)-H(18C)	109.5	C(24A)-C(23A)-P(22)	116.8(3)
H(18B)-C(18A)-H(18C)	109.5	C(25A)-C(24A)-C(23A)	121.4(4)
C(20A)-C(19A)-P(21)	131.0(6)	C(25A)-C(24A)-H(24A)	119.3
C(20B)-C(19A)-P(21)	128.5(7)	C(23A)-C(24A)-H(24A)	119.3
C(20A)-C(19A)-H(19C)	104.5	C(26A)-C(25A)-C(24A)	120.3(4)
P(21)-C(19A)-H(19C)	104.5	C(26A)-C(25A)-H(25A)	119.8
C(20A)-C(19A)-H(19D)	104.5	C(24A)-C(25A)-H(25A)	119.8
P(21)-C(19A)-H(19D)	104.5	C(25A)-C(26A)-C(27A)	118.9(3)
H(19C)-C(19A)-H(19D)	105.7	C(25A)-C(26A)-H(26A)	120.6
C(19A)-C(20A)-H(20A)	109.5	C(27A)-C(26A)-H(26A)	120.6
C(19A)-C(20A)-H(20B)	109.5	C(26A)-C(27A)-C(28A)	120.9(3)
H(20A)-C(20A)-H(20B)	109.5	C(26A)-C(27A)-H(27A)	119.6
C(19A)-C(20A)-H(20C)	109.5	C(28A)-C(27A)-H(27A)	119.6
H(20A)-C(20A)-H(20C)	109.5	C(27A)-C(28A)-C(23A)	120.8(3)
H(20B)-C(20A)-H(20C)	109.5	C(27A)-C(28A)-H(28A)	119.6
C(19A)-C(20B)-H(20D)	109.5	C(23A)-C(28A)-H(28A)	119.6
C(19A)-C(20B)-H(20E)	109.5	C(34A)-C(29A)-C(30A)	117.8(3)
C(34A)-C(29A)-P(22)	123.0(3)	H(1SA)-O(1S)-H(1SB)	102.1
C(30A)-C(29A)-P(22)	119.1(3)	C(47)-P(3)-C(53)	100.1(7)
C(31A)-C(30A)-C(29A)	121.8(3)	C(47)-P(3)-C(41)	106.5(8)
C(31A)-C(30A)-H(30A)	119.1	C(53)-P(3)-C(41)	96.2(8)
C(29A)-C(30A)-H(30A)	119.1	C(42)-C(41)-C(46)	115.8(13)
C(30A)-C(31A)-C(32A)	119.9(3)	C(42)-C(41)-P(3)	127.3(11)

C(30A)-C(31A)-H(31A)	120.1	C(46)-C(41)-P(3)	116.7(12)
C(32A)-C(31A)-H(31A)	120.1	C(43)-C(42)-C(41)	122.1(14)
C(33A)-C(32A)-C(31A)	119.2(3)	C(43)-C(42)-H(42)	118.9
C(33A)-C(32A)-H(32A)	120.4	C(41)-C(42)-H(42)	118.9
C(31A)-C(32A)-H(32A)	120.4	C(44)-C(43)-C(42)	124.5(15)
C(32A)-C(33A)-C(34A)	120.8(3)	C(44)-C(43)-H(43)	117.7
C(32A)-C(33A)-H(33A)	119.6	C(42)-C(43)-H(43)	117.7
C(34A)-C(33A)-H(33A)	119.6	C(43)-C(44)-C(45)	112.0(14)
C(29A)-C(34A)-C(33A)	120.5(3)	C(43)-C(44)-H(44)	124.0
C(29A)-C(34A)-H(34A)	119.8	C(45)-C(44)-H(44)	124.0
C(33A)-C(34A)-H(34A)	119.8	C(44)-C(45)-C(46)	125.0(15)
C(40A)-C(35A)-C(36A)	118.6(3)	C(44)-C(45)-H(45)	117.5
C(40A)-C(35A)-P(22)	121.4(3)	C(46)-C(45)-H(45)	117.5
C(36A)-C(35A)-P(22)	120.0(3)	C(41)-C(46)-C(45)	119.4(13)
C(37A)-C(36A)-C(35A)	120.6(3)	C(41)-C(46)-H(46)	120.3
C(37A)-C(36A)-H(36A)	119.7	C(45)-C(46)-H(46)	120.3
C(35A)-C(36A)-H(36A)	119.7	C(48)-C(47)-C(52)	115.8(12)
C(38A)-C(37A)-C(36A)	120.2(4)	C(48)-C(47)-P(3)	115.5(10)
C(38A)-C(37A)-H(37A)	119.9	C(52)-C(47)-P(3)	127.9(11)
C(36A)-C(37A)-H(37A)	119.9	C(49)-C(48)-C(47)	119.3(13)
C(37A)-C(38A)-C(39A)	119.4(3)	C(49)-C(48)-H(48)	120.3
C(37A)-C(38A)-H(38A)	120.3	C(47)-C(48)-H(48)	120.3
C(39A)-C(38A)-H(38A)	120.3	C(50)-C(49)-C(48)	128.6(14)
C(38A)-C(39A)-C(40A)	120.6(3)	C(50)-C(49)-H(49)	115.7
C(38A)-C(39A)-H(39A)	119.7	C(48)-C(49)-H(49)	115.7
C(40A)-C(39A)-H(39A)	119.7	C(49)-C(50)-C(51)	110.6(12)
C(35A)-C(40A)-C(39A)	120.6(4)	C(49)-C(50)-H(50)	124.7
C(35A)-C(40A)-H(40A)	119.7	C(51)-C(50)-H(50)	124.7
C(39A)-C(40A)-H(40A)	119.7	C(50)-C(51)-C(52)	122.7(13)
C(50)-C(51)-H(51)	118.6	C(60)-C(61)-C(62)	143.0
C(52)-C(51)-H(51)	118.6	C(60)-C(61)-H(61A)	101.2
C(47)-C(52)-C(51)	121.8(13)	C(62)-C(61)-H(61A)	101.2
C(47)-C(52)-H(52)	119.1	C(60)-C(61)-H(61B)	101.2
C(51)-C(52)-H(52)	119.1	C(62)-C(61)-H(61B)	101.2
C(54)-C(53)-C(58)	117.7(13)	H(61A)-C(61)-H(61B)	104.5
C(54)-C(53)-P(3)	123.5(12)	C(63')-C(62)-C(61)	122.9

C(58)-C(53)-P(3)	118.7(12)	C(62)-C(63)-H(63B)	109.5
C(55)-C(54)-C(53)	118.7(13)	H(63A)-C(63)-H(63B)	109.5
C(55)-C(54)-H(54)	120.7	C(62)-C(63)-H(63C)	109.5
C(53)-C(54)-H(54)	120.7	H(63A)-C(63)-H(63C)	109.5
C(56)-C(55)-C(54)	127.3(14)	H(63B)-C(63)-H(63C)	109.5
C(56)-C(55)-H(55)	116.4	C(62)-C(63')-H(63D)	109.5
C(54)-C(55)-H(55)	116.4	C(62)-C(63')-H(63E)	109.5
C(55)-C(56)-C(57)	112.8(14)	H(63D)-C(63')-H(63E)	109.5
C(55)-C(56)-H(56)	123.6	C(62)-C(63')-H(63F)	109.5
C(57)-C(56)-H(56)	123.6	H(63D)-C(63')-H(63F)	109.5
C(56)-C(57)-C(58)	123.0(14)	H(63E)-C(63')-H(63F)	109.5
C(56)-C(57)-H(57)	118.5		
C(58)-C(57)-H(57)	118.5		
C(53)-C(58)-C(57)	120.4(13)		
C(53)-C(58)-H(58)	119.8		
C(57)-C(58)-H(58)	119.8		
C(60)-C(59)-H(59A)	109.5		
C(60)-C(59)-H(59B)	109.5		
H(59A)-C(59)-H(59B)	109.5		
C(60)-C(59)-H(59C)	109.5		
H(59A)-C(59)-H(59C)	109.5		
H(59B)-C(59)-H(59C)	109.5		
C(61)-C(60)-C(59)	136.9		
C(61)-C(60)-H(60A)	102.9		
C(59)-C(60)-H(60A)	102.9		
C(61)-C(60)-H(60B)	102.9		
C(59)-C(60)-H(60B)	102.9		
H(60A)-C(60)-H(60B)	105.1		
C(63)-C(62)-C(61)	141.9		
C(63)-C(62)-H(62A)	101.5		
C(61)-C(62)-H(62A)	101.5		
C(63)-C(62)-H(62B)	101.5		
C(61)-C(62)-H(62B)	101.5		
H(62A)-C(62)-H(62B)	104.6		
C(62)-C(63)-H(63A)	109.5		

Table D-4.5: Anisotropic displacement parameters ($\text{\AA}^2 \times 10^3$) for Compound 7. The anisotropic displacement factor exponent takes the form: $-2\pi^2 [h^2 a^{*2} U_{11} + \dots + 2 h k a^{*} b^{*} U_{12}]$

	U ₁₁	U ₂₂	U ₃₃	U ₂₃	U ₁₃	U ₁₂
Ru(1)	15(1)	14(1)	25(1)	5(1)	3(1)	2(1)
P(11)	20(1)	21(1)	32(1)	12(1)	5(1)	3(1)
P(12)	17(1)	15(1)	22(1)	5(1)	5(1)	4(1)
N(11)	33(2)	31(2)	24(2)	3(1)	4(1)	9(1)
N(12)	25(2)	27(2)	34(2)	7(1)	5(1)	4(1)
C(1)	17(2)	21(2)	30(2)	6(1)	4(1)	7(1)
C(2)	22(2)	22(2)	30(2)	5(1)	9(1)	9(1)
C(3)	22(2)	21(2)	24(2)	4(1)	5(1)	4(1)
C(4)	27(2)	23(2)	27(2)	0(1)	6(2)	5(1)
C(5)	47(3)	38(2)	25(2)	-3(2)	-4(2)	11(2)
C(6)	86(3)	99(3)	40(2)	-6(2)	-12(2)	21(2)
C(7)	86(3)	99(3)	40(2)	-6(2)	-12(2)	21(2)
C(8)	86(3)	99(3)	40(2)	-6(2)	-12(2)	21(2)
C(9)	18(2)	25(2)	31(2)	7(2)	0(1)	4(1)
C(10)	16(2)	20(2)	32(2)	4(1)	0(1)	0(1)
C(11)	15(2)	21(2)	39(2)	4(2)	0(2)	-2(1)
C(12)	20(2)	20(2)	41(2)	9(2)	0(2)	-2(1)
C(13)	32(2)	27(2)	28(2)	6(2)	10(2)	7(2)
C(14)	35(2)	37(2)	45(3)	4(2)	16(2)	7(2)
C(15)	40(2)	27(2)	35(2)	1(2)	3(2)	9(2)
C(16)	56(3)	48(3)	43(3)	19(2)	19(2)	25(2)
C(17)	32(2)	21(2)	45(2)	15(2)	-2(2)	1(2)
C(18)	37(2)	20(2)	60(3)	13(2)	-1(2)	7(2)
C(19)	33(2)	49(3)	49(3)	26(2)	19(2)	12(2)
C(20)	35(3)	151(7)	50(3)	48(4)	17(2)	22(3)
C(21)	29(2)	19(2)	32(2)	9(2)	4(2)	4(1)
C(22)	29(2)	44(2)	35(2)	19(2)	3(2)	5(2)
C(23)	33(2)	18(2)	28(2)	12(1)	12(2)	13(1)
C(24)	34(2)	44(2)	36(2)	19(2)	16(2)	22(2)

C(25)	51(3)	67(3)	47(3)	31(2)	31(2)	38(2)
-------	-------	-------	-------	-------	-------	-------

	U11	U22	U33	U23	U13	U12
C(26)	88(4)	61(3)	45(3)	30(2)	45(3)	50(3)
C(27)	79(3)	36(2)	29(2)	7(2)	19(2)	22(2)
C(28)	43(2)	24(2)	28(2)	7(2)	10(2)	9(2)
C(29)	19(2)	14(2)	25(2)	2(1)	3(1)	3(1)
C(30)	26(2)	18(2)	33(2)	9(2)	2(2)	4(1)
C(31)	23(2)	22(2)	41(2)	10(2)	-4(2)	5(1)
C(32)	19(2)	21(2)	46(2)	10(2)	4(2)	3(1)
C(33)	23(2)	24(2)	37(2)	12(2)	9(2)	5(1)
C(34)	20(2)	23(2)	25(2)	5(1)	5(1)	6(1)
C(35)	13(2)	18(2)	28(2)	9(1)	5(1)	4(1)
C(36)	20(2)	22(2)	28(2)	8(1)	9(1)	6(1)
C(37)	21(2)	21(2)	36(2)	11(2)	12(2)	9(1)
C(38)	18(2)	30(2)	35(2)	17(2)	9(2)	10(1)
C(39)	17(2)	34(2)	26(2)	10(2)	4(1)	9(1)
C(40)	17(2)	21(2)	30(2)	7(1)	7(1)	5(1)
Ru(2)	29(1)	33(1)	17(1)	2(1)	3(1)	11(1)
P(21)	36(1)	27(1)	40(1)	-3(1)	-1(1)	10(1)
P(22)	17(1)	22(1)	17(1)	4(1)	4(1)	6(1)
N(21)	51(2)	45(2)	38(2)	21(2)	20(2)	23(2)
N(22)	117(4)	50(3)	24(2)	4(2)	10(2)	16(3)
C(1A)	30(2)	46(2)	24(2)	9(2)	-4(2)	10(2)
C(2A)	38(2)	50(2)	23(2)	12(2)	1(2)	17(2)
C(3A)	37(2)	45(2)	27(2)	12(2)	9(2)	18(2)
C(4A)	46(2)	49(3)	26(2)	17(2)	13(2)	24(2)
C(5A)	73(3)	53(3)	45(3)	28(2)	33(2)	28(3)
C(6A)	167(8)	113(6)	101(6)	81(5)	82(6)	89(6)
C(7A)	91(5)	86(4)	48(3)	27(3)	39(3)	18(3)
C(8A)	82(4)	77(4)	68(4)	29(3)	34(3)	1(3)
C(9A)	29(2)	40(2)	28(2)	5(2)	8(2)	13(2)
C(10A)	35(2)	50(3)	29(2)	8(2)	16(2)	18(2)
C(11A)	52(3)	48(3)	24(2)	4(2)	12(2)	22(2)
C(12A)	75(3)	45(3)	29(2)	6(2)	16(2)	22(2)

C(13A)	175(7)	52(3)	24(2)	5(2)	5(4)	12(4)
--------	--------	-------	-------	------	------	-------

	U11	U22	U33	U23	U13	U12
C(14A)	247(10)	58(4)	30(3)	14(3)	-1(5)	14(5)
C(15A)	220(9)	63(4)	29(3)	1(3)	32(4)	16(5)
C(16A)	176(6)	80(5)	39(3)	13(3)	-31(4)	21(5)
C(17A)	52(3)	42(3)	71(3)	-25(3)	16(2)	4(2)
C(18A)	61(3)	67(4)	47(3)	-26(3)	2(2)	5(3)
C(19A)	48(3)	49(3)	181(7)	52(4)	-1(3)	15(2)
C(20A)	77(7)	44(6)	83(7)	29(5)	40(5)	27(5)
C(20B)	48(3)	49(3)	181(7)	52(4)	-1(3)	15(2)
C(21A)	55(3)	24(2)	30(2)	4(2)	-2(2)	7(2)
C(22A)	82(4)	28(2)	57(3)	13(2)	3(3)	5(2)
C(23A)	21(2)	19(2)	19(2)	2(1)	4(1)	7(1)
C(24A)	26(2)	54(3)	39(2)	26(2)	16(2)	19(2)
C(25A)	29(2)	63(3)	46(3)	31(2)	14(2)	27(2)
C(26A)	34(2)	27(2)	24(2)	9(2)	5(2)	11(2)
C(27A)	30(2)	33(2)	25(2)	11(2)	11(2)	10(2)
C(28A)	23(2)	31(2)	25(2)	8(2)	6(1)	11(2)
C(29A)	20(2)	23(2)	17(2)	5(1)	2(1)	7(1)
C(30A)	24(2)	20(2)	26(2)	6(1)	5(1)	7(1)
C(31A)	19(2)	26(2)	28(2)	9(2)	4(1)	5(1)
C(32A)	23(2)	31(2)	33(2)	10(2)	6(2)	13(2)
C(33A)	29(2)	20(2)	38(2)	8(2)	6(2)	10(2)
C(34A)	19(2)	22(2)	27(2)	9(1)	3(1)	5(1)
C(35A)	15(2)	26(2)	25(2)	9(1)	4(1)	8(1)
C(36A)	22(2)	28(2)	25(2)	9(2)	5(1)	5(1)
C(37A)	25(2)	26(2)	26(2)	6(1)	1(1)	6(1)
C(38A)	19(2)	26(2)	41(2)	12(2)	5(2)	7(1)
C(39A)	26(2)	29(2)	38(2)	16(2)	15(2)	8(2)
C(40A)	24(2)	31(2)	26(2)	9(2)	8(1)	11(2)
O(1S)	250(30)	190(20)	90(12)	30(13)	30(14)	150(20)
O(2S)	250(30)	190(20)	90(12)	30(13)	30(14)	150(20)
P(3)	125(4)	102(3)	92(3)	39(3)	7(3)	12(3)
C(41)	133(10)	147(16)	95(9)	66(11)	16(8)	51(10)

C(42)	108(11)	260(30)	189(16)	147(19)	23(10)	26(15)
-------	---------	---------	---------	---------	--------	--------

	U11	U22	U33	U23	U13	U12
C(43)	149(14)	320(30)	270(20)	180(20)	134(15)	161(16)
C(44)	270(20)	200(30)	280(30)	150(20)	170(20)	150(20)
C(45)	280(20)	170(20)	205(17)	118(16)	165(17)	170(20)
C(46)	234(19)	123(15)	103(9)	43(10)	73(10)	103(14)
C(47)	176(16)	90(9)	83(7)	59(6)	17(7)	47(10)
C(48)	65(9)	207(19)	128(11)	54(9)	55(8)	49(11)
C(49)	81(10)	141(13)	150(12)	67(9)	67(9)	30(10)
C(50)	160(14)	63(8)	74(8)	34(7)	56(8)	43(9)
C(51)	190(20)	148(19)	106(12)	7(10)	3(11)	87(16)
C(52)	210(20)	137(15)	72(8)	30(8)	32(8)	106(15)
C(53)	118(13)	101(8)	95(11)	33(8)	17(10)	29(8)
C(54)	202(18)	159(16)	97(14)	-9(12)	51(14)	95(14)
C(55)	164(18)	156(15)	80(13)	-66(12)	-22(11)	103(15)
C(56)	300(30)	122(15)	54(12)	-34(10)	-66(16)	64(15)
C(57)	230(30)	96(11)	65(10)	21(10)	10(30)	-29(16)
C(58)	177(17)	102(12)	121(16)	33(12)	26(14)	-13(11)
C(59)	280(30)	150(19)	82(12)	57(12)	9(14)	120(19)
C(60)	290(40)	500(60)	190(30)	-60(30)	-60(30)	290(40)
C(61)	62(9)	134(13)	189(18)	83(11)	27(10)	37(9)
C(62)	89(15)	320(30)	260(30)	-140(30)	-76(17)	77(17)
C(63)	141(11)	159(11)	159(11)	49(6)	33(7)	57(8)
C(63')	141(11)	159(11)	159(11)	49(6)	33(7)	57(8)

Table D-4.6: Hydrogen coordinates ($\times 10^4$) and isotropic displacement parameters ($\text{\AA}^2 \times 10^3$) for Compound 7.

	x	y	z	U(eq)
H(1A)	5458	3144	-246	27
H(1B)	5242	3967	-252	27
H(2)	6151	4483	915	29
H(3)	6040	2956	949	28
H(4)	7341	4380	1918	33
H(6A)	8695	2999	2952	126
H(6B)	9480	3810	3449	126
H(6C)	9454	3611	2661	126
H(7A)	6727	3956	3188	126
H(7B)	7755	4023	3782	126
H(7C)	7041	3205	3269	126
H(8A)	9118	4820	2656	126
H(8B)	9140	4948	3441	126
H(8C)	8104	4998	2920	126
H(9A)	9053	3911	-53	31
H(9B)	9391	3489	534	31
H(10)	8998	4383	1355	30
H(11)	8908	5248	386	34
H(12)	8188	5411	1624	35
H(14D)	6226	6027	1483	61
H(14E)	6667	6528	2256	61
H(14F)	6936	5744	2032	61
H(15D)	8940	6443	2526	55
H(15E)	8729	7252	2730	55
H(15F)	9554	7142	2261	55
H(16D)	8400	7619	1426	68
H(16E)	7575	7668	1906	68
H(16F)	7103	7168	1133	68
H(17C)	8012	5416	-613	42
H(17D)	7182	5074	-1351	42

	x	y	z	U(eq)
H(18D)	5661	4931	-875	61
H(18E)	6453	5803	-612	61
H(18F)	6476	5241	-131	61
H(19A)	9204	4442	-859	49
H(19B)	8636	3556	-1236	49
H(20G)	7983	3878	-2230	114
H(20H)	9306	4182	-1976	114
H(20I)	8614	4764	-1847	114
H(21C)	6263	2949	-1696	34
H(21D)	5484	3353	-1362	34
H(22D)	5178	3277	-2514	55
H(22E)	6435	3791	-2399	55
H(22F)	5598	4155	-2080	55
H(24)	9060	2630	-538	41
H(25)	9764	2156	-1417	55
H(26)	8577	1323	-2424	63
H(27)	6685	1016	-2573	56
H(28)	5949	1483	-1692	38
H(30)	4898	2148	-1241	32
H(31)	3086	1329	-1473	37
H(32)	2624	508	-801	36
H(33)	3963	519	116	33
H(34)	5787	1311	335	28
H(36)	7488	1021	-437	27
H(37)	8247	386	275	30
H(38)	8848	941	1441	31
H(39)	8794	2170	1888	30
H(40)	8076	2827	1173	27
H(1AA)	5532	7899	7062	43
H(1AB)	4926	7207	6358	43
H(2A)	6018	7896	5756	44
H(3A)	6653	9158	6920	41
H(4A)	7598	8958	5779	44

	x	y	z	U(eq)
H(6AA)	7424	10713	5625	155
H(6AB)	8601	11246	5602	155
H(6AC)	8276	11283	6310	155
H(7AA)	8955	9406	5331	109
H(7AB)	8993	10115	5011	109
H(7AC)	7830	9563	5034	109
H(8AA)	9951	10982	6804	115
H(8AB)	10302	10999	6109	115
H(8AC)	10234	10267	6399	115
H(9AA)	8768	7455	7399	39
H(9AB)	9545	8360	7618	39
H(10A)	9057	8428	6478	44
H(11A)	8159	6805	6167	49
H(12A)	7765	7771	5309	59
H(14A)	6953	7851	4354	185
H(14B)	7044	7433	3626	185
H(14C)	8073	7676	4273	185
H(15A)	8027	6283	3942	168
H(15B)	6923	6052	3347	168
H(15C)	6948	5618	3932	168
H(16A)	5301	5961	4207	166
H(16B)	5263	6367	3604	166
H(16C)	5324	6836	4350	166
H(17A)	6598	5763	6003	76
H(17B)	5824	5282	6380	76
H(18A)	4688	5348	5442	104
H(18B)	5245	6257	5609	104
H(18C)	4492	5905	6067	104
H(19C)	7184	5597	7415	112
H(19D)	8087	6033	7094	112
H(20A)	8928	6910	8170	93
H(20B)	8957	6051	8101	93
H(20C)	8091	6339	8456	93

	x	y	z	U(eq)
H(20D)	7900	5243	6777	140
H(20E)	8892	5634	7448	140
H(20F)	8772	6063	6864	140
H(21A)	5993	6706	8013	47
H(21B)	5037	6532	7347	47
H(22A)	4772	5212	7154	90
H(22B)	4638	5559	7891	90
H(22C)	5754	5378	7811	90
H(24A)	9228	8127	8648	42
H(25A)	9746	7591	9512	48
H(26A)	8496	7152	10129	33
H(27A)	6765	7335	9914	34
H(28A)	6264	7911	9075	31
H(30A)	5117	7714	8014	28
H(31A)	3578	8056	8191	29
H(32A)	3702	9354	8508	33
H(33A)	5363	10292	8597	35
H(34A)	6912	9949	8416	28
H(36A)	8480	9567	9349	30
H(37A)	9992	10687	9768	32
H(38A)	10993	11160	9042	34
H(39A)	10420	10543	7887	35
H(40A)	8886	9441	7461	31
H(1SA)	1388	9087	7116	194
H(1SB)	2056	9381	6577	194
H(42)	3394	7923	5043	219
H(43)	4659	8387	4478	244
H(44)	4340	7962	3295	244
H(45)	2443	7348	2726	208
H(46)	1169	6761	3265	165
H(48)	194	8129	5297	151
H(49)	869	9059	6288	139
H(50)	2195	9057	7206	109

	x	y	z	U(eq)
H(51)	3351	8315	6870	180
H(52)	2725	7344	5862	155
H(54)	2619	6276	4465	180
H(55)	2716	5112	4585	174
H(56)	1445	4268	4950	220
H(57)	-149	4621	5088	182
H(58)	-288	5814	5003	176
H(59A)	6120	8299	2653	241
H(59B)	6735	8571	3442	241
H(59C)	7228	9020	2936	241
H(60A)	6098	9524	2827	400
H(60B)	5181	8857	2941	400
H(61A)	6562	10099	3764	146
H(61B)	5954	9409	4013	146
H(62A)	5011	10268	3472	324
H(62B)	4522	9633	3815	324
H(63A)	4440	10672	4266	226
H(63B)	5753	11063	4428	226
H(63C)	5254	10413	4779	226
H(63D)	4950	10931	4340	226
H(63E)	6002	11099	4028	226
H(63F)	6052	10774	4681	226

Table D-4.7: Torsion angles [°] for Compound 7.

Ru(1)-C(1)-C(2)-C(3)	-65.9(3)
C(1)-C(2)-C(3)-C(4)	176.6(3)
Ru(1)-C(2)-C(3)-C(4)	113.1(3)
C(1)-C(2)-C(3)-Ru(1)	63.5(3)
C(5)-N(11)-C(4)-C(3)	177.9(4)
C(2)-C(3)-C(4)-N(11)	169.1(4)
Ru(1)-C(3)-C(4)-N(11)	-114.4(4)
C(4)-N(11)-C(5)-C(6)	-134.3(5)
C(4)-N(11)-C(5)-C(7)	105.4(5)
C(4)-N(11)-C(5)-C(8)	-17.6(6)
Ru(1)-C(9)-C(10)-C(11)	-66.2(3)
C(9)-C(10)-C(11)-C(12)	-179.6(3)
Ru(1)-C(10)-C(11)-C(12)	116.1(3)
C(9)-C(10)-C(11)-Ru(1)	64.3(3)
C(13)-N(12)-C(12)-C(11)	179.9(3)
C(10)-C(11)-C(12)-N(12)	164.5(3)
Ru(1)-C(11)-C(12)-N(12)	-118.4(4)
C(12)-N(12)-C(13)-C(15)	64.5(4)
C(12)-N(12)-C(13)-C(16)	-176.5(3)
C(12)-N(12)-C(13)-C(14)	-59.2(4)
C(19)-P(11)-C(17)-C(18)	-177.8(3)
C(21)-P(11)-C(17)-C(18)	74.1(3)
Ru(1)-P(11)-C(17)-C(18)	-50.0(3)
C(17)-P(11)-C(19)-C(20)	-54.9(5)
C(21)-P(11)-C(19)-C(20)	51.4(5)
Ru(1)-P(11)-C(19)-C(20)	177.8(4)
C(19)-P(11)-C(21)-C(22)	-68.4(4)
C(17)-P(11)-C(21)-C(22)	36.0(4)
Ru(1)-P(11)-C(21)-C(22)	162.4(3)
C(35)-P(12)-C(23)-C(28)	117.3(3)
C(29)-P(12)-C(23)-C(28)	16.4(3)
Ru(1)-P(12)-C(23)-C(28)	-117.9(3)
C(35)-P(12)-C(23)-C(24)	-58.6(3)
C(29)-P(12)-C(23)-C(24)	-159.5(3)

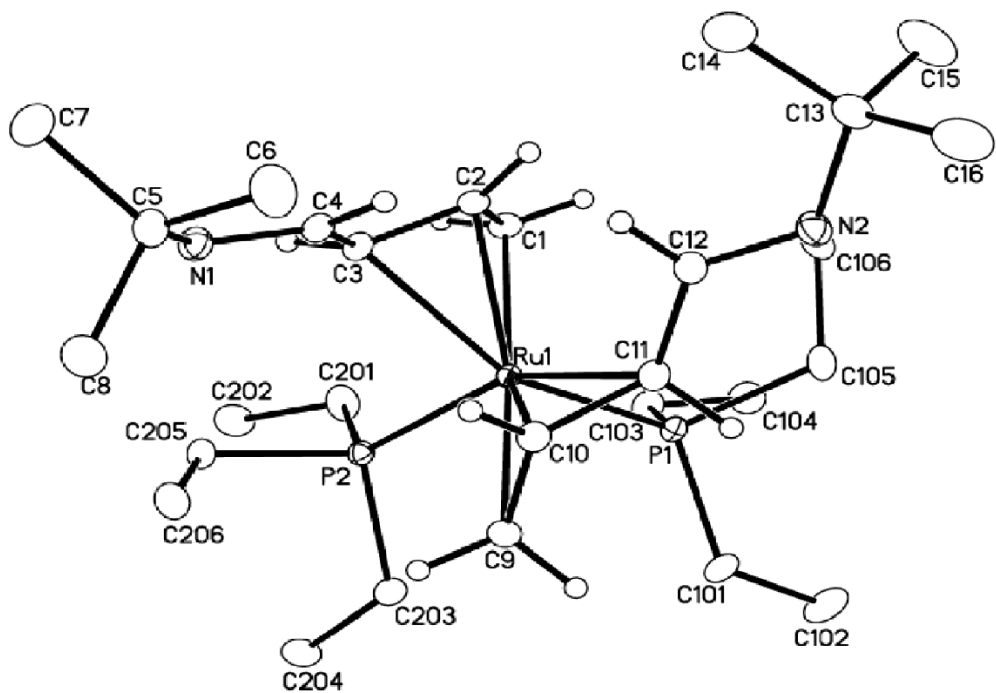
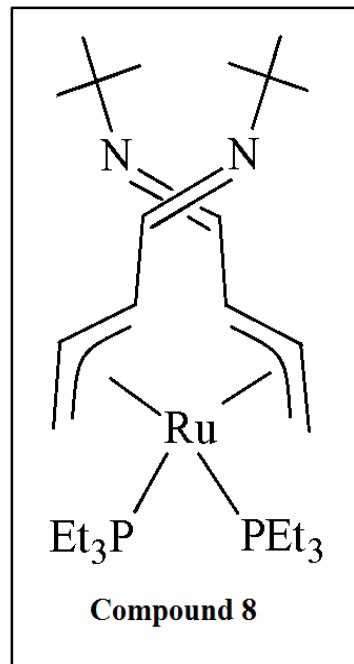
Ru(1)-P(12)-C(23)-C(24)	66.2(3)
C(28)-C(23)-C(24)-C(25)	-1.1(6)
P(12)-C(23)-C(24)-C(25)	175.1(3)
C(23)-C(24)-C(25)-C(26)	-0.2(7)
C(24)-C(25)-C(26)-C(27)	1.7(7)
C(25)-C(26)-C(27)-C(28)	-1.8(7)
C(24)-C(23)-C(28)-C(27)	1.0(6)
P(12)-C(23)-C(28)-C(27)	-174.8(3)
C(26)-C(27)-C(28)-C(23)	0.5(6)
C(35)-P(12)-C(29)-C(34)	18.0(3)
C(23)-P(12)-C(29)-C(34)	117.5(3)
Ru(1)-P(12)-C(29)-C(34)	-108.3(3)
C(35)-P(12)-C(29)-C(30)	-165.6(3)
C(23)-P(12)-C(29)-C(30)	-66.1(3)
Ru(1)-P(12)-C(29)-C(30)	68.1(3)
C(34)-C(29)-C(30)-C(31)	-2.7(5)
P(12)-C(29)-C(30)-C(31)	-179.2(3)
C(29)-C(30)-C(31)-C(32)	1.5(6)
C(30)-C(31)-C(32)-C(33)	0.8(6)
C(31)-C(32)-C(33)-C(34)	-1.7(6)
C(30)-C(29)-C(34)-C(33)	1.8(5)
P(12)-C(29)-C(34)-C(33)	178.3(3)
C(32)-C(33)-C(34)-C(29)	0.4(6)
C(29)-P(12)-C(35)-C(40)	-108.1(3)
C(23)-P(12)-C(35)-C(40)	147.8(3)
Ru(1)-P(12)-C(35)-C(40)	20.6(3)
C(29)-P(12)-C(35)-C(36)	67.4(3)
C(23)-P(12)-C(35)-C(36)	-36.8(3)
Ru(1)-P(12)-C(35)-C(36)	-163.9(2)
C(40)-C(35)-C(36)-C(37)	1.2(5)
P(12)-C(35)-C(36)-C(37)	-174.4(3)
C(35)-C(36)-C(37)-C(38)	0.9(5)
C(36)-C(37)-C(38)-C(39)	-2.2(5)
C(37)-C(38)-C(39)-C(40)	1.3(5)
C(36)-C(35)-C(40)-C(39)	-2.1(5)
P(12)-C(35)-C(40)-C(39)	173.4(3)

C(38)-C(39)-C(40)-C(35)	0.9(5)
Ru(2)-C(1A)-C(2A)-C(3A)	-67.3(4)
C(1A)-C(2A)-C(3A)-C(4A)	-178.4(4)
Ru(2)-C(2A)-C(3A)-C(4A)	116.3(4)
C(1A)-C(2A)-C(3A)-Ru(2)	65.3(4)
C(5A)-N(21)-C(4A)-C(3A)	-176.6(4)
C(2A)-C(3A)-C(4A)-N(21)	163.6(4)
Ru(2)-C(3A)-C(4A)-N(21)	-119.3(4)
C(4A)-N(21)-C(5A)-C(8A)	-123.7(5)
C(4A)-N(21)-C(5A)-C(7A)	0.0(7)
C(4A)-N(21)-C(5A)-C(6A)	120.1(6)
Ru(2)-C(9A)-C(10A)-C(11A)	-66.3(4)
C(9A)-C(10A)-C(11A)-C(12A)	179.8(4)
Ru(2)-C(10A)-C(11A)-C(12A)	115.0(4)
C(9A)-C(10A)-C(11A)-Ru(2)	64.8(3)
C(13A)-N(22)-C(12A)-C(11A)	179.2(6)
C(10A)-C(11A)-C(12A)-N(22)	165.0(5)
Ru(2)-C(11A)-C(12A)-N(22)	-115.9(5)
C(12A)-N(22)-C(13A)-C(16A)	-109.3(7)
C(12A)-N(22)-C(13A)-C(15A)	134.3(7)
C(12A)-N(22)-C(13A)-C(14A)	12.6(11)
C(19A)-P(21)-C(17A)-C(18A)	171.6(5)
C(21A)-P(21)-C(17A)-C(18A)	68.8(5)
Ru(2)-P(21)-C(17A)-C(18A)	-56.3(5)
C(21A)-P(21)-C(19A)-C(20A)	-74.2(8)
C(17A)-P(21)-C(19A)-C(20A)	-178.1(8)
Ru(2)-P(21)-C(19A)-C(20A)	54.4(9)
C(21A)-P(21)-C(19A)-C(20B)	148.4(7)
C(17A)-P(21)-C(19A)-C(20B)	44.5(8)
Ru(2)-P(21)-C(19A)-C(20B)	-83.0(8)
C(19A)-P(21)-C(21A)-C(22A)	-51.1(4)
C(17A)-P(21)-C(21A)-C(22A)	49.1(4)
Ru(2)-P(21)-C(21A)-C(22A)	175.2(3)
C(29A)-P(22)-C(23A)-C(28A)	18.4(3)
C(35A)-P(22)-C(23A)-C(28A)	122.7(3)
Ru(2)-P(22)-C(23A)-C(28A)	-114.7(3)

C(29A)-P(22)-C(23A)-C(24A)	-161.6(3)
C(35A)-P(22)-C(23A)-C(24A)	-57.2(3)
Ru(2)-P(22)-C(23A)-C(24A)	65.4(3)
C(28A)-C(23A)-C(24A)-C(25A)	1.6(6)
P(22)-C(23A)-C(24A)-C(25A)	-178.4(4)
C(23A)-C(24A)-C(25A)-C(26A)	0.9(7)
C(24A)-C(25A)-C(26A)-C(27A)	-2.3(7)
C(25A)-C(26A)-C(27A)-C(28A)	1.1(6)
C(26A)-C(27A)-C(28A)-C(23A)	1.5(6)
C(24A)-C(23A)-C(28A)-C(27A)	-2.8(5)
P(22)-C(23A)-C(28A)-C(27A)	177.2(3)
C(23A)-P(22)-C(29A)-C(34A)	114.6(3)
C(35A)-P(22)-C(29A)-C(34A)	13.7(3)
Ru(2)-P(22)-C(29A)-C(34A)	-112.8(3)
C(23A)-P(22)-C(29A)-C(30A)	-68.5(3)
C(35A)-P(22)-C(29A)-C(30A)	-169.5(3)
Ru(2)-P(22)-C(29A)-C(30A)	64.0(3)
C(34A)-C(29A)-C(30A)-C(31A)	-1.6(5)
P(22)-C(29A)-C(30A)-C(31A)	-178.6(3)
C(29A)-C(30A)-C(31A)-C(32A)	0.0(5)
C(30A)-C(31A)-C(32A)-C(33A)	1.5(6)
C(31A)-C(32A)-C(33A)-C(34A)	-1.4(6)
C(30A)-C(29A)-C(34A)-C(33A)	1.7(5)
P(22)-C(29A)-C(34A)-C(33A)	178.5(3)
C(32A)-C(33A)-C(34A)-C(29A)	-0.2(6)
C(29A)-P(22)-C(35A)-C(40A)	-116.8(3)
C(23A)-P(22)-C(35A)-C(40A)	139.4(3)
Ru(2)-P(22)-C(35A)-C(40A)	13.2(3)
C(29A)-P(22)-C(35A)-C(36A)	65.4(3)
C(23A)-P(22)-C(35A)-C(36A)	-38.3(3)
Ru(2)-P(22)-C(35A)-C(36A)	-164.5(2)
C(40A)-C(35A)-C(36A)-C(37A)	-0.4(5)
P(22)-C(35A)-C(36A)-C(37A)	177.4(3)
C(35A)-C(36A)-C(37A)-C(38A)	-1.1(6)
C(36A)-C(37A)-C(38A)-C(39A)	1.7(5)
C(37A)-C(38A)-C(39A)-C(40A)	-0.8(6)

C(36A)-C(35A)-C(40A)-C(39A)	1.2(5)
P(22)-C(35A)-C(40A)-C(39A)	-176.5(3)
C(38A)-C(39A)-C(40A)-C(35A)	-0.6(6)
C(47)-P(3)-C(41)-C(42)	10.8(16)
C(53)-P(3)-C(41)-C(42)	-91.6(15)
C(47)-P(3)-C(41)-C(46)	-163.7(13)
C(53)-P(3)-C(41)-C(46)	93.9(14)
C(46)-C(41)-C(42)-C(43)	3.6(16)
P(3)-C(41)-C(42)-C(43)	-170.9(16)
C(41)-C(42)-C(43)-C(44)	-5(2)
C(42)-C(43)-C(44)-C(45)	9(3)
C(43)-C(44)-C(45)-C(46)	-12(4)
C(42)-C(41)-C(46)-C(45)	-7(2)
P(3)-C(41)-C(46)-C(45)	168.5(14)
C(44)-C(45)-C(46)-C(41)	12(3)
C(53)-P(3)-C(47)-C(48)	-146.4(11)
C(41)-P(3)-C(47)-C(48)	114.0(12)
C(53)-P(3)-C(47)-C(52)	44.2(16)
C(41)-P(3)-C(47)-C(52)	-55.4(16)
C(52)-C(47)-C(48)-C(49)	0.1(16)
P(3)-C(47)-C(48)-C(49)	-170.7(11)
C(47)-C(48)-C(49)-C(50)	-7.3(17)
C(48)-C(49)-C(50)-C(51)	13(2)
C(49)-C(50)-C(51)-C(52)	-12(3)
C(48)-C(47)-C(52)-C(51)	0(3)
P(3)-C(47)-C(52)-C(51)	169.3(16)
C(50)-C(51)-C(52)-C(47)	7(3)
C(47)-P(3)-C(53)-C(54)	-101.7(13)
C(41)-P(3)-C(53)-C(54)	6.3(13)
C(47)-P(3)-C(53)-C(58)	81.5(15)
C(41)-P(3)-C(53)-C(58)	-170.5(14)
C(58)-C(53)-C(54)-C(55)	-0.4(16)
P(3)-C(53)-C(54)-C(55)	-177.2(12)
C(53)-C(54)-C(55)-C(56)	-1.2(18)
C(54)-C(55)-C(56)-C(57)	3(3)
C(55)-C(56)-C(57)-C(58)	-4(3)

C(54)-C(53)-C(58)-C(57)	0(3)
P(3)-C(53)-C(58)-C(57)	176.5(17)
C(56)-C(57)-C(58)-C(53)	3(4)
C(59)-C(60)-C(61)-C(62)	-163.1
C(60)-C(61)-C(62)-C(63')	-141.5
C(60)-C(61)-C(62)-C(63)	-172.2



Molecular Structure of Compound 8

Table D-5.1: Crystal data and structure refinement for Compound 8.

Empirical formula	$C_{28} H_{58} N_2 P_2 Ru$	
Formula weight	585.77	
Temperature	100(2) K	
Wavelength	0.71073 Å	
Crystal system	Triclinic	
Space group	P 1 bar	
Unit cell dimensions	$a = 9.1351(6)$ Å	$\alpha = 78.638(2)^\circ$.
	$b = 12.0450(7)$ Å	$\beta = 85.286(3)^\circ$.
	$c = 14.3466(9)$ Å	$\gamma = 88.256(3)^\circ$.
Volume	$1542.25(17)$ Å ³	
Z	2	
Density (calculated)	1.261 Mg/m ³	
Absorption coefficient	0.630 mm ⁻¹	
F(000)	628	
Crystal size	$0.298 \times 0.253 \times 0.216$ mm ³	
Theta range for data collection	1.452 to 36.384°.	
Index ranges	$-15 \leq h \leq 15, -20 \leq k \leq 20, -23 \leq l \leq 23$	
Reflections collected	116324	
Independent reflections	14895 [R(int) = 0.0408]	
Completeness to theta = 25.242°	99.5 %	
Absorption correction	Semi-empirical from equivalents	
Max. and min. transmission	0.7471 and 0.7082	
Refinement method	Full-matrix least-squares on F ²	
Data / restraints / parameters	14895 / 0 / 310	
Goodness-of-fit on F ²	1.049	
Final R indices [I>2sigma(I)]	R1 = 0.0239, wR2 = 0.0550	
R indices (all data)	R1 = 0.0285, wR2 = 0.0572	
Extinction coefficient	n/a	
Largest diff. peak and hole	0.666 and -0.614 e.Å ⁻³	

Table D-5.2: Atomic coordinates ($\times 10^4$) and equivalent isotropic displacement parameters ($\text{\AA}^2 \times 10^3$) for Compound 8. U(eq) is defined as one third of the trace of the orthogonalized \mathbf{U}^{ij} tensor.

	x	y	z	U(eq)
Ru(1)	173(1)	440(1)	2447(1)	8(1)
P(1)	1860(1)	1475(1)	1330(1)	10(1)
P(2)	-882(1)	1964(1)	3070(1)	10(1)
N(1)	-2718(1)	-1804(1)	4403(1)	14(1)
N(2)	1881(1)	-2388(1)	1228(1)	15(1)
C(1)	1900(1)	147(1)	3491(1)	13(1)
C(2)	1005(1)	-810(1)	3572(1)	12(1)
C(3)	-509(1)	-745(1)	3891(1)	12(1)
C(4)	-1461(1)	-1705(1)	3935(1)	12(1)
C(5)	-3668(1)	-2768(1)	4381(1)	15(1)
C(6)	-3061(1)	-3605(1)	3761(1)	22(1)
C(7)	-3950(1)	-3394(1)	5418(1)	21(1)
C(8)	-5107(1)	-2242(1)	4008(1)	21(1)
C(9)	-1640(1)	636(1)	1460(1)	12(1)
C(10)	-1174(1)	-504(1)	1722(1)	12(1)
C(11)	276(1)	-825(1)	1420(1)	12(1)
C(12)	799(1)	-1989(1)	1692(1)	12(1)
C(13)	2391(1)	-3568(1)	1528(1)	17(1)
C(14)	1680(2)	-4217(1)	2469(1)	29(1)
C(15)	4045(1)	-3507(1)	1599(1)	31(1)
C(16)	2115(2)	-4177(1)	714(1)	29(1)
C(101)	1136(1)	2290(1)	236(1)	17(1)
C(102)	2151(1)	2948(1)	-568(1)	24(1)
C(103)	2885(1)	2513(1)	1811(1)	15(1)
C(104)	4373(1)	2938(1)	1315(1)	18(1)
C(105)	3344(1)	659(1)	801(1)	16(1)
C(106)	4169(1)	-189(1)	1513(1)	19(1)
C(201)	211(1)	2753(1)	3753(1)	18(1)
C(202)	-555(1)	3433(1)	4451(1)	21(1)

	x	y	z	U(eq)
C(203)	-1527(1)	3109(1)	2128(1)	16(1)
C(204)	-2430(1)	4101(1)	2396(1)	19(1)
C(205)	-2537(1)	1652(1)	3899(1)	13(1)
C(206)	-3749(1)	1029(1)	3547(1)	17(1)

Table D-5.3: Bond lengths [Å] for Compound 8.

Ru(1)-C(2)	2.1507(8)	Ru(1)-C(2)	2.1507(8)
Ru(1)-C(10)	2.1571(8)	Ru(1)-C(10)	2.1571(8)
Ru(1)-C(1)	2.2372(9)	Ru(1)-C(1)	2.2372(9)
Ru(1)-C(9)	2.2437(9)	Ru(1)-C(9)	2.2437(9)
Ru(1)-C(11)	2.3142(8)	Ru(1)-C(11)	2.3142(8)
Ru(1)-C(3)	2.3231(8)	Ru(1)-C(3)	2.3231(8)
Ru(1)-P(1)	2.3274(3)	Ru(1)-P(1)	2.3274(3)
Ru(1)-P(2)	2.3442(2)	Ru(1)-P(2)	2.3442(2)
P(1)-C(101)	1.8412(10)	P(1)-C(101)	1.8412(10)
P(1)-C(105)	1.8510(9)	C(7)-H(7B)	0.9800
P(1)-C(103)	1.8526(9)	C(7)-H(7C)	0.9800
P(2)-C(205)	1.8455(9)	C(8)-H(8A)	0.9800
P(2)-C(203)	1.8496(9)	C(8)-H(8B)	0.9800
P(2)-C(201)	1.8557(9)	C(8)-H(8C)	0.9800
N(1)-C(4)	1.2783(12)	C(9)-C(10)	1.4132(12)
N(1)-C(5)	1.4776(12)	C(9)-H(9A)	0.9900
N(2)-C(12)	1.2805(11)	C(9)-H(9B)	0.9900
N(2)-C(13)	1.4750(12)	C(10)-C(11)	1.4246(12)
C(1)-C(2)	1.4140(12)	C(10)-H(10)	1.0000
C(1)-H(1A)	0.9900	C(11)-C(12)	1.4561(12)
C(1)-H(1B)	0.9900	C(11)-H(11)	1.0000
C(2)-C(3)	1.4248(12)	C(12)-H(12)	0.9500
C(2)-H(2)	1.0000	C(13)-C(14)	1.5249(15)
C(3)-C(4)	1.4570(12)	C(13)-C(15)	1.5285(16)
C(3)-H(3)	1.0000	C(13)-C(16)	1.5366(15)
C(4)-H(4)	0.9500	C(14)-H(14A)	0.9800
C(5)-C(8)	1.5319(14)	C(14)-H(14B)	0.9800
C(5)-C(7)	1.5343(14)	C(14)-H(14C)	0.9800
C(5)-C(6)	1.5345(13)	C(15)-H(15A)	0.9800
C(6)-H(6A)	0.9800	C(15)-H(15B)	0.9800
C(6)-H(6B)	0.9800	C(15)-H(15C)	0.9800
C(6)-H(6C)	0.9800	C(16)-H(16A)	0.9800
C(7)-H(7A)	0.9800	C(16)-H(16B)	0.9800
C(16)-H(16C)	0.9800	C(206)-H(20N)	0.9800

C(101)-C(102)	1.5249(14)
C(101)-H(10A)	0.9900
C(101)-H(10B)	0.9900
C(102)-H(10C)	0.9800
C(102)-H(10D)	0.9800
C(102)-H(10E)	0.9800
C(103)-C(104)	1.5343(13)
C(103)-H(10F)	0.9900
C(103)-H(10G)	0.9900
C(104)-H(10H)	0.9800
C(104)-H(10I)	0.9800
C(104)-H(10J)	0.9800
C(105)-C(106)	1.5246(15)
C(105)-H(10K)	0.9900
C(105)-H(10L)	0.9900
C(106)-H(10M)	0.9800
C(106)-H(10N)	0.9800
C(106)-H(10O)	0.9800
C(201)-C(202)	1.5285(13)
C(201)-H(20A)	0.9900
C(201)-H(20B)	0.9900
C(202)-H(20C)	0.9800
C(202)-H(20D)	0.9800
C(202)-H(20E)	0.9800
C(203)-C(204)	1.5251(13)
C(203)-H(20F)	0.9900
C(203)-H(20G)	0.9900
C(204)-H(20H)	0.9800
C(204)-H(20I)	0.9800
C(204)-H(20J)	0.9800
C(205)-C(206)	1.5284(13)
C(205)-H(20K)	0.9900
C(205)-H(20L)	0.9900
C(206)-H(20M)	0.9800
C(206)-H(20O)	0.9800

Table D-5.4. Bond angles [°] for Compound 8.

C(2)-Ru(1)-C(10)	104.38(3)	C(103)-P(1)-Ru(1)	113.67(3)
C(2)-Ru(1)-C(1)	37.53(3)	C(205)-P(2)-C(203)	102.85(4)
C(10)-Ru(1)-C(1)	139.85(3)	C(205)-P(2)-C(201)	100.61(4)
C(2)-Ru(1)-C(9)	138.81(3)	C(203)-P(2)-C(201)	102.17(5)
C(10)-Ru(1)-C(9)	37.40(3)	C(205)-P(2)-Ru(1)	116.28(3)
C(1)-Ru(1)-C(9)	176.16(3)	C(203)-P(2)-Ru(1)	112.15(3)
C(2)-Ru(1)-C(11)	92.07(3)	C(201)-P(2)-Ru(1)	120.41(3)
C(10)-Ru(1)-C(11)	36.95(3)	C(4)-N(1)-C(5)	120.51(7)
C(1)-Ru(1)-C(11)	114.20(3)	C(12)-N(2)-C(13)	120.64(8)
C(9)-Ru(1)-C(11)	64.98(3)	C(2)-C(1)-Ru(1)	67.91(5)
C(2)-Ru(1)-C(3)	36.89(3)	C(2)-C(1)-H(1A)	116.9
C(10)-Ru(1)-C(3)	90.21(3)	Ru(1)-C(1)-H(1A)	116.9
C(1)-Ru(1)-C(3)	65.05(3)	C(2)-C(1)-H(1B)	116.9
C(9)-Ru(1)-C(3)	111.23(3)	Ru(1)-C(1)-H(1B)	116.9
C(11)-Ru(1)-C(3)	101.02(3)	H(1A)-C(1)-H(1B)	113.9
C(2)-Ru(1)-P(1)	118.11(2)	C(1)-C(2)-C(3)	119.58(7)
C(10)-Ru(1)-P(1)	108.76(2)	C(1)-C(2)-Ru(1)	74.56(5)
C(1)-Ru(1)-P(1)	88.96(2)	C(3)-C(2)-Ru(1)	78.15(5)
C(9)-Ru(1)-P(1)	94.67(2)	C(1)-C(2)-H(2)	120.2
C(11)-Ru(1)-P(1)	85.15(2)	C(3)-C(2)-H(2)	120.2
C(3)-Ru(1)-P(1)	153.64(2)	Ru(1)-C(2)-H(2)	120.2
C(2)-Ru(1)-P(2)	109.93(2)	C(2)-C(3)-C(4)	120.20(7)
C(10)-Ru(1)-P(2)	119.03(2)	C(2)-C(3)-Ru(1)	64.97(5)
C(1)-Ru(1)-P(2)	92.78(2)	C(4)-C(3)-Ru(1)	120.94(6)
C(9)-Ru(1)-P(2)	88.00(2)	C(2)-C(3)-H(3)	114.0
C(11)-Ru(1)-P(2)	152.98(2)	C(4)-C(3)-H(3)	114.0
C(3)-Ru(1)-P(2)	88.65(2)	Ru(1)-C(3)-H(3)	114.0
P(1)-Ru(1)-P(2)	97.354(9)	N(1)-C(4)-C(3)	122.96(8)
C(101)-P(1)-C(105)	99.84(5)	N(1)-C(4)-H(4)	118.5
C(101)-P(1)-C(103)	105.05(4)	C(3)-C(4)-H(4)	118.5
C(105)-P(1)-C(103)	102.81(4)	N(1)-C(5)-C(8)	105.71(7)
C(101)-P(1)-Ru(1)	116.83(3)	N(1)-C(5)-C(7)	106.36(8)
C(105)-P(1)-Ru(1)	116.68(3)	C(8)-C(5)-C(7)	109.75(8)
N(1)-C(5)-C(6)	116.09(8)	C(12)-C(11)-Ru(1)	122.61(6)

C(8)-C(5)-C(6)	109.25(8)	C(10)-C(11)-H(11)	113.3
C(7)-C(5)-C(6)	109.50(8)	C(12)-C(11)-H(11)	113.3
C(5)-C(6)-H(6A)	109.5	Ru(1)-C(11)-H(11)	113.3
C(5)-C(6)-H(6B)	109.5	N(2)-C(12)-C(11)	122.07(8)
H(6A)-C(6)-H(6B)	109.5	N(2)-C(12)-H(12)	119.0
C(5)-C(6)-H(6C)	109.5	C(11)-C(12)-H(12)	119.0
H(6A)-C(6)-H(6C)	109.5	N(2)-C(13)-C(14)	116.16(8)
H(6B)-C(6)-H(6C)	109.5	N(2)-C(13)-C(15)	105.75(8)
C(5)-C(7)-H(7A)	109.5	C(14)-C(13)-C(15)	109.35(10)
C(5)-C(7)-H(7B)	109.5	N(2)-C(13)-C(16)	106.26(8)
H(7A)-C(7)-H(7B)	109.5	C(14)-C(13)-C(16)	109.98(9)
C(5)-C(7)-H(7C)	109.5	C(15)-C(13)-C(16)	109.08(9)
H(7A)-C(7)-H(7C)	109.5	C(13)-C(14)-H(14A)	109.5
H(7B)-C(7)-H(7C)	109.5	C(13)-C(14)-H(14B)	109.5
C(5)-C(8)-H(8A)	109.5	H(14A)-C(14)-H(14B)	109.5
C(5)-C(8)-H(8B)	109.5	C(13)-C(14)-H(14C)	109.5
H(8A)-C(8)-H(8B)	109.5	H(14A)-C(14)-H(14C)	109.5
C(5)-C(8)-H(8C)	109.5	H(14B)-C(14)-H(14C)	109.5
H(8A)-C(8)-H(8C)	109.5	C(13)-C(15)-H(15A)	109.5
H(8B)-C(8)-H(8C)	109.5	C(13)-C(15)-H(15B)	109.5
C(10)-C(9)-Ru(1)	67.97(5)	H(15A)-C(15)-H(15B)	109.5
C(10)-C(9)-H(9A)	116.9	C(13)-C(15)-H(15C)	109.5
Ru(1)-C(9)-H(9A)	116.9	H(15A)-C(15)-H(15C)	109.5
C(10)-C(9)-H(9B)	116.9	H(15B)-C(15)-H(15C)	109.5
Ru(1)-C(9)-H(9B)	116.9	C(13)-C(16)-H(16A)	109.5
H(9A)-C(9)-H(9B)	113.9	C(13)-C(16)-H(16B)	109.5
C(9)-C(10)-C(11)	119.32(8)	H(16A)-C(16)-H(16B)	109.5
C(9)-C(10)-Ru(1)	74.63(5)	C(13)-C(16)-H(16C)	109.5
C(11)-C(10)-Ru(1)	77.53(5)	H(16A)-C(16)-H(16C)	109.5
C(9)-C(10)-H(10)	120.3	H(16B)-C(16)-H(16C)	109.5
C(11)-C(10)-H(10)	120.3	C(102)-C(101)-P(1)	121.37(7)
Ru(1)-C(10)-H(10)	120.3	C(102)-C(101)-H(10A)	107.0
C(10)-C(11)-C(12)	120.69(8)	P(1)-C(101)-H(10A)	107.0
C(10)-C(11)-Ru(1)	65.52(4)	C(102)-C(101)-H(10B)	107.0
P(1)-C(101)-H(10B)	107.0	C(202)-C(201)-H(20B)	107.2
H(10A)-C(101)-H(10B)	106.7	P(2)-C(201)-H(20B)	107.2

C(101)-C(102)-H(10C)	109.5	H(20A)-C(201)-H(20B)	106.9
C(101)-C(102)-H(10D)	109.5	C(201)-C(202)-H(20C)	109.5
H(10C)-C(102)-H(10D)	109.5	C(201)-C(202)-H(20D)	109.5
C(101)-C(102)-H(10E)	109.5	H(20C)-C(202)-H(20D)	109.5
H(10C)-C(102)-H(10E)	109.5	C(201)-C(202)-H(20E)	109.5
H(10D)-C(102)-H(10E)	109.5	H(20C)-C(202)-H(20E)	109.5
C(104)-C(103)-P(1)	119.63(7)	H(20D)-C(202)-H(20E)	109.5
C(104)-C(103)-H(10F)	107.4	C(204)-C(203)-P(2)	120.18(7)
P(1)-C(103)-H(10F)	107.4	C(204)-C(203)-H(20F)	107.3
C(104)-C(103)-H(10G)	107.4	P(2)-C(203)-H(20F)	107.3
P(1)-C(103)-H(10G)	107.4	C(204)-C(203)-H(20G)	107.3
H(10F)-C(103)-H(10G)	106.9	P(2)-C(203)-H(20G)	107.3
C(103)-C(104)-H(10H)	109.5	H(20F)-C(203)-H(20G)	106.9
C(103)-C(104)-H(10I)	109.5	C(203)-C(204)-H(20H)	109.5
H(10H)-C(104)-H(10I)	109.5	C(203)-C(204)-H(20I)	109.5
C(103)-C(104)-H(10J)	109.5	H(20H)-C(204)-H(20I)	109.5
H(10H)-C(104)-H(10J)	109.5	C(203)-C(204)-H(20J)	109.5
H(10I)-C(104)-H(10J)	109.5	H(20H)-C(204)-H(20J)	109.5
C(106)-C(105)-P(1)	115.33(7)	H(20I)-C(204)-H(20J)	109.5
C(106)-C(105)-H(10K)	108.4	C(206)-C(205)-P(2)	115.61(6)
P(1)-C(105)-H(10K)	108.4	C(206)-C(205)-H(20K)	108.4
C(106)-C(105)-H(10L)	108.4	P(2)-C(205)-H(20K)	108.4
P(1)-C(105)-H(10L)	108.4	C(206)-C(205)-H(20L)	108.4
H(10K)-C(105)-H(10L)	107.5	P(2)-C(205)-H(20L)	108.4
C(105)-C(106)-H(10M)	109.5	H(20K)-C(205)-H(20L)	107.4
C(105)-C(106)-H(10N)	109.5	C(205)-C(206)-H(20M)	109.5
H(10M)-C(106)-H(10N)	109.5	C(205)-C(206)-H(20N)	109.5
C(105)-C(106)-H(10O)	109.5	H(20M)-C(206)-H(20N)	109.5
H(10M)-C(106)-H(10O)	109.5	C(205)-C(206)-H(20O)	109.5
H(10N)-C(106)-H(10O)	109.5	H(20M)-C(206)-H(20O)	109.5
C(202)-C(201)-P(2)	120.41(7)	H(20N)-C(206)-H(20O)	109.5
C(202)-C(201)-H(20A)	107.2		
P(2)-C(201)-H(20A)	107.2		

Table D-5.5: Anisotropic displacement parameters ($\text{\AA}^2 \times 10^3$) for Compound 8. The anisotropic displacement factor exponent takes the form: $-2\pi^2 [h^2 a^{*2} U^{11} + \dots + 2 h k a^{*} b^{*} U^{12}]$

	U^{11}	U^{22}	U^{33}	U^{23}	U^{13}	U^{12}
Ru(1)	9(1)	8(1)	7(1)	-1(1)	0(1)	0(1)
P(1)	10(1)	11(1)	9(1)	-2(1)	0(1)	-1(1)
P(2)	11(1)	9(1)	9(1)	-2(1)	0(1)	0(1)
N(1)	15(1)	12(1)	14(1)	-2(1)	2(1)	-1(1)
N(2)	16(1)	12(1)	16(1)	-4(1)	1(1)	1(1)
C(1)	13(1)	13(1)	12(1)	-1(1)	-3(1)	0(1)
C(2)	13(1)	11(1)	11(1)	0(1)	-2(1)	1(1)
C(3)	14(1)	11(1)	10(1)	-1(1)	1(1)	-1(1)
C(4)	15(1)	11(1)	10(1)	0(1)	1(1)	0(1)
C(5)	14(1)	13(1)	16(1)	-2(1)	3(1)	-2(1)
C(6)	22(1)	17(1)	28(1)	-10(1)	4(1)	-4(1)
C(7)	20(1)	19(1)	20(1)	3(1)	2(1)	-4(1)
C(8)	16(1)	24(1)	21(1)	-3(1)	-2(1)	0(1)
C(9)	12(1)	13(1)	12(1)	-2(1)	-2(1)	1(1)
C(10)	12(1)	12(1)	12(1)	-4(1)	-2(1)	-2(1)
C(11)	14(1)	11(1)	11(1)	-4(1)	-1(1)	-1(1)
C(12)	14(1)	12(1)	12(1)	-4(1)	0(1)	-1(1)
C(13)	18(1)	13(1)	19(1)	-4(1)	-2(1)	3(1)
C(14)	36(1)	17(1)	29(1)	4(1)	4(1)	5(1)
C(15)	18(1)	28(1)	46(1)	-10(1)	-6(1)	6(1)
C(16)	42(1)	18(1)	31(1)	-12(1)	-13(1)	10(1)
C(101)	16(1)	24(1)	10(1)	2(1)	-1(1)	-2(1)
C(102)	22(1)	30(1)	14(1)	6(1)	-2(1)	-10(1)
C(103)	15(1)	14(1)	14(1)	-3(1)	0(1)	-5(1)
C(104)	14(1)	19(1)	21(1)	-2(1)	-1(1)	-6(1)
C(105)	13(1)	18(1)	16(1)	-6(1)	3(1)	-1(1)
C(106)	15(1)	19(1)	24(1)	-6(1)	2(1)	2(1)
C(201)	17(1)	20(1)	19(1)	-12(1)	-1(1)	-2(1)
C(202)	27(1)	20(1)	20(1)	-11(1)	-6(1)	6(1)

	U^{11}	U^{22}	U^{33}	U^{23}	U^{13}	U^{12}
C(203)	20(1)	13(1)	13(1)	-1(1)	0(1)	4(1)
C(204)	22(1)	14(1)	20(1)	-4(1)	-5(1)	6(1)
C(205)	14(1)	13(1)	12(1)	-2(1)	2(1)	0(1)
C(206)	14(1)	17(1)	20(1)	-4(1)	1(1)	-2(1)

Table D-5.6: Hydrogen coordinates ($\times 10^4$) and isotropic displacement parameters ($\text{\AA}^2 \times 10^3$) for Compound 8.

	x	y	z	U(eq)
H(1A)	2929	81	3229	15
H(1B)	1786	568	4020	15
H(2)	1440	-1537	3433	14
H(3)	-703	-342	4437	14
H(4)	-1133	-2284	3599	15
H(6A)	-2876	-3204	3100	33
H(6B)	-3778	-4202	3789	33
H(6C)	-2141	-3944	3998	33
H(7A)	-3039	-3766	5641	31
H(7B)	-4706	-3964	5454	31
H(7C)	-4284	-2851	5819	31
H(8A)	-5480	-1686	4388	31
H(8B)	-5833	-2837	4058	31
H(8C)	-4929	-1865	3339	31
H(9A)	-2628	837	1722	15
H(9B)	-1393	1018	791	15
H(10)	-1866	-1086	2095	14
H(11)	584	-470	745	14
H(12)	322	-2467	2230	15
H(14A)	1833	-3811	2980	43
H(14B)	2127	-4976	2614	43
H(14C)	625	-4283	2416	43
H(15A)	4500	-3072	1001	46
H(15B)	4469	-4274	1715	46
H(15C)	4228	-3134	2126	46
H(16A)	1055	-4243	679	44
H(16B)	2569	-4934	834	44
H(16C)	2545	-3740	109	44
H(10A)	592	1753	-44	21

	x	y	z	U(eq)
H(10B)	404	2838	433	21
H(10C)	1582	3265	-1111	35
H(10D)	2920	2439	-765	35
H(10E)	2603	3564	-342	35
H(10F)	2236	3184	1823	18
H(10G)	3047	2173	2482	18
H(10H)	4243	3308	654	28
H(10I)	5060	2296	1322	28
H(10J)	4766	3482	1652	28
H(10K)	2913	245	360	19
H(10L)	4060	1200	417	19
H(10M)	4922	-584	1168	29
H(10N)	3478	-741	1890	29
H(10O)	4638	212	1938	29
H(20A)	878	2198	4117	21
H(20B)	839	3283	3284	21
H(20C)	-1256	3971	4119	31
H(20D)	179	3847	4703	31
H(20E)	-1078	2916	4978	31
H(20F)	-648	3428	1725	19
H(20G)	-2116	2753	1721	19
H(20H)	-2778	4577	1818	28
H(20I)	-1819	4551	2707	28
H(20J)	-3275	3813	2833	28
H(20K)	-2237	1191	4506	16
H(20L)	-2951	2375	4040	16
H(20M)	-4109	1499	2971	25
H(20N)	-4560	877	4044	25
H(20O)	-3356	312	3401	25

Table D-5.7: Torsion angles [°] for Compound 8.

Ru(1)-C(1)-C(2)-C(3)	-66.31(7)
C(1)-C(2)-C(3)-C(4)	177.04(8)
Ru(1)-C(2)-C(3)-C(4)	112.63(8)
C(1)-C(2)-C(3)-Ru(1)	64.41(7)
C(5)-N(1)-C(4)-C(3)	176.83(8)
C(2)-C(3)-C(4)-N(1)	163.94(9)
Ru(1)-C(3)-C(4)-N(1)	-118.89(9)
C(4)-N(1)-C(5)-C(8)	-122.04(9)
C(4)-N(1)-C(5)-C(7)	121.31(9)
C(4)-N(1)-C(5)-C(6)	-0.77(13)
Ru(1)-C(9)-C(10)-C(11)	-65.73(7)
C(9)-C(10)-C(11)-C(12)	178.92(8)
Ru(1)-C(10)-C(11)-C(12)	114.73(8)
C(9)-C(10)-C(11)-Ru(1)	64.19(7)
C(13)-N(2)-C(12)-C(11)	179.50(8)
C(10)-C(11)-C(12)-N(2)	159.00(9)
Ru(1)-C(11)-C(12)-N(2)	-122.09(8)
C(12)-N(2)-C(13)-C(14)	-6.91(14)
C(12)-N(2)-C(13)-C(15)	-128.39(10)
C(12)-N(2)-C(13)-C(16)	115.76(10)
C(105)-P(1)-C(101)-C(102)	-49.99(9)
C(103)-P(1)-C(101)-C(102)	56.25(9)
Ru(1)-P(1)-C(101)-C(102)	-176.75(7)
C(101)-P(1)-C(103)-C(104)	-73.28(8)
C(105)-P(1)-C(103)-C(104)	30.76(8)
Ru(1)-P(1)-C(103)-C(104)	157.81(6)
C(101)-P(1)-C(105)-C(106)	-176.74(7)
C(103)-P(1)-C(105)-C(106)	75.23(8)
Ru(1)-P(1)-C(105)-C(106)	-49.88(8)
C(205)-P(2)-C(201)-C(202)	-28.60(9)
C(203)-P(2)-C(201)-C(202)	77.18(9)
Ru(1)-P(2)-C(201)-C(202)	-157.82(7)
C(205)-P(2)-C(203)-C(204)	46.00(9)
C(201)-P(2)-C(203)-C(204)	-58.03(9)

Ru(1)-P(2)-C(203)-C(204)	171.67(7)
C(203)-P(2)-C(205)-C(206)	72.47(7)
C(201)-P(2)-C(205)-C(206)	177.70(7)
Ru(1)-P(2)-C(205)-C(206)	-50.48(7)

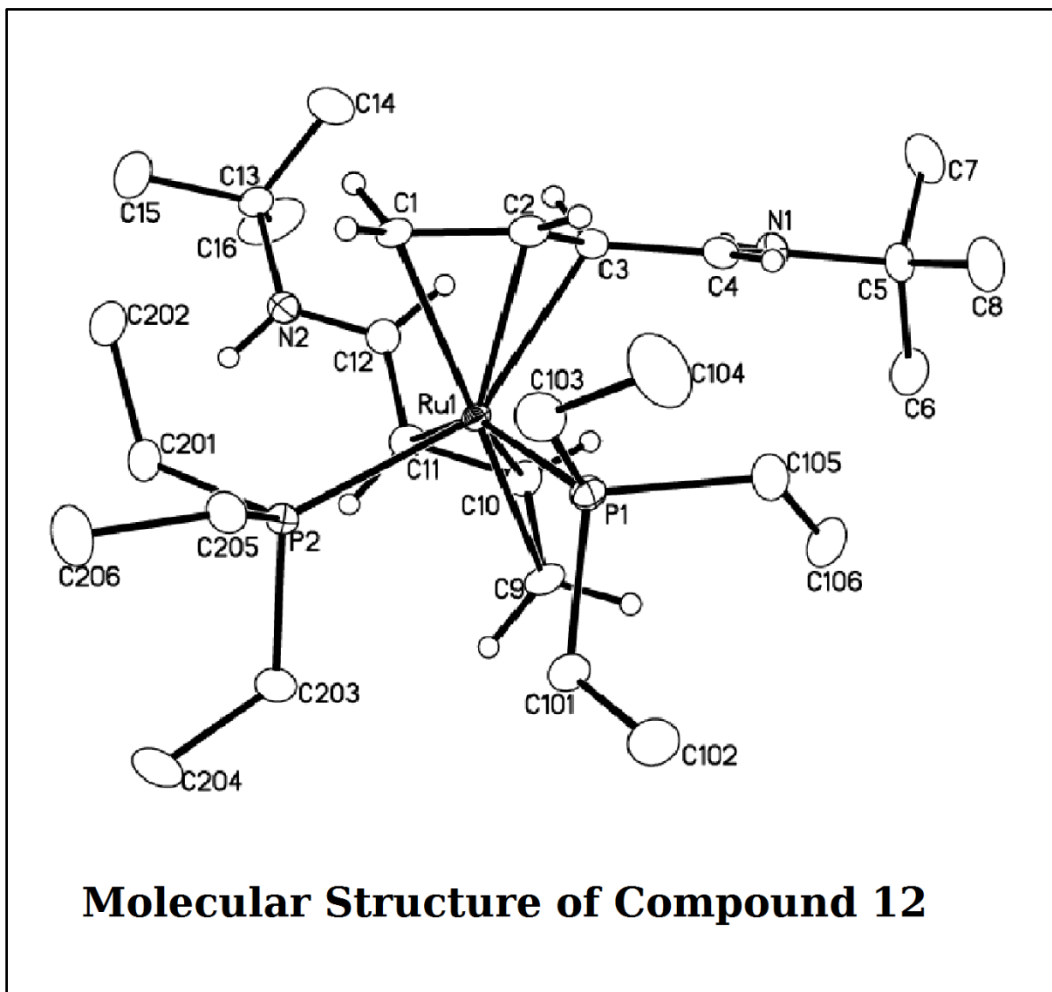
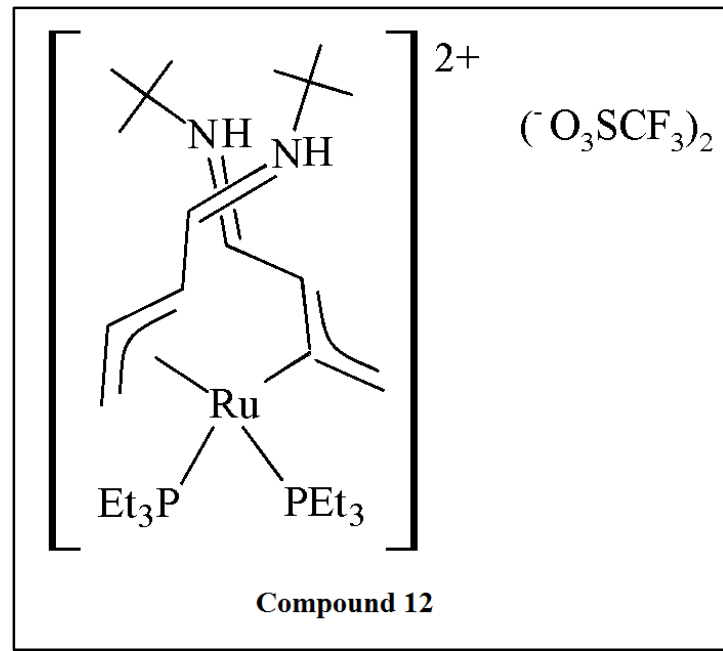


Table D-6.1: Crystal data and structure refinement for Compound 12.

Empirical formula	$C_{34} H_{68} F_6 N_2 O_7 P_2 Ru S_2$	
Formula weight	958.03	
Temperature	100(2) K	
Wavelength	0.71073 Å	
Crystal system	Monoclinic	
Space group	P 2 ₁ /c	
Unit cell dimensions	$a = 13.0975(3)$ Å	$\alpha = 90^\circ$.
	$b = 24.4595(6)$ Å	$\beta = 114.4530(10)^\circ$.
	$c = 15.4017(4)$ Å	$\gamma = 90^\circ$.
Volume	$4491.48(19)$ Å ³	
Z	4	
Density (calculated)	1.417 Mg/m ³	
Absorption coefficient	0.582 mm ⁻¹	
F(000)	2008	
Crystal size	$0.292 \times 0.213 \times 0.104$ mm ³	
Theta range for data collection	1.665 to 30.492°.	
Index ranges	$-18 \leq h \leq 18, -34 \leq k \leq 34, -20 \leq l \leq 21$	
Reflections collected	99883	
Independent reflections	13680 [R(int) = 0.0505]	
Completeness to theta = 25.242°	100.0 %	
Absorption correction	Semi-empirical from equivalents	
Max. and min. transmission	0.8622 and 0.8050	
Refinement method	Full-matrix least-squares on F ²	
Data / restraints / parameters	13680 / 14 / 503	
Goodness-of-fit on F ²	1.018	
Final R indices [I>2sigma(I)]	R1 = 0.0312, wR2 = 0.0691	
R indices (all data)	R1 = 0.0415, wR2 = 0.0740	
Extinction coefficient	n/a	
Largest diff. peak and hole	0.632 and -0.619 e.Å ⁻³	

Table D-6.2: Atomic coordinates ($\times 10^4$) and equivalent isotropic displacement parameters ($\text{\AA}^2 \times 10^3$) for Compound 12. U(eq) is defined as one third of the trace of the orthogonalized U^{ij} tensor.

	x	y	z	U(eq)
Ru(1)	789(1)	2143(1)	8998(1)	10(1)
P(1)	1776(1)	1350(1)	9027(1)	13(1)
P(2)	-877(1)	1658(1)	8748(1)	12(1)
N(1)	3422(1)	3196(1)	9263(1)	16(1)
N(2)	-1151(1)	3509(1)	8955(1)	16(1)
C(1)	1112(1)	2242(1)	10536(1)	16(1)
C(2)	2113(1)	2275(1)	10406(1)	16(1)
C(3)	2267(1)	2725(1)	9884(1)	15(1)
C(4)	3205(1)	2767(1)	9655(1)	15(1)
C(5)	4363(1)	3282(1)	8975(1)	17(1)
C(6)	3841(2)	3352(1)	7893(1)	27(1)
C(7)	4929(2)	3815(1)	9463(2)	29(1)
C(8)	5196(2)	2813(1)	9281(2)	25(1)
C(9)	352(2)	2208(1)	7416(1)	17(1)
C(10)	408(1)	2718(1)	7853(1)	16(1)
C(11)	-443(1)	2865(1)	8164(1)	15(1)
C(12)	-345(1)	3318(1)	8750(1)	15(1)
C(13)	-1078(1)	3970(1)	9604(1)	16(1)
C(14)	114(2)	4041(1)	10357(2)	37(1)
C(15)	-1851(2)	3826(1)	10081(2)	33(1)
C(16)	-1463(2)	4484(1)	9011(2)	42(1)
C(101)	1042(1)	875(1)	8046(1)	19(1)
C(102)	1678(2)	356(1)	8011(2)	28(1)
C(103)	2120(2)	914(1)	10096(1)	21(1)
C(104)	3295(2)	668(1)	10584(2)	36(1)
C(105)	3128(1)	1426(1)	8938(1)	21(1)
C(106)	3060(2)	1716(1)	8037(2)	27(1)
C(201)	-1936(1)	2031(1)	9015(1)	18(1)
C(202)	-1583(2)	2238(1)	10034(1)	22(1)

	x	y	z	U(eq)
C(203)	-1731(1)	1453(1)	7505(1)	19(1)
C(204)	-2761(2)	1091(1)	7276(2)	32(1)
C(205)	-670(1)	1032(1)	9469(1)	17(1)
C(206)	-1653(2)	793(1)	9636(2)	26(1)
S(1)	1712(1)	4560(1)	8428(1)	17(1)
F(1)	1213(1)	3939(1)	6919(1)	36(1)
F(2)	-214(1)	4182(1)	7172(1)	31(1)
F(3)	576(1)	4765(1)	6601(1)	35(1)
O(1)	1828(1)	4054(1)	8958(1)	20(1)
O(2)	2710(1)	4727(1)	8334(1)	33(1)
O(3)	1090(1)	4980(1)	8647(1)	30(1)
C(17)	772(2)	4354(1)	7220(1)	19(1)
S(2)	6142(1)	3084(1)	6744(1)	18(1)
F(4)	7650(1)	3721(1)	6559(1)	36(1)
F(5)	6070(1)	4115(1)	6245(1)	43(1)
F(6)	6226(1)	3546(1)	5238(1)	38(1)
O(4)	6766(1)	2628(1)	6623(1)	29(1)
O(5)	6517(1)	3271(1)	7721(1)	26(1)
O(6)	4939(1)	3055(1)	6217(1)	23(1)
C(18)	6539(2)	3648(1)	6167(1)	24(1)
O(1S)	4393(13)	829(6)	7359(10)	45(1)
O(1S')	3773(2)	627(1)	7249(2)	45(1)
C(1S)	3771(2)	710(1)	6347(2)	44(1)
C(2S)	4298(2)	207(1)	6126(2)	39(1)
C(3S)	4822(2)	-94(1)	7072(2)	40(1)
C(4S)	4754(2)	310(1)	7785(2)	38(1)

Table D-6.3: Bond lengths [Å] for Compound 12.

Ru(1)-C(10)	2.1472(16)	C(6)-H(6B)	0.9800
Ru(1)-C(2)	2.1683(16)	C(6)-H(6C)	0.9800
Ru(1)-C(1)	2.2407(16)	C(7)-H(7A)	0.9800
Ru(1)-C(9)	2.2660(16)	C(7)-H(7B)	0.9800
Ru(1)-P(1)	2.3209(4)	C(7)-H(7C)	0.9800
Ru(1)-C(3)	2.3331(15)	C(8)-H(8A)	0.9800
Ru(1)-P(2)	2.3719(4)	C(8)-H(8B)	0.9800
Ru(1)-C(11)	2.3781(16)	C(8)-H(8C)	0.9800
P(1)-C(101)	1.8321(17)	C(9)-C(10)	1.405(2)
P(1)-C(105)	1.8419(17)	C(9)-H(9A)	0.9900
P(1)-C(103)	1.8551(18)	C(9)-H(9B)	0.9900
P(2)-C(203)	1.8423(17)	C(10)-C(11)	1.429(2)
P(2)-C(201)	1.8430(17)	C(10)-H(10)	1.0000
P(2)-C(205)	1.8445(17)	C(11)-C(12)	1.401(2)
N(1)-C(4)	1.299(2)	C(11)-H(11)	1.0000
N(1)-C(5)	1.489(2)	C(12)-H(12)	0.9500
N(1)-H(1)	0.8800	C(13)-C(16)	1.511(3)
N(2)-C(12)	1.306(2)	C(13)-C(15)	1.519(3)
N(2)-C(13)	1.484(2)	C(13)-C(14)	1.521(3)
N(2)-H(2)	0.8800	C(14)-H(14A)	0.9800
C(1)-C(2)	1.408(2)	C(14)-H(14B)	0.9800
C(1)-H(1A)	0.9900	C(14)-H(14C)	0.9800
C(1)-H(1B)	0.9900	C(15)-H(15A)	0.9800
C(2)-C(3)	1.425(2)	C(15)-H(15B)	0.9800
C(2)-H(2A)	1.0000	C(15)-H(15C)	0.9800
C(3)-C(4)	1.415(2)	C(16)-H(16A)	0.9800
C(3)-H(3)	1.0000	C(16)-H(16B)	0.9800
C(4)-H(4)	0.9500	C(16)-H(16C)	0.9800
C(5)-C(8)	1.518(2)	C(101)-C(102)	1.530(2)
C(5)-C(6)	1.526(3)	C(101)-H(10A)	0.9900
C(5)-C(7)	1.532(3)	C(101)-H(10B)	0.9900
C(6)-H(6A)	0.9800	C(102)-H(10C)	0.9800
C(102)-H(10D)	0.9800	S(1)-C(17)	1.8256(18)

C(102)-H(10E)	0.9800	F(1)-C(17)	1.341(2)
C(103)-C(104)	1.528(3)	F(2)-C(17)	1.330(2)
C(103)-H(10F)	0.9900	F(3)-C(17)	1.336(2)
C(103)-H(10G)	0.9900	S(2)-O(4)	1.4405(14)
C(104)-H(10H)	0.9800	S(2)-O(6)	1.4445(12)
C(104)-H(10I)	0.9800	S(2)-O(5)	1.4496(13)
C(104)-H(10J)	0.9800	S(2)-C(18)	1.828(2)
C(105)-C(106)	1.527(3)	F(4)-C(18)	1.336(2)
C(105)-H(10K)	0.9900	F(5)-C(18)	1.327(2)
C(105)-H(10L)	0.9900	F(6)-C(18)	1.338(2)
C(106)-H(10M)	0.9800	O(1S)-C(4S)	1.416(13)
C(106)-H(10N)	0.9800	O(1S)-C(1S)	1.459(15)
C(106)-H(10O)	0.9800	O(1S')-C(1S)	1.403(3)
C(201)-C(202)	1.527(2)	O(1S')-C(4S)	1.434(3)
C(201)-H(20A)	0.9900	C(1S)-C(2S)	1.516(3)
C(201)-H(20B)	0.9900	C(1S)-H(1S1)	0.9900
C(202)-H(20C)	0.9800	C(1S)-H(1S2)	0.9900
C(202)-H(20D)	0.9800	C(2S)-C(3S)	1.520(3)
C(202)-H(20E)	0.9800	C(2S)-H(2SA)	0.9900
C(203)-C(204)	1.526(2)	C(2S)-H(2SB)	0.9900
C(203)-H(20F)	0.9900	C(3S)-C(4S)	1.507(3)
C(203)-H(20G)	0.9900	C(3S)-H(3SA)	0.9900
C(204)-H(20H)	0.9800	C(3S)-H(3SB)	0.9900
C(204)-H(20I)	0.9800	C(4S)-H(4S1)	0.9900
C(204)-H(20J)	0.9800	C(4S)-H(4S2)	0.9900
C(205)-C(206)	1.530(2)		
C(205)-H(20K)	0.9900		
C(205)-H(20L)	0.9900		
C(206)-H(20M)	0.9800		
C(206)-H(20N)	0.9800		
C(206)-H(20O)	0.9800		
S(1)-O(2)	1.4336(14)		
S(1)-O(3)	1.4344(13)		
S(1)-O(1)	1.4551(13)		

Table D-6.4: Bond angles [°] for Compound 12.

C(10)-Ru(1)-C(2)	122.80(6)	C(103)-P(1)-Ru(1)	115.27(6)
C(10)-Ru(1)-C(1)	132.55(6)	C(203)-P(2)-C(201)	100.21(8)
C(2)-Ru(1)-C(1)	37.20(6)	C(203)-P(2)-C(205)	105.93(8)
C(10)-Ru(1)-C(9)	37.02(6)	C(201)-P(2)-C(205)	102.28(8)
C(2)-Ru(1)-C(9)	143.78(6)	C(203)-P(2)-Ru(1)	115.29(6)
C(1)-Ru(1)-C(9)	169.28(6)	C(201)-P(2)-Ru(1)	116.27(6)
C(10)-Ru(1)-P(1)	120.10(5)	C(205)-P(2)-Ru(1)	114.96(5)
C(2)-Ru(1)-P(1)	84.09(5)	C(4)-N(1)-C(5)	128.38(14)
C(1)-Ru(1)-P(1)	102.09(5)	C(4)-N(1)-H(1)	115.8
C(9)-Ru(1)-P(1)	88.29(4)	C(5)-N(1)-H(1)	115.8
C(10)-Ru(1)-C(3)	86.28(6)	C(12)-N(2)-C(13)	126.95(14)
C(2)-Ru(1)-C(3)	36.69(6)	C(12)-N(2)-H(2)	116.5
C(1)-Ru(1)-C(3)	64.44(6)	C(13)-N(2)-H(2)	116.5
C(9)-Ru(1)-C(3)	111.42(6)	C(2)-C(1)-Ru(1)	68.60(9)
P(1)-Ru(1)-C(3)	100.24(4)	C(2)-C(1)-H(1A)	116.8
C(10)-Ru(1)-P(2)	108.04(5)	Ru(1)-C(1)-H(1A)	116.8
C(2)-Ru(1)-P(2)	122.53(5)	C(2)-C(1)-H(1B)	116.8
C(1)-Ru(1)-P(2)	89.05(4)	Ru(1)-C(1)-H(1B)	116.8
C(9)-Ru(1)-P(2)	93.13(5)	H(1A)-C(1)-H(1B)	113.8
P(1)-Ru(1)-P(2)	92.996(15)	C(1)-C(2)-C(3)	118.90(15)
C(3)-Ru(1)-P(2)	152.24(4)	C(1)-C(2)-Ru(1)	74.19(9)
C(10)-Ru(1)-C(11)	36.38(6)	C(3)-C(2)-Ru(1)	77.96(9)
C(2)-Ru(1)-C(11)	120.83(6)	C(1)-C(2)-H(2A)	120.5
C(1)-Ru(1)-C(11)	106.29(6)	C(3)-C(2)-H(2A)	120.5
C(9)-Ru(1)-C(11)	63.52(6)	Ru(1)-C(2)-H(2A)	120.5
P(1)-Ru(1)-C(11)	151.50(4)	C(4)-C(3)-C(2)	122.45(15)
C(3)-Ru(1)-C(11)	94.37(6)	C(4)-C(3)-Ru(1)	119.63(11)
P(2)-Ru(1)-C(11)	84.91(4)	C(2)-C(3)-Ru(1)	65.35(9)
C(101)-P(1)-C(105)	101.26(8)	C(4)-C(3)-H(3)	113.7
C(101)-P(1)-C(103)	102.60(8)	C(2)-C(3)-H(3)	113.7
C(105)-P(1)-C(103)	103.68(8)	Ru(1)-C(3)-H(3)	113.7
C(101)-P(1)-Ru(1)	114.64(6)	N(1)-C(4)-C(3)	123.59(15)
C(105)-P(1)-Ru(1)	117.34(6)	N(1)-C(4)-H(4)	118.2
C(3)-C(4)-H(4)	118.2	C(11)-C(10)-H(10)	120.1

N(1)-C(5)-C(8)	112.11(14)	Ru(1)-C(10)-H(10)	120.1
N(1)-C(5)-C(6)	106.81(13)	C(12)-C(11)-C(10)	122.57(15)
C(8)-C(5)-C(6)	111.30(16)	C(12)-C(11)-Ru(1)	112.22(11)
N(1)-C(5)-C(7)	105.48(14)	C(10)-C(11)-Ru(1)	62.99(9)
C(8)-C(5)-C(7)	110.55(14)	C(12)-C(11)-H(11)	115.9
C(6)-C(5)-C(7)	110.39(16)	C(10)-C(11)-H(11)	115.9
C(5)-C(6)-H(6A)	109.5	Ru(1)-C(11)-H(11)	115.9
C(5)-C(6)-H(6B)	109.5	N(2)-C(12)-C(11)	124.78(15)
H(6A)-C(6)-H(6B)	109.5	N(2)-C(12)-H(12)	117.6
C(5)-C(6)-H(6C)	109.5	C(11)-C(12)-H(12)	117.6
H(6A)-C(6)-H(6C)	109.5	N(2)-C(13)-C(16)	108.22(15)
H(6B)-C(6)-H(6C)	109.5	N(2)-C(13)-C(15)	106.28(14)
C(5)-C(7)-H(7A)	109.5	C(16)-C(13)-C(15)	111.20(17)
C(5)-C(7)-H(7B)	109.5	N(2)-C(13)-C(14)	111.14(14)
H(7A)-C(7)-H(7B)	109.5	C(16)-C(13)-C(14)	110.27(18)
C(5)-C(7)-H(7C)	109.5	C(15)-C(13)-C(14)	109.67(17)
H(7A)-C(7)-H(7C)	109.5	C(13)-C(14)-H(14A)	109.5
H(7B)-C(7)-H(7C)	109.5	C(13)-C(14)-H(14B)	109.5
C(5)-C(8)-H(8A)	109.5	H(14A)-C(14)-H(14B)	109.5
C(5)-C(8)-H(8B)	109.5	C(13)-C(14)-H(14C)	109.5
H(8A)-C(8)-H(8B)	109.5	H(14A)-C(14)-H(14C)	109.5
C(5)-C(8)-H(8C)	109.5	H(14B)-C(14)-H(14C)	109.5
H(8A)-C(8)-H(8C)	109.5	C(13)-C(15)-H(15A)	109.5
H(8B)-C(8)-H(8C)	109.5	C(13)-C(15)-H(15B)	109.5
C(10)-C(9)-Ru(1)	66.90(9)	H(15A)-C(15)-H(15B)	109.5
C(10)-C(9)-H(9A)	117.0	C(13)-C(15)-H(15C)	109.5
Ru(1)-C(9)-H(9A)	117.0	H(15A)-C(15)-H(15C)	109.5
C(10)-C(9)-H(9B)	117.0	H(15B)-C(15)-H(15C)	109.5
Ru(1)-C(9)-H(9B)	117.0	C(13)-C(16)-H(16A)	109.5
H(9A)-C(9)-H(9B)	114.0	C(13)-C(16)-H(16B)	109.5
C(9)-C(10)-C(11)	119.30(15)	H(16A)-C(16)-H(16B)	109.5
C(9)-C(10)-Ru(1)	76.09(9)	C(13)-C(16)-H(16C)	109.5
C(11)-C(10)-Ru(1)	80.64(10)	H(16A)-C(16)-H(16C)	109.5
C(9)-C(10)-H(10)	120.1	H(16B)-C(16)-H(16C)	109.5
C(102)-C(101)-P(1)	116.61(13)	H(10N)-C(106)-H(10O)	109.5
C(102)-C(101)-H(10A)	108.1	C(202)-C(201)-P(2)	117.31(12)

P(1)-C(101)-H(10A)	108.1	C(202)-C(201)-H(20A)	108.0
C(102)-C(101)-H(10B)	108.1	P(2)-C(201)-H(20A)	108.0
P(1)-C(101)-H(10B)	108.1	C(202)-C(201)-H(20B)	108.0
H(10A)-C(101)-H(10B)	107.3	P(2)-C(201)-H(20B)	108.0
C(101)-C(102)-H(10C)	109.5	H(20A)-C(201)-H(20B)	107.2
C(101)-C(102)-H(10D)	109.5	C(201)-C(202)-H(20C)	109.5
H(10C)-C(102)-H(10D)	109.5	C(201)-C(202)-H(20D)	109.5
C(101)-C(102)-H(10E)	109.5	H(20C)-C(202)-H(20D)	109.5
H(10C)-C(102)-H(10E)	109.5	C(201)-C(202)-H(20E)	109.5
H(10D)-C(102)-H(10E)	109.5	H(20C)-C(202)-H(20E)	109.5
C(104)-C(103)-P(1)	119.17(14)	H(20D)-C(202)-H(20E)	109.5
C(104)-C(103)-H(10F)	107.5	C(204)-C(203)-P(2)	119.74(14)
P(1)-C(103)-H(10F)	107.5	C(204)-C(203)-H(20F)	107.4
C(104)-C(103)-H(10G)	107.5	P(2)-C(203)-H(20F)	107.4
P(1)-C(103)-H(10G)	107.5	C(204)-C(203)-H(20G)	107.4
H(10F)-C(103)-H(10G)	107.0	P(2)-C(203)-H(20G)	107.4
C(103)-C(104)-H(10H)	109.5	H(20F)-C(203)-H(20G)	106.9
C(103)-C(104)-H(10I)	109.5	C(203)-C(204)-H(20H)	109.5
H(10H)-C(104)-H(10I)	109.5	C(203)-C(204)-H(20I)	109.5
C(103)-C(104)-H(10J)	109.5	H(20H)-C(204)-H(20I)	109.5
H(10H)-C(104)-H(10J)	109.5	C(203)-C(204)-H(20J)	109.5
H(10I)-C(104)-H(10J)	109.5	H(20H)-C(204)-H(20J)	109.5
C(106)-C(105)-P(1)	114.71(13)	H(20I)-C(204)-H(20J)	109.5
C(106)-C(105)-H(10K)	108.6	C(206)-C(205)-P(2)	119.62(12)
P(1)-C(105)-H(10K)	108.6	C(206)-C(205)-H(20K)	107.4
C(106)-C(105)-H(10L)	108.6	P(2)-C(205)-H(20K)	107.4
P(1)-C(105)-H(10L)	108.6	C(206)-C(205)-H(20L)	107.4
H(10K)-C(105)-H(10L)	107.6	P(2)-C(205)-H(20L)	107.4
C(105)-C(106)-H(10M)	109.5	H(20K)-C(205)-H(20L)	106.9
C(105)-C(106)-H(10N)	109.5	C(205)-C(206)-H(20M)	109.5
H(10M)-C(106)-H(10N)	109.5	C(205)-C(206)-H(20N)	109.5
C(105)-C(106)-H(10O)	109.5	H(20M)-C(206)-H(20N)	109.5
H(10M)-C(106)-H(10O)	109.5	C(205)-C(206)-H(20O)	109.5
H(20M)-C(206)-H(20O)	109.5	C(1S)-C(2S)-C(3S)	104.17(19)
H(20N)-C(206)-H(20O)	109.5	C(1S)-C(2S)-H(2SA)	110.9
O(2)-S(1)-O(3)	116.79(9)	C(3S)-C(2S)-H(2SA)	110.9

O(2)-S(1)-O(1)	114.21(8)	C(1S)-C(2S)-H(2SB)	110.9
O(3)-S(1)-O(1)	114.52(9)	C(3S)-C(2S)-H(2SB)	110.9
O(2)-S(1)-C(17)	103.56(9)	H(2SA)-C(2S)-H(2SB)	108.9
O(3)-S(1)-C(17)	103.20(8)	C(4S)-C(3S)-C(2S)	103.96(19)
O(1)-S(1)-C(17)	101.88(8)	C(4S)-C(3S)-H(3SA)	111.0
F(2)-C(17)-F(3)	107.62(14)	C(2S)-C(3S)-H(3SA)	111.0
F(2)-C(17)-F(1)	106.88(15)	C(4S)-C(3S)-H(3SB)	111.0
F(3)-C(17)-F(1)	107.73(15)	C(2S)-C(3S)-H(3SB)	111.0
F(2)-C(17)-S(1)	111.90(12)	H(3SA)-C(3S)-H(3SB)	109.0
F(3)-C(17)-S(1)	111.60(12)	O(1S)-C(4S)-C(3S)	111.1(6)
F(1)-C(17)-S(1)	110.87(12)	O(1S')-C(4S)-C(3S)	104.18(19)
O(4)-S(2)-O(6)	115.74(8)	O(1S)-C(4S)-H(4S1)	109.4
O(4)-S(2)-O(5)	114.26(8)	C(3S)-C(4S)-H(4S1)	109.4
O(6)-S(2)-O(5)	114.88(8)	O(1S)-C(4S)-H(4S2)	109.4
O(4)-S(2)-C(18)	103.38(9)	C(3S)-C(4S)-H(4S2)	109.4
O(6)-S(2)-C(18)	103.16(8)	H(4S1)-C(4S)-H(4S2)	108.0
O(5)-S(2)-C(18)	102.98(9)		
F(5)-C(18)-F(4)	107.55(16)		
F(5)-C(18)-F(6)	108.02(16)		
F(4)-C(18)-F(6)	107.69(15)		
F(5)-C(18)-S(2)	111.68(13)		
F(4)-C(18)-S(2)	110.91(13)		
F(6)-C(18)-S(2)	110.83(13)		
C(4S)-O(1S)-C(1S)	104.4(10)		
C(1S)-O(1S')-C(4S)	106.35(19)		
O(1S')-C(1S)-C(2S)	106.94(19)		
O(1S)-C(1S)-C(2S)	107.3(5)		
O(1S)-C(1S)-H(1S1)	110.3		
C(2S)-C(1S)-H(1S1)	110.3		
O(1S)-C(1S)-H(1S2)	110.3		
C(2S)-C(1S)-H(1S2)	110.3		
H(1S1)-C(1S)-H(1S2)	108.5		

Table D-6.5: Anisotropic displacement parameters ($\text{\AA}^2 \times 10^3$) for Compound 12. The anisotropic displacement factor exponent takes the form: $-2\pi^2 [h^2 a^{*2} U^{11} + \dots + 2 h k a^{*} b^{*} U^{12}]$

	U^{11}	U^{22}	U^{33}	U^{23}	U^{13}	U^{12}
Ru(1)	11(1)	11(1)	8(1)	0(1)	4(1)	0(1)
P(1)	14(1)	12(1)	15(1)	-2(1)	7(1)	0(1)
P(2)	12(1)	14(1)	11(1)	-1(1)	4(1)	-1(1)
N(1)	14(1)	17(1)	18(1)	2(1)	7(1)	1(1)
N(2)	14(1)	17(1)	16(1)	-2(1)	6(1)	-1(1)
C(1)	18(1)	21(1)	10(1)	-4(1)	6(1)	-3(1)
C(2)	17(1)	17(1)	12(1)	-2(1)	4(1)	-1(1)
C(3)	14(1)	18(1)	13(1)	-3(1)	6(1)	-3(1)
C(4)	15(1)	16(1)	14(1)	-2(1)	4(1)	-2(1)
C(5)	12(1)	23(1)	19(1)	2(1)	8(1)	-1(1)
C(6)	24(1)	38(1)	22(1)	6(1)	12(1)	6(1)
C(7)	19(1)	26(1)	39(1)	-1(1)	10(1)	-4(1)
C(8)	18(1)	26(1)	33(1)	8(1)	12(1)	5(1)
C(9)	23(1)	19(1)	10(1)	0(1)	8(1)	0(1)
C(10)	17(1)	18(1)	12(1)	4(1)	6(1)	2(1)
C(11)	17(1)	15(1)	13(1)	2(1)	5(1)	2(1)
C(12)	15(1)	16(1)	13(1)	5(1)	5(1)	2(1)
C(13)	20(1)	14(1)	15(1)	-2(1)	8(1)	-1(1)
C(14)	22(1)	50(1)	35(1)	-23(1)	7(1)	-4(1)
C(15)	43(1)	28(1)	42(1)	-13(1)	31(1)	-14(1)
C(16)	79(2)	21(1)	28(1)	7(1)	24(1)	15(1)
C(101)	22(1)	18(1)	21(1)	-6(1)	12(1)	-2(1)
C(102)	29(1)	20(1)	40(1)	-14(1)	18(1)	-4(1)
C(103)	22(1)	15(1)	23(1)	3(1)	8(1)	2(1)
C(104)	23(1)	37(1)	40(1)	15(1)	3(1)	6(1)
C(105)	17(1)	17(1)	31(1)	-5(1)	13(1)	-1(1)
C(106)	30(1)	27(1)	36(1)	-8(1)	25(1)	-5(1)
C(201)	14(1)	20(1)	20(1)	2(1)	9(1)	1(1)
C(202)	21(1)	25(1)	25(1)	-3(1)	14(1)	1(1)

	U^{11}	U^{22}	U^{33}	U^{23}	U^{13}	U^{12}
C(203)	16(1)	24(1)	14(1)	-4(1)	3(1)	-2(1)
C(204)	24(1)	43(1)	25(1)	-13(1)	5(1)	-15(1)
C(205)	16(1)	15(1)	18(1)	1(1)	7(1)	-2(1)
C(206)	22(1)	27(1)	32(1)	9(1)	13(1)	-3(1)
S(1)	15(1)	14(1)	20(1)	-2(1)	6(1)	0(1)
F(1)	47(1)	36(1)	22(1)	-7(1)	12(1)	15(1)
F(2)	20(1)	31(1)	32(1)	-2(1)	1(1)	-6(1)
F(3)	43(1)	32(1)	25(1)	13(1)	9(1)	6(1)
O(1)	20(1)	20(1)	19(1)	3(1)	7(1)	2(1)
O(2)	19(1)	31(1)	47(1)	9(1)	12(1)	-5(1)
O(3)	32(1)	22(1)	32(1)	-11(1)	9(1)	7(1)
C(17)	24(1)	17(1)	17(1)	0(1)	8(1)	4(1)
S(2)	12(1)	24(1)	15(1)	-1(1)	3(1)	-1(1)
F(4)	18(1)	54(1)	36(1)	3(1)	11(1)	-10(1)
F(5)	40(1)	23(1)	67(1)	4(1)	25(1)	3(1)
F(6)	34(1)	60(1)	21(1)	8(1)	11(1)	-5(1)
O(4)	25(1)	28(1)	28(1)	-2(1)	5(1)	8(1)
O(5)	15(1)	45(1)	15(1)	-6(1)	4(1)	-5(1)
O(6)	13(1)	31(1)	21(1)	-2(1)	3(1)	-3(1)
C(18)	17(1)	31(1)	25(1)	1(1)	8(1)	-1(1)
O(1S)	55(2)	44(1)	52(1)	15(1)	38(1)	26(1)
O(1S')	55(2)	44(1)	52(1)	15(1)	38(1)	26(1)
C(1S)	52(1)	40(1)	37(1)	10(1)	16(1)	18(1)
C(2S)	48(1)	40(1)	30(1)	7(1)	18(1)	10(1)
C(3S)	48(1)	43(1)	34(1)	10(1)	21(1)	21(1)
C(4S)	40(1)	44(1)	30(1)	5(1)	16(1)	9(1)

Table D-6.6: Hydrogen coordinates ($\times 10^4$) and isotropic displacement parameters ($\text{\AA}^2 \times 10^3$) for Compound 12.

	x	y	z	U(eq)
H(1)	2951	3470	9153	20
H(2)	-1807	3347	8678	19
H(1A)	841	2583	10714	19
H(1B)	1012	1913	10868	19
H(2A)	2719	1998	10700	19
H(3)	2018	3083	10042	18
H(4)	3704	2465	9796	18
H(6A)	3441	3017	7592	41
H(6B)	4433	3424	7676	41
H(6C)	3314	3659	7717	41
H(7A)	4373	4110	9280	43
H(7B)	5529	3908	9266	43
H(7C)	5247	3766	10157	43
H(8A)	5502	2772	9976	38
H(8B)	5807	2889	9088	38
H(8C)	4815	2474	8977	38
H(9A)	954	2122	7207	20
H(9B)	-401	2079	6973	20
H(10)	981	2994	7871	19
H(11)	-1225	2754	7733	19
H(12)	359	3500	9019	18
H(14A)	379	3696	10698	56
H(14B)	126	4326	10810	56
H(14C)	605	4149	10049	56
H(15A)	-2614	3770	9592	50
H(15B)	-1853	4126	10503	50
H(15C)	-1586	3491	10455	50
H(16A)	-950	4567	8713	63
H(16B)	-1468	4789	9421	63

	x	y	z	U(eq)
H(16C)	-2221	4428	8514	63
H(10A)	334	764	8082	23
H(10B)	839	1074	7438	23
H(10C)	1179	115	7504	43
H(10D)	1936	166	8625	43
H(10E)	2326	455	7880	43
H(10F)	1984	1133	10578	25
H(10G)	1577	607	9913	25
H(10H)	3448	441	10127	55
H(10I)	3341	444	11125	55
H(10J)	3849	964	10811	55
H(10K)	3647	1633	9500	25
H(10L)	3455	1059	8963	25
H(10M)	2527	1523	7474	41
H(10N)	3802	1717	8025	41
H(10O)	2807	2093	8034	41
H(20A)	-2188	2349	8580	21
H(20B)	-2592	1788	8862	21
H(20C)	-2249	2358	10122	33
H(20D)	-1066	2547	10149	33
H(20E)	-1209	1944	10485	33
H(20F)	-1986	1791	7124	23
H(20G)	-1229	1261	7270	23
H(20H)	-3145	1039	6585	49
H(20I)	-3272	1267	7509	49
H(20J)	-2526	736	7589	49
H(20K)	-398	743	9166	20
H(20L)	-57	1106	10103	20
H(20M)	-2267	704	9022	40
H(20N)	-1913	1062	9972	40
H(20O)	-1409	461	10023	40
H(1S1)	3815	1024	5958	52
H(1S2)	2972	640	6201	52

	x	y	z	U(eq)
H(2SA)	4875	311	5897	46
H(2SB)	3723	-21	5635	46
H(3SA)	4398	-431	7059	48
H(3SB)	5611	-192	7224	48
H(4S1)	4223	173	8041	45
H(4S2)	5501	346	8323	45

Table D-6.7: Torsion angles [°] for Compound 12.

Ru(1)-C(1)-C(2)-C(3)	66.18(14)
C(1)-C(2)-C(3)-C(4)	-174.82(15)
Ru(1)-C(2)-C(3)-C(4)	-110.66(15)
C(1)-C(2)-C(3)-Ru(1)	-64.16(13)
C(5)-N(1)-C(4)-C(3)	-178.71(16)
C(2)-C(3)-C(4)-N(1)	-173.02(16)
Ru(1)-C(3)-C(4)-N(1)	108.91(16)
C(4)-N(1)-C(5)-C(8)	-5.8(2)
C(4)-N(1)-C(5)-C(6)	116.32(19)
C(4)-N(1)-C(5)-C(7)	-126.21(18)
Ru(1)-C(9)-C(10)-C(11)	-70.66(14)
C(9)-C(10)-C(11)-C(12)	168.41(15)
Ru(1)-C(10)-C(11)-C(12)	100.25(15)
C(9)-C(10)-C(11)-Ru(1)	68.16(13)
C(13)-N(2)-C(12)-C(11)	177.06(15)
C(10)-C(11)-C(12)-N(2)	170.95(16)
Ru(1)-C(11)-C(12)-N(2)	-117.79(15)
C(12)-N(2)-C(13)-C(16)	94.9(2)
C(12)-N(2)-C(13)-C(15)	-145.61(18)
C(12)-N(2)-C(13)-C(14)	-26.3(2)
C(105)-P(1)-C(101)-C(102)	50.26(16)
C(103)-P(1)-C(101)-C(102)	-56.69(16)
Ru(1)-P(1)-C(101)-C(102)	177.60(12)
C(101)-P(1)-C(103)-C(104)	98.61(16)
C(105)-P(1)-C(103)-C(104)	-6.47(18)
Ru(1)-P(1)-C(103)-C(104)	-136.09(14)
C(101)-P(1)-C(105)-C(106)	66.89(14)
C(103)-P(1)-C(105)-C(106)	172.99(13)
Ru(1)-P(1)-C(105)-C(106)	-58.66(14)
C(203)-P(2)-C(201)-C(202)	175.39(13)
C(205)-P(2)-C(201)-C(202)	66.45(14)
Ru(1)-P(2)-C(201)-C(202)	-59.64(14)
C(201)-P(2)-C(203)-C(204)	-60.23(17)
C(205)-P(2)-C(203)-C(204)	45.79(17)

Ru(1)-P(2)-C(203)-C(204)	174.13(13)
C(203)-P(2)-C(205)-C(206)	-72.14(16)
C(201)-P(2)-C(205)-C(206)	32.38(16)
Ru(1)-P(2)-C(205)-C(206)	159.32(13)
O(2)-S(1)-C(17)-F(2)	179.83(12)
O(3)-S(1)-C(17)-F(2)	-57.98(14)
O(1)-S(1)-C(17)-F(2)	61.03(13)
O(2)-S(1)-C(17)-F(3)	-59.49(14)
O(3)-S(1)-C(17)-F(3)	62.69(14)
O(1)-S(1)-C(17)-F(3)	-178.29(12)
O(2)-S(1)-C(17)-F(1)	60.61(14)
O(3)-S(1)-C(17)-F(1)	-177.20(13)
O(1)-S(1)-C(17)-F(1)	-58.19(14)
O(4)-S(2)-C(18)-F(5)	-177.36(13)
O(6)-S(2)-C(18)-F(5)	61.70(15)
O(5)-S(2)-C(18)-F(5)	-58.13(15)
O(4)-S(2)-C(18)-F(4)	-57.41(15)
O(6)-S(2)-C(18)-F(4)	-178.35(13)
O(5)-S(2)-C(18)-F(4)	61.82(15)
O(4)-S(2)-C(18)-F(6)	62.15(14)
O(6)-S(2)-C(18)-F(6)	-58.79(14)
O(5)-S(2)-C(18)-F(6)	-178.61(12)
C(4S)-O(1S')-C(1S)-O(1S)	-63.9(8)
C(4S)-O(1S')-C(1S)-C(2S)	32.5(3)
C(4S)-O(1S)-C(1S)-O(1S')	64.3(9)
C(4S)-O(1S)-C(1S)-C(2S)	-31.1(10)
O(1S')-C(1S)-C(2S)-C(3S)	-12.5(3)
O(1S)-C(1S)-C(2S)-C(3S)	26.0(7)
C(1S)-C(2S)-C(3S)-C(4S)	-10.8(3)
C(1S)-O(1S)-C(4S)-O(1S')	-61.3(10)
C(1S)-O(1S)-C(4S)-C(3S)	24.4(11)
C(1S)-O(1S')-C(4S)-O(1S)	67.0(9)
C(1S)-O(1S')-C(4S)-C(3S)	-39.3(3)
C(2S)-C(3S)-C(4S)-O(1S)	-8.2(8)
C(2S)-C(3S)-C(4S)-O(1S')	30.0(3)

References

- (1) MiTeGen, LLC, PO Box 3867, Ithaca, NY, 14852
- (2) Bruker Analytical X-Ray, Madison, WI, **2008**.
- (3) Bruker-SHELXTL: Sheldrick, G.M. *Acta Crystallogr.* **2008**, *A64*, 112-122.